KINETIC INVESTIGATIONS OF COMPLEXES OF COBALT(III) CONTAINING CO-ORDINATED MALONATE

A THESIS

presented to the University

of London for the degree of

DOCTOR OF PHILOSOPHY

by

Martin Alan Richard Smith.

Bedford College,

Regent's Park,

LONDON, N.W.1

July, 1971.

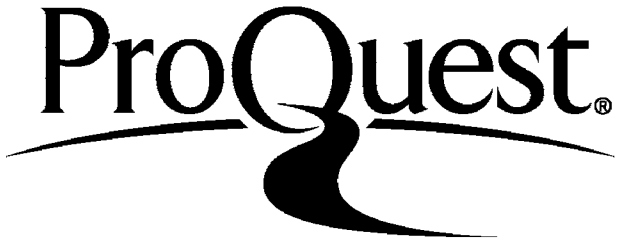

ABSTRACT

Part One.

The acid-catalysed deuteration of the active methylene group in the complexes: $[Coen_2mal]^+$, $[CoBipy_2mal]^+$ and $[Comal_2en]^-$, (where en = ethylenediamine, mal = malonate and Bipy = 2,2' bipyridyl), has been studied in the temperature range 20-45°C. The reaction was found to be of the first order in both acid and complex concentrations in the range pD2-3. The relative rates of deuteration are discussed in terms of a keto-enolate cation mechanism. The stereospecific deuteration of the methylene protons in $[Comal_2en]^-$ is discussed in terms of the conformational flexibility of the six membered chelate ring. Absolute assignment of the magnetically inequivalent geminal protons in the latter complex followed the interpretation of the pmr spectra of the complex anions, $[CoEthylmal_2en]^-$ and $[Comal_2Bipy]^-$ in acidic and in basic solution.

Part Two.

The kinetics and mechanisms of the base and of the acid hydrolysis of the α-monosubstituted complex cations $[Coen_2Ethylmal]^+$ and $[Coen_2Benzylmal]^+$ have been investigated spectrophotometrically in the temperature range 18-60°C. In basic solution the reaction proceeds in two identifiable stages. Both obey the rate law:

$$\text{Rate} = k_1[\text{complex}] + k_2[\text{complex}][OH^-] + k_3[\text{complex}][OH^-]^2.$$

The second term is dominant in dilute base ($[OH^-] < 1M$), and the combined first and third in concentrated base ($[OH^-] > 1.50M$), at 25°C. In acidic solution, the reaction proceeds in two stages. In the pH range studied (2-4), the first shows half order dependence on acid, whilst the second is independent of acid.
Mechanisms consistent with the kinetics are discussed.

ACKNOWLEDGEMENTS.

The author wishes to express his gratitude to his supervisor, Dr.M.E.Farago for her constant help and encouragement throughout this work.

I am also indebted to Professor G.H. Williams for the provision of laboratory facilities.

I am especially grateful to my wife, Gwen, for typing and reproducing this thesis. In this context, thanks are also due to Mr.G.M.Paterson for allowing the library's stencilling equipment to be used and to Mr.T.Hatt for drawing Figure 8.

Lastly the award of a studentship from the Science Research Council is gratefully recognised.

CONTENTS.

GENERAL INTRODUCTION

1. THE ESTABLISHMENT OF RATE LAWS.

Experimental determination of rates involves examination of the change in concentration of a reactant with time, with the condition that the method of measurement interferes in no way with the reacting system.

There are two basic methods for mixing reactants and following the course of a reaction in solution. The static method and the flow method. The latter, for measuring very fast rates, is dealt with in ref.24. In the former, reactants are preheated, because of the high heat capacity of liquids, to the required temperature and then mixed. The reaction solution is then accurately thermostated. Subsequent monitoring of one concentration or another necessitates a completely discriminating method of analysis. For example, the whole reaction solution may be monitored by say, NMR, to which only one constituent responds, whilst an identical solution under the same conditions, may be intermittently sampled, the reaction quenched and concentrations of say, a metal, determined by classical methods of analysis.

The net result is, therefore, a set of concentration versus time plots. Most reactions do not proceed in a single stage, but in a series of reaction steps. In the first of these, which are often reversible, intermediates are formed which subsequently react in later stages to form products. Each step behaves as a unique reaction having its own transition complex, and the rate of each step is proportional to the concentration of each reactant in the step. The overall rate is a product of the effect of each step i.e. if one step is predominantly slow, its rate determines the overall rate of reaction, and the complexity of the rate law will, very likely, depend upon the complexity or otherwise of this step.

Rates may be determined from concentration, time plots by tangent drawing although this is not very accurate and improved methods have been devised(40).

If it is suspected that a reaction is obeying an elementary rate law, linear plots may be constructed from the standard integrated form of that rate law - see Table 1.

TABLE 1.

Reaction Type	Initial Conditions	Rate Law	Integrated Law	Plot	Reaction Order
$A \longrightarrow$ products	$[A]=[A_o]$	$-\frac{dA}{dt} = k_o$	$[A]=[A_o]-k_o t$	$[A]/t$	zero
$A \longrightarrow$ products	$[A]=[A_o]$	$-\frac{dA}{dt} = k_o[A]$	$\ln[A]=\ln[A_o]-k_o t$	$\ln[A]/t$	first
$2A \longrightarrow$ products $A+B \longrightarrow$ products	$[A]=[A_o]$ $[A]=[B]$	$-\frac{dA}{dt} = k_2[A]^2$	$\frac{1}{[A]} = \frac{1}{[A_o]} + k_2 t$	$1/[A]/t$	second
$A+B \longrightarrow$ products.	$[A]\neq[B]$	$-\frac{dA}{dt} = k_2'[A][B]$	$\ln\frac{[B]}{[A]} = \ln\frac{[A_o]}{[A_o]} + ([B_o]-[A_o])k_2' t$	$\ln\frac{[B]}{[A]}/t$	second
$A+B+C \longrightarrow$ products	$[A]=[B]=[C]$	$-\frac{dA}{dt} = k_3[A][B][C]$	$1/[A]^2 = 1/[A_o]^2 + k_3 t$	$1/[A]^2/t$	third
$2A+B \longrightarrow$ products	$[A_o]=2[B_o]$	$-\frac{dB}{dt} = k_3'[A]^2[B]$	$\frac{1}{[B]^2} = \frac{1}{[B_o]^2} + 4k_3' t$	$1/[B]^2/t$	third.

Such plots must be linear for at least 90%, (about three half lives), of reaction in order to verify that the correct law has been chosen and the rate constants so obtained must be reproducible.

For a complex reaction many proceedures may be adopted(40,Ch.3). However, there are two standard procedures:

(i) The method of initial rates. The initial rate for the reaction:

$$aA + bB + cC \longrightarrow \text{products}$$

is given by:

$$(\text{Initial Rate})_1 = k[A]^a[B]^b[C]^c \qquad (1)$$

If we now vary the concentration of A by a factor of x, we obtain:

$$(\text{Initial Rate})_2 = k[xA]^a[B]^b[C]^c \qquad (2)$$

Dividing (2) by (1) thus gives:

$$\frac{(\text{Initial Rate})_2}{(\text{Initial Rate})_1} = x^a \qquad (3)$$

The order of reaction w.r.t. A,a, is thereby determined. By varying the concentration of each reactant in turn b and c may also be determined, and if no other subsequent steps are slow, a rate law of complex orders in A,B and C may be built up. The serious limit to the method is the difficulty in experimentally measuring initial rates.

(ii) The isolation method. Here all concentrations, except the one to be examined, are kept in large excess. This results in the rate varying during the course of a reaction in a manner dependent on only the isolated reactant. The reaction order w.r.t. this isolated component may then be established by selecting an appropriate integrated rate equation, or by initial rates. Difficulty arises in keeping the rate of the isolated reactant low enough to measure, whilst maintaining a large excess of the others. Rate dependence on the reagent in excess may also be determined. For instance, in the simple reaction:

$$A + B \longrightarrow C$$

If [B] is kept constant by having a large excess then initial and finite time conditions are:

at t = o [A]= a [B]=b

at t = t [A]= (a-x) [B]=b.

Therefore, $\frac{dx}{dt} = k_2(a-x)b$ (4)

Integrating (4) $\ln \frac{a_o}{(a-x)} = bk_2t$ or $\ln a_o/t = k_2b$ —— (5)
$a-x$

The left hand side of (5) is standard first-order,log concentration,time plot, the slope of which is called the "pseudo-first-order" rate constant. Varying [B] whilst still maintaining it in "first-order" excess gives a set of k_1, b data. The term b may contain several terms itself,which may be found by fitting a linear relationship to the k_1, b data.

This extension of the isolation method is conveniently used in the study of kinetics of hydrolysis of transition metal complexes by the technique of spectrophotometry. Here the concentration of A, the complex, is necessarily small whilst B,which may be acid or base, can be easily kept in large excess or if this results in the hydrolysis being too fast, by buffering with non-interfe ring buffering agents.

2.FACTORS AFFECTING RATES IN SOLUTION.

Reaction between two species in solution is thought to occur in three stages:(a)diffusion of one species to the other,(b) the chemical change,and(c) diffusion of the products away from each other. Much work has been done on the influence of solvation, solvent and ionic strength (61) on reaction rates. The electrostatic effect on the combination of charged ions in terms of collision theory (72 and 85) must also be considered.

The influence of ionic strength on the rates of reaction between ions has been discussed,(27,17,14 and 85). Bronstead and Bjerrum (17,14) postulate that the rate of reaction is proportional to the <u>concentration</u> of the activated complex rather than its <u>activity</u>.

Thus,in the reaction, $A + B \rightleftharpoons X^* \longrightarrow$ products.

$$\text{Rate} = k'[X^*] \quad (6)$$

and the equilibrium between A,B and X^* may be represented as:

$$K = \frac{[X^*]}{[A][B]} \cdot \frac{F_*}{F_A F_B} \quad (7)$$

where the F's are activity coefficents. Introducing (7) into (6) gives:

$$\text{Rate} = k[A][B] = k_o[A][B]\ \frac{F_A F_B}{F_*} \qquad (8)$$

Using the Debye-Hückel relationship:

$$\log_{10} f = -Qz^2 \sqrt{\mu} \qquad (9)$$

where z = valency, μ = ionic strength and Q = a constant, and taking logs of expression (8) we eventually arrive at:

$$\log_{10} k = \log_{10} k_o + 2\ QZ_A Z_B \sqrt{\mu} \qquad (10)$$

Evaluating Q for aqueous solution at 25°C and substituting we arrive at expression (11) which shows the effect of ionic strength on the rate of reaction between two ions of valency Z_A and Z_B:

$$\log_{10} k = \log_{10} k_o + 1.02\ Z_A Z_B \sqrt{\mu}\ . \qquad (11)$$

A plot of $\log_{10} k$ versus $\sqrt{\mu}$ should give a straight line of slope depending on valencies Z_A and Z_B. The validity of equn. (11) has been repeatedly tested and holds for a number of reactions. In concentrated solution where Debye-Hückel theory breaks down, the equation no longer holds satisfactorily. Explanation of this can usually be had in terms of ion pairing, either (a) reducing the true ionic strength of the solution, or (b) changing the electrostatic interactions between the ions if one of them is involved in ion pairing.
The maintainance of ionic strength at a constant value with an inert solute (such as perchlorate) during the course of a kinetic determination is essential.
Throughout this research concentrations have been used rather than activities. Especially in those studies using very concentrated hydroxide, and throughout the other work, the rates quoted are not absolute values. Nevertheless, they bear the same relationship to the absolute values as the concentration does to the activity of the components of the solutions studied.

3.LIGAND FIELD THEORY.

The term "Ligand Field Theory" applies to the Molecular Orbital description of ligand field splitting.

(i)Molecular Orbital Theory,describes the combination of metal and ligand orbitals to give a new set of orbitals, one of each new pair of which is more stable and the other less stable than either of the original orbitals. Figure 1 demonstrates the five angular distributions for all sets of d electrons chosen as being primarily independent whilst not all being of the same shape. Considering octahedral ligand distribution, providing the symmetry of the orbitals on the metal and on the ligands is suitable, shown for example in Figure 2, the new set of molecular orbitals formed will have an energy distribution as shown schematically in Figure 3. The most important result, is the combination of the e_g orbitals with ligand orbitals to give doubly degenerate bonding and antibonding molecular orbitals, whilst the t_{2g} orbitals are unaffected by σ bonding in this way. The separation between the t_{2g} and antibonding e_g molecular orbitals is known as the ligand field splitting, 10Dq.

(ii)Valence Bond Theory.In octahedral, six co-ordinate, complexes, six hybrid orbitals are visualised,identical, except for being pointed towards six differant directions in space each defined by a unique set of Cartesian co-ordinates. The six atomic orbitals used are the $d_{x^2-y^2}$, d_{z^2},s,p_x,p_y and p_z. Six σ bonds are then formed by each hybrid orbital accepting a pair of electrons from each ligand. The d_{xy},d_{xz} and d_{yz} orbitals of the metal,rotated 45° from the hybrid orbitals are suitably placed for π bonding with either p or d orbitals on the ligands. Pauling (78) has postulated that if the ligand has any such orbitals vacant and the metal has the required filled orbitals, π overlap will occur and help strengthen the co-ordinate bond, (a) by double bonding and (b) by reducing charge density on the metal.

(iii)Crystal Field Theory. Although comparatively simple, the theory is valuable in deriving energy level diagrams which may be used without further recourse. The theory was first formulated by Bethe (11) and considers the ligands purely as

FIGURE 1. The d orbitals.

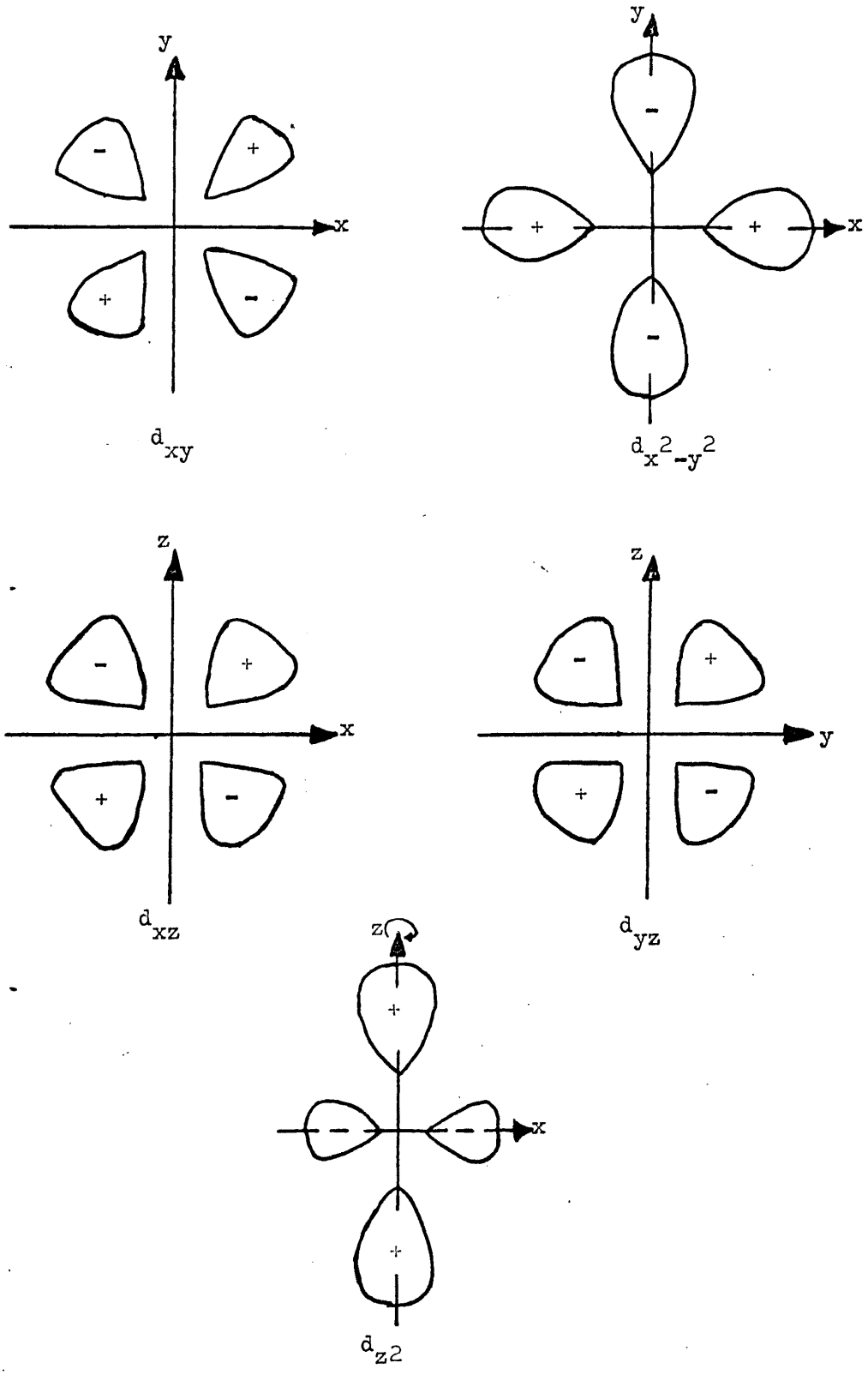

FIGURE 2. The σ bonding orbitals of an octahedral complex involving (a) the $3d_{x^2-y^2}$ orbital and (b) the $3d_{z^2}$ orbital.

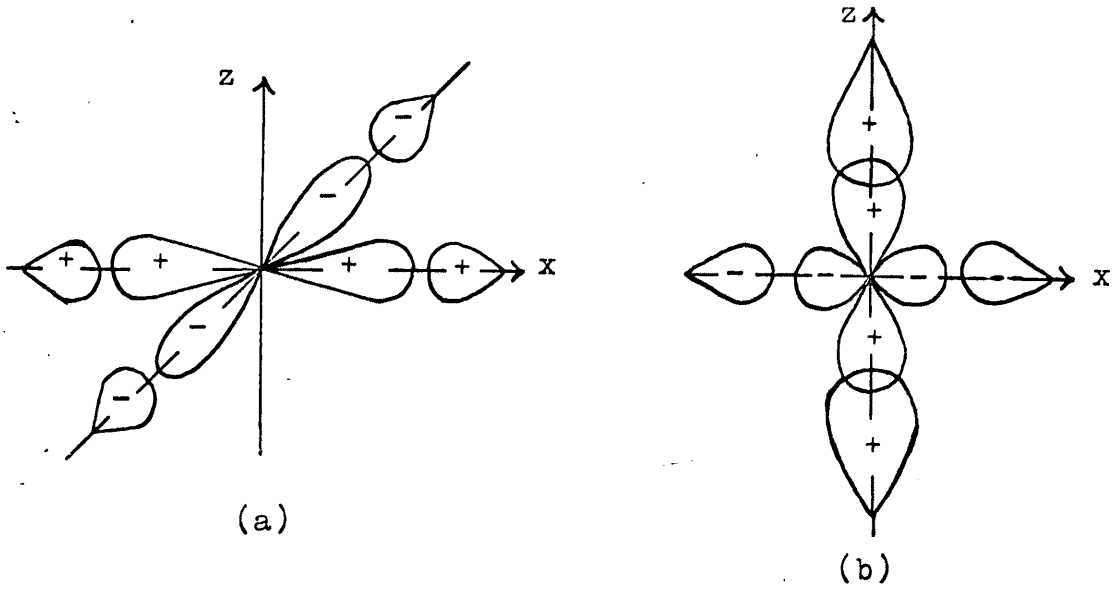

FIGURE 3. The molecular-orbital energy level diagram for an octahedral complex. Note, the actual order of the a_{1g}, t_{1u} and e_g (bonding) orbitals is unknown.

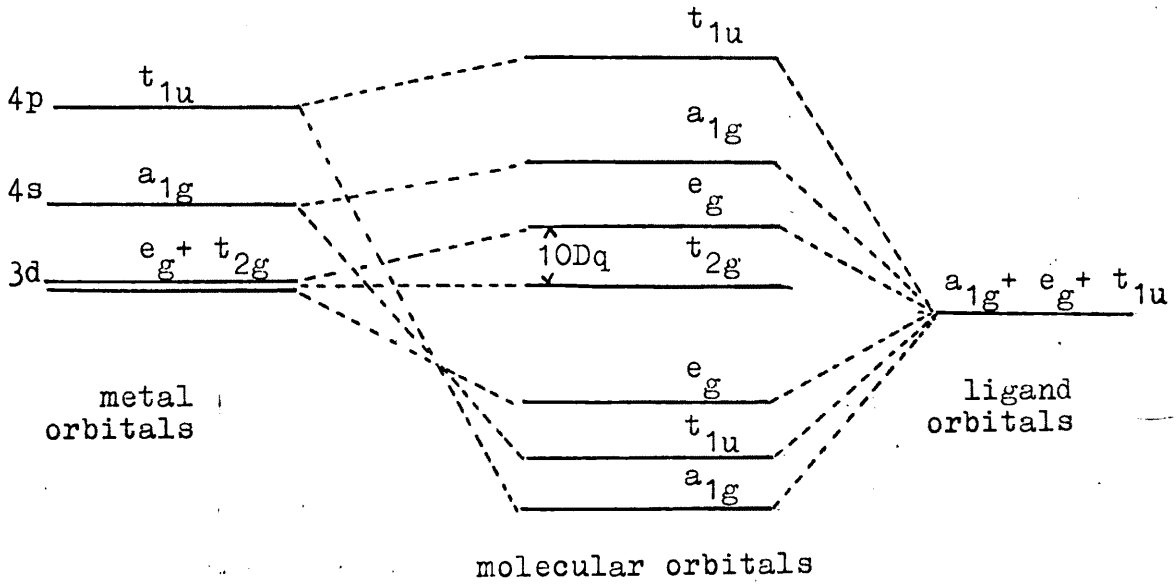

point charges. Modifications to include orbital overlap, orbital overlap plus electrostatic interaction, covalence, etc., have been numerous and not without success, (see for example, 77). The theory derives from the coulombic effect of an octahedral array of six negative ions around the metal ion. The angular distribution of charge in the d_{xy}, d_{yz} and d_{zx} orbitals project between the negative charges of the ligands, whilst that in the $d_{x^2-y^2}$ and d_{z^2} orbitals points directly at the ligands, thereby attaining a higher energy and lifting the degeneracy of the isolated d orbitals of the metal.

There is no net change in energy. Thus, the destabilisation of the $d_{x^2-y^2}$ and d_{z^2} orbitals, known together as the e_g orbitals, is equal to the total stabilisation of the d_{xy}, d_{yz} and d_{zx} orbitals, known collectively as the t_{2g} orbitals. The energy difference between e_g and t_{2g} orbitals is 10Dq, the ligand field strength.

(iv)Electronic Spectra. Almost all Co^{3+} complex ions derive from the octahedral, low spin, $(t_{2g})^6$, arrangement.From this are derived, from coupling of the various characteristic microstates of the free ion ("Russel-Saunders coupling"), net energy terms, whose energy distribution is shown in Figure 4 (29). In the absence of a ligand field the ground state is ^5D and since transitions between Russel-Saunders states of differant multiplicity is formally forbidden and since the selection rule $\triangle L=0\pm1$ applies, non co-ordination compounds of Co^{3+} and similar transition metal ions are only weakly coloured. In the presence of a ligand field the Russel-Saunders energy terms are split into terms of lower symmetry as shown in Figure 4. The ground state for Co^{3+} is usually $^1A_{1g}$, but under the influence of weak ligand fields, which give rise to high spin configurations, e.g. in $[CoF_6]^{3-}$, the ground state is $^5T_{2g}$. One absorption band is expected in the high spin case, ($^5T_{2g} \longrightarrow {}^5E_g$ transition), and two in the low spin case ($^1A_{1g} \longrightarrow {}^1T_{1g}$ and $^1A_{1g} \longrightarrow {}^1T_{2g}$). The Laporte Selection Rule formally forbids even these transitions on the basis that re-arrangments within any quantum shell are not allowed. Mixing of d and p orbitals in transition metal complexes provides the mechanism for the transitions but they are nonetheless extremely weak in comparison to other allowed electronic spectral transitions.

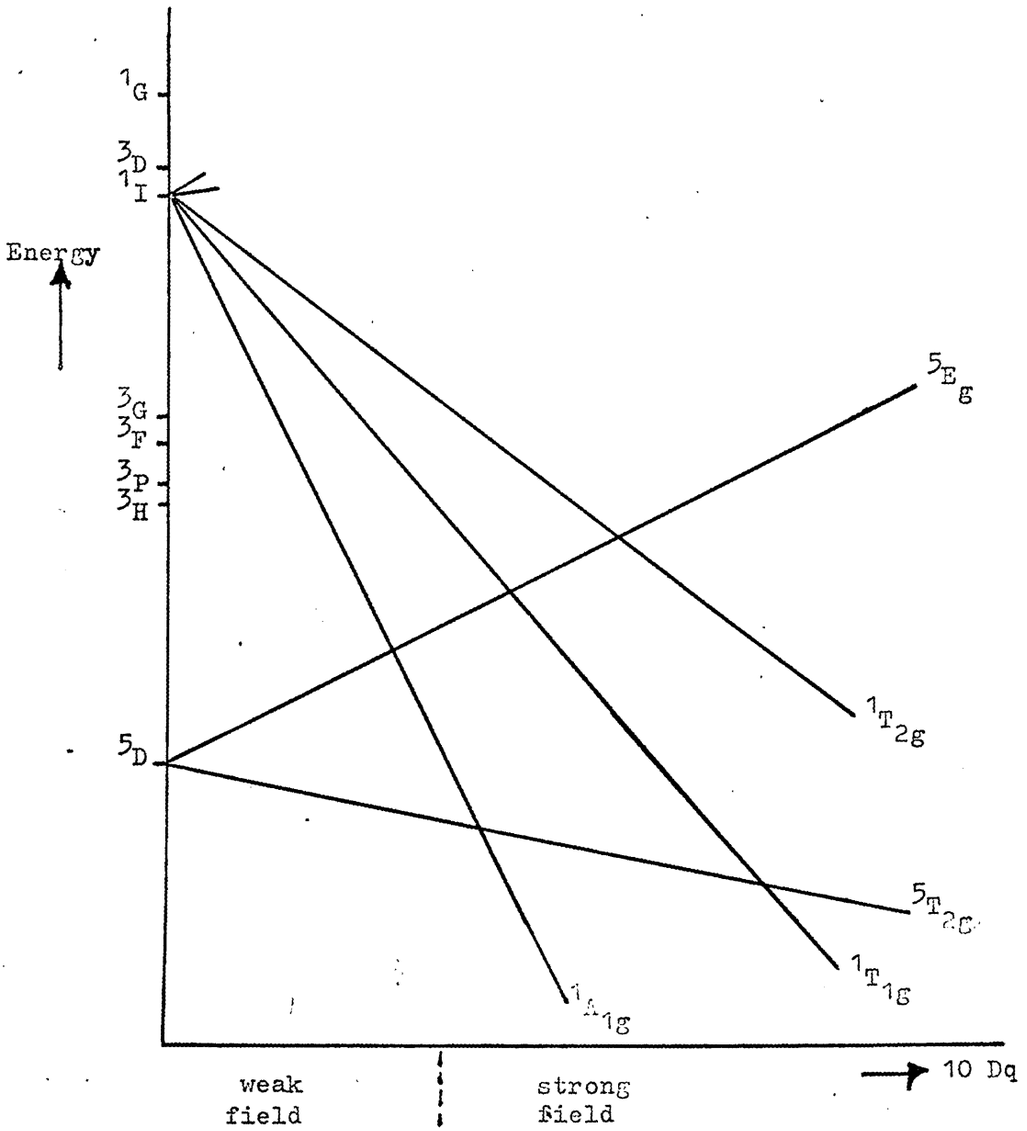

FIGURE 4. Simplified energy level diagram for a d^6 ion in an octahedral ligand field.

Low spin complexes of the type $[CoX_6]^{n+}$ have O_h symmetry and for these, electronic spectra are predicted accurately. This is also the case with complexes of D_3 symmetry, (e.g.$[Co\ en_3]^{3+}$). Lowering symmetry still further, as in the case of cis and trans complexes of the type $[CoA_4B_2]^{n+}$, produces further splitting of the $^1T_{1g}$ level into $^1E_{1g}$ and $^1A_{2g}$ levels. In the case of the cis complex the latter splitting is negligable and one observes only two bands. In the case of the trans complex, however, three bands are found (8) corresponding to the transitions $^1A_{1g} \longrightarrow {}^1E_g$, $^1A_{1g} \longrightarrow {}^1A_{2g}$ and $^1A_{1g} \longrightarrow {}^1T_{2g}$. Ballhausen (7) has conclusively demonstrated the relative splittings of the $^1T_{1g}$ level in cis and trans complexes by considering the tetragonal contributions of each isomer to the crystal field potential.

4.KINETIC APPLICATIONS OF CRYSTAL FIELD THEORY

The observation that high spin octahedral complexes with one, two and more than three d electrons undergo substitution reactions at high velocity whilst those having three d electrons or a low spin configuration react comparitively slowly, was first correlated by Taube (10a). The former class of compounds he called labile, whilst the second were designated inert. The arrangement of d electrons provides the correlating factor. For example, complexes of $Cr^{3+}(d^3)$ and $Co^{3+}(d^6$low spin) react very slowly in solution and are conveniently studied, whilst Mn^{2+} and $Fe^{3+}(d^5$high spin) react rapidly and are not easy to study by conventional means. There is not, however, a necessary correlation between the reactivity of a complex and its thermodynamic stability. Ammines of Cr^{3+}, for example, although no more stable thermodynamically than metal complexes classified as labile e.g. of Sc^{3+} or Ti^{2+}, may be studied easily in solution, whilst the latter complexes would rapidly decompose under identical conditions.

The inertness of such configurations as octahedral d^6 may be easily understood in terms of the effect of an incoming substituting ligand on the charge distribution of the attacked ion. Octahedral high spin d^5, for example, has no special features resisting the approach of a seventh ligand and the reaction is substantially equivalent to a similar reaction of a nontransition metal ion such as Mg^{2+}. If the mechanism is

associative, (see next section), it is enough to bring the incoming ligand to approximately the same distance from the metal as the other six already there in order to achieve equality of bond strength between incoming and departing ligands. On the other hand, in the case of a similar attack on a metal ion of configuration $(t_{2g})^6$, the incoming ligand must force an electron from the t_{2g} orbitals into the e_g, in order to achieve equivalence with the other six ligands. Thus the attack of the seventh ligand is strongly resisted by the complex in order to preserve its previously stable nature.

Basolo and Pearson (10a) have calculated the Crystal Field Stabilisation Energies (C.F.S.E.) of a number of configurations: octahedral, tetrahedral, square and those that may be considered as reaction intermediate structures; pentagonal bipyramidal (associative), and trigonal bipyramidal and square pyramidal (dissociative), in both weak and strong crystal fields and correlated the values obtained with the lability or inertness of various complexes.

For example, using the pentagonal bipyramidal structure as that of the activated complex in the S_N2 substitution mechanism of an octahedral complex, Basolo and Pearson calculated the difference between original octahedral, and activated C.F.S.E. This may be considered to be at least a contribution to the total activation energy, $\triangle$ E. The calculations, which necessarily involve a number of assumptions, for all d configurations in both weak and strong fields, are summarised in Table 2, reproduced from (10a) - Basolo and Pearson. A large value of $\triangle$ E predicts inertness whilst a small value predicts high reactivity. It may be seen from Table 2, that the inertness of Co^{3+} (low spin) and Cr^{3+} is well predicted on this model. Similar relative values of reactivity are obtained if the calculations are made for a dissociative mechanism involving a square pyramidal intermediate.

TABLE 2.

	STRONG FIELD			WEAK FIELD		
System	Octa-hedral	Pentagonal Bipyramid.	C.F.A.E.	Octa-hedral	Pentagonal Bipyramid.	C.F.A.E.
d^0	0	0	0	0	0	0
d^1	4	5.28	-1.28	4	5.28	-1.28
d^2	8	10.56	-2.56	8	10.56	-2.56
d^3	12	7.74	4.26	12	7.74	4.26
d^4	16	13.02	2.98	6	4.93	1.07
d^5	20	18.30	1.70	0	0	0
d^6	24	15.48	8.52	4	5.28	-1.28
d^7	18	12.66	5.34	8	10.56	-2.56
d^8	12	7.74	4.26	12	7.74	4.26
d^9	6	4.93	1.07	6	4.93	1.07
d^{10}	0	0	0	0	0	0

5. MECHANISMS OF SUBSTITUTION REACTIONS IN OCTAHEDRAL TRANSITION METAL COMPLEXES.

Ingold extended his theories of substitution at a tetrahedral carbon atom to substitutions in octahedral transition metal complexes, (for example see 54). Ingold divided the substitution reactions into two classes: the S_N1, (substitution nucleophilic unimolecular), mechanism and the S_N2, (substitution nucleophilic bimolecular), mechanism. In the former, slow rate controlling heterolysis is followed by fast addition of the incoming nucleophile. Thus:

$$M\text{-}X \longrightarrow M^+ + X^-$$
$$M^+ + Y^- \longrightarrow M\text{-}Y$$

In the latter mechanism, the reaction takes place in one bimolecular step in which a new metal-ligand bond is partly formed whilst that of the outgoing ligand is weakened. Thus:

$$Y^- + M\text{-}X \longrightarrow Y.....M.....X \longrightarrow Y\text{-}M + X^-$$

As outlined in the first section (p.6), since the total rate is made up of interplay between individual stages, we would expect the S_N1 mechanism to be independent of Y^-, since the rate determining step does not involve the incoming nucleophile, whilst in the S_N2 mechanism the rate should be dependant on the nucleophilic character of Y^-.

There have been many developments and extensions of Ingold's classification in order to account for mechanisms intermediate between the two extremes. Basolo and Pearson (10a) sub-divided the classification into S_N1 and S_N1 (lim), and S_N2 and S_N2(lim). In the former pair, the limiting case refers to a reaction in which definite evidence for a reduced co-ordination number can be found, whilst the non-limiting case obeys, say, the kinetic requirements of a dissociative process even though no evidence can be found for a reduced co-ordination number. The limiting case in the associative mechanism refers to that case when the rate depends only on bond making, whilst the non-limiting case has equality between bond making and bond breaking.

Langford and Gray (67) remove emphasis both from the molecularity of the reaction and from the nucleophilicity of the substituting ligand. In their scheme the incoming ligand may occupy the appropriate place in an outer co-ordination sphere purely by accident, ('accidental bimolecularity'), energy is transferred rapidly and the new complex may be formed without the new ligand having contributed at all to the activation energy. Thus, stoichiometrically the reaction is bimolecular, but the intimate mechanism, involving energy transfer to attain the transition state, is unimolecular. In the light of these postulations, the following classification was derived.

(i) D, dissociative. Analogous to the S_N1 (lim) mechanism. The intermediate has reduced co-ordination number.

(ii) A, associative. Analogous to the S_N2 (lim) mechanism. The intermediate has increased co-ordination number.

(iii) I, interchange. The leaving group moves from inner to outer co-ordination sphere, as the incoming group moves from outer to inner. The co-ordination number of the first co-ordination sphere is at no time altered. Subdivisions of

the I process are: associative interchange, I_a, where the activation energy is affected mostly by the incoming ligand, and dissociative interchange, I_d, when the incoming ligand has little effect on the activation energy.

It is frequently found that, for anions other than hydroxide, the rate of substitution is <u>independent</u> of the substituting nucleophile. This is not necessarily symptomatic of a D or S_N1 (lim) process, but a consequence of rate determining substitution by water, followed by a fast anation reaction as the co-ordinated water is replaced by a ligand.

Hydrolysis is greatly facilitated by the presence of hydroxide, even in catalytic amounts. Explanation of the second order kinetics observed at first(98,55,56),was made in terms of a bimolecular process.

Mechanisms introduced to explain kinetics differing from second order include: the S_N1 conjugate base (S_N1CB) mechanism, the S_N2CB mechanism,as well as those involving formation of ion pairs and electron transfer.

The S_N1CB mechanism, introduced by Garrick (42) involves deprotonation of an acidic group in the complex and may be used to explain a limiting rate, if one is reached, in concentrated base. The acidic proton may come from an ammine group or any other source containing acidic protons (35). Subsequent steps involve slow heterolysis to give a five co-ordinate intermediate (the D process) and rapid addition of water to give the products. For example:

$$[Co(NH_3)_5X]^{n+} + OH^- \underset{}{\overset{K}{\rightleftharpoons}} [Co(NH_3)_4NH_2X]^{(n-1)+} + H_2O \qquad (A)$$

$$[Co(NH_3)_4NH_2X]^{(n-1)+} \xrightarrow[slow]{k} [Co(NH_3)_4NH_2]^{n+} + X^- \qquad (B)$$

$$[Co(NH_3)_4NH_2]^{n+} + H_2O \xrightarrow{fast} [Co(NH_3)_5OH]^{n+} \qquad (C)$$

If the conjugate base reacts directly with water, this constitutes an S_N2CB mechanism:

$$[Co(NH_3)_4NH_2X]^{(n-1)+} + H_2O \longrightarrow [Co(NH_3)_5OH]^{n+} + X^- \qquad (D)$$

From B $\quad$ Rate $= k[\text{Conjugate Base}]$ $\quad$ (12)

From A $\quad [\text{Conj.Base}] = [\text{Conj. Acid}][OH^-]K$ $\quad$ (13)

Also, $[\text{Total Complex}] = [\text{Conj.Acid}]+[\text{Conj.Base}]$ $\quad$ (14)

Thus, $[Conj.Base] = K[OH^-]([Total\ Complex]-[Conj.Base])$ (15)

Then, $[Conj.Base] = \frac{K[OH^-][Total\ Complex]}{1+ K[OH^-]}$ (16)

Substituting (16) in (12),

$$Rate = \frac{kK[OH^-][Total\ Complex]}{1+ K[OH^-]} \quad (17)$$

When $K[OH^-] \gg 1$, Rate = $kK[OH^-][Complex]$ and therefore, overall second order kinetics are observed. If, however, $K[OH^-] \ll 1$, Rate = k[Complex], i.e. the rate becomes independent of hydroxide and a first order limiting rate is reached. This means that equilibrium(A)lies predominantly to the right, and all the complex is in the form of the conjugate base.

Experimental evidence for conjugate base mechanisms is plentiful. The rate of hydrogen exchange of ammine protons (9), is about 10^5 times faster than base hydrolysis. This provides good evidence in favour of a fast deprotonation equilibrium. Oxygen^{18} studies of $[Co(NH_3)_5X]^{2+}$, (49) where X= chlorine, bromine, iodine support an S_N1CB mechanism. The isotopic fraction of the products of hydrolysis is invariant no matter what the nature of X. When X= fluorine, variation does occur and this was taken as symptomatic of an S_N2CB mechanism. Further hydrolysis studies (22) of substituted cobalt (III) pentammines in competition with added anions, Y^-: $Y=N_3^-$, SCN^-, CH_3COO^-, SO_4^{2-} and PO_4^{2-}, showed the formation of some $[Co(NH_3)_5Y]^{2+}$. The ratio of $[Co(NH_3)_5Y]^{2+}$: $[Co(NH_3)_5OH]^{2+}$ was found to be dependent on the concentration of Y^- and independent of hydroxide and was therefore taken as an indication of an S_N1CB rather than an S_N2CB mechanism, where not only should the rate be independent of hydroxide but dependent on X^-, the leaving group.

Tobe et al (83) have demonstrated the existence of a conjugate base during the course of the base hydrolysis of trans-$[Cod_4\text{-cyclam}Cl_2]^+$, ($d_4$-cyclam = N,N',N'',N'''-tetradeuterio -1,4,8,11 -tetraazocyclotetradecane), in 2,6-dimethylpiperidine /HCl buffer. After about 30% reaction, first the unreacted trans-$[Cod_4\text{-cyclam}Cl_2]^+$ was precipitated as the insoluble perchlorate, followed by the reaction product, also precipitated as trans-$[Cod_4\text{-cyclam}Cl_2]ClO_4$. The extent of hydrogen exchange in both unreacted substrate and product

was determined from the N-H and N-D stretching absorptions. Approximately 20% exchange occured in the unreacted substrate and about 40% in the product. No exchange occured in trans-$[Cod_4\text{-cyclam(OH)(Cl)}]^+$ under identical conditions. The extra exchange in the product must therefore take place as it is being formed. Only in the S_N1CB mechanism does hydrogen exchange accompany base hydrolysis and it must therefore apply here.

Further, the results indicate that reaction(A)(p.20) should be subject to some general base catalysis. The ion pair and associative mechanisms require specific hydroxide catalysis. Reaction with the ionic base, azide, obeys a two term rate law, of which only one can be ascribed to a hydroxide dependence.

Treating the conjugate base mechanism from the Valence Bond viewpoint (81), π overlap occures between the filled p orbitals of the nitrogen of the amido group and either the filled d_{xy} orbital of the metal, or the p_x orbital if the metal shared by the metal and ligand in σ bonding. The overlap represents a repulsive force directed at the ligand cis to the amido group.

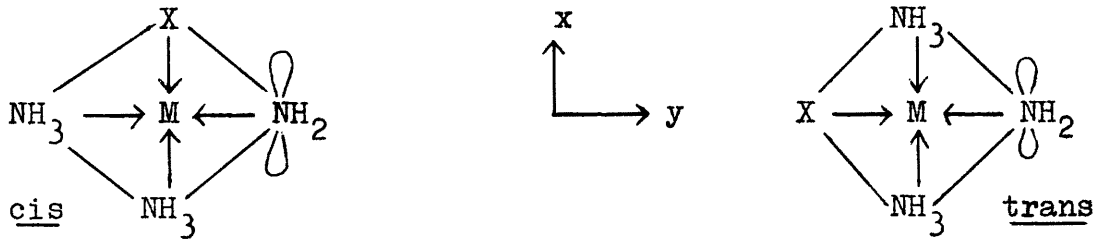

(The ammonias above the plane are ommitted for clarity).

Nordmeyer (75) has used the argument that the amido group in an S_N1CB mechanism is formed preferentially cis to the leaving group, X, to explain product distributions in base hydrolysis reactions of the complex ions: $[Co(NH_3)_5X]^{2+}$ and $[Coen_2LX]^{n+}$. Good agreement is found between observed and predicted results. Pearson and Basolo (80) have previously calculated the fractions of trigonal bipyramidal intermediates produced from cis and trans forms of $[Coen_2LX]^{n+}$ in an S_N1CB mechanism. The following scheme shows the stereochemistry they proposed:

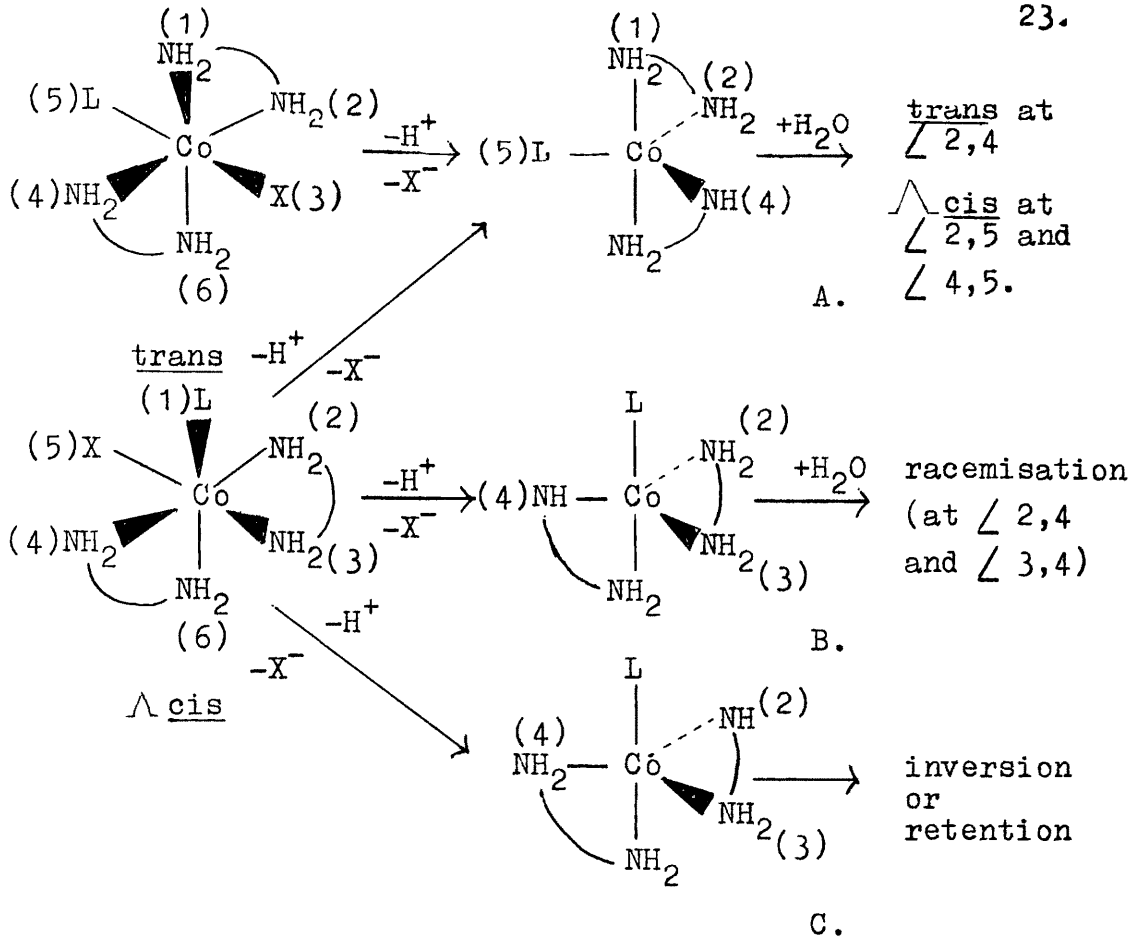

The amido group is most favourably formed in the trigonal plane, (79) allowing strong metal to ligand π bonding. If the ethylendiamine chelate containing the amido group is contained <u>within</u> the trigonal plane, the intermediate C, is assymetric and the two ends of the ethylendiamine ligand are distinguishable. Different amounts of the two <u>cis</u> enantiomers result on addition of water. For instance Λ* <u>cis</u> $[Coen_2NH_3Cl]^{2+}$ gives 24% Δ <u>cis</u>, (calculated, 20%). Otherwise -as in B - the intermediate is symmetrical and only racemic product can result from it. Good experimental agreement is found with predicted results, thereby lending proof to the S_N1CB mechanism. For instance, it is predicted by the above scheme, that the <u>cis</u> isomer must never give less <u>cis</u> product than the <u>trans</u> isomer. This is never violated in the list of reactions compiled by Basolo and Pearson.

The S_N2 ion pair mechanism, analogous to the I_a process, has also been suggested (26), as a result of anomolous kinetics. The hydrolysis of $[Co(NH_3)_5Cl]^{2+}$ and $[Coen_2NH_3Cl]^{2+}$ has been suggested to go by an S_N2 ion pair mechanism.

* Λ uses the notation of Piper(82) to describe right handed chirality about the C_2 axis.

$$[Co(NH_3)_5Cl]^{2+} \underset{}{\overset{K}{\rightleftharpoons}} ([Co(NH_3)_5Cl]^{2+}.OH) \quad (E)$$

$$([Co(NH_3)_5Cl]^{2+}.OH) \xrightarrow[slow]{k} ([Co(NH)_3OH]^{2+}.Cl) \xrightarrow{fast}$$

$$[Co(NH_3)_5OH]^{2+} + Cl^- \quad (F)$$

From this proposed mechanism, and in the presence of a large, 'first-order', excess of hydroxide, the rate law:

$$1/k_{obs} = 1/Kk[OH^-] + 1/k \quad (18)$$

- was calculated. From(18),plots of $1/k_{obs}$ versus $1/[OH^-]$ gave straight line plots. However, the rate law would also fit a dissociative process, K being the acid dissociation constant. K, was found to decrease along the series: $(NH_3)_5$, $(NH_3)en_2$, (NH_3)trien, and this was taken as diagnostic of an ion pair mechanism, since increase in the size of the complex molecule would be expected to decrease the possibility of ion pair formation.

The possibility of an electron transfer mechanism in base hydrolysis has been comprehensively reviewed by Gillard(44). In the case of $[Co(NH_3)_5X]^{2+}$, the proposed rate controlling step is formation of a Co^{2+} intermediate from an ion pair, thus:

$$([Co^{3+}(NH_3)_5X].OH)^+ \underset{}{\overset{slow}{\rightleftharpoons}} ([(NH_3)_5Co^{2+}X]OH\cdot)^+ \quad (G)$$

Esr studies of such reactions have not succeeded in showing the presence of radicals. Some evidence may be furnished in terms of electron affinities of the series: Co^{3+}, Cr^{3+}, Ru^{3+} and Rh^{3+}. Co^{3+} has the highest value (35.5ev) and is observed to react fastest.

Although studies of neither racemisation nor inversion of configuration were undertaken during the course of this project, isomeric changes were followed. For the sake of completeness, Basolo and Pearson's classical treatment of the stereochemical consequences of an S_N1 (lim),(or D) or S_N2(lim),(or A), process (10b), is included in this introduction.

(i)S_N2 or displacement mechanism in the complex type ⌒ cis $M(AA)_2LX$.

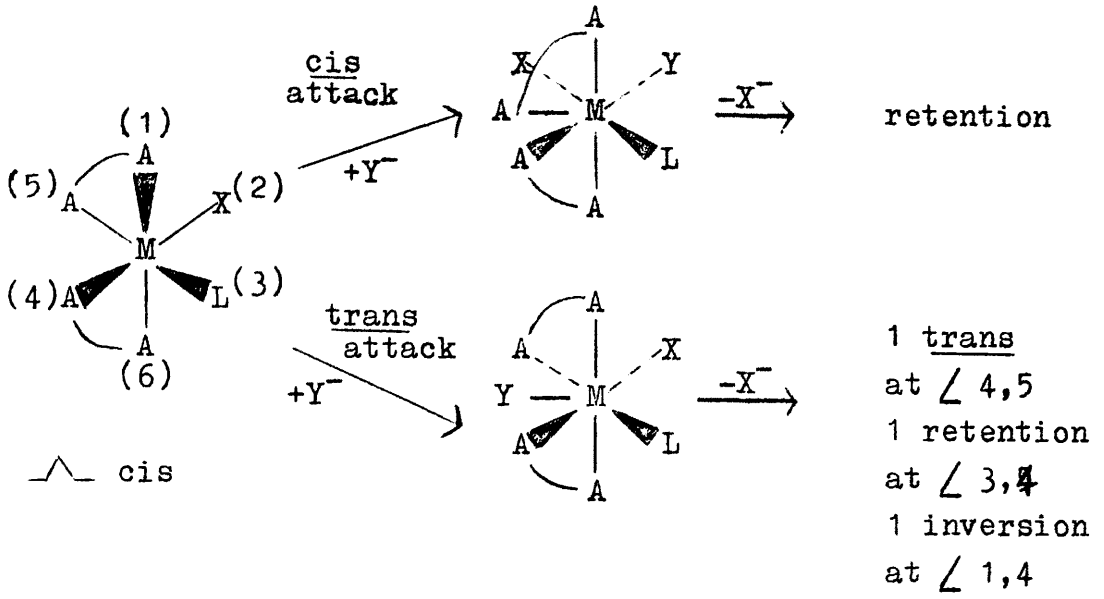

The seven co-ordinate pentagonal bipyramidal intermediate may be formed by attack of the incoming group Y^- adjacent to the departing group, cis attack, or opposite to the departing group, trans attack. The adjacent ligand shifts along the octahedral edge allowing the incoming group to enter. Basolo and Pearson also outline the more likely attack on the octahedral face, to give an intermediate seven co-ordinate octahedral-wedge structure. But, since the stereochemical consequences are identical to those of edge displacement, this is not dealt with here. Cis attack in the above example leads to retention of configuration, (as it always does), whilst trans attack, depending on its direction, may with equal probability give trans product, ⌒ cis product or inversion of configuration. Optical activity is therefore lost either by production of the trans isomer and/or by the equal probability of formation of the two intermediates giving equal amounts of the two cis enantiomorphs.

(ii)The S_N1 or dissociation mechanism - requires the formation of a five co-ordinate intermediate, either a trigonal bipyramid or a tetragonal pyramid. On the assumption that in the case of the tetragonal pyramidal intermediate, the entering group Y^- enters the intermediate in the same position as that vacated by the outgoing group, no re-arrangement takes place during the course of the reaction. This seems likely in

the light of: a) minimum atomic motion being needed to form the new octahedron and b) according to valence bond theory the vacant d^2sp^3 hybrid orbital points directly toward the incoming group. The following scheme outlines the stereochemical changes accompanying this mechanism for the complex type $\angle\!\!\!\backslash$ cis $M(AA)_2LX$.

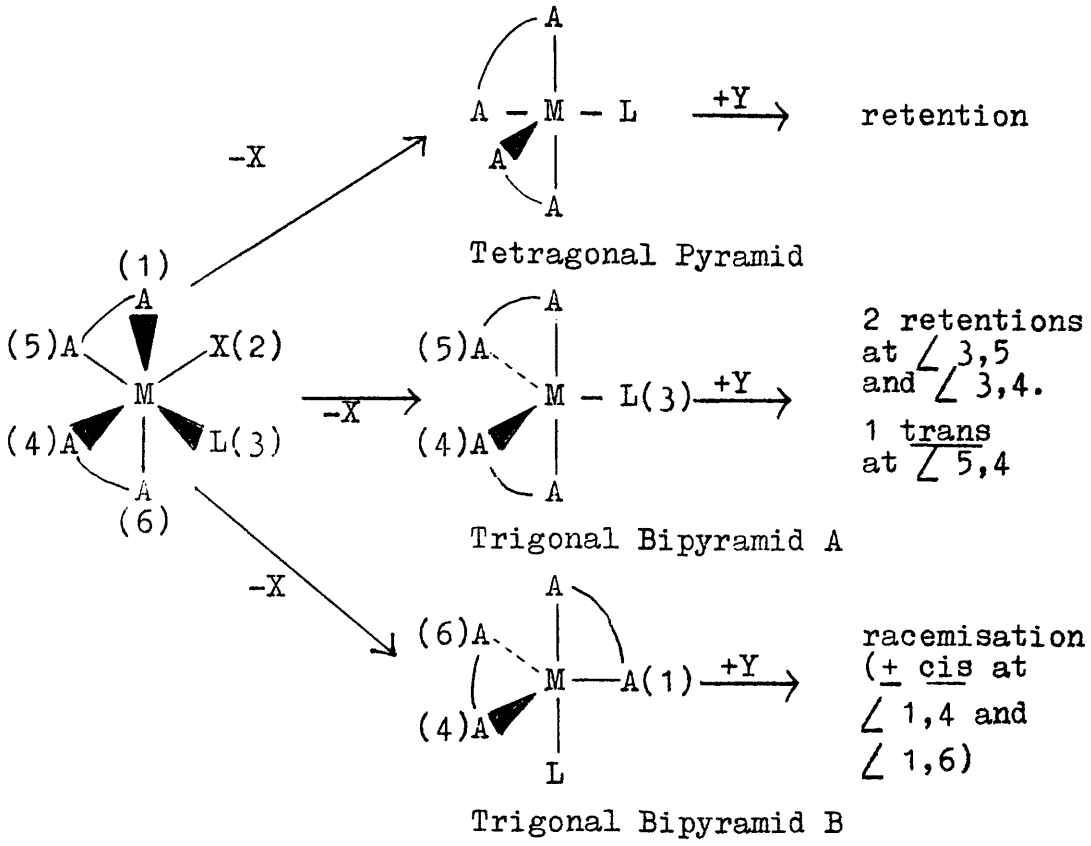

Loss of optical activity in the S_N1 mechanism, may take place via <u>either</u> intermediate, but any retention of optical activity <u>must</u> take place via A. Inversion is not possible - unless the chelate ring in the trigonal plane in B is not symmetrical. This makes B assymetric and capable of reacting with inversion or retention of configuration in unequal amounts. In the S_N1CB mechanism (p.23) where the amido group is formed in the ethylenediamine chelate lying in the trigonal plane, this is the case, permitting a route to net inversion or retention via B (or intermediate C, p.23).
Stereochemical re-arrangements are considerably more numerous in an S_N1 or S_N1CB mechanism than in an S_N2.
Tobe(99) has drawn a comparison between the extent of steric change accompanying aquation in a dissociative mechanism and the entropy of activation. As well as well known <u>trans</u> systems

such as $[Coen_2(Cl)(OH)]^+$, $[Coen_2(NCS)(Cl)]^+$, $[Coen_2N_3Cl]^+$, $[Coen_2Cl_2]^+$ and $[Rhen_2Cl_2]^+$, some trans complexes having the stereoretentive quadridentate ligand, cyclam (1,4,8,11 - tetraazacyclotetradecane), instead of en_2 were also examined. These underwent aquation, as expected, with retention configuration. However, it was only after deriving entropy data that a systematic correlation was obtained. In every case steric change is associated with a higher entropy of activation than is retention of configuration.

Such a correlation did not, however, explain the results of the aquation of the corresponding cis isomers, which react largely without steric change,unless, as had been deemed unlikely, a bimolecular mechanism could be invoked. In order to explain more fully the entropy values obtained, it was proposed that when there are four amine groups cis to the same leaving group, the higher entropy values are diagnostic of a trigonal bipyramidal intermediate and the lower are diagnostic of a tetragonal pyramidal intermediate - which precludes steric change.

Furthermore, it was proposed that the energy difference between the two intermediates is not large. A direct consequence of this pertains to substitution reactions of the cis complex $[Coen_2Cl_2]^+$ in nonaqueous solution (100) and the Hg^{2+} catalysed aquation (23) which take place with stereochemical change. Both had been ascribed a trigonal bipyramidal intermediate to account for the observed change. However, if the energy difference is small, a change of solvent or leaving group might be expected to push the interplay of configuration - deciding factors over to a tetragonal pyramid. Such modifications would therefore react without steric change - as is observed.in aqueous solution.

PART ONE

Pmr Studies of Complexes of Cobalt(III) Containing Co-ordinated Malonate.

INTRODUCTION.

1.NUCLEAR MAGNETIC RESONANCE SPECTROSCOPY (NMR).

Atomic nuclei with odd atomic number, odd mass number, or both possess magnetic moments. For example; ^{1}H(I, the nuclear spin quantum number = $\frac{1}{2}$), has magnetic moment μ = 2.75 magnetons, ^{13}C (I=$\frac{1}{2}$), has μ = 0.70, ^{19}F,(I=$\frac{1}{2}$), has μ = 2.63 and ^{31}P,(I=$\frac{1}{2}$),has μ = 1.13 - are the most common available for study by NMR. The most common application is to protons: proton magnetic resonance,(pmr).
In a magnetic field a magnetic nucleus aligns its axis at quantised angles to the field direction and precesses about that direction. There are (2I + 1) angles available. Thus, for a nucleus with spin $\frac{1}{2}$, there are two such angles. These may be regarded as with, or against the applied magnetic field, H_0. The quantised angles are equally separated by an energy difference of $\mu H_0/I$. On applying an oscillating, (radio frequency), field to the magnetically quantised sample, energy is absorbed, and transitions take place between adjacent levels. The resonance condition:

$$h\upsilon = \frac{\mu H_0}{I} \qquad (19)$$

can be met by fixing υ and varying H_0, or vice versa. In practice the former technique is used. 'Sweep coils' near the pole pieces of a large magnet are used for this purpose. The RF field derives from a coil wound round the sample compartment powered by an RF oscillator. Absorption of energy is detected by a receiver coil with its axis perpendicular to the main field. As the field is swept, the characteristic absorptions are detected by the receiver coil and displayed on a recorder. Signal strength is proportional to H_0 and consequently high fields are used. For instance, 14,000 gauss with a 60 MHz oscillator, or 23,000 gauss with a 100 MHz oscillator.

2.SPECTRUM PARAMETERS.

(i) The Chemical Shift - is the frequency separation of

individual nuclei from a selected reference signal, e.g. tetramethyl silane (TMS) for ^1H. Valence electrons are induced by an applied field to circulate in a plane perpendicular to the field. This results in the generation of an electric current producing a subsidiary field in opposition to the main field, which must then be increased to induce resonance. The extent of this diamagnetic shielding varies from nucleus to nucleus depending on its environment, giving each a characteristic chemical shift. The shift is proportional to field strength and is usually expressed as a fraction, (in ppm), of the field - although it can be stated as a fraction of the oscillator frequency, producing a field independent value. In olefinic systems electrons circulate in the plane of the bond axis and since attached protons are outside the circulation, they experience a reverse induced field, and are shifted downfield. In aromatic systems the effect is enhanced as electrons can circulate over several bonds, and aromatic protons subsequently resonate at even lower fields than olefinic protons.
Steric compression (downfield shift) and conformational rigidity (up or downfield shift), account for long range intramolecular chemical shift effects. The phenomenon is also solvent and concentration dependent.

(ii) Spin-spin coupling. Two nuclei fairly close together may interact via a perturbation of the electronic wave function, each producing a small permanent field at each other. If they are equivalent no effect is observed. If inequivalent, since each has (2I + 1) precession angles, each of which produces a differant magnetic effect on the neighbouring nucleus, each splits the resonance line of the other. Thus, in I, proton a can have energy levels, $+\mu H_0$ and $-\mu H_0$.

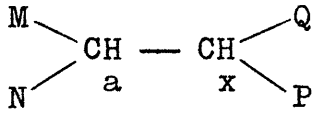

I

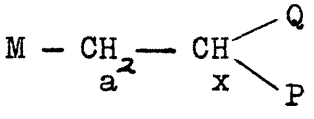

II

$2\mu H_0$ is a very small energy difference and Boltzmann distribution predicts that the levels have almost equal populations, i.e. equal numbers of molecules have the a

proton in each level. Equal numbers of x protons thus experience each of two slightly different fields and so produce two spectral lines of equal intensity - a doublet. The x protons exert an identical splitting effect on the a proton line. The separation of the two lines of each doublet is the coupling constant, J_{ax}. In structure II, the two a protons have combinations of spins: ++,+-,-+,--, the second and third being equivalent. The x proton line is thus split into a 1:2:1 triplet whilst the a line remains as a doublet. Further, three equivalent protons have spin combinations: +++,++-(3),--+(3),---, and thus split adjacent protons into 1:3:3:1 quartets - and so on. Spin interaction falls off rapidly with distance. In benzene, for instance, ortho, meta and para coupling constants are: 6-9 Hz, 1-3 Hz and 0-1 Hz respectively. Whilst quantum mechanics states that spin interactions must take place through bonds, there have been several reports of 'through-space' coupling in the literature. Although notably ^{19}F - ^{19}F and ^{19}F - ^{1}H(74 and 84),several ^{1}H - ^{1}H examples have been reported((6) and p.72).

Spin interaction must take place over a time interval which is long compared to the reciprocal of the coupling constant. Chemical exchange separating a pair of nuclei in a time shorter than this will remove spin coupling. Furthermore, the energy states must be constant over the interaction period. This is why spin coupling involving a nucleus of spin$>\frac{1}{2}$, (Cobalt,I = 7/2, ^{35}Chlorine,I = 3/2), is seldom seen. Relaxation takes place via the electric quadrupole moment and is usually much more rapid than that of any adjacent spin $\frac{1}{2}$ nuclei.

Spectra of spin $\frac{1}{2}$ nuclei are characteristically sharp lined, since the nuclear spin relaxation mechanisms are inefficient. Broadening of lines may be due to several factors, explanation of which is sometimes useful. The presence of paramagnetic material shortens the relaxation time thereby broadening a line. Alternatively, unresolved spin coupling, or time dependent internal rotation and chemical exchange may result in the same effect. An electric quadrupole moment can assist relaxation by interaction with the fluctuating electric field gradient at the nucleus. Hence, ^{1}H - ^{14}N lines are always broad.

Both chemical shift and spin coupling are subject to time averaging. For instance, rapid conformational exchange in which a nucleus has different chemical shifts and coupling constants will result in the spectrum consisting of the time average of the individual parameters. Slow exchange produces superimposed spectra of individual conformers, whilst intermediate rates result in broad-line spectra,(see Section 3). Intermolecular exchange averages chemical shifts but removes coupling, as described above.

3.SPECTRUM NOTATION.

The pmr patterns that arise from structures I and II (p.30) comprise "first-order" spectra. Such simple splitting is only observed when the coupling constant is much smaller than the separation of the resonance positions of the uncoupled protons. The limit to a first-order pattern is reached, according to Bible(13) at $\Delta\partial \sim 6J$. For large values of J (e.g. geminal coupling) higher order patterns result and analysis must frequently be based on formal mathematical grounds. An excellent summary of first, and higher order spectra, containing up to seven individual spins, has been collected by Bishop in Mooney(73).

$$\underset{\underline{a}}{-CH-}\underset{\underline{b}}{CH-}\underset{\underline{c}}{CH_2}$$

III

Structure III and the resulting pmr patterns in Figure 5 demonstrate the multitude of results that may be obtained from a first-order system. Figure 5(i),(ii) and (iii) are conventional splittings by one, two and three adjacent protons respectively. Figure 5(iv) shows the signal of the b proton in III when J_{AB} is greater than J_{BC}, whilst Figure 5(v) shows the result when $J_{AB}=J_{BC}$. Figure 5(vi) demonstrates the special case when $J_{AB}=2J_{BC}$.

First order spectra may equally well derive from coupling to nuclei of spin $> \frac{1}{2}$. For example, the ^{19}F spectrum of NF_3 is a 1:1:1 triplet due to coupling with ^{14}N,I = 1. Coupling causes splitting into (2I+1) components of equal intensity. The

FIGURE 5. First order splitting patterns.

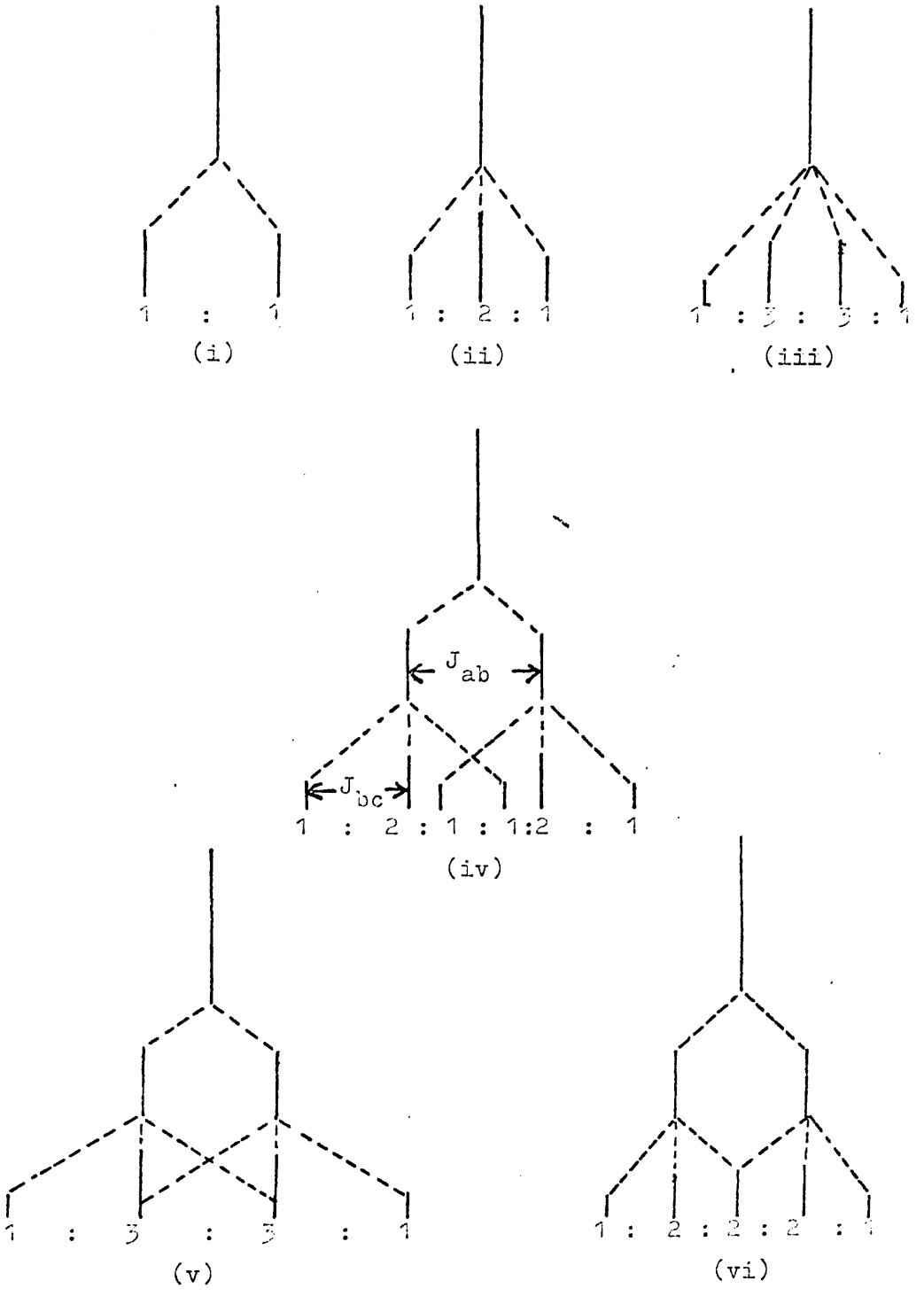

difference from a 1:2:1 triplet arises because the F nuclei 'see' the three orientations of the ^{14}N nucleus with equal probability. The one central component missing is because the component spins within the ^{14}N nucleus cannot be anti-parallel.

When the first order condition $\Delta\delta > 6J$ is not met, the resultant higher order pattern is characterised by three changes in the first order spectrum.(1)Integral ratios of peak intensities become distorted,(2) extra peaks appear, and (3) spacing of peaks becomes unequal. Figure 6A(12) shows the effect of decreasing $\Delta\delta$ in going from a first order A_2X_2 pattern to an A_4 signal, (where the equivalent nuclei show one peak although strongly coupled). Figure 6A(b),(c) and (d) approximate to $[A_2B_2]$ systems, although they may be nearer to $[AB]_2$.

Bible(13) has treated the simplest two spin second order system, the AB system, in exact terms. In the special case, $\Delta\delta_{AB} = \sqrt{3}\, J_{AB}$, the peaks are equally separated and have relative intensities, 1:3:3:1. However, regardless of the value of $\Delta\delta_{AB}/J$, the doublet components are each separated by exactly J_{AB}. Numbering peaks from low to high field 1-4, the relative intensities of peaks 1 and 2, and of 4 and 3 are in the same ratio as the separation of the inner peaks (2-3) to the separation of the outer peaks (1-4).

$$\frac{\text{Intensity of 1 or 4}}{\text{Intensity of 2 or 3}} = \frac{\text{Separation 2-3}}{\text{Separation 1-4}} \qquad (20)$$

If the measured value of J_{AB} is placed on one side of a right triangle, (Fig.6B), and the separation of peaks 1 and 3 on the hypotenuse, the completing side $= \Delta\delta_{AB} \cdot \frac{1}{2}\Delta\delta_{AB}$ from the centre of the pattern then gives δ_A and δ_B.

The total spread of the AB pattern (1-4) is given by:

$$(1\text{-}4) = \frac{2J(\text{Intensity of 2 or 3})}{(1\text{-Intensity of 1 or 4})} \qquad (21)$$

Confusion may arise between a first order quartet, (the A pattern of an A_2X_3 system for instance), and the $\Delta\delta_{AB} = \sqrt{J}_{AB}$ system. Changing solvent may aleviate this difficulty,(since

$\triangle\delta$ is often sensative to solvent, whilst J is not), by destroying $\triangle\delta_{AB} = \sqrt{3}\,J$ equality.

Bible has also pointed out that the inner peaks of a first order pattern tend to 'lean' toward one another,(Figure 6A(a)), in distribution of intensities. This is a consequence of higher order interaction and can be detected even when $\triangle\delta = 20J$. AB patterns, however, show this distortion only in the total ratio of the doublets, and not in the 'inner' signals. This means may also be used to distinguish between first order and regular AB patterns.

Bible proceeds to treat the ABX system in equally exact terms, and various four spin systems in a more qualitative manner.

Precise definition of an nmr system in terms of a notation implying both chemical-shift and coupling parameters has been adopted only in the case of spin $\frac{1}{2}$ spectra, since these account for most high resolution spectra. Bernstein et al in Emsley et al(32) propose the use of different capital letters for each chemical shift. Letters close in the alphabet, (A,B,C), are used if coupling is of the same order of magnitude as the chemical shift difference, whilst widely separated letters, (A,M,P,X), signify large shift separations. Thus structure III,(p.32), in view of the spectra of Figure 5 constitutes an AMX system.

Bernstein's notation, however, did not distinguish between systems having two coupled nuclei co-incidentally having the same chemical shift, whilst still being non-equivalent in the spin coupling sense. Richards and Schaefer(32) propose the use of primes to designate this case i.e. AA', whilst using subscripts to denote nuclei of complete equivalency. However, Haigh(50), in pointing out the cumbersome nature of Richards and Shaefer's notation, proposes a further method based on the use of brackets to enclose any part of the spin system which is equivalent in the spin-coupling sense. A subscript outside the brackets shows the sub-system is symmetry repeated and has couplings across the bracketed halves as well as within each. Thus, an $AA'BB'$ system in Richards and Shaefer's notation becomes $[AB]_2$, whilst A_2B_2,(having complete, spin and shift, equivalence), is denoted $[A_2B_2]$. The absence of brackets remains, as in Bernstein's system, as a general term not implying any symmetry.

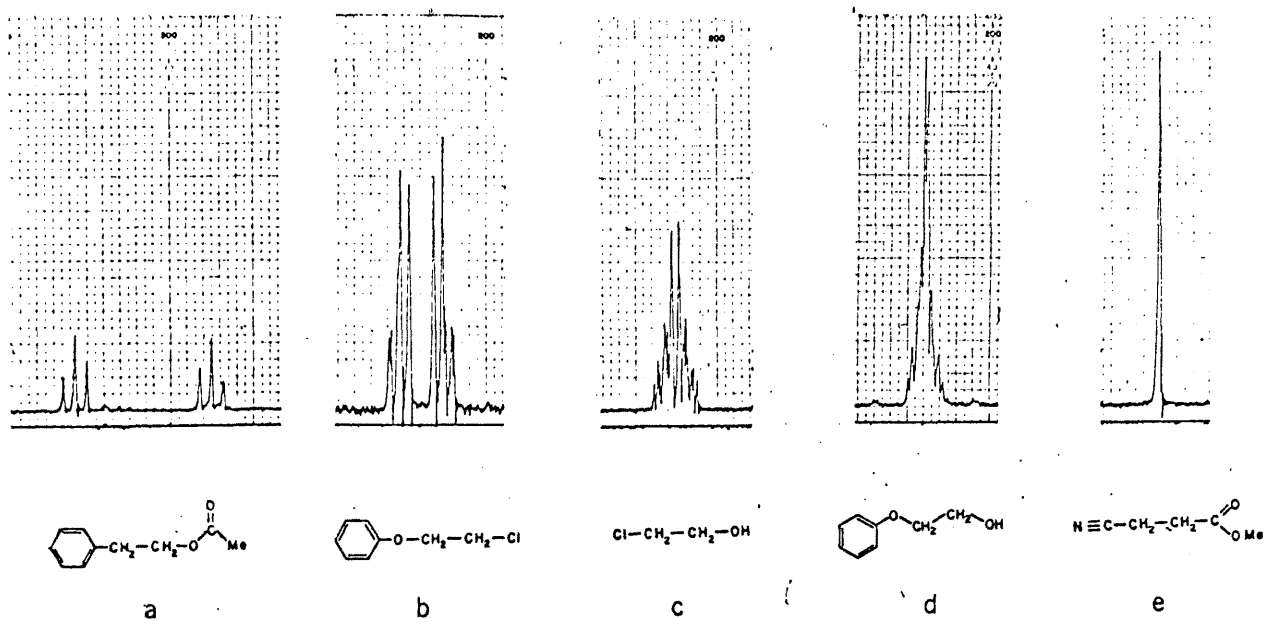

Figure 6A. The effect of decreasing $\Delta\partial_{AB} / J_{AB}$ on the spin-spin splitting pattern of an A_2X_2 system.

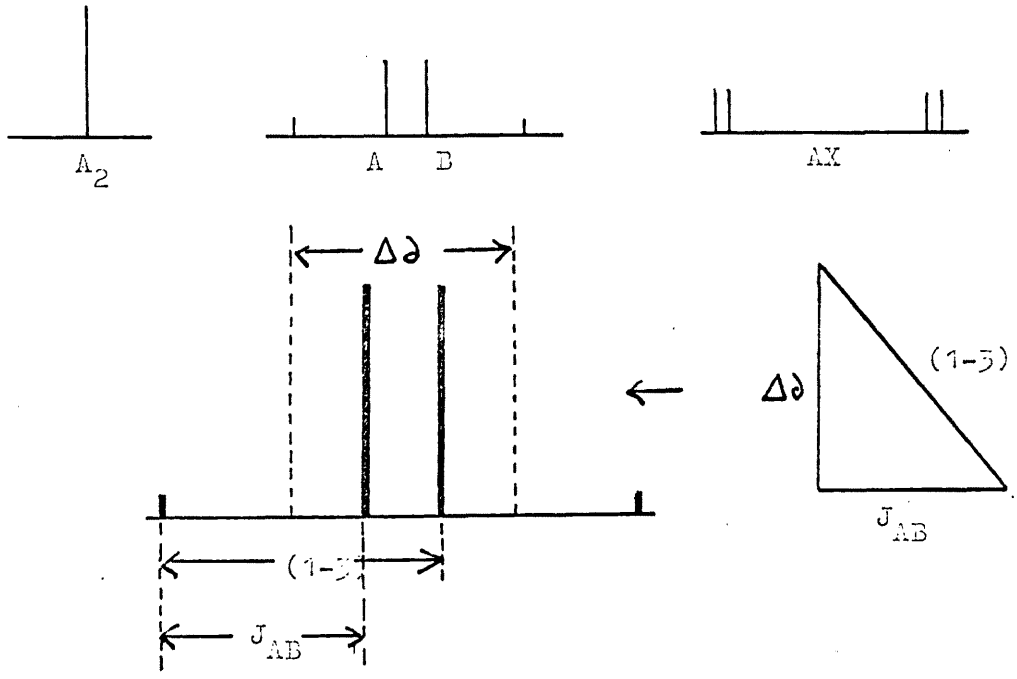

Figure 6B. Analysis of an AB system.

4. NMR IN CONFORMATIONAL ANALYSIS.

Both NMR parameters, the chemical shift and spin coupling, can be extensively applied to conformational analysis.

(i) The use of the chemical shift. Chemical shifts are subject to time averaging, depending on how fast conformers are interconverting compared with the NMR time scale.(Section 2 p.32). In those compounds whose energy barrier to exchange between conformational sites is as low as 5 kcal/mole (ethane, cyclohexanone), exchange is fast compared to the NMR scale even at the lowest temperatures available, and the time average is therefore always observed. However, there are many compounds having additional steric and/or electronic factors that result in the energy barrier between exchange sites being raised and individual conformers have been observed.
In cyclohexane-d_{11}(5), the sharp singlet observed at ambient temperature splits to a sharp doublet at -100°C,($\triangle\partial_{AB}$= 28Hz). The high field peak is due to the conformer having axial hydrogen and the low field peak to that with equatorial hydrogen. H-D unresolved coupling was removed by irradiation at the deuterium frequency. (Saturating rf radiation applied at a particular resonance's frequency will decouple any spin interaction of that nucleus with any adjacent nuclei). The rate constant for the exchange of conformational sites, as measured at the 'coalescence' temperature, T_c, is given by:

$$K = \frac{\partial_{oAB}}{\sqrt{2}} \qquad (22)$$

-where ∂_{oAB} is the <u>maximum</u> shift between spectra of the nuclei in different sites. Above coalescence, the line width may be used as a measure of the rate exchange, using the approximation:

$$K = \partial_{oAB} / 2\partial\nu \qquad (23)$$

-where $\partial\nu$ is the line width due to exchange broadening. Below coalescence the separation of the doublet is used:

$$K = [\tfrac{1}{2}(\partial^2_{oAB} - \partial^2_{AB})]^{\frac{1}{2}} \qquad (24)$$

- where δ_{AB} is the shift difference at any temperature below coalescence.

Application of the Arrhenius equation and the appropriate thermodynamic expressions then give a complete thermodynamic description of the exchange process. Instead of 'blotting out' all the proton signals but one, by using the d_{11} compound, ^{19}F NMR of 1,1-difluorocyclohexane, and higher fluoro analogues, has been used,(107), assisted by an iterative computer programme, to deduce conformational exchange parameters. Extension of these techniques to such systems as: decalin, seven and higher membered rings and nitrogen inversion is summarised by Thomas in Part Two of ref.(73).

(ii) The use of coupling constants. This subject is summarised by Thomas in(73). In conformationally exchanging sites, coupling constants are time-averaged. Anet(4), has expressed the time averaged coupling constants for 3,3',4,4',5,5', -hexadeuterocyclohexanol, an $[AB]_2X$ system, as the sum of the appropriate mole fractions of each conformer's coupling constants. Using the <u>cis</u> and <u>trans</u> 4-t-butyl derivatives, he was able to find the individual AX and BX coupling constants corresponding to those of each 4,4'-d_2 conformer, and hence deduce all the required exchange parameters.

Karplus(59,60), has proposed the following relationships between vicinal coupling constants in saturated systems and the dihedral angle between the coupled protons.

$$J_1 = K_1\cos^2\phi + c \qquad 0 \leqslant \phi \leqslant 90^\circ \qquad (25)$$

$$J_2 = K_2\cos^2\phi + c \qquad 90^\circ \leqslant \phi \leqslant 180^\circ \qquad (26)$$

-where K_1 and K_2 are constants depending on the nature of the C-C bond, and where the c's are constants which are either very small or zero. He later(60), refined the equation:

$$J_{HH'} = A + B\cos\phi + C\cos 2\phi \qquad (27)$$

In saturated,non-strained systems, the $\cos^2$ rule is followed closely for coupling constants over three bonds. Many anomalies have been reported, but these apply in the main to strained and unsaturated ring systems- although the Karplus

equation is by no means always inapplicable to such systems. The equation is invaluable in recognising and predicting coupling constants of protons in individual conformations.

The use of geminal coupling constants in conformational analysis is, as yet, of little value. Pople and Bonther-By(108) have, however, outlined a molecular-orbital treatment of two-bond coupling. According to their theory, the hyperconjugative withdrawal of electrons from the antisymmetric bonding orbital of a $-CH_2$ group by the π electron system of a carbonyl group, (if one is present), is at a maximum when the H-H internuclear axis is perpendicular to the nodal plane of the π system, thus producing a more negative coupling constant. Magnitudes of such geminal couplings have proved useful in recognising either fixed or time-averaged conformations of ring systems containing inequivalent geminal protons and one or more carbonyl groups.

The extension of pmr to conformational analysis of inorganic chelate rings is less well known. There are, however, several reports in the literature. Cobalt(III) complexes are well suited to such studies because of their chemical inertness, lack of ligand exchange and non-occurence of proton-electron interaction. Woldbye(105) has ascribed two pairs of doublets in the pmr spectrum of $[Co(meso\text{-}2,3\text{-diaminobutane})_3]^{3+}$ to axial and equatorial methyl groups split by the adjacent proton.

The most extensive investigations have been into co-ordinated ethylenediamine and propylenediamine.

Here it is pertinent to outline the decisions of the Commission on the Nomenclature of Inorganic Chemistry of the International Union of Pure and Applied Chemistry(57), on octahedral metal complexes.

Sargeson(in 25) designated conformations of the five membered ethylenediamine chelate as k and k', whilst Corey and Bailar Jr(28) in using k and k', employed them in the opposite sense. To avoid these and similar confusions with respect to conformation and configuration, the Commission outlined a nomenclature independent of symmetry and devoid of chemical significance.

The basic principle is that two skew lines, which are not

orthogonal, define a helical system. If one skew line determines the axis of a helix on a cylinder, whose radius is equal to the length of the two line's one common normal, the other line makes up a tangent to the helix. Two such pairs of nonorthogonal skew lines, seen in projection, define right and left handed helicity respectively thus:

Right handed helicity, as in (a), is assigned the Greek letter delta, and left handed, as in (b), is assigned lambda. Capital letters Δ and Λ refer to configuration and small letters δ and λ to conformation.

Configuration. The rule is that the two donor atoms of a chelate ring define a line and two such lines define a helix, i.e. for a cis-bis-bidentate complex:

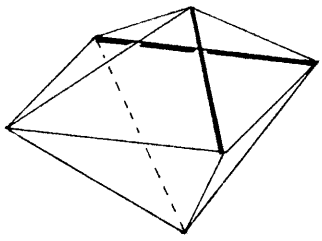

-where the edges spanned by each chelate ring are heavily lined. One line is the axis of the helix and the other the tangent at the normal. The tangent describes a right handed helix and the configuration is designated Δ .
With tris-bidentate complexes, any one of three possible pairs of chelate rings defines the configuration as for cis-bis-bidentate complexes.

Conformation. Here the helix is defined by the two skew lines, (a) joining the donor atoms and (b) joining the atoms adjacent to the donor atoms. The conformation is thereby described as having right (δ) or left (λ) handed helicity with respect to the axis defined by one of the chosen lines.

Note. Where both atoms adjacent to the donor atoms are above the plane determined by the metal and donor atoms, but still form skew lines, the nomenclature applies. It does not apply to nonhelical chelate rings defined, for example, by a five membered ring in its 'envelope' form, or a six membered ring in either 'boat' or 'chair' forms, i.e.

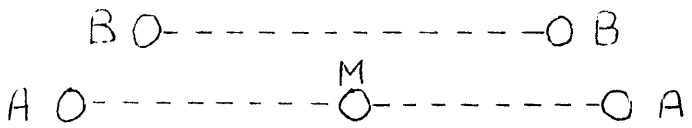

This does not necessarily preclude chirality. Once chemical nature is restored to the chelate, i.e. a means of distinction, the complex may be found to be chiral.
The notation of Piper(82) which refers chirality to a symmetry axis and that of Liehr(66) which applies to conformation were found to be analogous to the nomenclature of the Commission.
Sargeson's k conformation and Corey and Bailar's k' are designated as having right handed helicity, and the k' and k forms as describing a left handed helix.

The C protons of $[Coen_3]^{3+}$ are expected to show three equivalent, 24 line,$[A_2B_2]$ patterns, but instead show a single broad resonance, half width 21 Hz narrowing to 18 Hz when the $-NH_2$ groups are deuterated. Cooling to $-39^{\circ}C$ in D_2O/D_2SO_4 produced no resolution of the band but did produce further broadening. Sargeson in Carlin(25) attributes the observed spectrum to (a) rapid conformational exchange and (b) $\sim$ 30% of the $\partial\partial\lambda$ configuration that is expected to be present, causing complex overlap of the $[A_2B_2]$ pattern.
Complexes of the type $[Coen_2X_2]^{n+}$ have C_2 symmetry, the two fold axis being in the plane of the cobalt and the two X groups. This results in the $-CH_2CH_2-$ groups being equivalent, providing the cobalt-ethylenediamine rings have the same conformation. If the conformers are rigid (k,inversion $< 10\ sec^{-1}$) an ABCD pattern (56 lines) would result. An averaged conformation would be expected to give an $[A_2B_2]$ pattern since each $-CH_2$ group would experience a different averaged field.
<u>cis</u>$[Co(en)_2(OH_2)_2]^{3+}$ is notable for the resolution of its

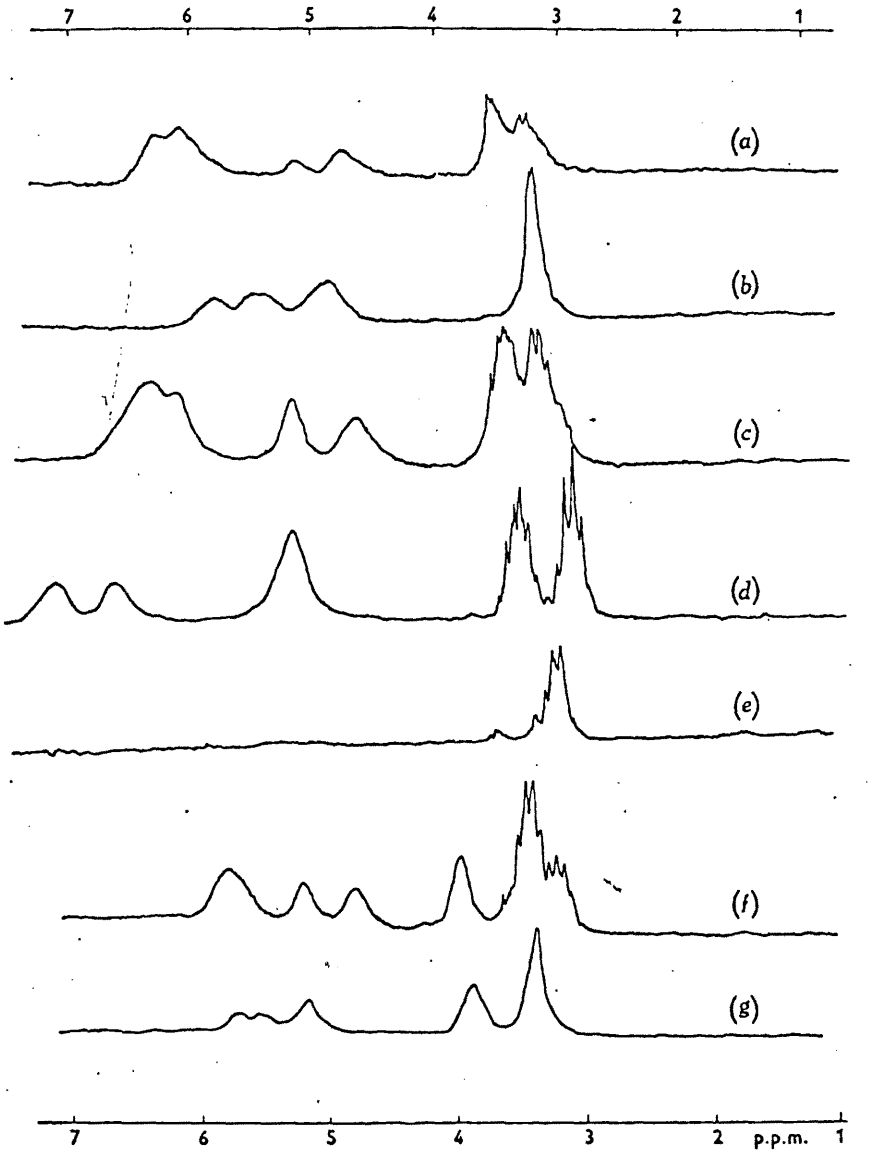

Figure 7. 100MHz pmr spectra of:
(a) cis-$[CoCl_2en_2]Cl$; (b) cis-$[Co(NO_2)_2en_2]Cl$;
(c) cis-$[CoCl(H_2O)en_2]SO_4$; (d) cis-$[Co(H_2O)_2en_2](ClO_4)_3$;
(e) cis-$[Co(N_3)_2en_2]ClO_4$(in D_2O);
(f) cis-$[CoClNH_3en_2]Br_2$;
(g) cis-$[Co(NH_3)_2en_2](ClO_4)_3$ in 1.8M D_2SO_4.

C-proton signal, into something showing good resemblance to an $[A_2B_2]$ pattern (Figure 7(d)). Resolution is attributed to retention of conformation, which in turn is attributed to the aquo ligands since, in general, cis-$[Coen_2X_2]^{n+}$ complexes do not show splitting of the C-proton signal. Buckingham et al(19) suggest that resolution of the $-CH_2CH_2-$ signal arises from different averaged fields rather than slow conformational exchange. It is conceivable that hydrogen bonding to the $-NH_2$ groups could produce both slow conformational exchange and a different averaged field at each pair of C-protons. Figure 7 shows a selection of $[Coen_2X_2]^{n+}$ spectra from(19).

Mixed ethylenediamine (en), propylenediamine (pn) complexes show evidence for the presence of more than one conformation in the N-proton region. For complexes containing (-)pn, all D isomers give two N-H signals, whereas the L isomers show no splitting. Since L(-) and D(-), $[Coen_2(-)pn]^{3+}$ can exist in only one configuration, this splitting cannot be attributed solely to a mixture of geometrical isomers but is instead attributed to a less stable pn conformer present in the D(-) pn complexes. The racemate, L(-)$[Co(-)pn_2(+)pn]^{3+}$. D(-)[Co (+)pn_2(-)pn]$^{3+}$, where each ion contains both proposed conformers, shows two N-H bands, thereby confirming the assignment. (+)$[Coen_3]^{3+}$ also shows two poorly resolved N-H bands and this has been attributed to the $\delta\delta\lambda$ form as well as the more favoured $\delta\delta\delta$ conformer,(19).

$-NH_2(CH_2)_2NH_2$ - chelate rings show excellent resolution into recognisable $[AB]_2$ patterns when part of a multidentate aminocarboxylate ligand such as $EDTA^{4-}$(ethylenediamine - N,N,N',N' -tetracetate)(65)- see Figure 8, II. Here, the configuration about the N atoms cannot invert without changing all four acetate bridging positions, thus holding the ethylenediamine ring conformation rigid.

Of spectra in the series $[Coen_2acac]^{2+}$, $[Coen_2tfac]^{2+}$ and $[Coen_2hfac]^{2+}$,(where acac = acetylacetone, tfac = trifluoro-acetylacetone and hfac = hexafluoroacetylacetone), only the last named compound shows any fine structure of the $-(CH_2)_2$ signal(19).

Conformations of the six membered malonato ligand, where only methylene protons are available to respond to pmr, are discussed later in this work.

5. THE USE OF DEUTERATION IN PMR SPECTROSCOPY.

Deuterium, ^2H, has no magnetic moment and therefore deuteration of sufficiently labile protons results in the collapse of their pmr signals and subsequent identification.
The technique is frequently used as a diagnostic tool in both organic and inorganic pmr spectroscopy.
Deuterated solvents:- D_2O, d_6- dimethyl sulphoxide, d_6- benzene, d- chloroform, are used extensively as 'window' solvents in pmr spectroscopy. Deuteration may be used to 'block out' all signals except the one under study before recording the spect-rum, e.g. in the determination of conformational exchange rates of d_{11}-cyclohexane, (see section 4.p.37), or is allowed to proceed during several spectrum runs, enabling acidic protons, such as those of an ammine, to be readily identified. The rate of deuteration itself may provide evidence as to the identity and environment of a particular proton.

Good evidence for the operation of a conjugate base mechanism has been found(9) by demonstrating that hydrogen exchange in basic solution proceeds at a rate $\sim 10^5$ times faster than base hydrolysis.
Recently, the rate of hydrogen exchange at an assymetric nitrogen centre has been extensively used(48,51,20,21) to demonstrate that the configuration about the nitrogen is retained most of the time that the proton is off the quaternary nitrogen site. Such complex cations as:.$[Co(NH_3)_4(Nmeen)]^{3+}$ (Nmeen = N methylethylenediamine)(20), $[Co(NH_3)_4(Nmegly)]^{2+}$ (where Nmegly = N methylglycinate)(51), $[Pt(Meen)(NH_3)_2]^{2+}$ and $[Pt(Meen)(phen)]^{2+}$(48), $[Pt(Meen)(en)]^{2+}$(21) and the octahedral Pt(IV) complex $[Pt(Meen)(en)Cl_2]^{2+}$(21), all have as their sole source of optical activity the chelate N atom. Both racemisation and hydrogen exchange are found to follow the rate law:

$$\text{Rate} = k_2[\text{complex}][OH^-] \qquad (28)$$

- and since k_2 for the deuteration, compared to k_2 for the racemisation is found to vary between 10^2 and 10^5, this was taken, in all cases, as a strong implication that since the

hydrogen may come off the assymetric atom without inversion of configuration about the atom, this is why such metal complexes can be resolved into enantiomers, having a quaternary nitrogen as their source of chirality, in the first place. It was previously thought(88) that although such N-atoms lack the lone pair of electrons that cause rapid inversion about trigonal nitrogen atoms, the acidity and lability of the amino hydrogen would preclude any attempts to resolve compounds containing them.
Buckingham et al(20) propose two possibilities, (a) a deprotonation equilibrium and (b) an ion pair equilibrium, which can lead to a common intermediate, to account for the racemisation mechanism.
The deuteration itself was followed by monitoring the decoupling of the $NH-CH_3$ proton's spins as deuterium replaced hydrogen on the amino nitrogen.

Since 1965 there has been a succession of reports in the literature concerning the use of deuteration of α- hydrogen atoms in tetra-,penta- and hexadentate aminocarboxylate complexes as an aid to assignment of these proton's signals. Williams and Busch(104) first demonstrated the ability of a central metal ion to increase the acidity of ligand α - hydrogens by noting the deuteration of such protons in Co(III) aminocarboxylate complexes in alkaline D_2O.
Co-ordination to a metal ion localises the carbonyl group that was previously delocalised over two O-C-O bonds in the unco-ordinated acid, thereby increasing the acidity of the α-hydrogens. The situation is analogous to that in β-keto and carboxylate esters where the α-hydrogens can be removed by a base such as ethoxide and can effect nucleophilic displacement as carbanions.
Deuteration may also occur readily in acidic D_2O by a keto-enol mechanism(97).
Although primarily concerned with Co(III) there have been reports of pmr spectra of aminocarboxylate complexes of rhodium(III), palladium(II) and platinum(II)(89 - 92).
Terrill and Reilley(97) have demonstrated that the acid-catalysed deuteration of 'out-of-plane' glycinate α-hydrogen atoms in $CoCyDTA^-$, H_A and H_B in Figure 8, I, where CyDTA =

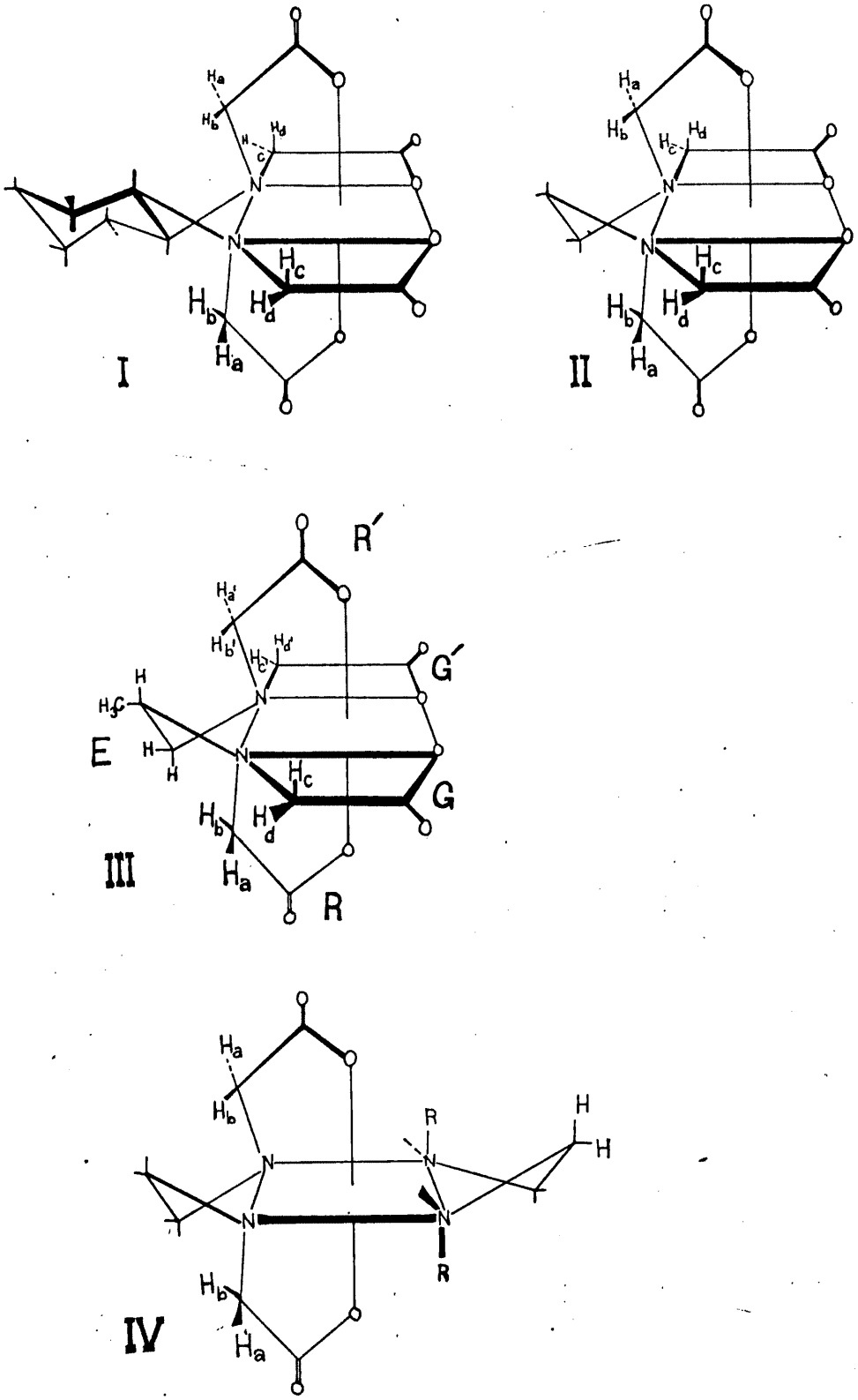

Figure 8. Co(III)-aminocarboxylate chelates.
I.Co(III)CyDTA$^-$ II.Co(III)EDTA$^-$ III.Co(III)PDTA$^-$ and
IV.Co(III)EDDA(diamine)$^+$.

trans -1,2 cyclohexanediamine - N,N,N',N'- tetracetate, is stereospecific. The high field portion of the spectrum diminishes in intensity approximately 10 times faster than the low field portion. The stereospecificity was ascribed to sheltering of H_B from solvent attack by the diamine 'backbone' of the ligand, and has been shown to always occur in complexes of this nature.

The complex is symmetrical about the C_2 axis and consequently each pair of 'out-of-plane' and 'in-plane' glycinate α-protons are equivalent. Each geminal proton, however, experiences a different field and an AB pattern for each of the two equivalent pairs results. Assignment of H_A and H_B was made on the strength of the deuteration reaction stereospecificity. The upfield signals were assigned to H_A and the downfield signals to H_B. The theory of steric compression(6) and orbital interaction(97) was invoked to explain this unexpected distribution of the chemical shifts.

Random co-ordination of d_2-$CyDTA^{4-}$ was used to assign H_C and H_D. This was laborious and ambiguous and a more accurate method of assigning 'in-plane' glycinate protons has recently been evolved(96),which will be dealt with subsequently. There have been no reports to date concerning the deuteration of 'in-plane' α -protons in Co(III) complexes. Terrill et al(33) have, however, observed that the deuteration of 'out-of-plane' glycinate methylene protons in paramagnetic nickel(II) complexes of PDTA, EDTA and CyDTA is 10^4 times faster than that of 'in-plane' groups.

Work of this nature has recently been summarised by Legg et al(63). Subsequent to the summary of Legg et al, Sudmeier et al (93)have made extensive use of the stereospecific deuteration of 'out-of-plane' glycinate protons, redox scrambling of 'in-plane' and deuterated 'out-of-plane' glycinate rings and weak field irradiation, (spin 'tickling'), at 100 MHz to conclusively assign all glycinate protons in $CoPDTA^-$, Figure 8,III, (PDTA = propylenediamine, N,N,N',N'- tetracetate) $CoCyDTA^-$, Figure 8,I and $CoEDTA^-$, Figure 8,II (EDTA = ethylenediamine, N,N,N',N'- tetracetate.

Redox scrambling primarily involves electrolytic reduction of the complex containing partly deuterated 'out-of-plane' glycinate protons. The resulting Co(II) compound being extremely labile

interchange 'out-of-plane' and 'in-plane' rings, causing mixing of H_A with H_C, and H_B with H_D. Subsequent re-oxidation then readily enables H_D to be recognised as having mixed randomly with the decoupled H_B.

Weak field irradiation causes further splitting into submulti-plets. For instance, 'tickling' the highest field signal of an AB quartet splits the lowest field signal of that quartet into a broad doublet and the next to lowest into a sharp doublet. Using this technique, Sudmeier et al separated the 16 peaks comprising 4 AB patterns from the propylendiamine 'backbone' signals in $CoPDTA^-$. In this complex the C_2 axis is destroyed by the presence of methyl group on the propylen-diamine backbone. Each set of protons from H_A to H_D is thereby rendered inequivalent, (see Figure 8, III).

However, since H_A was deuterated more rapidly than $H_{A'}$ and H_B faster than $H_{B'}$, assignment of 'out-of-plane' protons was accomplished wholly on the evidence of stereospecific deuteration. Assignment of H_C, $H_{C'}$, H_D and $H_{D'}$ was accomplished by redox scrambling of, (i) H_A and (ii) $H_A + H_{A'}$ deuterated 'out-of-plane' protons. H_C was shown to occur downfield of H_D.

$CoEDTA^-$ was much easier to assign. Here the C_2 axis is restored and only two pairs of geminal protons are seen, as two AB quartets. Stereospecific deuteration alone enabled assignment to be made, although 100 MHz was needed because of the small shift differences involved at 60 MHz. H_C and H_D were assigned by analogy with $CoPDTA^-$.

$CoCyDTA^-$ proved simplest of all, since no 'backbone' signals occur in the vicinity of the two AB patterns. H_A was allowed to go to 90% deuteration, (enabling assignment of H_A and H_B), which results in the growth of a decoupled H_B singlet between the downfield pair. The solution was then redox scrambled, thereby randomising D_A with H_C and H_B with H_D. The singlet that occured on reoxidation, between the high field pair of the H_CH_D AB pattern enabled the assignment of H_D to high field and H_C to low field. This confirmed Terrill and Reilley's earlier assignment(97) but was much more convenient than the technique they used(p.47).

Another observation to arise from Sudmeier et al's paper was

the diagnostic ability of the magnitude of the gylcinate protons geminal coupling constants. J_{AB}= -18 Hz for 'out-of-plane' rings and J_{AB}= -16 Hz for 'in-plane' rings. (The absolute sign of the coupling was made by analogy to aliphatic $-CH_2$ groups in similar compounds. See for example(16)). Pople and Bonther-By's M.O. treatment of geminal coupling was invoked here(see p.38). Since 'out-of-plane' glycinate groups are more planar(102) than 'in-plane' groups, according to Pople and Bonther-By, the 'out-of-plane' glycinate ring should have the more negative coupling constant, since the H-H internuclear axis is more perpendicular to the nodal plane of the carbonyl π system. The coupling constants obtained were always in agreement with the assignments made by other means, thereby enabling future assignment of 'in-' or 'out-of-plane' glycinate or similar rings merely by noting the coupling constants of any inequivalent, geminal protons contained within them.

6.THE STEREOSPECIFIC DEUTERATION OF THE α-HYDROGEN ATOMS IN TRANS- Co(III)EDDA(en)$^+$.

Quantitive assessment of the acid catalysed deuteration of 'out-of-plane' glycinate protons in Co(III)CyDTA$^-$, Figure 8, I(97) and of the base catalysed reaction in Co(III)EDTA$^-$, Figure 8, II(104), has been made. The work of Sudmeier and Occupati(93) on trans-CoEDDA(en)$^+$, Figure 8,IV, since the mechanisms and kinetics of previous workers were invoked(97, 104), and since the complex contains only 'out-of-plane' glycinate rings, is,however, the most comprehensive in making a comparison with [Comal$_2$en]$^-$.
The compound and its pmr spectrum were first reported by Legg and Cooke(64) although several assignments were tentative.
A series of Sudmeier and Occupati's spectra taken at varying intervals during the course of the acid catalysed deuteration are reproduced from(93),in Figure 9. The reaction is stereospecific and the decoupled singlet, d, emerges between the upfield pair. Therefore, the factor shielding H_B from solvent attack stereochemically, is also responsible for the larger diamagnetic shielding of H_B, i.e. the diamine 'backbone' of the aminocarboxylate ligand. The high field position of H_B is not found in the analogous CyDTA^{4-}, PDTA^{4-} and EDTA^{4-} complexes. Here, the decoupled singlet of the 'out-of-plane'

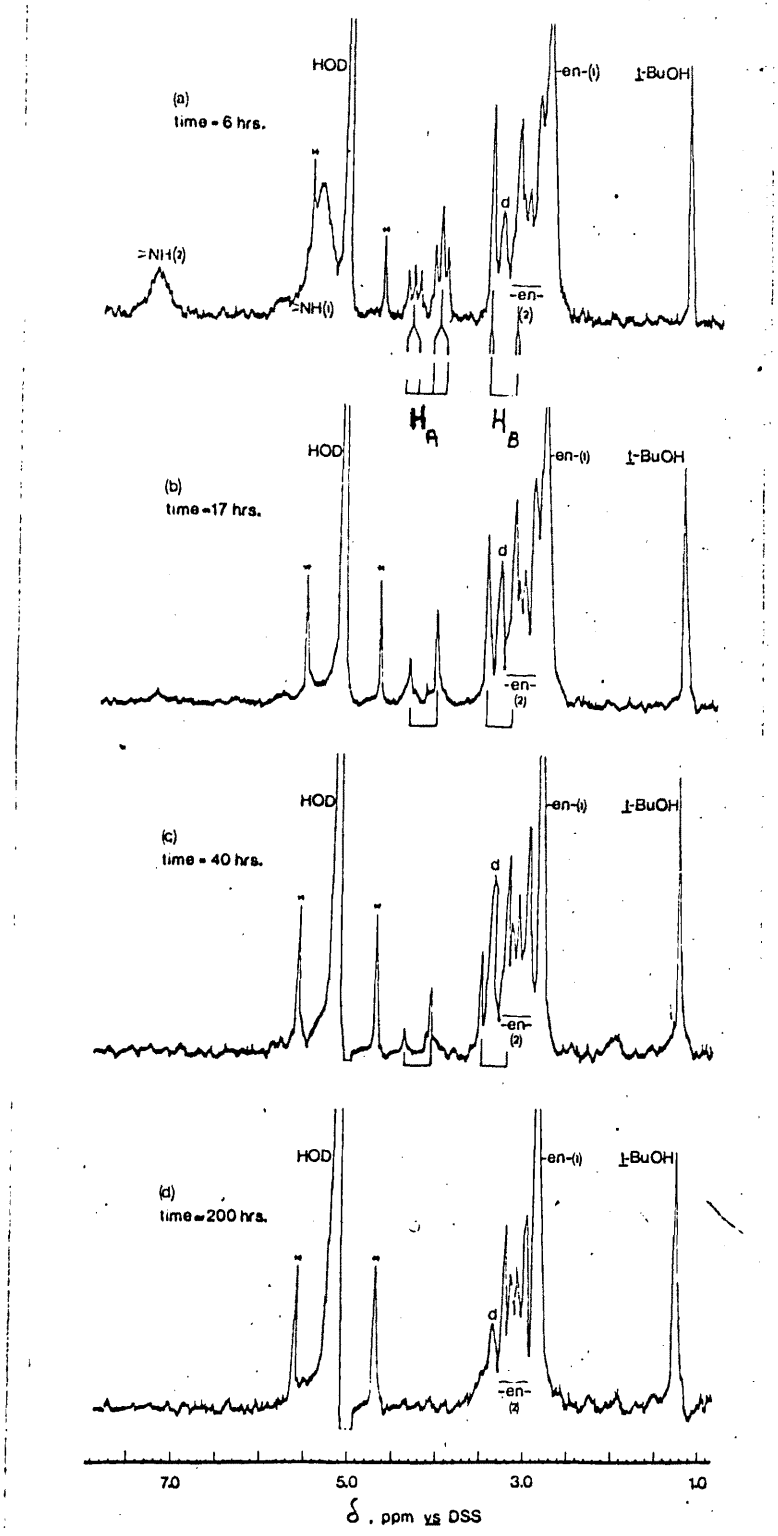

Figure 9. Pmr spectra demonstrating the stereospecificity of the acid-catalysed deuteration of trans-[CoEDDA(en)]$^+$.

glycinate protons emerges between the low field pair. The theory of stereochemical compression(6) was invoked to account for a large downfield shift of H_B, whilst still allowing it relative inaccessibility to solvent. Applying the Karplus equation,(p.38), to H-N-C-H coupling, Sudmeier et al conclusively assigned the downfield pair, (J_{NHCH}= 8 Hz), in CoEDDA(en)$^+$, to H_A, and the high field pair, (J_{NHCH}= < 1 Hz), to H_B - Figure 9,(a).

The stereospecific deuteration in acidic and in basic media, (the complex is insusceptible to hydrolysis in either), was monitored by the loss in intensity of the downfield portion of the AB pattern, (H_A), Figure 9,(b), and the eventual loss in intensity of the decoupled singlet,(H_B), Figure 9,(c) and (d).

In acidic D_2O the deuteration was carried out at about molar acid and 95°C for the complexes Co(III)EDDA(en)$^+$, CoEDDA(dmen)$^+$ and CoEDDA(deen)$^+$, (where dmen = N,N'- dimethylethylenediamine and deen = N,N' - diethylethylenediamine). When far from equilibrium, the reaction, in all cases, was found to follow the rate law:

$$-\frac{d[CoYH_A]}{dt} = k_{D(Acid)}[CoYH_A][D_3O^+] + k_{D(Base)}[CoYH_A][OD^-] \qquad (29)$$

- being first order in complex, acid and base. A similar equation applies to the subsequent deuteration of H_B. In acidic D_2O, the base catalysed term in equation (29) is negligable and the reaction proceeds according to a rate law given by the acid catalysed term only. The rate data and stereospecificity in acidic medium are given in Table 3.
k_D applies to the deuteration of H_A, and k_D^d,(where 'd' denotes 'decoupled'), to that of H_B.

Table 3. Data at 95°C.

Diamine	$10^5 k_{D(Acid)}$ $M^{-1}secs^{-1}$	$10^5 k^d_{D(Acid)}$ $M^{-1}secs^{-1}$	$\frac{k_{D(Acid)}}{k^d_D(Acid)}$
en	2.0 ± 0.4	2.0 ± 0.5	10 ± 3
dmen	3.4 ± 0.7	3.1 ± 0.7	11 ± 3
deen	6 ± 1	2.7 ± 0.5	22 ± 3

The base catalysed deuteration was promoted considerably more easily, (pD $\sim$ 9, 14-55°C), and showed much higher degrees of stereospecificity; (1.3 $\pm$ 0.3) x 10^2, (1.5 $\pm$ 0.4) x 10^2 and (2.2 $\pm$ 0.5) x 10^2 for Co(III)EDDA(en)$^+$, Co(III)EDDA(dmen)$^+$ and Co(III)EDDA(deen)$^+$ respectively. Since the method of catalysis should have no effect on the degree of protection of H_B by the ethylenediamine 'backbone', the markedly lower degree of stereospecificity in the acid catalysed deuteration was ascribed to the production,(from an enolate cation) of a dechelated species. This has free rotation about the α-carbon -nitrogen bond, and is thus able to react in a nonstereospecific manner, as in Scheme 1.

Scheme 1.

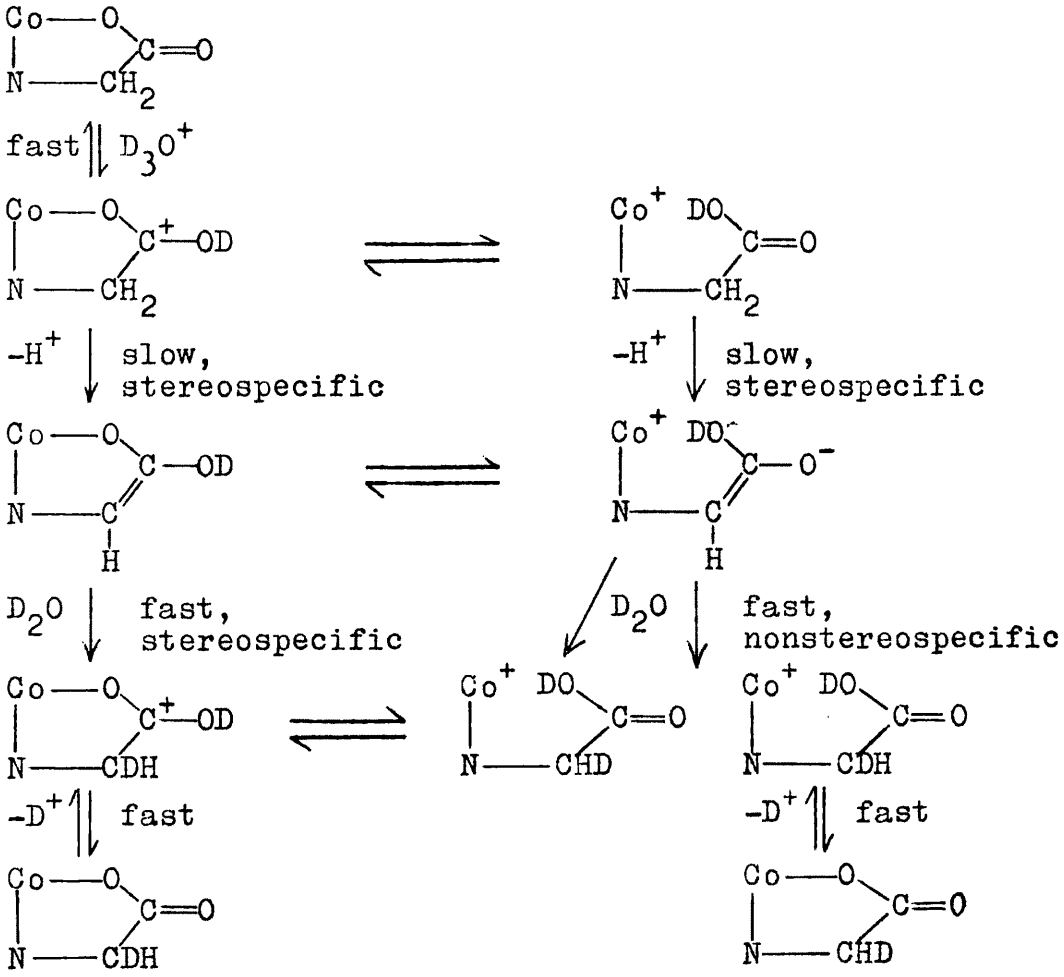

Rate controlling C-H bond rupture is indicated by the magnitude of the primary isotope effect ($\sim$5). The base catalysed reaction, where the first term in equation(29) is negligable, involves slow stereospecific deprotonation by OD^-,

followed by fast stereospecific addition of D^+ from D_2O. Thus, it is protonation of the carbonyl group in acidic solution that weakens the carbon-oxygen bond and reduces the degree of stereospecificity as described.

It is found that the alkyl groups of the diamine ligand enhance the deuteration rate in both acid and base. Although, since only one kind of alkyl substituent resonance is observed, conformational interchange between puckered forms is fast, Sudmeier and Occupati state that on the basis of molecular models and on the deuteration rates themselves, the conformation shown in Figure 8,IV, is most favourable i.e. having alkyl groups remote from the α-hydrogens. This would support the conclusion that the effect of N substituents situated on the ethylenediamine ligand is inductive rather than stereochemical.

Sudmeier and Occupati do not discuss the effect of the alkyl substituents on the stereospecificity of the reaction. An increasing inductive effect, deen > dmen > en, tending to reduce the polarizability of the Co-O bond, and hence precluding bond rupture and tendency to nonstereospecificity cannot apply, since a similar effect on the degree of stereospecificity was observed in both acid and base.

The effect is probably a consequence of the alkyl groups substituent effect on the ease of attaining the transition state, whilst the low degree of stereospecificity in acid is a direct consequence of protonation of the carbonyl group.

The effects on the ease of reaction and on the stereospecificity of the acid catalysed deuteration of out-of-plane glycinate protons in trans-Co(III)EDDA(diamine)$^+$, of: (i) the size of the glycinate ring (5 membered), (ii) the presence of one carbonyl group and (iii) the possibility of a dechelated species, are to be born in mind during the ensuing discussions on the stereospecific deuteration of $[Comal_2en]^-$.

EXPERIMENTAL

1. MATERIALS

Analar laboratory reagents were used wherever possible. D_2O (99.5% minimum isotopic purity) was obtained from Norsk Hydro-electrisk Kvætstofaktieselskab, NaOD from Koch-Light Ltd., (90% isotopic purity) and D_2SO_4 (99%) also from Koch-Light Ltd.

Benzylmalonic acid was obtained from Kodak Ltd., and ethylmalonic acid from Koch-Light Ltd. and Ralph N. Emanuel Research Chemicals Ltd.

Tertiary butyl alcohol was used always freshly distilled. The fraction boiling between 83-85°C was collected.

Stock deutero-acid solutions were prepared by the addition of D_2SO_4 to D_2O, the pD being measured on a Pye Dynacap pH meter after the appropriate correction factor: pD = 'pH' + 0.4(47,68) had been applied. Acid strength was checked by titrating random samples against standard base, on the pH meter, under a flow of nitrogen. The second derivative of the curve of mls of base added versus pH was constructed to obtain the end point. Agreement was always obtained to within $\pm$0.02 pH units between pre-prepared and checked samples.

Stock deutero-base solutions were prepared by the addition of a solution of borax/boric acid (0.1M in total borate) in D_2O, to a 0.1M solution of NaOD in D_2O, to obtain the required pD measured on a Dynacap pH meter.

All stock deuterated solvents were stored in a deep freeze between experiments.

2. PREPARATION OF COMPLEXES.

(i) $K[Comal_2en]H_2O$, was prepared by the method of Dwyer *et al*(30) without modification other than reprecipitating the product with ethanol from aqueous solution two or three more times than reported, in order to remove a persistent pink impurity. Pure yield about 60%.

Analysis.	Calculated for	$K[CoC_8H_{12}N_2O_8]H_2O$
		% C,25.30;H,3.68;N,7.37;K,10.33.
	Found,	% C,26.20;H,3.77;N,6.94;K,10.28

On addition of the complex to D_2O/D_2SO_4 solution, pD~2.5, the pD is observed to fall to a value of ~ 2.9, although thereafter remains constant to within ± 0.01 pH units. This cannot be the effect of the molecule of water of crystallisation since this would introduce < ½% of water into the acid solution, albeit unbuffered. The 'self-buffering' effect that is,in fact, occuring is discussed, together with the much more substantial one of $[Comal_3]^{3-}$, at the end of this section (p. 61).

(ii) $[Coen_2mal]Cl$. Werner's method(103) for the preparation of this complex was considered somewhat unwieldy and a modification was used that does not involve the isolation of the bimalonate sludge.
$[Coen_2CO_3]Cl$,prepared by the method of Dwyer(31), (17gm, 0.062 mole) was dissolved, with warming, in 60 ml of water. Malonic acid (6.5gm, 0.0625mole) was then added and the solution heated to the boiling point; whereupon it was vigorously stirred, or transferred to a separating funnel and shaken, until all effervescence ceased. Sodium chloride (8 grms) was added to the hot solution and it was left in a refridgerator for three days. The carmine-red leaf crystals were subsequently filtered at the pump, washed with a little ice water and ethanol, recrystallised from the minimum of hot water, and subsequently dried in vacuo over $CaCl_2$.
Yield, 40% (7.4gm).

Analysis	Calculated for	$[CoC_7H_{18}N_4O_4]Cl$.
		% C,26.54;H,5.69;N,17.70
	Found	% C,26.37;H,5.87;N,17.22

(iii) $[Coen_2mal]Br$.

$[Coen_2CO_3]Cl$ (9.0gm, 0.033mole) was dissolved in water (30 ml). Silver oxide, freshly precipitated from silver nitrate (5.96gm) and excess base, was added and the solution well stirred. $[Coen_2CO_3]OH$ was then filtered free from excess Ag_2O and AgCl and malonic acid added (3.5gm, 0.0335mole). The solution was heated to boiling and vigorously stirred until effervescence ceased. Potassium bromide (6gm) was then added and the solution allowed to cool in the refridgerator. The red,needle crystals

were filtered at the pump, washed with ice-water and ethanol and recrystallised from the minimum of hot water. The pure complex was washed on the filter in a similar manner and dried in vacuo over $CaCl_2$.

Analysis	Calculated for	$[CoC_7H_{18}N_4O_4]Br$.
		% C,23.25;H,4.99;N,15.53;Br,22.15
	Found	% C,24.00;H,5.09;N,13.39;Br,22.02 22.45

In view of the other three analyses, the figure returned for nitrogen was deemed unimportant.

(iv) $[CoBipy_2mal]Br.H_2O$, was prepared from $[CoBipy_2Cl_2]Cl.2H_2O$ by a method similar to that of $[Cophen_2Cl_2]Cl.3H_2O$(1), where phen= 1,10 phenanthroline,and $[Cophen_2mal]Cl.6H_2O$(2).

(a) $[CoBipy_2Cl_2]Cl.2H_2O$. Cobalt chloride hexahydrate, (5gm, 0.02mole), and 2,2' bipyridyl, (6.55gm, 0.04mole), were warmed together in 6ml of water, until a brown solution was obtained. Upon cooling in ice a yellow-brown material was precipitated.
Chlorine gas was then passed into the solution for 75 minutes, during which time the cobalt(II) material was oxidised to the red-grey cobalt(III) product. This was then filtered at the pump and well washed with ice-water and ether. The brown filtrate yields further product on reoxidising and working up the liquor.
Crude yield $\sim$ 50%.
The crude product was dissolved in 40ml of boiling water and 10ml of concentrated hydrochloric acid added. On cooling, dark purple,leaf-like crystals were deposited. The recrystallised $[CoBipy_2Cl_2]Cl.2H_2O$ was obtained in about 60% yield from the crude product, and was used without analysis.

(b) $[CoBipy_2mal]Br.H_2O$. Dichlorobis-(2,2' bipyridyl) cobalt(III) chloride dihydrate, (0.6gm, 0.0012mole), in water, (5ml), was ground in a mortar with silver oxide, freshly precipitated from silver nitrate, (0.95gm), and excess alkali. The resulting solution was filtered from excess Ag_2O and AgCl and treated with malonic acid, (0.25gm, 0.0024mole), at the boiling point. Boiling was continued for five minutes, after which time

potassium bromide, (1gm), was added and the solution cooled in ice. The resulting crystals, which were a somewhat deeper red than the analogous ethylenediamine complex, were filtered at the pump, washed with a little ice-water, ethanol and ether and air-dried.
Pure yield ~ 30% after recrystallisation from the minimum of boiling water.

Analysis Calculated for $[CoC_{23}H_{18}N_4O_4]Br.H_2O$

% C,48.40;H,3.51;N,9.82

Found % C,48.86;H,3.86;N,9.46

48.76 3.82

(v) $[Coen_2Etmal]Br.H_2O$.

$[Coen_2CO_3]Cl$, (10gm, 0.0365mole) in water (50ml) was treated with Ag_2O freshly precipitated from silver nitrate (11gms), and excess hydroxide. On filtering free from excess Ag_2O and AgCl, the filtrate was heated and ethylmalonic acid (5g, 0.038mole) added. Considerable shaking and stirring near the boiling point was necessary to remove all signs of effervescence. Potassium bromide (8gm) was subsequently added and the solution cooled in ice. The product was a somewhat deeper red than $[Coen_2mal]Br$. Recrystallisation was from the minimum of hot water, and the pure product was dried in vacuo over calcium chloride.

Analysis Calculated for $[CoC_9H_{22}N_4O_4]Br.H_2O$

% C,26.60;H,5.92;N,13.78;Br,20.55

Found % C,25.89;H,5.96;N,13.39;Br,21.27 $\pm$0.2

(vi) $K[CoEtmal_2en]H_2O$.

(a) Ethylenediamine ethylmalonate. Ethylenediamine, (0.88ml, 0.015mole), was added slowly to a stirred solution of ethylmalonic acid in ethanol,(1.72gm, 0.015mole). The white solid was collected at the pump, washed with ethanol and dried in vacuo over calcium chloride.
Yield, 2.5gm - 95%.
(b) A solution of potassium carbonate, (2.1gm, 0.015mole), in

water (30ml), was neutralised by ethylmalonic acid, (2.0gm, 0.015mole), and 2gm added in excess. The solution was then warmed and cobalt carbonate, (1.53gm, 0.013mole), added. Upon cooling to 30°C, (no higher), ethylenediamine ethylmalonate, (2.3gm, 0.012mole), was added, followed by lead dioxide, (3.1gm, 0.013mole).

Oxidation was accomplished by the slow addition of glacial acetic acid, (1.55ml), to the hot solution,(65-70°C), over a period of 20 minutes. During this time, the colour of the solution changed from pink to deep purple.

When oxidation was complete, (absence of Co(II) material was confirmed by the reaction of alcoholic thiocyanate), the hot solution was filtered from excess dioxide,(twice), and caesium chloride,(1.2gm), added.

Upon standing in a refridgerator overnight a white material (impurity as the caesium salt),was deposited which was filtered off and discarded.The solution was then allowed to evapourate spontaneously.Over a period of 7 days various amounts of the white impurity were deposited,filtered off and discarded.After 7 days,the product began to crystallise; whereupon the solution was cooled in an ice bath.The first fraction consisted of a gelatinous purple material, which was discarded as impure.Subsequent fractions consisted of beautiful purple needles.These were filtered at the pump, well washed on the filter with ice-water and ice-cold ethanol and dried in vacuo over phosphorous pentoxide. Three crops in all were obtained from the liquor.

Attempts to recrystallise the product from water resulted in disproportionation on warming,(although the complex is quite stable at room temperature). Reprecipitation from aqueous solution by the slow addition of ethanol resulted in the deposition of a gelatinous sludge,whilst the use of other organic solvents gave oils. Analysis of the original product, and its pmr spectrum, however, leave little doubt as to its purity. Most impurity was initially precipitated by the addition of caesium chloride.

Yield 10%

Analysis. Calculated for $K[CoC_{12}H_{20}N_2O_8]H_2O$

% C,32.80; H,5.08; N,6.45; O,33.10

Found % C,31.62; H,5.35; N,6.14; O,33.44

5.30

(vii) $K_3[Comal_3]3H_2O$ - was prepared, with one modification, by the method of Al-Obadie and Sharpe(76).
The complex appears to be quite susceptible to photoreduction in ethanolic solution, and precipitation of the product from aqueous solution by ethanol was always preceeded by precipitation of a pink material, (cobaltous malonate). Upon filtering from dioxide after oxidation therefore, ethanol, (400ml using Al-Obadie's quantities), was quickly added with stirring to the warm solution, the resulting pink impurity removed, and a further 300ml of ethanol added. Whereupon the vivid green product came down.
Yield $\sim$ 30%.

Analysis. Calculated for $K_3[CoC_9H_6O_{12}]3H_2O$.
% C,20.16;H,2.25
Found % C,20.25;H,2.38.

(viii) $[Comal_2Bipy]^-$ was obtained as the double salt, $[CoBipy_2mal][Comal_2Bipy]3H_2O$.

The analogous oxalato complexes have been reported(18) and were also obtained as $[CoBipy_2\,ox]I$ and $Ba([Co\,ox_2Bipy])_2$, from the double complex.

2,2' bipyridyl (0.45gm, 0.029mole) was dissolved in hot, 30% aqueous ethanol (9ml) and a solution of $K_3[Comal_3]3H_2O$ (1.39gm, 0.026mole), in water (5ml) added. The reaction mixture was then heated, with great care, until it turned a deep red colour. It was then cooled in ice.
The solution occasionally had to be reduced in volume to ensure crystallisation - this necessitated great care or the brown $[CoBipy_3]^{3+}$ cation resulted. The purple-red powder obtained was washed on the filter with a small amount of ice water, absolute ethanol and ether and air dried. It was analysed without further purification.
Yield, 20-60% (based on $[Comal_3]^{3-}$).

Analysis Calculated for $[CoC_{23}H_{18}N_4O_4][CoC_{16}H_{12}N_2O_8]3H_2O$.
% C,49.50;H,3.84;N,8.89
Found % C,49.64;H,3.80;N,8.98.

Numerous attempts were made to split the complex into its

component halves. Precipitation of the cation with I^- proved successful but left behind a yellow-brown solution, probably of $[CoBipy_3]I_3$.
The cation was also successfully removed with sodium tetraphenyl borate, leaving a vivid purple solution behind. Attempts to work this up resulted in deposition of colourless solids ($B(Ph)_4^-$) and a colour change to red ($[CoBipy_2mal]^+$) and through to brown ($[CoBipy_3]^{+3}$).

(ix) $[Cophen_2mal][Comal_2phen]3H_2O$.

1,10 phenanthroline, (0.5gm, 0.0027mole) was dissolved in warm, 33% aqueous ethanol (11ml) and added to a solution of $K_3[Comal_3]3H_2O$ (1.34gm, 0.0025mole) in water (5ml). The solution was heated just to boiling point whereupon it changed from green to dark brown. Immersion in an ice/salt bath soon resulted in the deposition of the purple-red product, (of a somewhat darker hue than the bipyridyl analogue). The product was washed with ice-water, ethanol and ether, air dried, and again analysed without further purification.
Yield, 40% (based on $[Comal_3]^{3-}$).

Analysis	Calculated for	$[CoC_{27}H_{18}N_4O_4][CoC_{18}H_{12}N_2O_8]3H_2O$.
		% C,53.10;H,3.57;N,8.27
	Found	% C,53.35;H,3.72;N,8.44.

Attempts to split this complex into its component halves were even less successful than in the previous case. Whatever reagent was used to remove $[CoBipy_2mal]^+$ resulted in disproportionation of the product, the colour changing from red-purple to brown ($[Cophen_3]^{3+}$) almost immediately. $[Cophen_2mal][Comal_2phen]3H_2O$ proved of little value. Its pmr spectrum was unobtainable because of its extreme insolubility in all solvents - even using microcell technique.

Microanalyses for C,H,N, and O were carried out by Alfred Bernhardt of Elbach über Engelskirchen, West Germany and Dr F.B. Strauss of Oxford, England. Halide was analysed gravimetrically and by potentiometric titration,and potassium was determined by flame photometry(39).

(x) The nature of $[Comal_2en]^-$ and $[Comal_3]^-$ in solution.

It has been shown by McAfferty and Mason(70) from circular

dichroism (C.D.) spectra that $[Co(C_2O_4)_3]^{3-}$ exists in solution partly in the open ring form.

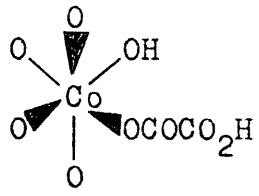

C.D. detects the reduction in symmetry in going from the fully chelated form (D_3) to ring-opened form (C_2).
Upon dissolving $[Comal_2en]^-$ and $[Comal_3]^{3-}$ in an unbuffered, weakly acidic solution (pH2.5) to give a 0.100M solution, the pH changes from 2.5 to about 2.8 and 2.5 to 5.5 respectively. This self buffering effect could only come about as a result of a ring opened form analogous to the above. Furthermore, the effect depends strongly on the presence of the third malonate ring - $[Coen_2mal]^+$ does not alter the pH of a solution pH2.5.
The effect could come about as a result of the following sequence.

$$[Comal_3]^{3-} + H_2O \rightleftharpoons [Comal_3H_2O]^{3-} \underset{H^+}{\overset{OH^-}{\rightleftharpoons}} [Comal_3OH]^{4-} + H_2O \qquad \text{(H.)}$$

- the second stage providing the buffering effect. Since $[Comal_2en]^-$ showed a markedly less tendancy to exist in the proposed dechelated form and since Sudmeier and Occupati(93) have proposed a similar form of Co(III)EDDA(en)$^+$ to account for low stereospecificity in acid solution, the complex was suitable for study of the effect of chelation on the lability of α-hydrogens. $[Comal_3]^{3-}$,however, was considered unsuitable on these grounds.
A spectrophotometric survey of the complexes in a range of buffers is presented in Appendix I.

The uv-visible spectra of $[Coen_2mal]^+$, $[CoBipy_2mal]^+$ and $[Comal_2en]^-$ in 0.25M acid show no change over a period of time up to six months. Any species involving dechelation of malonate in $[Comal_2en]^-$ must therefore be formed in a fast preequilibrium.

3.PMR SPECTRA AND KINETIC MEASUREMENTS

All spectra, with the exception of [$CoBipy_2mal$][$Comal_2Bipy$], were recorded on a Varian HA60,60MHz nmr spectrometer.[$CoBipy_2mal$][$Comal_2Bipy$] was recorded on a Varian HA100,100MHz instrument at Harwell Institute. Temperatures were varied by means of the Varian variable temperature accessory. The manufacturer's claim to an error of $\pm 1^{o}C$ could not be bettered, and occasionally even greater error was incurred. Activation parameters are therefore subject to large error. Temperatures were checked by measuring shift differences in methanol and ethylene glycol and refering to the manufacturer's calibration chart. Ice-water or ice-methanol were used as the heat sink.
Chemical shifts were conveniently measured relative to tertiary butyl alcohol or HOD as internal standards, usually on a sweep width of 500Hz at a scan rate of $1Hz.sec.^{-1}$ Peak areas were measured using the spectrometer's electronic integrator at a scan rate of $5Hz.sec.^{-1}$

The acid catalysed deuterium exchange rates were determined in sulphuric acid solution at the temperatures indicated for each complex. 'Dummy runs' monitored by pH meter indicated no change in pH during the course of a run. The stock acid solution and nmr tubes, containing weighed amounts of complex. to be used were preheated or precooled in a water bath at the appropriate temperature. No attempt was made to maintain ionic strength. After addition of stock acid and rapid transfer to the spectrometer, peak areas were continuously monitored. For those solutions in which exchange was fast, the tubes were left in the spectrometer's probe throughout the run. Otherwise, the tubes were kept in a water bath at the required temperature between readings. Integration was run from 3.20ppm,(versus t-BuOH), upfield, in order to avoid the big HOD signal. Where present, the ethylenediamine $-CH_2CH_2-$ signal was included in the integral. Since this is not subject to deuteration, the malonato α-hydrogen is expressed as a fraction of it, in order to allow for variation in the spectrometer's output power. In the case of $[CoBipy_2mal]^{+}$ the initial integral was made as large as possible, without incurring too large a signal/noise ratio, and the field kept constantly shimmed. Complexes used were $K[Comal_2en]H_2O$, $[Coen_2mal]Cl$ or $[Coen_2mal]Br$,

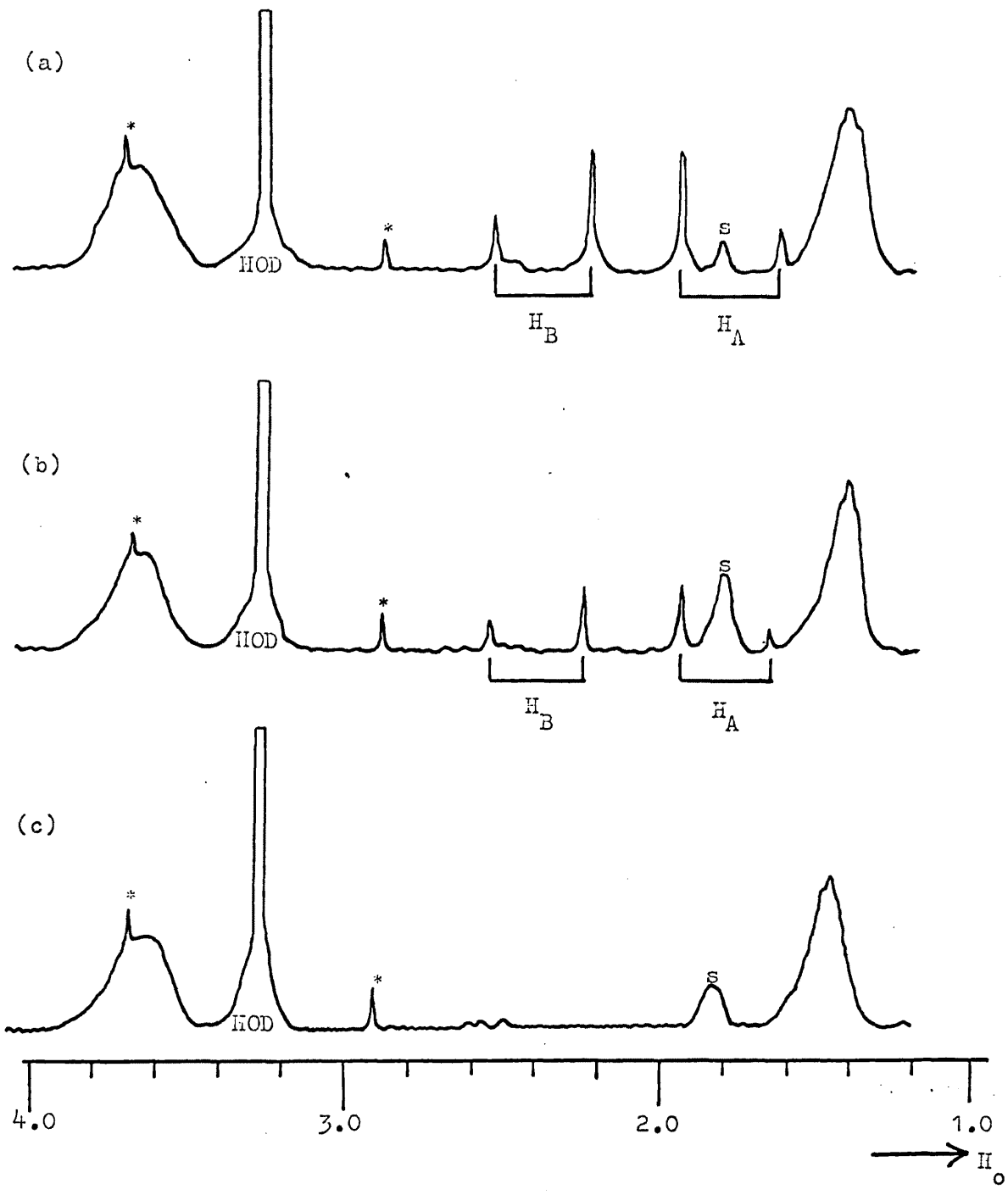

Figure 10. Pmr spectra of $Comal_2en^-$ in 0.0016 M D_2SO_4/D_2O , (a) after 2 minutes, (b) after 20 minutes and (c) after 100 minutes - at 37°C.

and [CoBipy$_2$mal]Br.H_2O. [Complex] was always 0.100M.

4. K[Comal$_2$en]H_2O.

The pmr spectrum of this complex has been reported previously (19,106). As recorded by the author it is reproduced in Figure 10a.

Asterisks denote spinning side bands. The broad peak (half width 12Hz) at 1.47ppm is assigned to the ethylenediamine -$-CH_2CH_2-$ protons. Its broadness is ascribed to unresolved coupling to the $-NH_2$ protons. Careful examination in a well shimmed field reveals shoulders on either side of the main peak; the whole representing a rudimentary triplet. Addition of deutero base causes rapid sharpening of the signal to a half width of about 2Hz. In view of this, and since there is no fine structure, we may conclude that: (a) each methylene group is in an identical field, and (b) conformational interchange of the ethylenediamine chelate ring is fast, (> 100 sec.$^{-1}$).

The broad peak at 3.75ppm is readily assigned to the two equivalent $-NH_2$ groups, since it disappears rapidly on addition of deutero base. The readily identifiable AB pattern, centred at 2.11ppm, immediately downfield of the en $-CH_2CH_2-$ signal, is assigned to the malonato α-hydrogen atoms.

Disregarding conformational interchange for the moment, it may be seen that an AB pattern is inevitable, since in any conformation there will always be one pair of protons, H_B, between the two malonate rings, and one pair, H_A, outside the rings, adjacent to the amino groups of the ethylenediamine ligand.

As we have seen, (p.32), for intramolecular processes such as conformational exchange, that are fast compared to the nmr time scale, both chemical shifts and coupling constants are subject to time averaging. The time average as 'seen' by the spectrometer will consist of the weighted mean of all conformationally attainable structures. A prefered conformation will contribute more to the time average than will an energetically unfavourable conformation.

As will be seen, the reaction is stereospecific, in that the downfield protons are deuterated first. Therefore, the difference in averaged chemical environment of H_A and H_B is

a consequence of the same factor(s) that govern the stereospecificity of the reaction - and we may assume that no steric compression factors operate. However, the assignment of H_A or H_B to the high field AB signals, and to an average sheltered environment, is a matter for conjecture.

All other things being equal, we may consider the inherent repulsive terms contained in each conformation. Figure 11(a) shows the two malonate rings in the intermediate 'skew-boat' conformation, whilst Figure 11(b) and (c) show the rigid 'chair' and mobile 'boat' forms. Energetically, the chair form is most unfavourable. It contains eclipsed lone electron pairs; O_1 and O_3, O_2 and O_4, and O_1 and O_2, as well as various less significant lone pair-bonding pair interactions. In comparison the boat conformer has only lone pairs on O_1 and O_2 eclipsed. In view of this we may expect the mobile conformers to contribute more to the average than the rigid chair form.

However, we must consider the inter-ligand steric interactions.

In one pair of boat conformers, the H_A's may approach to within $0.5A^{\circ}$ of N_1 and N_2, whilst in the other pair, the H_B's may approach to within $0.7A^{\circ}$ of the carbonyl oxygens O_3, and the co-ordinated oxygens O_1 and O_2. Measurements were estimated from Dreiding models. Both boat conformations, therefore, contain repulsion terms other than those inherent to the conformation. On raising the temperature of an acidic solution of $[Comal_2en]^-$ to as high as $80^{\circ}C$ and lowering it to $20^{\circ}C$, no conformational consequences were observed. The activation energy for exchange is therefore likely to be $\sim$ 5 kcal.mole^{-1}, exchange is <u>always</u> fast compared to the nmr time scale and we may consider the net conformation as comprising of the weighted mean of the above energy terms.

Furthermore, since molecular models indicate that in the intermediate 'skew-boat' and rigid 'chair' forms neither H_A nor H_B is liable to preferential attack, either malonate-malonate or H_2N-malonate repulsion is likely to be stronger, thereby rendering H_A or H_B in an average sheltered environment. The average nature of the environment then decides the degree of stereospecificity.

The relative motion of the malonate rings must also be considered.

Disregarding the 'chair' form, (or accepting a set contribution

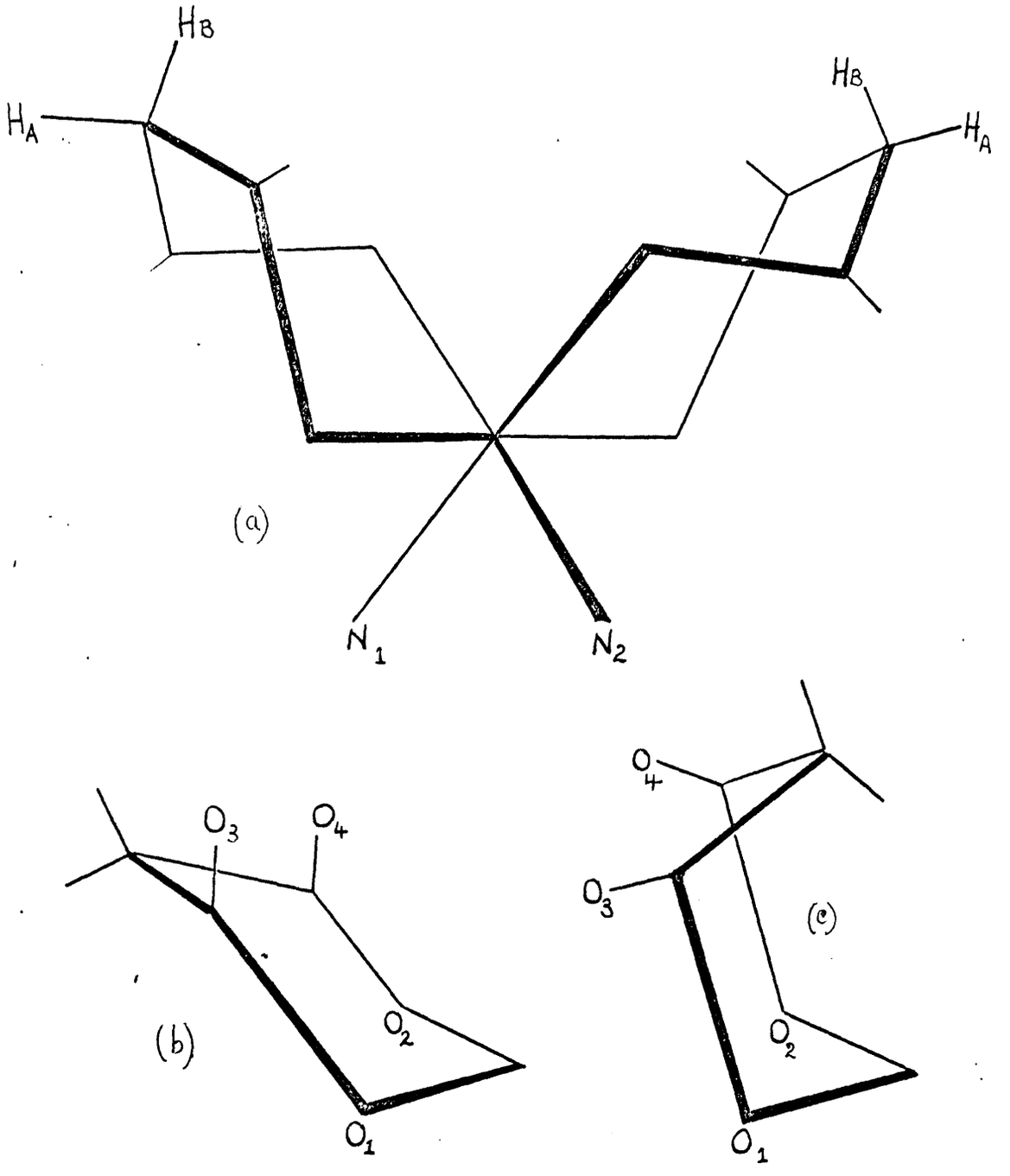

Figure 11. Conformations of co-ordinated malonate.
(a)'skew-boats',(b) 'chair' and (c) 'boat' conformations

from it), the rings can be envisaged as moving from 'boat', through 'skew-boat' and back again in two ways - Figure 12.

(i) Their motion can be considered to be like that of bent windscreen wipers on a central pivot. As H_{A1}(Fig.12(a)) and N_1 are juxtaposed in the 'boat' conformation, malonate ring 2 has H_{B2} and O_{11} of ring 1 adjacent. Repulsion occurs and both rings move back through the intermediate skew boats,(Fig.11(a)), until H_{A2} and N_2, and H_{B1} and O_{12} are adjacent (Fig.12(b)) - and so on.

(ii) With the two rings moving, 'in phase'. Each 'boat' conformer tries to occupy the central position,(Fig.12(c)), incures a large repulsion in the form of atom-lone pair interactions; H_{B2}-O_{11}, H_{B1}-O_{12}, H_{A1}-O_{32} and H_{A2}-O_{31}, and reverts through 'skew-boat' to the conformations having H_{A1} and N_1 and H_{A2} and N_2 adjacent.

The competing repulsion terms in (i) are H_A-bonding pair interaction and H_B-lone pair interaction and in (ii) H_A-bonding pair and the four atom-lone pair interactions outlined above. The repulsive effect of the eclipsed lone-pairs is generally considered to be more significant than that of eclipsed bonding pairs(46). Therefore, whether the relative methods of malonate ring conformational interchange follows model (i),(ii) or both, the conformers having H_A's and N_1 and N_2 adjacent are rendered relatively stable.
Without further evidence, stereospecificity of reaction is very likely due to average sheltering of H_A by the ethylenediamine amino groups. Confirmatory evidence was undertaken nevertheless. Other steric factors were introduced; in the malonate ligand in $[CoEtmal_2en]^-$ and in the fixed ligand in $[Comal_2Bipy]^-$.

(a) The use of ethylmalonate.
The spectrum of $[Coen_2Etmal]^+$ in weakly acidic (pD$\sim$4)D_2O is shown in Fig. 13(a). Shifts were conveniently measured upfield of HOD, (as lock signal), which occurs 3.50ppm downfield of t-BuOH at 60 MHz. The α-carbon-ethyl group comprises a first-order A_3M_2X system. No additional signals appear and we may therefore assume that conformational interchange is fast. The broadening of the centre peaks of the M signal is due to the slight inequality of J_{AM}(7Hz) and J_{MX}(6Hz).

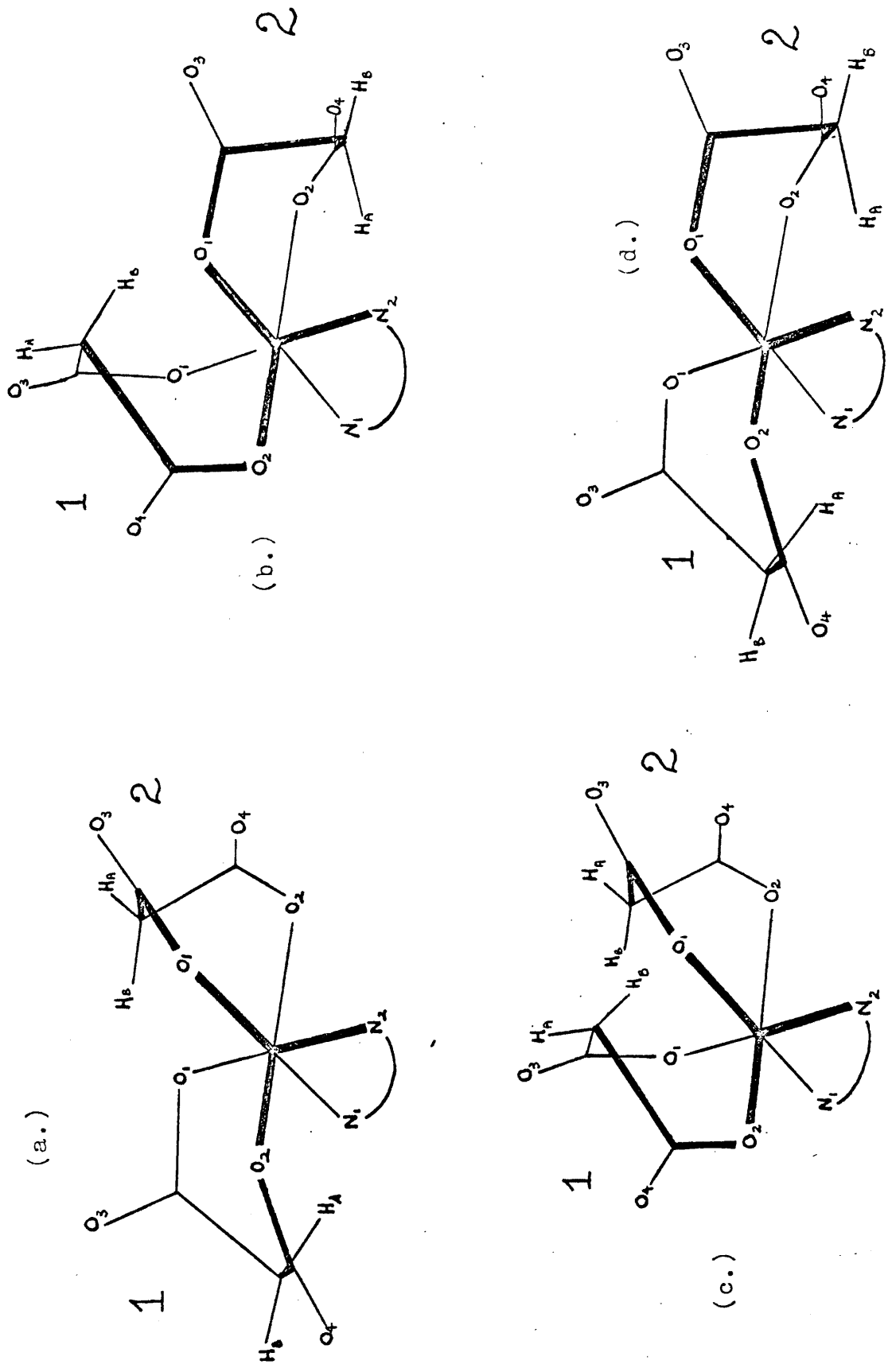

Figure 12: Interactions incurred by the mobile conformers of co-ordinated malonate in $[Conal_2en]^-$.

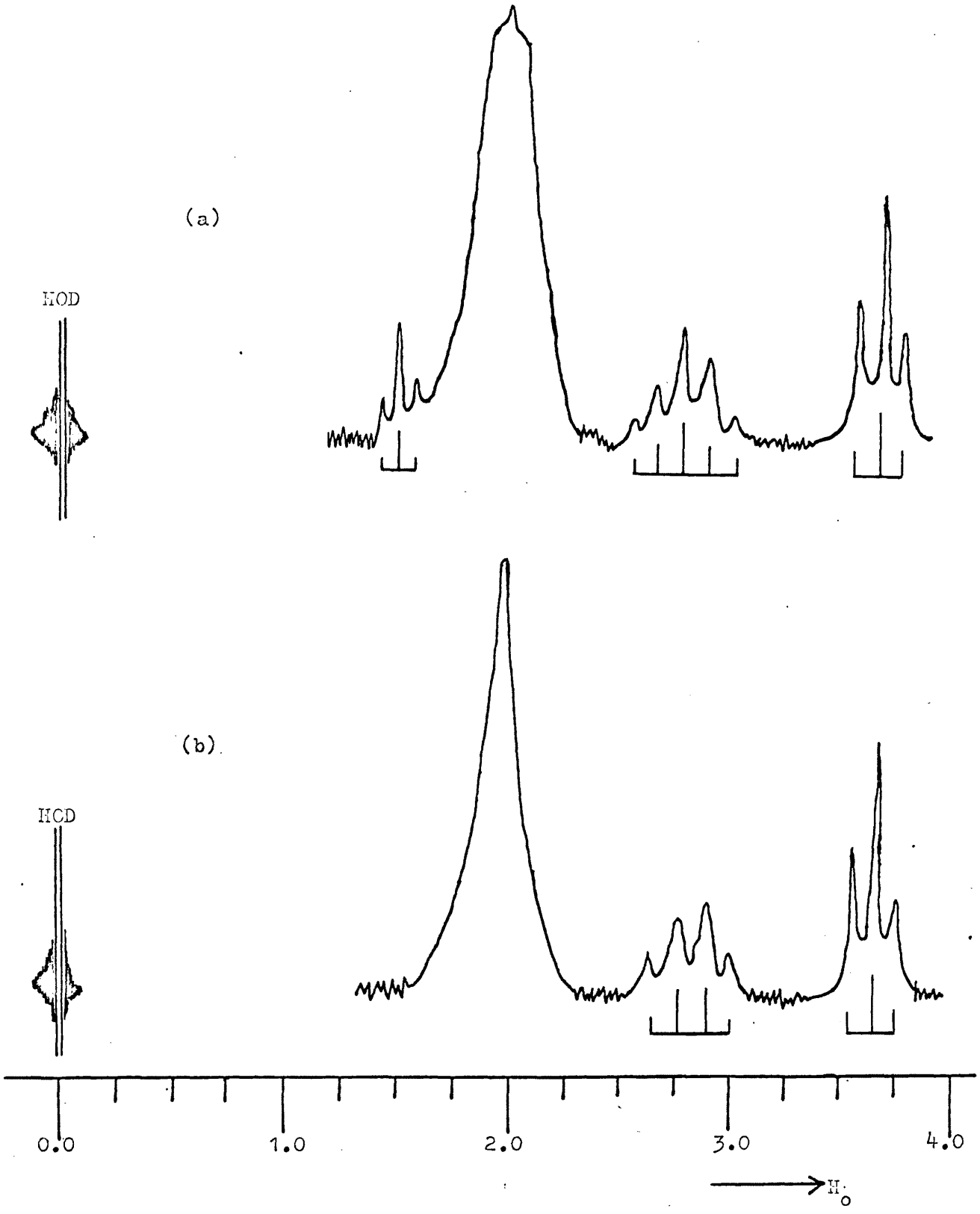

Figure 13. Pmr spectra of (a) $[Co(NH_2\text{-}(CH_2)_2\text{-}NH_2)_2(C_2H_5CH(COO)_2)]^+$ and (b) $[Co(ND_2\text{-}(CH_2)_2\text{-}ND_2)_2(C_2H_5CD(COO)_2)]^+$ - in acidic D_2O.

The broad peak at 1.48ppm is assigned to the ethylenediamine $-(CH_2)_2-$protons. The nature of this signal is dealt with further in section 5 - on $[Coen_2mal]^+$.
Spectral assignments are summarised in Table 4.
Deuteration of the α - protons by the addition of deutero-base caused, as expected, the collapse of the M quintet to a quartet,(Fig.13(b)).

Note. Spectra were recorded quickly because of the complex's susceptibility to acid and to base hydrolysis, (Part Two). No variation in chemical shifts was observed during the process of recording spectra. Acid $\sim$ pD4 and NaOD/borate buffer, pD$\sim$8.5 was used to record initial spectra and to deuterate amino protons respectively.

Table 4.

60MHz spectral assignments of $[Coen_2Etmal]^+$, (δ ppm versus t-BuOH).

Signal	δ ppm.	
$-NH_2$ cis	-3.13	
$-NH_2$ trans	-4.14	
$-(CH_2)-$ en	-1.48	
malonate		
C-H	-1.90(triplet)	J_{MX}= 6 Hz
$-CH_2$	-0.72(quintuplet)	J_{AM}= 7 Hz
$-CH_3$	+0.04(triplet)	

The 60MHz spectrum of $[CoEtmal_2en]^-$ in weakly acidic D_2O is shown in Figure 14(a). Shifts were again conveniently measured relative to the HOD lock signal.
The complex consists of a mixture of two geometrical isomers defined by the position of the ethyl groups relative to the ethylenediamine amino groups. (i) Having H_A's, (Fig.11), = ethyl (2 syn), and (ii) having the H_B's = ethyl,(2 anti). Isomers having H_{A1}= ethyl and H_{B2}= ethyl, (syn-anti), and H_{B1}= ethyl and H_{A2} = ethyl,(anti-syn), are indistinguishable

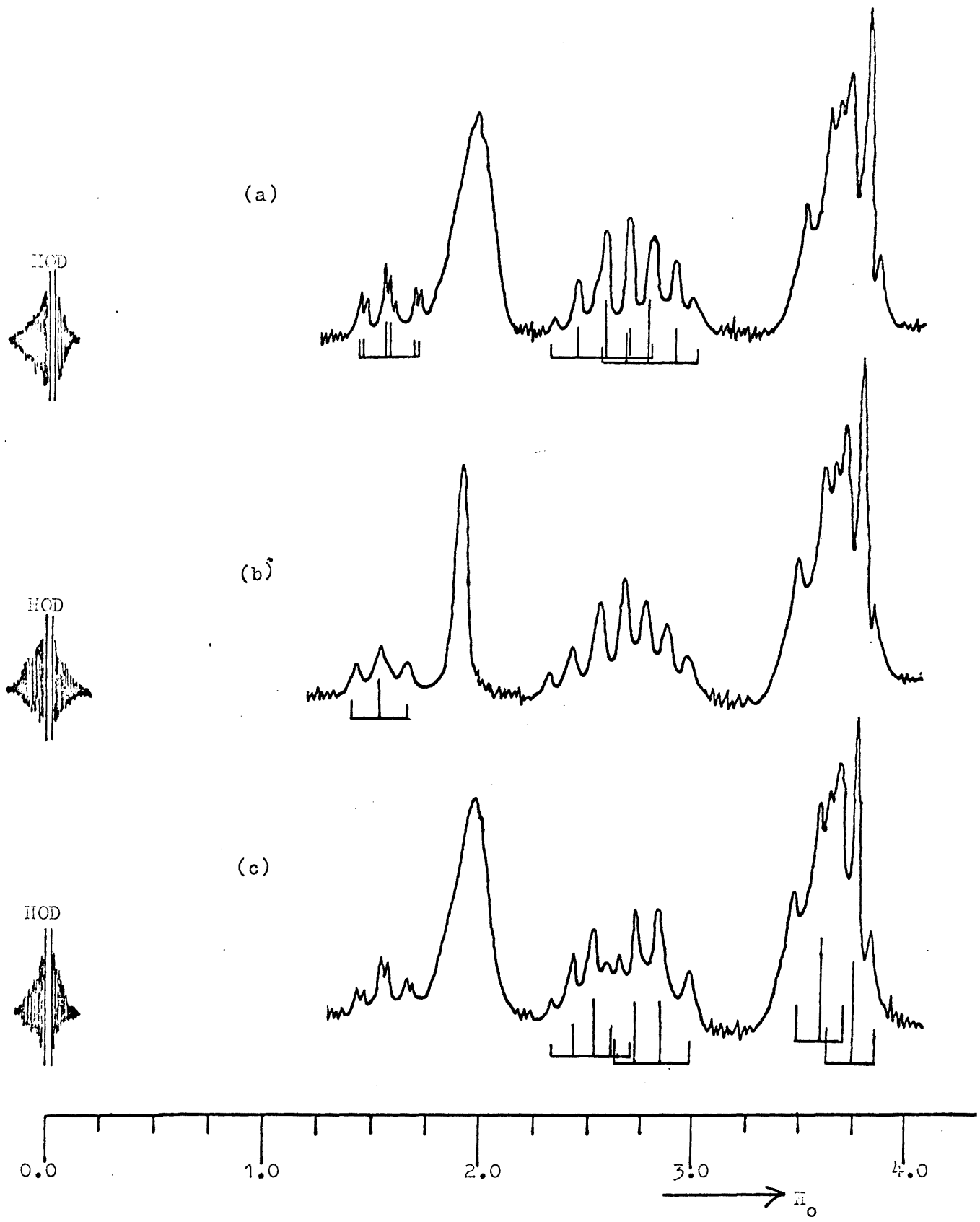

Figure 14. Pmr spectra of Co(syn-anti-Etmal)$_2$en$^-$ (a) after 2 minutes in D_2SO_4/D_2O, pD 3, (b) after 2 minutes in $NaOD/D_2O$ and (c) after 6 hours in D_2SO_4/D_2O, pD 3.

from the extreme syn and anti isomers in the pmr spectrum of the complex.

The group of 7 peaks immediately upfield of the ethylenediamine $-CH_2$ signal, (which was assigned by analogy), is assigned, on the basis of integration, to two overlapping quintets. Such overlapping, (Fig.15), provides the observed 1:4:7:8:7:4:1 ratio, whereas a regular septuplet would show a ratio of 1:6:15:20:15:6:1. The two quintets are assigned to the $-CH_2$ protons of the ethyl groups of the syn and anti isomers. If the steric interactions are similar to those in $[Comal_2en]^-$ the high field quintet would be due to the syn isomer and the low field one to the anti isomer.

In the same way, the six signals upfield of the $-CH_2$ signals are assigned to two overlapping triplets derived from the methyl group of the ethyl side chain in the syn and anti isomers. No coincidence of individual isomers spin coupled signals occurs here.

Figure 15.

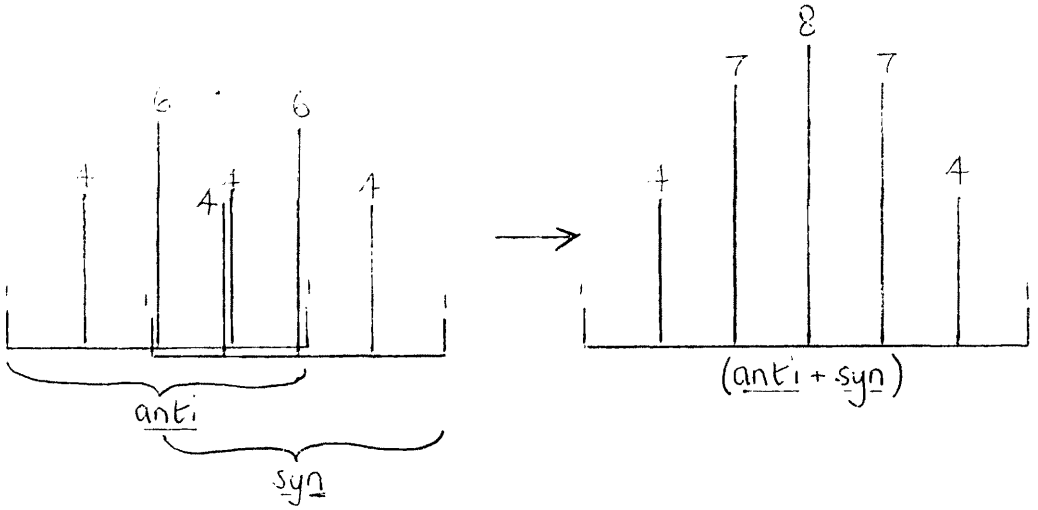

The α -hydrogen of the anti isomer is assigned to the group of peaks centred 1.66ppm upfield of HOD (-1.84ppm versus t-BuOH). The triplet structure derives from coupling to the adjacent $-CH_2$ group, (J = 7Hz). The fine structure ($J < 1.5$Hz) is assigned to 'trans-space' coupling between the α -proton and the ethylenediamine amino group. In the anti isomer strong mutual steric compression by the ethyl groups could result in such a phenomenon. ^1H-^1H 'trans-space' coupling has previously been observed in highly compressed 'cage' compounds by Anet et al(6).

Neutralisation of the acid solution with deuterobase, although

causing some loss of intensity of the triplet, nevertheless caused collapse of the fine structure (Fig.14(b)), presumably as a result of deuteration of the amino protons.
If such a conclusion is correct, we may conclude that the conformation having the H_A's and N_1 and N_2 juxtaposed is very much preferred.
No signal due to the syn isomer's α-hydrogen signal was observed. This is expected to occur to low field of that of the anti isomer, and since side bands of the HOD lock signal interfere in this region, it is probably lost amongst these signals.
Deuteration in acid solution (Fig.14(c)) caused the high field $-CH_2$ quintet to collapse to a quartet, without great decrease in intensity or loss of fine structure of the α-hydrogen signal. This supports the assignment of the syn isomer, which, if the repulsive terms involved in both malonate ring interconversions are as already postulated, contains H_B and will be preferentially deuterated relative to that containing H_A.

The pmr spectrum of $[CoEtmal_2en]^-$ points clearly to the dominance of the repulsive terms when H_B and donor oxygens are adjacent and we may readily assign H_A to the high field pair in the AB quartet of $[Comal_2en]^-$.

The assignments for $K[CoEtmal_2en]$ are summarised in Table 5. The isomeric mixture consists of overlapping A_3M_2XP and A_3M_2X patterns as already specified. Where $J_{AM} = 6.5Hz$, $J_{MX} = 7Hz$, $J_{XP} \sim 1.5Hz$, $J_{AX} = 0$, $J_{AP} = 0$ and $J_{MP} = 0$. Broadening of the centre peaks of the $-CH_2$ signal is due to the small difference between J_{AM} and J_{MX}.

Table 5.

60MHz spectral assignments of $[CoEtmal_2en]^-$ (δ ppm versus t-BuOH)

Signal	δ ppm
$-(CH_2)_2-$ en	-1.47
syn Et	
C-H	-
$-CH_2$	-0.57
$-CH_3$	+0.75
anti Et	
C-H	-1.84
$-CH_2$	-0.82
$-CH_3$	+0.64

(b) The use of 2,2' Bipyridyl.

The 100MHz spectrum of the malonato methylene protons in $[CoBipy_2mal][Comal_2Bipy]$ is shown in Figure 16(a). Shifts were recorded relative to TMS in d_6-DMSO, (dimethyl sulphoxide).

The singlet belongs to $[CoBipy_2mal]^+$. The equivalency of the methylene protons is explained in section 5.

The AB pattern arises from $[Comal_2Bipy]^-$ in an analogous manner to that in $[Comal_2en]^-$. The spectral assignments, converted to 60MHz and expressed relative to t-BuOH are summarised in Table 6. (t-BuOH is shifted 2.92ppm downfield of TMS at 60MHz).

Table 6.

60MHz spectral assignments of the malonato methylene protons of $[CoBipy_2mal][Comal_2Bipy]$ in d_6DMSO, (δ ppm versus t-BuOH).

Signal	δ ppm	
$-CH_2$	-1.97	
H_A	-1.53	J_{AB}= 16Hz
H_B	-3.15	

Since spectra were recorded in d_6-DMSO, the solvent effect on δ values of $[CoBipy_2mal]^+$ was taken as a blank. The methylene protons of $[CoBipy_2mal]^+$ (see section 6, p.89) in aqueous solution resonate at 2.11ppm downfield of t-butanol at 60MHz. d_6-DMSO, therefore, shifts spin equivalent αC -protons upfield by 0.14ppm.

The unsplit δ value of the high field protons in $[Comal_2en]^-$ is 1.84ppm and that of the low field protons, 2.36ppm.

Since no extra malonate-malonate repulsion is incurred in $[CoBipymal_2]^-$, the bipyridyl ligand is responsible for any anomolous effects. Its effect, therefore, is to shift the high field protons further upfield by 0.17ppm (relative to aqueous solution) and to shift the low field signal further downfield by 0.65ppm!

Furthermore, the value of J_{AB}(16Hz) using Pople and Bonther-By's(108) argument corresponds to that of geminal and inequivalent protons in a less planar ring than when J_{AB} = 18Hz (i.e.in

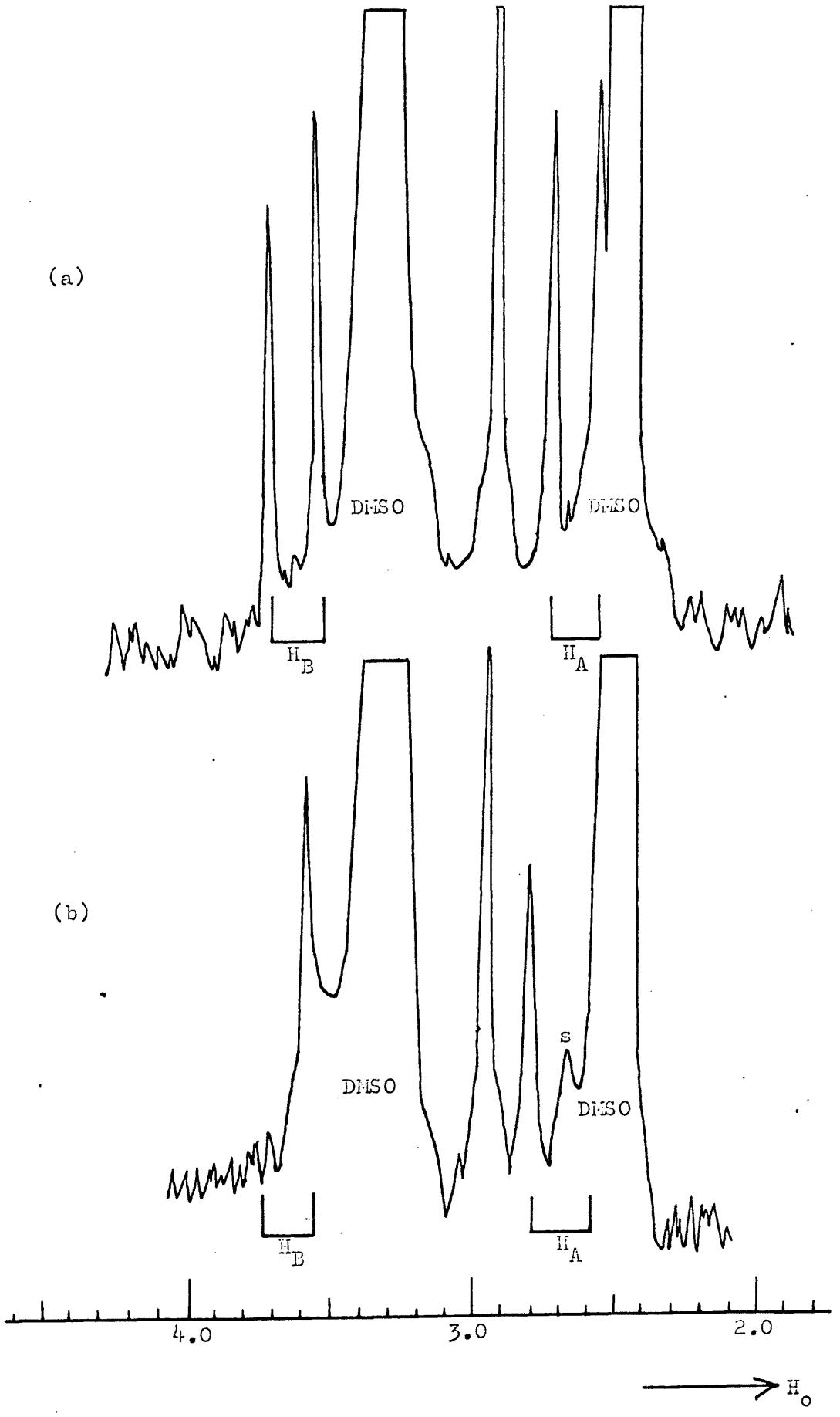

Figure 16. 100 MHz pmr spectra of $[CoBipy_2mal][Comal_2Bipy]$ in d_6-Dimethyl sulphoxide, (a) initially and (b) after deuteration.

Note. Chemical shifts are converted to 60 MHz versus t-BuOH in Table 7.

$[Comal_2en]^-$). The weighted mean, therefore, contains a higher contribution from the less planar, compared to the 'skew boat', 'boat' conformers.

On deuteration, (Figure 16(b)), the decoupled singlet appears between the high field signals. The same stereospecification factors, therefore, apply in $[CoBipymal_2]^-$ as did in $[Coenmal_2]^-$.

2,2' bipyridyl lacks the amino protons of ethylenediamine. The aromatic bonds, when the ligand is co-ordinated to a metal ion, are directed away from an approaching H_A atom as the malonate ring attempts to adopt the appropriate 'boat' conformation. The repulsive effect, therefore, lacks the relatively weak bonding pair-bonding pair interaction incurred with ethylenediamine. Nevertheless, the H_A's are encouraged to spend more time adjacent to N_1 and N_2. The proximity of the delocalised aromatic electrons would then be expected to provide the observed upfield shift.

In view of this evidence, the high field signals in the AB quartet are assigned to H_A. The large downfield shift of H_B is, however, of uncertain nature. Molecular models do not indicate any steric compression factors. A downfield shift of H_B was expected if the time average contains a larger contribution from the 'boat' conformer having increased shielding of H_A. However, a value of 0.65ppm was not expected. The answer could lie in the increased availability of H_B to solvent contact.

In the light of the assignments of $[CoEtmal_2en]^-$ and $[Comal_2Bipy]^-$ the absolute assignment of $[Comal_2en]^-$ is summarised in Table 7.

Table 7.

60MHz spectral assignments of $[Comal_2en]^-$ (δ ppm versus t-BuOH)

Signal	δ ppm	
$-H_A$	-1.84	J_{AB}= 18Hz
$-H_B$	-2.36	
$-(CH_2)_2-$ en	-1.47	
$-NH_2$ en	-3.75	

When deuteration of $[Comal_2en]^-$ was allowed to proceed at an experimental, self-buffered, pD of 2.80 at 37 ± 1°C, the area of the broad peak at 1.838ppm - denoted s, increased with time for the first 25 minutes or so of the reaction, (Fig.10(a) and (b)). Correspondingly, the AB pattern diminished in intensity: the low field pair, (H_B), due to deuteration, and the high field signals, (H_A), to a redistribution in intensity as H_A becomes decoupled from the deuterated H_B. The chemical shift of -1.838ppm corresponds exactly to the unsplit value of H_A calculated from standard AB spectrum analysis(p.34). The broadness of s is due to unresolved coupling to the geminal D_B atom.

Since no singlet appears between the low field pair of signals, H_B is deuterated entirely preferentially, and in this sense the reaction is stereospecific.

The acid catalysed deuteration rates were obtained by monitoring the largest of the H_B pair of signals, as already described (p.62).

The deuteration of H_B may be represented by:

$$CoXH_AH_B + D_3O^+ \longrightarrow CoXH_AD_B + HDO^+ \qquad (I.)$$

-where $CoXH_AD_B$ is the monodeuterated complex. Since, as described, the experimental pD remains constant throughout the run, pseudo-first order treatment may be applied to the kinetics, if the reaction is first order in complex.

$$-\frac{d(CoXH_AH_B)}{dt} = k_{D(Acid)}[CoXH_AH_B]^n[D_3O^+]^m \qquad (30)$$

Where m and n are reaction orders w.r.t. acid and complex concentrations respectively, and $k_{D(Acid)}$ is the rate constant for the acid-catalysed deuteration. Integrating (30) for a constant value of $[D_3O^+]^m$ (see p.9) and assuming n=1.

$$\frac{\ln[CoXH_AH_B]}{[CoXH_AH_B]_0} /t = k_{D(Acid)}[D_3O^+]^m \qquad (31)$$

$$\text{i.e.} \quad k'_{D(Acid)} = k_{D(Acid)}[D_3O^+]^m \qquad (32)$$

Where $k'_{D(Acid)}$ = the pseudo first-order rate constant, and $[CoXH_AH_B]_0$ = complex concentration at t = 0. Since I, the peak integral value, is directly proportional to $[CoXH_AH_B]$ at any time, equation (31) may be represented as:

$$\ln \frac{I}{I_0} /t = k_{D(Acid)}[D_3O^+]^m \qquad (33)$$

Plots of $\ln(I_1/I_2 - I_{1\infty}/I_{2\infty})$ against time were constructed, where I_1 = H_B peak integral and I_2 = the ethylenediamine $-CH_2$ peak integral, which is not subject to deuteration. I_∞ values were usually zero. Good straight lines over periods up to five half-lives (~95%) of reaction were obtained, thereby confirming the choice of n as unity. The slopes of these plots gave $k'_{D(Acid)}$, at each acid concentration studied.
Reaction order w.r.t. acid concentration was deduced by taking $\log_{10}$ of expression (32).

$$\log_{10}k'_{D(Acid)} = \log_{10}k_{D(Acid)} - mpD \qquad (34)$$

Least squares analysis of corresponding values of $\log_{10}k'_{D(Acid)}$ and pD using the standard regression in y expression for the slope a:

$$a = \frac{n\sum xy - \sum x \sum y}{n\sum(x^2) - [\sum x]^2} \qquad (35)$$

-where n= the number of x or y terms, gave values of m=1.0±0.1 for all temperatures. Second order rate constants, $k_{D(Acid)}$ were derived from equation (32) having m=1.

After about 30 minutes at pD 2.80 the decoupled α-hydrogen atoms, H_A, finally undergo deuteration, and the signal at 1.838ppm dereases in intensity(Fig.10(c).
The observed pseudo first order and second order rate constants for this stage of the reaction; $k'^{s}_{D(Acid)}$ and $k^{s}_{D(Acid)}$, were obtained in a similar manner to $k'_{D(Acid)}$ and $k_{D(Acid)}$.

Reproducibility of results. First order rate constants deduced at the probe temperature, 37°C, were reproducible to

within ± 5% of the mean. Use of the Varian variable temperature accessory, where difficulty was experienced in reproducing the required temperature from one run to another, gave an error of not greater than 17% overall, for any given set of conditions. Error in first order rate constants was calculated from % error in individual kinetic parameters. That in second order rate constants was derived from the corresponding error in the first order constants. The mean second order rate constants also included an error figure derived from the method of mean deviation.
The value of $k_{D(Acid)}$ at 25°C was obtained at a single pD value, and consequently is subject to more error than the corresponding values at 37°C and 44°C.

Results are summarised in Table 8. Mean values are summarised in Table 9 - from which Arrhenius plots were constructed. Error is included in the Arrhenius plots (Fig.17).

Table 8.

Deuteration rate constants of the active methylene protons in $[Comal_2en]^-$ in acidic D_2O.

(i) H_B data.

Temp. °C.	pD	$[D_3O^+]$ $M.L^{-1}$	$10^4 k'_{D(Acid)}$ sec^{-1}	$k_{D(Acid)}$ $L.M^{-1}sec^{-1}$
37±1	3.12	0.00076	6.58 ± 0.35	0.880 ± 0.045
	3.04	0.00091	7.52 ± 0.50	0.840 ± 0.055
	2.93	0.00118	10.10 ± 0.50	0.860 ± 0.040
	2.80	0.00160	13.30 ± 0.50	0.830 ± 0.030
44±1	3.12	0.00076	19.7 ± 1.0	2.59 ± 0.15
	3.04	0.00091	25.0 ± 1.5	2.74 ± 0.17
	2.93	0.00118	27.0 ± 2.0	2.30 ± 0.27
	2.80	0.00160	35.2 ± 2.0	2.20 ± 0.25
25±1	2.93	0.00118	1.80 ± 0.15	0.150 ± 0.013

Table 8 cont'd.

(ii) H_A data.

Temp. °C	pD	$[D_3O^+]$ $M.L^{-1}$	$10^4 k'^s_{D(Acid)}$ sec^{-1}	$k^s_{D(Acid)}$ $L.M^{-1}sec^{-1}$
37±1	3.12	0.00076	0.97 ± 0.15	0.13 ± 0.020
	3.04	0.00091	1.12 ± 0.20	0.12 ± 0.025
	2.93	0.00118	1.56 ± 0.25	0.13 ± 0.020
	2.80	0.00160	2.00 ± 0.25	0.125± 0.015
44±1	3.12	0.00076	3.15 ± 0.50	0.415± 0.070
	3.04	0.00091	3.83 ± 0.50	0.42 ± 0.055
	2.93	0.00118	4.24 ± 0.55	0.37 ± 0.050
	2.80	0.00160	5.44 ± 0.70	0.34 ± 0.060
25±1	2.93	0.00118	0.26 ± 0.06	0.022± 0.005

Table 9.

Stereospecific data for the deuteration of $[Comal_2en]^-$ in acidic D_2O

Temp. °C.	Mean $k_{D(Acid)}$ $L.M^{-1}sec^{-1}$	Mean $k^s_{D(Acid)}$ $L.M.^{-1}sec^{-1}$	$\frac{k_{D(Acid)}}{k^s_{D(Acid)}}$
37	0.850 ± 0.040	0.128 ± 0.02	6.65 ± 0.75
44	2.43 ± 0.20	0.383 ± 0.055	6.35 ± 0.75
25	0.152 ± 0.013	0.022 ± 0.005	6.85 ± 0.90

The mean stereospecific factor is therefore:

$$s = 6.60 \pm 0.80$$

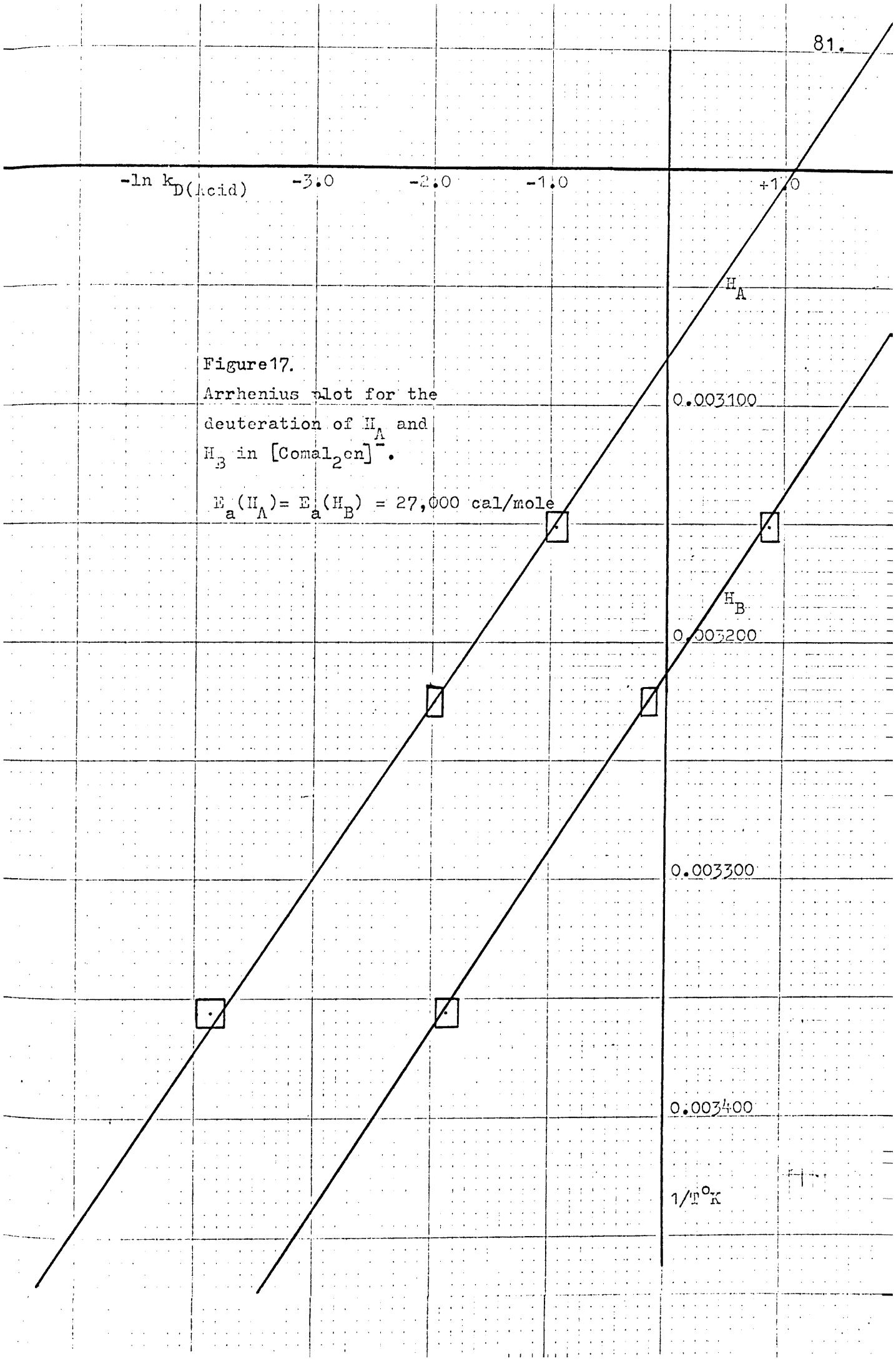

Figure 17.
Arrhenius plot for the deuteration of H_A and H_B in $[Comal_2en]^{-}$.

$E_a(H_A) = E_a(H_B) = 27,000$ cal/mole

The deuteration of H_B and H_A fits the Arrhenius relationships:

$$k_{D(Acid)} = 7.1 \times 10^{18} \exp[-27,000/RT] \quad (36)$$

$$k^{s}_{D(Acid)} = 1.2 \times 10^{18} \exp[-27,000/RT] \quad (37)$$

Within experimental error, the activation energy, E_a, of each stage, was found to be the same. Derived thermodynamic data is summarised in Table 10.

Table 10.
Activation parameters for the acid catalysed deuteration of the α-protons H_B and H_A of $[Comal_2en]^-$.

	E_a kcal/mole	$\triangle H^{\ddagger}$ kcal/mole (25°)	$\triangle G^{\ddagger}$ kcal/mole (25°)	$\triangle S^{\ddagger}$ eu.
$-H_B$	27.0 ± 3	26.4 ± 3	18 ± 7	26±10
$-H_A$	27.0 ± 3	26.4 ± 3	19.5± 2	22± 5

5. $[Coen_2mal]^+$

The pmr spectrum of this complex has been reported(19,106). It is shown, as recorded during the course of this work, in Figure 18(a).
As explained in the case of $[Coen_2Etmal]^+$, there is non-equivalence of the amino protons. One pair is cis to the ligating oxygen atoms of the malonate, and the other trans. This results in the two broad bands at -3.13ppm and -4.14ppm; easily recognisable by their ready dissappearance in deutero-base. When deuteration of these protons is carried out,(Figure, 18(c)), the broad peak at -1.47ppm sharpens from a half width of 12Hz, to one of 7.5Hz. In addition, the crude triplet structure, (c.f.$[Comal_2en]^-$), collapses. This peak is therefore assigned to the ethylenediamine $-(CH_2)_2-$ protons. In comparison, in $[Comal_2en]^-$, where the ethylenediamine methylene protons are equivalent, the signal of the latter protons sharpened to a half width of 2Hz on deuteration of the amino protons. We

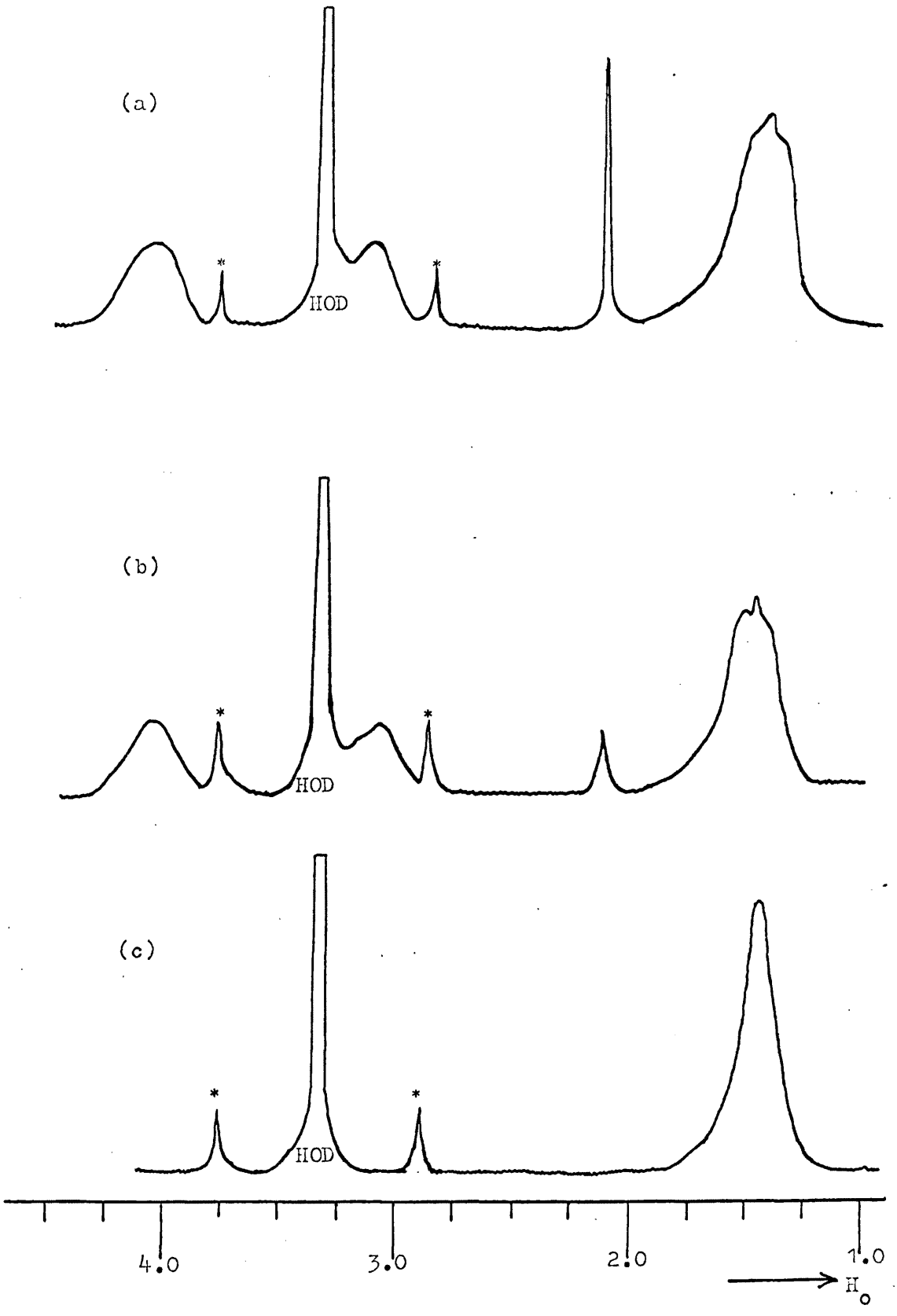

Figure 18. Pmr spectra of $Coen_2mal^+$ (a) after 2 minutes and (b) after 20 minutes in 0.0034 M D_2SO_4/D_2O, and (c) after 2 minutes in $NaOD/D_2O$, pD 8.8

may, therefore, conclude that, although conformational exchange between δ and λ forms of the ethylenediamine ring is fast, in $[Coen_2mal]^+$, the spectrometer 'sees' a different averaged field for each of two pairs of methylene protons. One pair is adjacent to an amino group cis to malonate oxygens and the other pair adjacent to a trans amino group. Buckingham et al's(19) conclusion that lack of resolution, where an $[A_2B_2]$ pattern should be observed, (even if conformational exchange is fast), is due to a complex overlap of signals, may pertain here.

Raising the temperature of the solution to 80°C produced a sharpening of the signal to 6Hz. This demonstrates an increased rate of conformational exchange. But nevertheless the chemical inequivalency of each pair of ethylenediamine methylene groups cannot be destroyed.

Replacing one malonate ligand in $[Comal_2en]^-$ by an ethylenediamine ligand results in the introduction of a twofold axis of symmetry through the α-carbon and cobalt atom, (Figure 19). When the malonate ring is in either of two possible 'skew boat' conformations, the α-protons are equivalent. This is the time averaged case, since 'boat' conformers will receive equal repulsive forces from interaction with the ethylenediamine amino groups. One sharp signal at -2.11ppm is observed, and this is reconciled with fast interchange between the two 'skew boat' conformers shown in Figure 19.

Spectral assignments are summarised in Table 11.

Table 11.

60MHz pmr spectral assignments of $[Coen_2mal]^+$ (δ ppm vs t-BuOH)

Signal	δ ppm
$-NH_2$ cis	-3.13
$-NH_2$ trans	-4.14
$-CH_2$ (en)	-1.47
$-CH_2$ (mal)	-2.11

By monitoring the malonate singlet intensity compared with that of the ethylenediamine methylene signal during the course

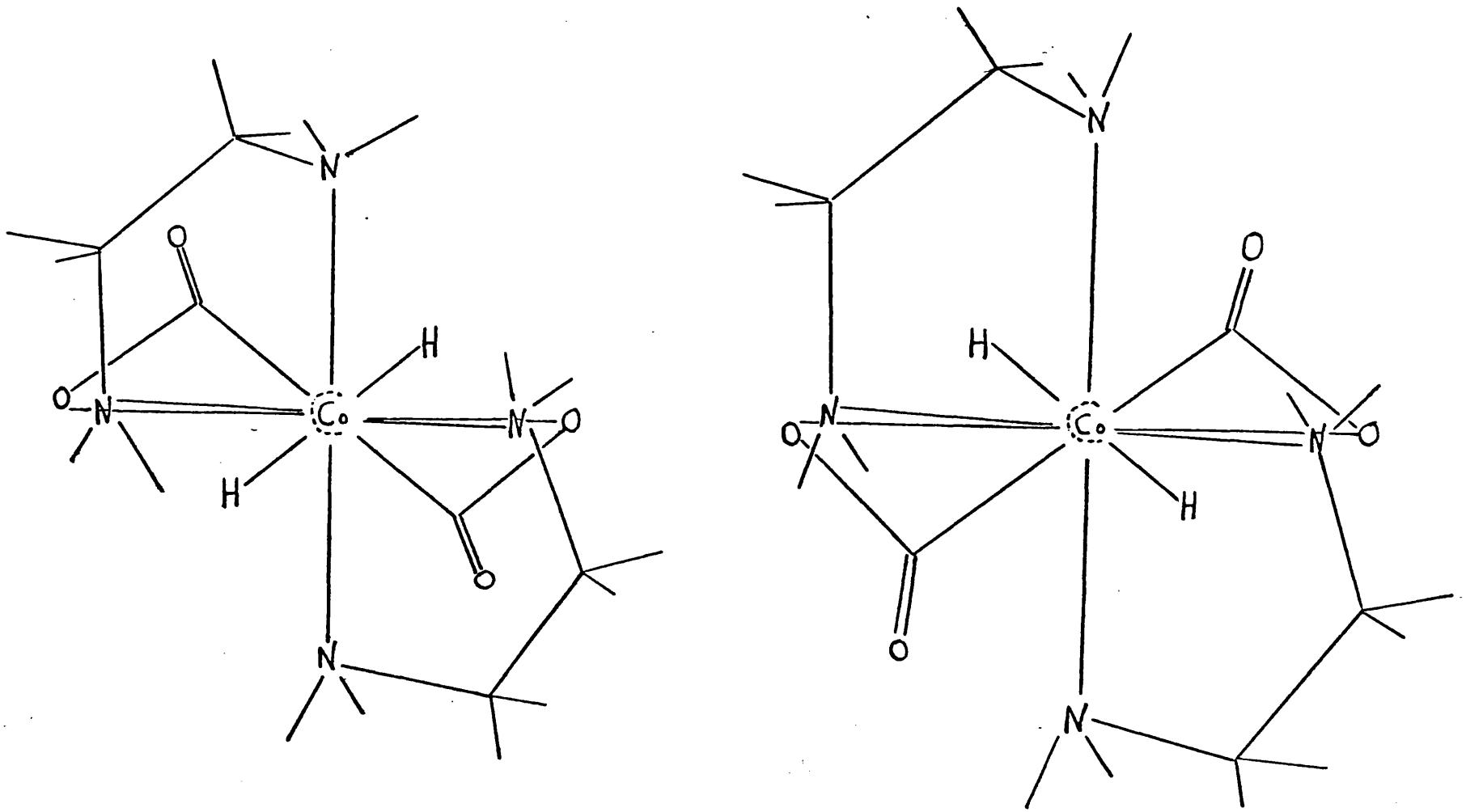

Figure 19: $[Coen_2mal]^+$ viewed down the cobalt-α-carbon (C_2) axis equivalence of α-hydrogens in the 'skew boat' conformations.

of deuteration, as described in the experimental section and treating the results in an identical manner to those of $[Comal_2en]^-$, the results summarised in Table 12 were obtained. Error was assessed as for $[Comal_2en]^-$.
m, the reaction order w.r.t. acid concentration was found to be 1.0 ± 0.02 at 37°C and 1.0 ± 0.1 for other temperatures.

Table 12.
Deuteration rate constants of the active methylene group in $[Coen_2mal]^+$ in acidic D_2O.

Temp °C	pD	$[D_3O^+]$ $M.L^{-1}$	$10^4 k'_{D(Acid)}$ sec^{-1}	$k_{D(Acid)}$ $L.M^{-1}sec^{-1}$
37 ± 0.5	2.37	0.0043	13.4 ± 0.5	0.312 ± 0.012
	2.47	0.0034	10.75± 0.4	0.316 ± 0.012
	2.68	0.0021	6.4 ± 0.35	0.307 ± 0.015
	2.87	0.00135	4.1 ± 0.3	0.304 ± 0.015
35 ± 0.5	2.68	0.0021	5.3 ± 0.35	0.252 ± 0.017
	2.87	0.00135	3.3 ± 0.3	0.246 ± 0.022
27 ± 1	2.04	0.0091	6.4 ± 0.5	0.070 ± 0.005
	2.43	0.0036	2.5 ± 0.5	0.070 ± 0.014
	2.55	0.0027	1.8 ± 0.4	0.067 ± 0.014
	2.62	0.0024	1.9 ± 0.4	0.079 ± 0.014
20 ± 1	2.04	0.0091	2.2 ± 0.3	0.024 ± 0.004

Table 13. Mean second order rate constants for $[Coen_2mal]^+$ in acidic D_2O.

Temp °C	$1/T°K$	$k_{D(Acid)}$ $L.M^{-1}sec^{-1}$	$\ln(k_{D(Acid)})$.
37 ± 0.5	0.003225	0.310 ± 0.013	-1.17 ± 0.04
35 ± 0.5	0.003246	0.250 ± 0.020	-1.35 ± 0.04
27 ± 1	0.003334	0.0715± 0.012	-2.64 ± 0.18
20 ± 1	0.003413	0.024 ± 0.004	-3.73 ± 0.18

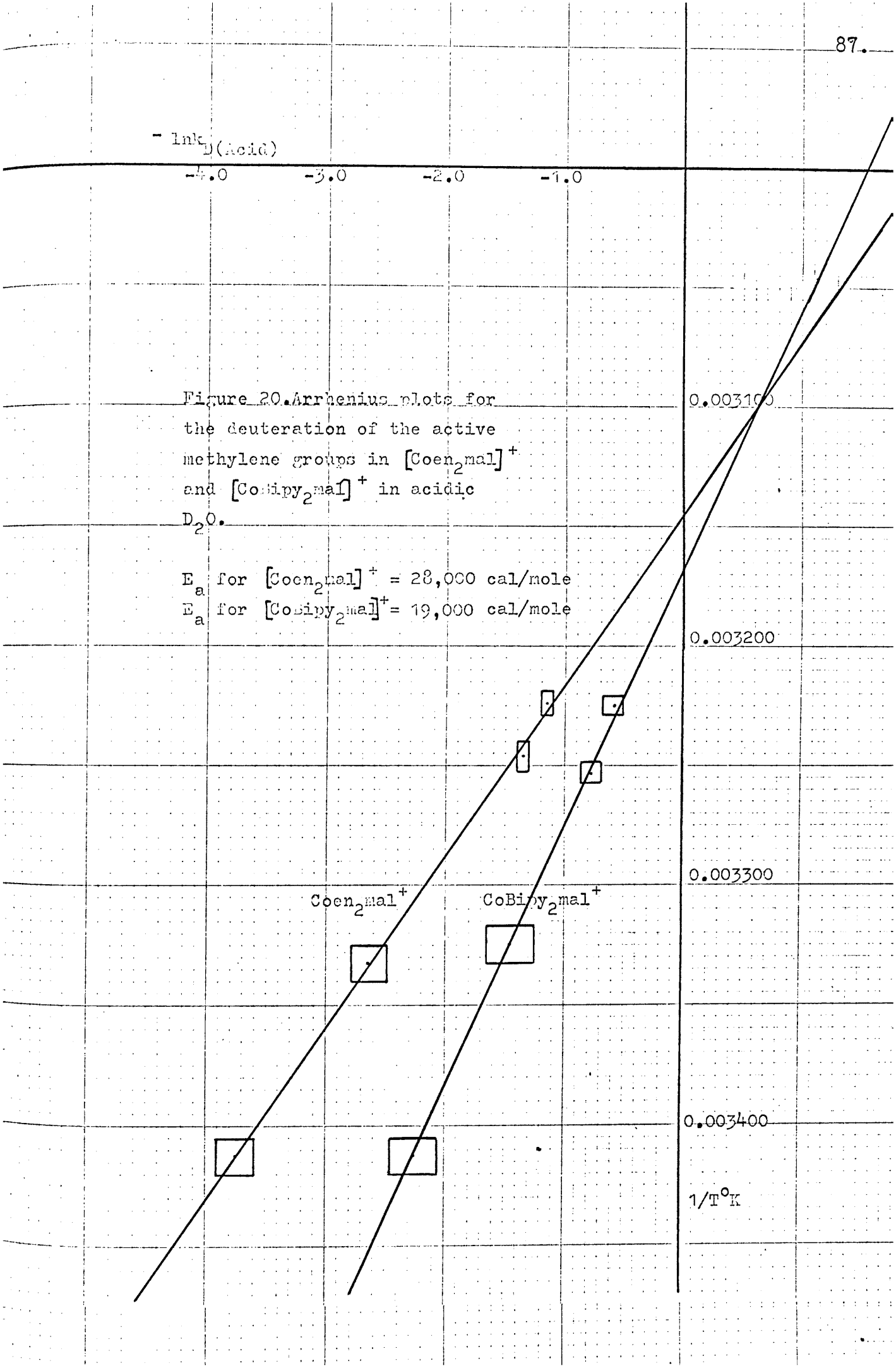

Figure 20. Arrhenius plots for the deuteration of the active methylene groups in $[Coen_2mal]^+$ and $[Cobipy_2mal]^+$ in acidic D_2O.

E_a for $[Coen_2mal]^+$ = 28,000 cal/mole
E_a for $[Cobipy_2mal]^+$ = 19,000 cal/mole

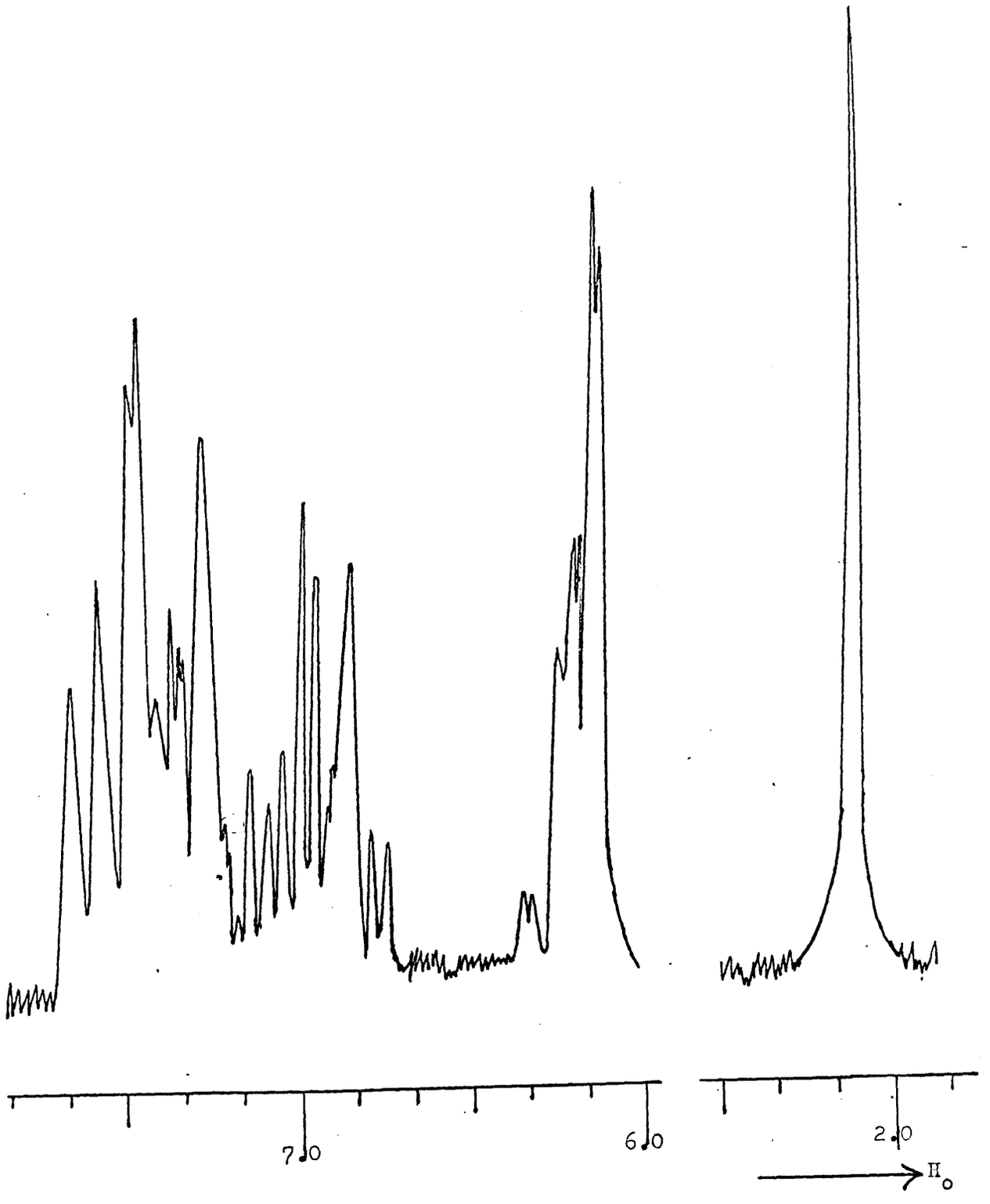

Figure 21. 60 MHz pmr spectrum of $[CoBipy_2ma]^+$ in 0.002 M D_2SO_4

An Arrhenius plot constructed from the data of Table 13 (Fig. 20) showed a linear relationship obeying the Arrhenius relationship.

$$k_{D(Acid)} = 1.3 \times 10^{19} e^{-28,000/RT} \qquad (38)$$

Activation parameters derived from this were: $E_a = 28 \pm 3$kcal/mole, $\Delta H^{\ddagger}(25^{\circ}C) = 27.4 \pm 3$kcal/mole, $\Delta G^{\ddagger}(25^{\circ}C) = 19.4 \pm 4$kcal/mole and $\Delta S^{\ddagger} = +27.0 \pm 6$ cal/deg/mole.

6.$[CoBipy_2mal]^+$.

The pmr spectrum of this complex is shown in Figure 21. The malonate methylene proton's signal occurs, as in $[Coen_2mal]^+$, at -2.11ppm. The same symmetry applies to both complexes.

The signals from the aromatic protons give the complex splitting pattern in the region -6 to -7ppm. Although a complete analysis was not necessary for this work, several characteristics of the pattern are apparent.
The signals are divided into two groups; one at about -7.3ppm and the other at about -6ppm, having relative intensities 3:1. The presence of an X proton, being separated by more than 6J from the other three is thereby confirmed. This is most likely to be derived from the 5,5' positions. The pmr spectra of cis and trans $[Cophen_2X_2]^+$ complexes have been reported and assigned(71) in terms of overlapping AB and ABX patterns. The cis complexes, as in the case of $[Coen_2mal]^+$, have each ligating N atom of each ligand cis and trans to X. Each half of the phenanthroline ligands thus experiences different fields and two overlapping ABX patterns and an AB pattern results. In the case of the trans complexes, there is an axis of symmetry through the 5,6 bond of each phenanthroline ligand and the cobalt atom. Each ABX pattern thus becomes equivalent and the 14 peaks of this and the 4 of the AB pattern were easily recognised. In the case of cis $[CoBipy_2mal]^+$ there is no separate two-spin system. The whole will comprise of two overlapping 4-spin systems each having an X component. An ABCX system(73) has a maximum of 50 lines, whilst the more likely possibility of $[AB_2X]$ has 30, all of which can be given explicitly.

Analysis on these grounds, however, is thwarted by there being two of such systems overlapping. The pmr spectrum of $[Comal_2Bipy]^-$ if $[CoBipy_2mal][Comal_2Bipy]$ could be split into its ions, or trans $[CoBipy_2X_2]^+$ would prove useful in this respect.

As described in the experimental section, the course of deuteration was monitored by measuring the malonato methylene proton's integral at as high an output as possible without incurring a high signal/noise ratio.
First order plots gave as good straight lines as obtained for $[Comal_2en]^-$ and $[Coen_2mal]^+$, even without the presence of a suitable 'reference' peak. Least squares analysis of the results gave a minimum correlation coefficient of 0.999.....
Treatment of the first-order rate constants was identical to that of the analogous ethylenediamine complex. **m**, the reaction order w.r.t. acid concentration was found to be 1.0 ± 0.02 at 37°C and 1.0 ± 0.1 at other temperatures. The results are summarised in Table 14.

Table 14.

Rate constants for the deuteration of active methylene protons in $[CoBipy_2mal]^+$ in acidic D_2O.

T°C	pD	$[D_3O^+]$ M.L.$^{-1}$	$10^4 k'_{D(Acid)}$ sec.$^{-1}$	$k_{D(Acid)}$ L.M.$^{-1}$sec^{-1}
37.0 ±	2.55	0.0028	14.3 ± 0.15	0.511 ± 0.006
0.5°C.	2.62	0.0024	13.3 ± 0.15	0.554 ± 0.007
	2.70	0.0020	11.1 ± 0.2	0.554 ± 0.010
	2.78	0.00165	9.7 ± 0.15	0.587 ± 0.020
34.5 ±	2.55	0.0028	12.3 ± 0.1	0.440 ± 0.004
0.5	2.70	0.0020	9.75± 0.1	0.475 ± 0.005
27.5 ±	2.04	0.0091	19.3 ± 1.5	0.212 ± 0.017
1	2.43	0.0037	7.4 ± 0.16	0.200 ± 0.005
	2.62	0.0034	5.6 ± 0.8	0.232 ± 0.033
	2.78	0.00165	4.8 ± 0.5	0.280 ± 0.030
20 ± 1	2.04	0.0091	9.5 ± 1.0	0.105 ± 0.010

Table 15.

Mean second order rate constants for $[CoBipy_2mal]^+$ in acidic D_2O.

T^oK	$1/T^oK$	$k_{D(Acid)}$ $L.M^{-1}sec.^{-1}$	$lnk_{D(Acid)}$
310 ± 0.5	0.003225	0.551 ± 0.015	-0.60 ± 0.10
307.5± 0.5	0.003253	0.457 ± 0.011	-0.78 ± 0.10
300.5± 1	0.003324	0.231 ± 0.023	-1.465 ± 0.20
293 ± 1	0.003413	0.105 ± 0.010	-2.26 ± 0.20

The mean second order rate constants (Table 15) were found to obey the Arrhenius relationship (Figure 20).

$$k_{D(Acid)} = 1.3 \times 10^{13}\ e^{-19,000/RT} \qquad (39)$$

Activation parameters derived as a result are: E_a = 19 ± 4kcal/mole, $\triangle H^{\ddagger}$ = 18.4 ± 4kcal/mole, $\triangle G^{\ddagger}(25^o)$ = 18.7 ± 5.5kcal/mole, $\triangle S^{\ddagger}$ = -1.0 ± 5 cal/deg/mole.

7. ADDITIONAL MEASUREMENTS.

(i) The base catalysed deuteration. At temperatures as low as 20°C and in borate/NaOD buffer at pD 8.8 all complexes showed no residual malonate α-proton signals one minute after initiation of the reaction. (One minute is the time taken to transfer the reaction mixture to the probe, adjust spinning-air against nitrogen pressure if working away from ambient temperature, lock and record the first integral). It would appear, therefore, to be impracticable to study the base catalysed reaction, where $t_{\frac{1}{2}} < 10$ secs in all cases.

(ii) Primary Isotope effect. $[Co(d_2\text{-mal})_2(d_4\text{-en})]^-$ and $[Co(d_4\text{-en})_2(d_2\text{-mal})]^+$ were prepared by allowing samples of the fully protonated complex to stand overnight in D_2O, rotary evaporating to dryness and repeating twice more. However, the large H_2O signal effectively obscured the malonato methylene signals making measurement of the latter impossible.

(iii) The effect of another electrophile. $[Comal_2en]^-$ was allowed to stand in freshly prepared bromine water and subsequ-

-ently precipitated by the addition of ethanol. Samples precipitated after 5 minutes or 5 hours showed the same extent of reaction. The AB pattern was found to diminish in intensity, and one sharp singlet was found to appear at -4.38ppm versus t-BuOH. i.e. Br^+ enters the complex stereospecifically. H_B is never completely brominated since the spin coupled AB pattern partly remains. Gravimetric analysis for Br^- revealed that about 60% of H_B had been substituted by Br^+. The analysis is complemented by the residual AB pattern.

DISCUSSION.

Table 16 summarises the second order rate constants for the acid catalysed deuteration of the active methylene protons in malonato and EDDA complexes of Co(III). Glycinate proton data is quoted from(93) at 95°C and malonate data at 37°C.

Table 16.

Note, H_A receives net sheltering in $[Comal_2en]^-$, whilst Sudmeier and Occupati assign their sheltered proton as H_B.

Complex	$k_{D(Acid)}$ $L.M^{-1}sec^{-1}$	$k^s_{D(Acid)}$ $L.M^{-1}sec^{-1}$	$k_{D(Acid)}/k^s_{D(Acid)}$
cis - $[Comal_2en]^-$	0.88	0.13	6.6 ± 0.8
trans-$[CoEDDA(en)]^+$	2.0×10^{-5}	2.0×10^{-6}	10 ± 3
trans-$[CoEDDA(dmen)]^+$	3.4×10^{-5}	3.1×10^{-6}	11 ± 3
trans-$[CoEDDA(deen)]^+$	6×10^{-5}	2.7×10^{-6}	22 ± 3
cis - $[Coen_2mal]^+$	0.31	-	-
cis - $[CoBipy_2mal]^+$	0.55	-	-

In explaining the low degree of stereospecificity of reaction in $[Comal_2en]^-$ compared to that in the trans-$[CoEDDA(diamine)]^+$ complexes, several factors must be invoked. The conformational mobility of co-ordinated malonate, the proximity of the sheltering moiety and the possibility of a nonstereospecific

reaction path.

It is impossible to specify absolutely the time averaged malonate conformation.

In the case of $[Coen_2mal]^+$, where the opposing repulsive forces displacing the co-ordinated malonate from conformation are exactly balanced, the average conformation is the 'skew boat' and one α -proton signal is observed. In $[Comal_2en]^-$, the 'skew boat' is unlikely to be the averaged conformations, - although certainly magnetic, and possibly steric inequivalency could arise from the 'skew boat'. The inequality of the repulsive forces acting on the malonate, irrespective of the relative motion of the two rings, has already been outlined (p.67) in some detail.

Within experimental error, the activation energies for the deuteration of H_A and H_B in $[Comal_2en]^-$ and the active methylene group in $[Coen_2mal]^+$, are the same, i.e. 28 $\pm$ 3kcal. $mole^{-1}$. This is good evidence for a lack of substantial steric and electronic difference in the environments of all three sets of protons. i.e. that the malonate rings are little displaced from the 'skew boat' conformations in $[Comal_2en]^-$.

Furthermore, the value of J_{AB}, 18Hz, in $[Comal_2en]^-$ compared with that in $[Comal_2Bipy]^-$, 16Hz, points(108) to a higher degree of planarity of the malonate ring in the former complex. The 'skew boat' is the most planar conformation available.

Contrary to these arguments, the second order rate constant for $[Coen_2mal]^+$, points to a substantial displacement from from the 'skew boat' in $[Comal_2en]^-$. Within experimental error, the rate constant lies midway between those for H_B and H_A. Any bias toward the value of H_A may be ascribed to the overall cationic charge of $[Coen_2mal]^+$, discouraging attack by an electrophilic species such as D_3O^+. It is unlikely that an approximately sterically equivalent environment provided by the 'skew boat' conformation would account for the relative rates in comparison to $[Coen_2mal]^+$, where malonate is in the 'skew boat' conformation.

Thus, although evidence exists for an averaged conformation of the malonate rings in $[Comal_2en]^-$ little displaced from the 'skew boat', the weightiest evidence lies on the side of a substantial displacement.

If this is indeed the case, it is interesting to note the

apparent lack of contribution from the steric factors involved to the energy of the transition state. This being so would point to the efficiency of D^+ as an electrophile. Quantitative investigation of Br^+ attack, which has been shown to be stereospecific (p.92) might prove informative as to the steric effect's contribution to the energy of the transition state, since the larger size of Br^+ would be expected to be more sensitive to such an effect.
No activation parameters for the acid catalysed deuteration of the trans-$[CoEDDA(diamine)]^+$ complexes are available for comparitive purposes.

Sudmeier and Occupati ascribe the sheltering of H_B in the trans-$[CoEDDA(diamine)]^+$ complexes to the ethylenediamine 'backbone' of the aminocarboxylate ligand. Molecular models indicate that H_B is situated approximately $1.5A^o$ from the octahedral edge spanned by the N atoms of the 'backbone', is protected by the 'backbone as a whole, and furthermore, is held in its sheltered position perminently because of the conformational rigidity, (apart from a limited 'puckering' ability), of the glycinate ring.
In comparison, $H_A(s)$ in $[Comal_2en]^-$ is situated, on average, between 0.5 and $2A^o$ from the ethylenediamine amino group(s).

A lack of stereospecificity in $[Comal_2en]^-$ of 30 $\pm$ 10% compared to that in $CoEDDA(en)^+$ would appear to be wholly ascribable to either, (a) a smaller sheltering factor or (b) a more remote environment - both as a result of time averaging.
As has been discussed, (b) is unlikely. Therefore, all other things being equal, the lower degree of stereospecificity in $[Comal_2en]^-$ is ascribed to the lesser sheltering effect of the amino groups.
"All other things" includes the nonstereospecific pathway postulated by Sudmeier and Occupati to account for the lower degree of stereospecificity found in the acid catalysed reaction compared to that in the base catalysed reaction. It is very unlikely that in the absence of such a nonstereospecific path, the steric factors already outlined would result in a degree of stereospecificity small enough to compare to that in the aminocarboxylate complexes which does include

the nonstereospecific route. Furthermore, in view of the self-buffering effect of $[Comal_2en]^-$ already noted (p.55) a dechelated species formed in a fast preequilibrium, able to react in a nonstereospecific manner in a distinct probability.

It may be noted from Table 16 that deuteration is effected considerably more easily in the malonato - than in the glycinato - containing complexes. $k_{D(Acid)}$(mal., 37°C): $k_{D(Acid)}$(gly., 95°C) is of the order 10^5:1.
It is proposed that, as in the case of the analogous amino-carboxylate complexes, a keto-enolate cation mechanism operates, having stereospecific and nonstereospecific reaction paths available. In addition, it is proposed that an appreciable fraction of the dechelated species, able to twist freely about the remaining donor oxygen-α-carbon and hence react in a nonstereospecific manner exists in a rapidly completed equilibrium with the starting complex. The greater ease of reaction found with $[Comal_2en]^-$ is ascribed to the presence of <u>two</u> carbonyl groups, which result in the production of resonance stabilised intermediates. <u>These</u> intermediates are expected to assist departure of a proton in the rate determining step in comparison to those of the aminocarboxylate complexes. - Scheme II(p.96).
Since the primary isotope effect was not investigated, an enolate mechanism is invoked by analogy with that for the aminocarboxylate complexes: $[CoEDTA]^-$(97) and <u>trans</u>-$[CoEDDA(en)]^+$(93). Sudmeier <u>et al</u>(94,95) have demonstrated enolate species in amino acid and aminocarboxylate complexes in 'superacid' medium at -80°C. ('Superacid' is the name given to such Friedel-Craft acids as; FSO_3-SbF_5-SO_2 or HF-SbF_5). Signals at low field, ascribed to $\diagdown C{=}OH^+$, were found in 'superacid', corresponding to protonated 'in-plane' and 'out-of-plane' carbonyl groups, which were absent in normal, aqueous solution.

Activation parameters for the deuteration of malonato complexes are summarised in Table 17.

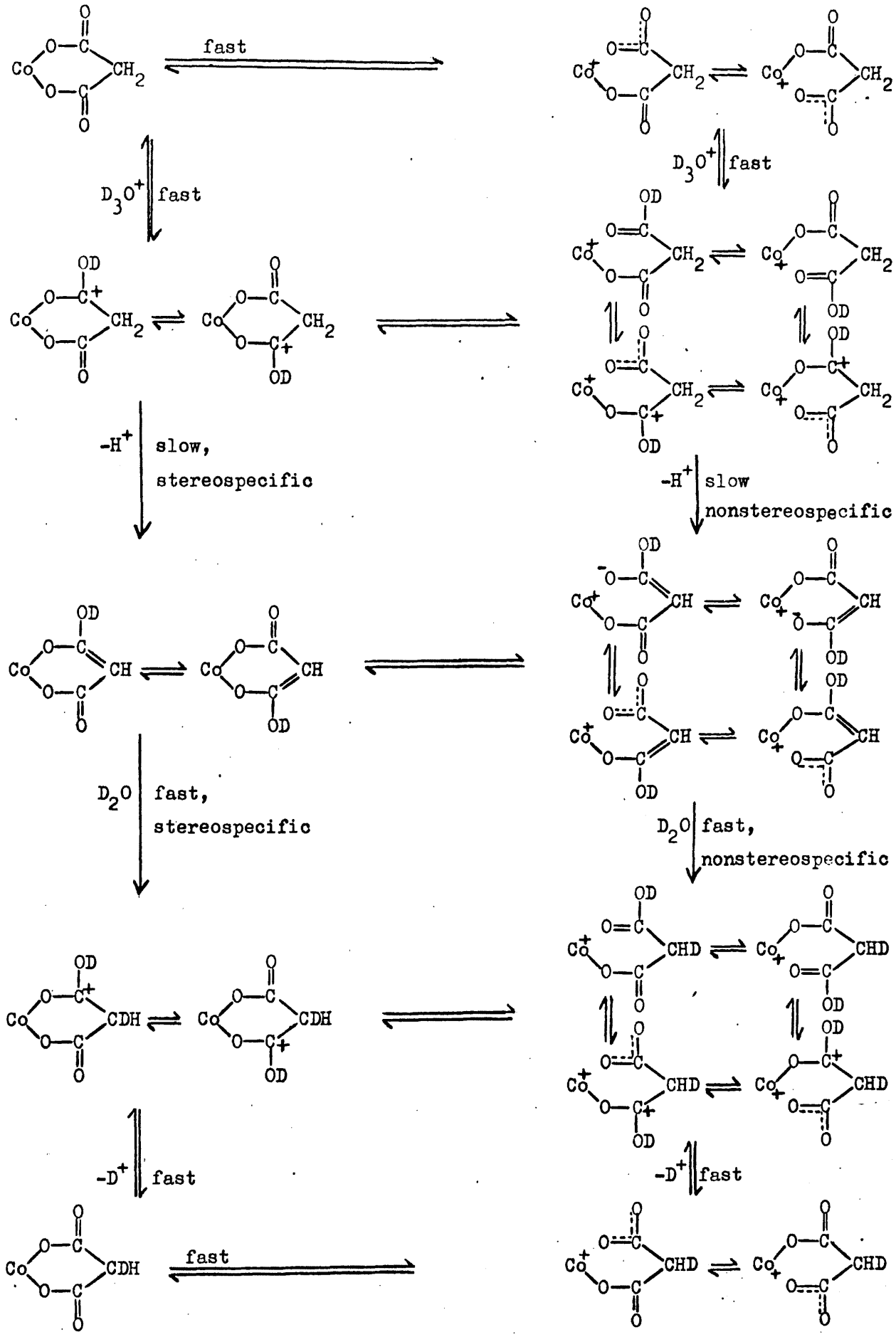
fast
D_3O^+ fast
OD
$-H^+$ slow, stereospecific
$-H^+$ slow nonstereospecific
nonstereospecific
D_2O fast, stereospecific
D_2O fast,
CH
CDH
CHD
$-D^+$ fast

SCHEME 3

Table 17.

Complex	E_a kcal.mole^{-1}	$\triangle H^{\ddagger}(25^{o})$ kcal.mole^{-1}	$\triangle G^{\ddagger}(25^{o})$ kcal.mole^{-1}	$\triangle S^{\ddagger}$ cal/deg/mole.
$[Comal_2en]^-$				
H_B	27 ± 3	26.4 ± 3	18.0 ± 7	+26.0 ± 10
H_A	27 ± 3	26.4 ± 3	19.5 ± 2	+22.0 ± 5
$[Coen_2mal]^+$	28 ± 3	27.4 ± 3	19.4 ± 4	+27.0 ± 6
$[CoBipy_2mal]^+$	19 ± 4	18.4 ± 4	18.7 ± 5.5	- 1.0 ± 5

It is proposed that the deuteration mechanisms for $[Coen_2mal]^+$ and $[CoBipy_2mal]^+$ involve keto-enolate intermediates as in the case of $[Comal_2en]^-$, but without those of the nonstereo-specific pathway. Dechelation is unlikely in view of the lack of self-buffering effect of these complexes - although it has been shown to occur in the case of the α-monosubstituted complexes $[CoEtmalen_2]^+$ and $[CoBzylmalen_2]^+$.(Part Two). Identical mechanisms are predicted from the equality of activation energies for H_B, H_A and $[Coen_2mal]^+$. The low value of E_a and also higher rates for $[CoBipy_2mal]^+$ are also reconcilable with the proposed mechanism.

π overlap can occur between the Co atom, d_{xy} orbital and the p_x orbital of the nitrogen of the bipyridyl ligand. Since the nitrogen is part of a π conjugated system, $p\pi$-$d\pi$ interaction with the cobalt atom and a net withdrawl of electrons from that atom into the aromatic rings would result in a similar withdrawl of electrons from the malonate rings, thereby polarising the $\backslash C{=}O$ bonds, and activating the carbonyl oxygens with respect to an incoming electrophile. Electron withdrawl from carboxylate ligands by an adjacent phenanthroline ligand has been demonstrated by infrared spectroscopy(36). Ir demonstrates the withdrawl by showing strengthening of the metal-oxygen bond in phenanthroline-carboxylate complexes compared to ammine and ethylenediamine-carboxylate complexes.

Such an effect is also expected for analogous bipyridyl complexes. As a result the acid catalysed deuteration is considerably facilitated in the case of $[CoBipy_2mal]^+$. Such a result is revealed thermodynamically in the form of a lower activation energy. A contribution to the lower value of E_a may also come from the reduced steric effect i.e. the lack of interferring amino-hydrogen atoms, already noted in the case of $[Comal_2Bipy]^-$(p.76).

Activation entropy $\triangle S^{\ddagger}$, values being substantially similar for $[Comal_2en]^-$ and $[Coen_2mal]^+$ reveal the virtual ineffectivness of the complexes overall charge in determining the transition state. The values may be attributed to release of water molecules of hydration in forming the transition state, (41b). The peculiarly low value for $[CoBipy_2mal]^+$ may be diagnostic of the complex having low affinity for water of hydration.

PART TWO

The base and the acid hydrolysis of the ethylmalonato- and the benzylmalonato-(bisethylenediamine) cobalt(III) cations.

INTRODUCTION.

1.THE BASE HYDROLYSIS OF THE DICARBOXYLATE-BISETHYLENEDIAMINE COBALT(III) CATIONS: $[Coen_2CO_3]^+$, $[Coen_2(C_2O_4)]^+$ and $[Coen_2mal]^+$.

The carbonato ion has been studied by Harris(62) and more recently by Farago(34). Farago found that the base catalysed reaction proceeds in two stages. First the ring opens, giving a hydroxo-carbonato intermediate, $[Coen_2(CO_3)(OH)]^o$, and secondly carbonate is abstracted to give dihydroxo product. Followed spectrophotometrically the intermediate is characterised by a large increase in absorbance around 30,000cm^{-1}.

As hydroxide concentration is increased the first stage rate becomes independent of base concentration whilst that of the second stage remains first order with respect to hydroxide. The first stage was therefore postulated to proceed by an S_N1CB, or ion pair mechanism (where$([Coen_2CO_3].OH)^o$ is the reactive species). Both predict limiting rates at high base concentration (p.21) when all the complex is in the form of the amido base or the ion pair respectively. The ring opening reaction was therefore postulated to go by cobalt-oxygen fission, since OH^- attack on the carbonyl carbon would not be expected to give a limiting rate. Taube(3) has also postulated cobalt-oxygen fission.

In dilute base, a plot of k_{obs} versus $[OH^-]$ was found to deviate from linearity(69). This was interpreted as being due to an acid catalysed path operating under the given conditions. This will be dealt with subsequently.

The ring opening reaction occured with retention of configuration. Loss of optical activity during the second stage, however, proceeded at a much faster rate than the hydrolysis reaction. A number of paths to racemisation or inversion were postulated, amongst which is the intramolecular mechanism for inversion of the cis-dihydroxo product later proposed by Farago(38).

In comparing carbonate exchange using $C^{14}O_3^-$ to racemisation, Harris(53) found a similar result to that of Pearce(69). Harris' conditions were at buffered pH $\sim$ 6.5, where the acid catalysed paths postulated by Pearce must operate.

The base hydrolysis of $[Coen_2(C_2O_4)]^+$ has been extensively investigated(87,3,37).

Harris et al(87) found second order kinetics at 71°C and $[OH^-]_{Max} = 10^{-2}M$. They postulated that dechelation, giving $[Coen_2(C_2O_4)(OH)]^0$ was rate determining. Under the conditions above, the products of the reaction are cis and trans $[Coen_2(OH)_2]^+$ in the equilibrium proportions proposed by Bjerrum and Rasmussen(15) as the product of isomerisation of the cis isomer.

Taube(3) has demonstrated by O^{18} exchange, that dechelation goes by carbon-oxygen fission:

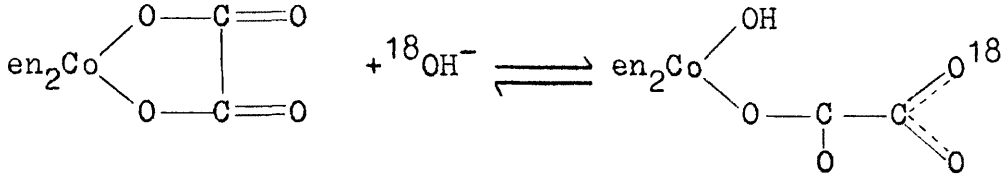

(J)

Intermediate

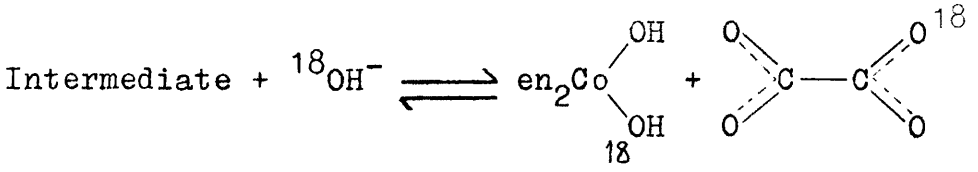

(K)

whilst abstraction of oxalate goes by normal metal-ligand cleavage.

Taube further suggested that terms higher order than first order in hydroxide may enter into the hydrolysis rate law.

Farago and Mason(37) have extended the work to high base concentrations (up to 4M) and low temperature. For the second stage, under Harris' conditions, Farago found simple second order kinetics, the products being the equilibrium mixture of the cis and trans dihydroxo ions. Since the rate of isomerisation of cis$[Coen_2(OH)_2]^+$ was much faster than the hydrolysis reaction(15), this was expected. Further, at low temperature and concentrated base, where hydrolysis is much faster than the isomerisation of cis$[Coen_2(OH)_2]^+$, the unisomerised cis dihydroxo product was expected. When the reaction was first-order w.r.t. hydroxide this was found. However, when a deviation from second-order kinetics was observed, (consistent with the suggestions of Taube), a mixture of cis and trans

$[Coen_2(OH)_2]^+$, indistinguishable from the cis/trans equilibrium mixture, was found, even when unisomerised cis was predicted.

The first stage of the reaction remains first order w.r.t. hydroxide.

Polarimetric studies show, under favourable conditions, a mutarotation,(indicating that dechelation goes with retention of configuration),followed by a rate of loss of optical activity equal to the rate of hydrolysis. No residual optical activity was observed under any of the conditions employed.

In view of the products and the kinetics the steric course of the second stage was ascribed two possibilities.

(a) A combination of the effects of the medium,(e.g. ion pairing),and of the leaving group on the distribution of intermediates in an S_N1CB mechanism (p.23).

In one instance intermediate B (p.23) produces racemic cis, and A is formed only at high base concentration to give trans.

In another, a change of medium alters the position of the incoming group in the trigonal bipyramid. i.e. A gives cis accompanied by net inversion from C, and at high base concentration gives trans with a corresponding decrease in net inversion from C.

(b) A change in the substrate, produced by OH^-, promoting a change to an associative mechanism. Such a species as:

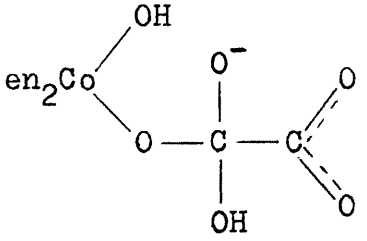

formed in concentrated alkali would be expected to decrease the acidity of the amine protons and encourage nucleophilic attack by a further OH^- molecule. Trans attack (p.25) would give, as observed, trans and racemic cis $[Coen_2(OH)_2]^+$.

Investigation of the base hydrolysis of $[Coen_2mal]^+$ is less well advanced.

In a preliminary survey Farago(34) found that the reaction

proceeded in one stage and that the rate, although showing first order dependence on $[OH^-]$ in dilute base, reached a limiting rate at about 2M $[OH^-]$. Products are the cis or cis/trans dihydroxo ion as expected according to conditions.

Subsequently, Farago(35) has ascribed the limiting rate to two possibilities.

(a) The reaction sequence is:

$$\underline{cis}[Coen_2mal]^+ + OH^- \xrightarrow{\text{slow } k} \underline{cis}[Coen_2mal.OH]^0 \qquad (L)$$

$$\underline{cis}[Coen_2mal.OH]^0 + OH^- \xrightarrow{fast} \underline{cis}[Coen_2(OH)_2]^+ \qquad (M)$$

$$\underline{cis}[Coen_2(OH)_2]^+ \rightleftharpoons \underline{trans}[Coen_2(OH)_2]^+ \qquad (N)$$

Dechelation is rate determining. $[Coen_2mal]^+$ can be removed from reaction (L) by formation of an unreactive conjugate base in a fast equilibrium:

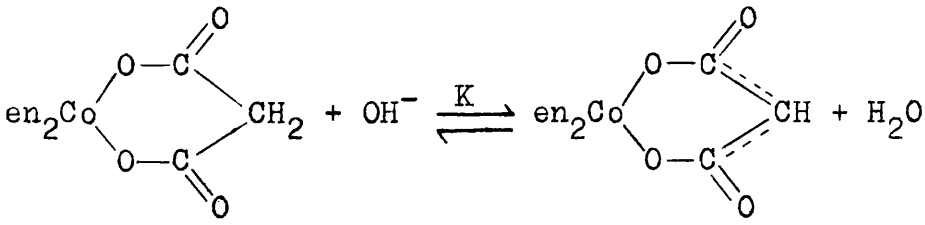

(P)

Total kinetics are: $$\text{Rate} = \frac{k[\text{complex}][OH^-]}{1 + K[OH^-]} \qquad (40)$$

i.e. in highly basic solution a limiting rate equal to k/K is predicted when equilibrium (P) lies dominantly to the right. At low $[OH^-]$ simple second order kinetics are observed, also as predicted.

(b) Dechelation is rapidly established in a fast preequilibrium (Q), followed by a rate determining dissociative process.

$$\underline{cis}[Coen_2mal]^+ + OH^- \underset{\text{fast}}{\overset{K'}{\rightleftharpoons}} \underline{cis}[Coen_2(mal)(OH)]^0 \qquad (Q)$$

$$\underline{cis}[Coen_2mal.OH]^{o} \xrightarrow{slow,k'} [Coen_2OH]^{2+} \qquad (R)$$

$$[Coen_2OH]^{2+} + OH^{-} \xrightarrow{fast} \underline{cis}[Coen_2(OH)_2]^{+} \qquad (S)$$

The direction of attack in reaction (S) being so as to give inversion or retention of configuration - as hydrolysis and loss of optical activity proceed at the same rates.
The rate equals $k'[C]_e$, where $[C]_e$ is the equilibrium concentration of the hydroxy-malonato intermediate. If [A] and [B] are the initial concentrations of complex and base. respectively, then:

$$\text{Rate} = \frac{k'K'[A][B]}{1 + K'[B]} \qquad (41)$$

When $[B] \ll 1$, simple second order kinetics are observed and the second order rate constant is equal to k'K' in equation (41). Derivation of the equilibrium constant from the second order rate constant or from the limiting first order rate constant in equation (40) gives identical results.
It is predicted also, that in concentrated base all the complex is in the form of the malonato-hydroxo intermediate and a limiting rate is reached, the rate constant being k'.

The reaction was found to follow the ionic strength dependence expression, (11)(p.10) proposed by Bronstead(17), to a reasonable degree of accuracy. Exact dependence is unlikely as Debye-Hückel theory does not usually apply at concentrations $> 10^{-2}$M. Nevertheless, scheme (b), involving a zero charged intermediate in the rate determining step would be expected to be independent of ionic strength. Scheme (a) would ideally be expected to show a linear log $k/\sqrt{\mu}$ relationship of slope 1.02 (at 25°) since it involves monopositive and mononegative ions in the rate determing step. Since this is in fact substantially true, it was taken as good evidence in favour of scheme (a).
Further, if dechelation proceeds via carbon-oxygen fission, by analogy with the oxalato complex, dechelation constitutes ester saponification.

Such reactions are characteristically irreversible(43) since the acid so formed easily loses a proton in the presence of the weakest of bases, to form a carboxylate anion which, in suppressing the electrophilic character of the carbonyl carbon, precludes reversibility of the reaction.

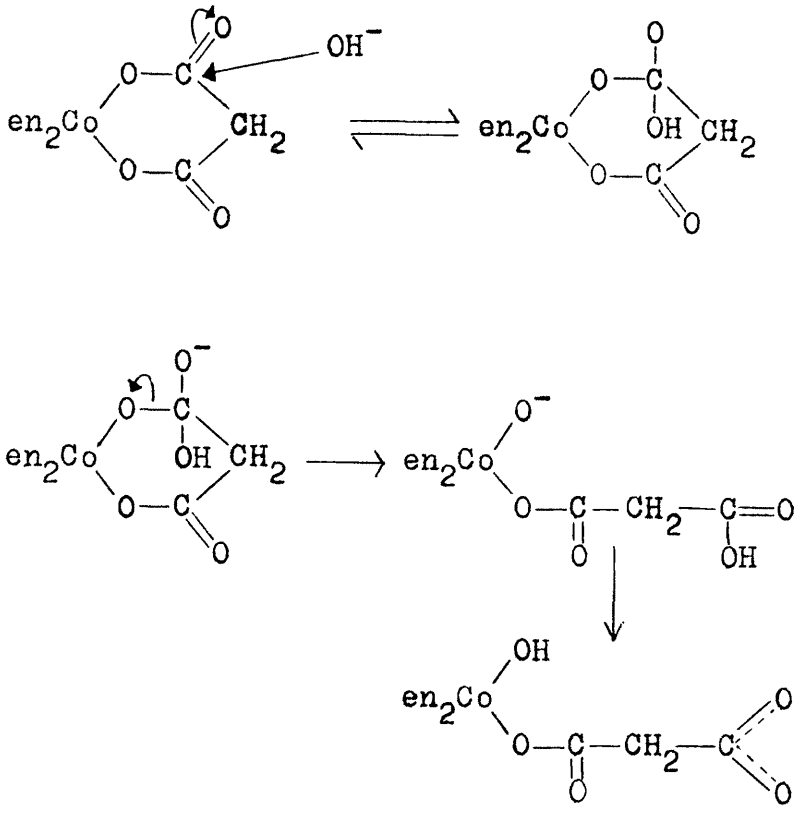

In such circumstances reaction (Q) would be invalid and scheme (b) unlikely.

Table 18.

Summary of the base hydrolysis of dicarboxylate bisethylenediamine cobalt(III) cations.

Complex	Dechelation fission	Ref.	Mechanism
$[Coen_2CO_3]^+$	Co - O	34,62	S_N1CB or S_N2 ion pair
$[Coen_2(C_2O_4)]^+$	C - O	3,37	S_N2
$[Coen_2mal]^+$	C - O	35	S_N2

The present work has introduced an extra effect in the hope of increasing the activation energy of the dechelation and hence rendering it observable. It is hoped that the effect will be substantially steric. Neither ethyl nor benzyl substituents on the α-position can conjugate, (benzyl not without tautomerism), any extra negative charge in the resonance stabilised intermediate established in (P) and hence render it and scheme (a) more favourable. A limiting rate observed in either dechelation or abstraction of substituted malonate would then confirm which scheme operates.

2. THE ACID CATALYSED HYDROLYSIS OF $[Coen_2CO_3]^+$.

Subsequent to the work of Harris et al(62) in which as a result of $C^{14}O_3^{2-}$ exchange in acid solution it was proposed that ring opening occurred, there have been several reports of the hydrolysis reaction itself.
Tong et al(101) proposed both acid-catalysed and noncatalysed pathways involving both protonated and unprotonated carbonate. However, unnecessary complication was introduced by working under non-buffered, non-pseudo first order conditions.
Harris and Sastri(52) obtained more convincing results over a large pH range (1 to 5). They proposed that ring opening is noncatalysed and that the only steps involving acidic species are protonation of the dechelated carbonate complex and subsequent hydrolysis of the resultant bicarbonato- species.

$$[Coen_2CO_3]^+ + H_2O \rightleftharpoons [Coen_2(H_2O)(CO_3)]^+ \quad (T)$$

$$[Coen_2(H_2O)(CO_3)]^+ + H^+ \rightleftharpoons [Coen_2(H_2O)(HCO_3)]^{2+} \; 1/K \quad (U)$$

$$[Coen_2(H_2O)(CO_3)]^+ + H_2O \xrightarrow{k_1} [Coen_2(OH)(H_2O)]^{2+} + HCO_3^- \quad (V)$$

$$[Coen_2(H_2O)(HCO_3)]^{2+} + H_2O \xrightarrow{k_2} [Coen_2(H_2O)_2]^{3+} + HCO_3^- \quad (W)$$

$$[Coen_2(H_2O)(HCO_3)]^{2+} + H_3O^+ \xrightarrow{k_3} [Coen_2(H_2O)_2]^{3+} + H_2CO_3 \quad (X)$$

Assuming that equilibrations (T) and (U) are established rapidly, the observed rate constant is given by:

$$k_{obs} = \frac{k_1K + k_2[H^+] + k_3[H^+]^2}{K + [H^+]} \qquad (42)$$

A 'best fit' computer programme demonstrated the substantial validity of rate equation (42).

Note: the production of an hydroxyaquo species provides a ready path to isomerisation, since this species has been shown to isomerise extremely rapidly(45).

By carrying out acid-base titrations in a flow apparatus Scheidegger and Schwarzenbach(86) found that ring opening in acid solution occurs by water attack on the cobalt, whilst in alkaline solution it goes by hydroxyl ion attack. Both hydroxo and carbonato ligands are subsequently susceptible to proton attack.

Jordon and Francis(58) used the equilibrium constants calculated by Scheidegger and Schwarzenbach to modify the rate expression (42) of Harris and Sastri. They proposed that ring opening involves hydroxyl ion attack and that the bicarbonato species produced are much more reactive than the carbonato species. k_2 and k_3 paths are those of Harris and Sastri whilst the k_1 path involves water attack on $[Coen_2(OH)(HCO_3)]^+$ rather than on $[Coen_2(H_2O)(CO_3)]^+$ to give the hydroxyaquo ion. Equilibria are:

$$[Coen_2CO_3]^+ + OH^- \rightleftharpoons [Coen_2(OH)(CO_3)]^0 \qquad K_0 \qquad (Y)$$

$$[Coen_2(OH)(CO_3)]^0 + H^+ \rightleftharpoons [Coen_2(OH)(HCO_3)]^+ \qquad 1/K_1 \qquad (Z)$$

$$[Coen_2(OH)(HCO_3)]^+ + H^+ \rightleftharpoons [Coen_2(H_2O)(HCO_3)]^{2+} \qquad 1/K_2 \qquad (A')$$

Equilibrium (A') is analogous to (U) proposed by Harris and Sastri, except that it involves the more reactive bicarbonato species. The total rate expression relating the observed pseudo first order rate constant to hydrogen ion dependence is then given by:

$$k_{obs} = \frac{k_1K_2 + k_2[H^+] + k_3[H^+]^2}{\frac{K_1K_2}{K_0K_W} + [H^+]} \qquad (43)$$

- where $K_W = [H^+][OH^-]$.

Using Scheidegger and Schwarzenbach's values for K_0,K_1 and K_2, k_1, k_2 and k_3 were evaluated. The values of K_2 also enabled Jordan to calculate these values according to Harris' rate law. Substantial agreement was found.

The present work presents only a preliminary survey of an analogous system. Whilst $[Coen_2(C_2O_4)]^+$(87) and $[Coen_2mal]^+$ (p. 61) are completely stable in acid solution, $[Coen_2Etmal]^+$ and $[Coen_2Bzylmal]^+$ are both observed to react readily at pH $\sim$ 3. Time did not permit the establishment of a complete rate law but good evidence was found for the various reactive species, from the kinetic dependence on $[H^+]$ and from the products of the reaction.

EXPERIMENTAL.

1. PREPARATION OF COMPLEXES.

$[Coen_2Etmal]Br.H_2O$ was prepared as already described (p.57).

$[Coen_2Bzylmal]Br.H_2O$ was prepared by a similar method, but with more difficulty.

$[Coen_2CO_3]Cl$,(6.1gm, 0.022mole), was dissolved with warming in 55ml of water. Silver oxide, freshly precipitated from silver nitrate, (8.5gm), and excess base, was added and the mixture well ground in a pestle and mortar. Silver chloride and excess dioxide were then filtered off and sodium bromide, (6.5gm), added. The solution was then heated to the boiling point and benzylmalonic acid, (4.3gm, 0.022mole), added with vigorous stirring. The solution was then alternatively heated and shaken in a separating funnel until all effervescence ceased. Finally, the volume of the solution was reduced to 45ml on a rotary evapourator, and the solution left to stand on ice. The deep red prismatic crystals that separated, were filtered at the pump and washed with a little ice-water and ethanol. Recrystallisation was from the minimum of boiling water. Yields were poor, and attempts to work up mother liquors resulted mainly in the deposition of yellow $[Coen_3]^{3+}$.

Maximum yield of recrystallised complex 20%.

Analysis: Calculated for $[CoC_{14}H_{24}N_4O_4]Br.H_2O$.

% C,35.90;H,5.56;N,11.95.

Found % C,36.07;H,5.58;N,11.49.

The uv-visible spectra of the two complexes, are shown in Figure 22. Ballhausen(7) has calculated the ligand field strength, 10Dq, associated with each d-d band under the influence of a strong ligand field (p.14). i.e:

$$\triangle E\ (^1A_{1g} \longrightarrow {}^1T_{2g}) = -115F_4 + 16F_2 + 10Dq \qquad (44)$$

$$\triangle E\ (^1A_{1g} \longrightarrow {}^1T_{1g}) = -35F_4 + 10Dq \qquad (45)$$

-where F_2 and F_4 are the Condon and Shortley ligand field

Figure 22. uv-visible spectra of :

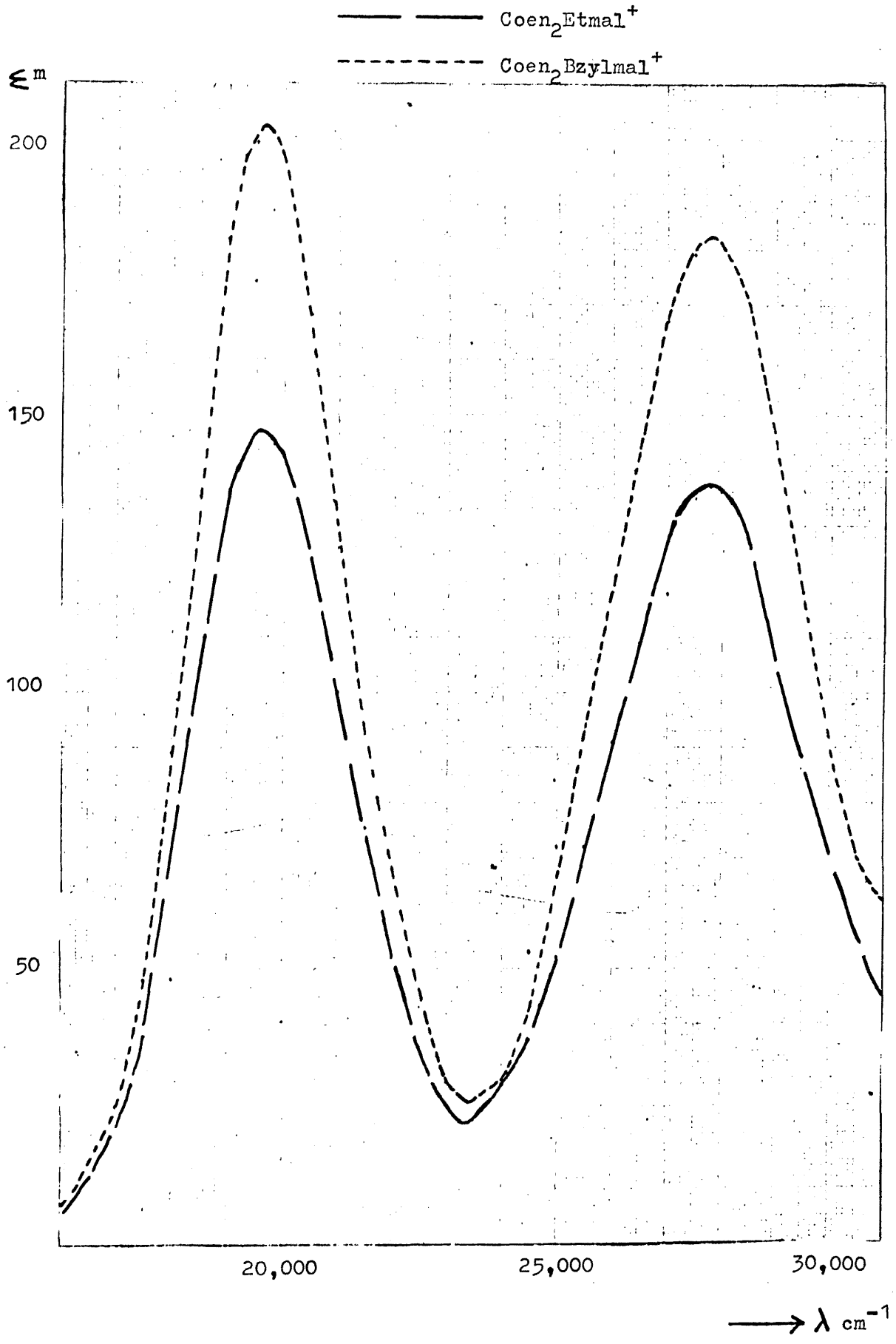

stabilisation parameters. Furthermore, a characteristic of the d^6 state is the approximation; $F_2 = 10F_4 = 1000cm^{-1}$. Using this approximation, 10Dq parameters are summarised in Table 19.

Table 19. Ligand field parameters for complexes of Co(III) containing co-ordinated malonate.

Complex	$^1A_{1g} \longrightarrow {}^1T_{1g}$ cm^{-1}	10Dq cm^{-1}	$^1A_{1g} \longrightarrow {}^1T_{2g}$ cm^{-1}	10Dq cm^{-1}
$[Coen_2mal]^+$	20,100	23,600	28,000	24,500
$[Coen_2Etmal]^+$	19,600	23,100	27,800	24,300
$[Coen_2Bzylmal]^+$	19,650	23,150	27,800	24,300

2. MEASUREMENT OF SPECTROPHOTOMETRIC RATES.

The main instrument used was an Unicam SP800 spectrophotometer fitted with a slave recorder and a repeat scan accessory, enabling up to four reactions to be followed simultaneously. Thermostating was by means of a water cooled thermostat/pump. For the lower temperatures studied, an extra coil immersed in a slush bath was incorporated into the thermostat circuit. Temperatures, checked using standard NPL thermometers, were always maintained to within $\pm$ 0.1°C.

Stock alkali was prepared from Volucan or BDH ampoules, and checked against known weights of potassium hydrogen phthallate. Stock solutions were always of the same concentration as the ionic strength required as constant for a set of $[OH^-]$ values under study.

Stock acid consisted of an acetate/HCl buffer, (0.100M in acetate), prepared according to the readings of a Pye Dynacap pH meter.

Ionic strength was maintained using NaCl. Perchlorate was found to precipitate both complexes when made up to the required strength in sodium perchlorate of the required ionic

strength. Complex/NaCl solutions are stable for at least eighteen months at room temperature.

Complex stock solutions were made up in NaCl of the required ionic strength. In this way, no matter in what proportions complex/NaCl, stock NaCl and stock NaOH are mixed to produce a range of values of $[OH^-]$, the ionic strength is automatically that of the stock NaCl solution.

Complex/NaCl, and NaCl/NaOH solutions were preheated in a divided vessel in a water bath to the required temperature, mixed, and rapidly transferred to the preheated cell in the thermostated cell compartment of the spectrophotometer. The reference cell always contained NaCl/NaOH solutions in the required proportions.

Both stages of the reaction were conveniently followed at $30,000cm^{-1}$. Checks at other wavelengths where the absorbance range was sufficient, showed that the rates for both stages were independent of wavelength.

For the measurements at 18^oC the reaction mixtures were kept in a thermostated water bath provided with an ice-cooled cooling coil and sampled at hourly intervals. The absorbance of each sample, quenched in an ice-methanol mixture, was then measured on an SP500 spectrophotometer.

RESULTS

1. THE BASE CATALYSED HYDROLYSIS.

(i) The Isomeric Course of the Reaction.

For both complexes, the reaction is observed to proceed in two stages. The first, by analogy to the spectrophotometric changes accompanying the base hydrolysis of $[Coen_2CO_3]^+$ and $[Coen_2(C_2O_4)]^+$, is ascribed to opening of the malonate ring. The reaction is characterised by a large increase in absorbance at the near uv end of the spectrum, so that the $^1A_{1g} \longrightarrow {}^1T_{2g}$ transition practically disappears, and by isobestic points at $18,600cm^{-1}$, $22,600cm^{-1}$, $26,700cm^{-1}$ and $29,100cm^{-1}$. This is demonstrated in Figure 23.

The second stage is characterised by a general fall in absorbance. There are no isobestic points. See Figure 24.

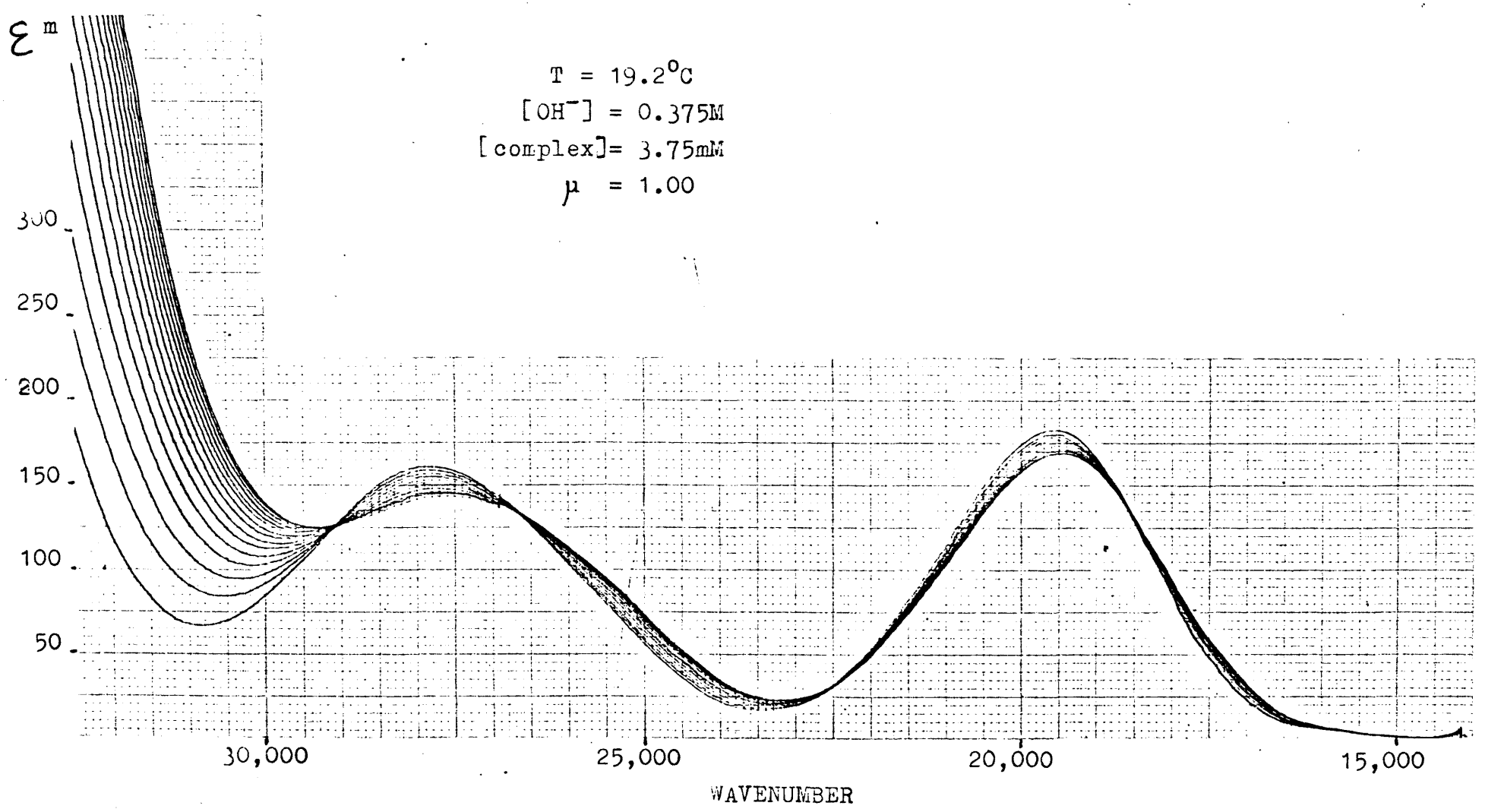

Figure 23, Spectral changes during the course of the ring opening stage of the base hydrolysis of $[Coen_2Bzylmal]^+$. Reaction was followed for ~ 35 minutes.

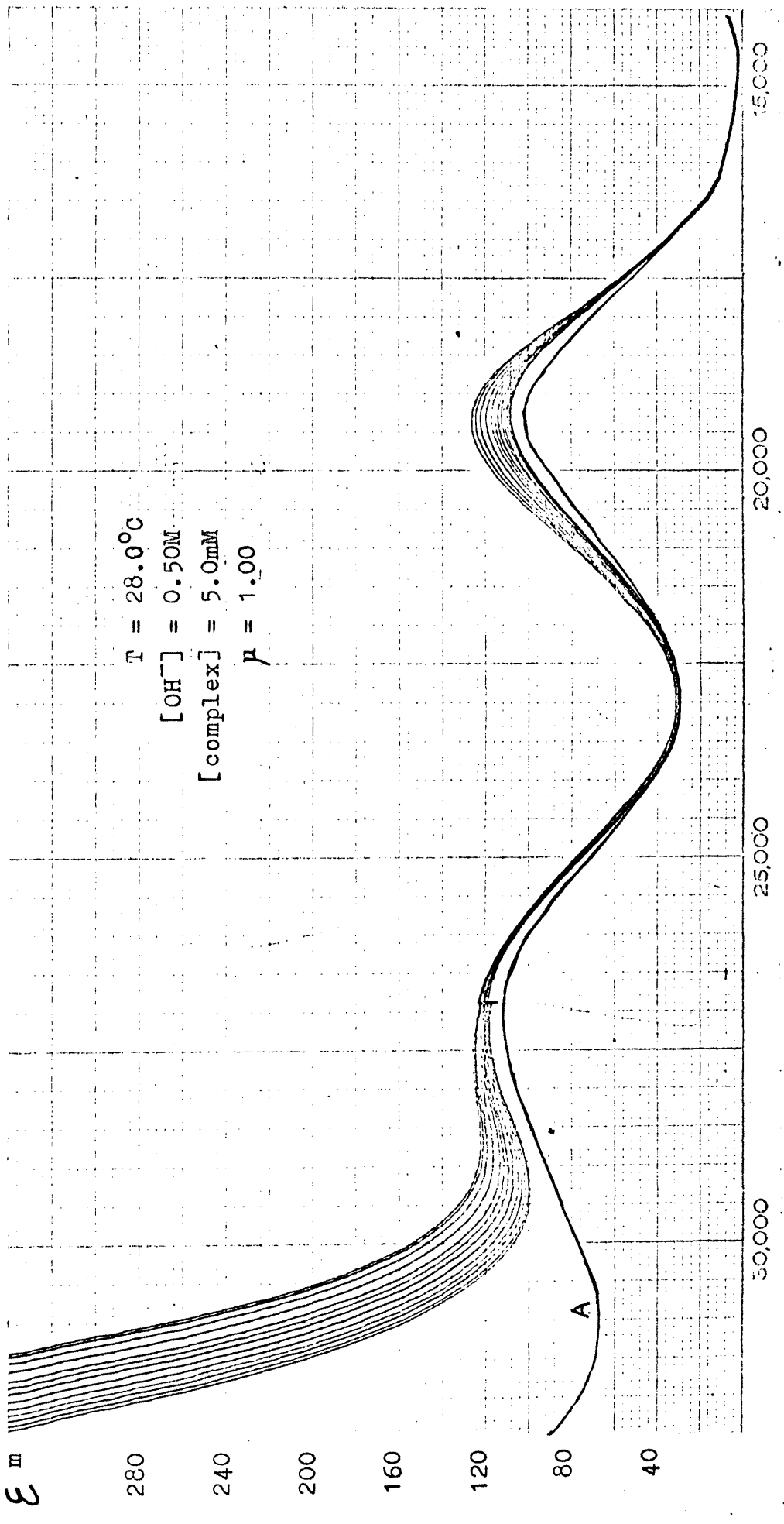

Figure 24. Spectral changes during the course of the second stage of the base hydrolysis of $[Coen_2Etmal]^+$. Reaction was followed for 9 hours (~ 2 half lives). Final spectrum (A) after 50 hours.

The product of the reaction is always cis-$[Coen_2(OH)_2]^+$ in equilibrium with the hydroxo-malonato intermediate produced in the first stage. Verification of the constitution of the final equilibrium mixture was undertaken as follows.
The ring opening stage was allowed to proceed under chosen conditions until the maximum amount of $[Coen_2(Rmal)(OH)]^0$ had accumulated. The reaction was then quenched by freezing. The conditions chosen were so that the effective product of the second stage would be cis-$[Coen_2(OH)_2]^+$. i.e. that the hydrolysis reaction would be very much faster than the isomerisation of the dihydroxo product. Since the latter is independent of $[OH^-]$(38,15) the required product can be effectively controlled by working at low temperature (27°C) and at high enough $[OH^-]$ to render $t_{\frac{1}{2}}^{isom.}/t_{\frac{1}{2}}^{hydrol.}$ at least 5,(where $t_{\frac{1}{2}}$ = the reaction half life).
Cis-$[Coen_2(OH)_2]^+$ was generated 'in situ' by the acid hydrolysis of $[Coen_2CO_3]ClO_4$ by perchloric acid and subsequent addition of alkali to pH12. This reaction does proceed with full retention of configuration(31). The solution of cis-$[Coen_2(OH)_2]^+$ was at the same concentration as '$[Coen_2(Rmal)(OH)]^0$' and was adjusted to the same ionic strength using sodium chloride. Molar extinction coefficient (ε_m) values corresponded to within ± 2% of the literature values(15).
The two solutions were then mixed in varying proportions. The mixtures were found to imitate the second stage reactions well, and the final spectrum of the hydrolysis reactions under conditions identical to those for the production of the $[Coen_2(Rmal)(OH)]^0$ solutions for the synthetic equilibrium mixtures, showed excellent agreement with spectra of cis-$[Coen_2(Rmal)(OH)]^0$/cis-$[Coen_2(OH)_2]^+$ mixtures at an approximate ratio of 1:9.
A specimen quasi 'equilibrium mixture' is reproduced in Figure 25 and can be compared to the authentic specimen in Figure 24.
Note the shift of the $^1A_{1g} \longrightarrow {}^1T_{2g}$ transition from 27,500cm^{-1} to 27,200cm^{-1} - a characteristic of the second stage reaction.
Table 20 summarises quasi and observed equilibrium mixtures for both complexes under varying conditions.

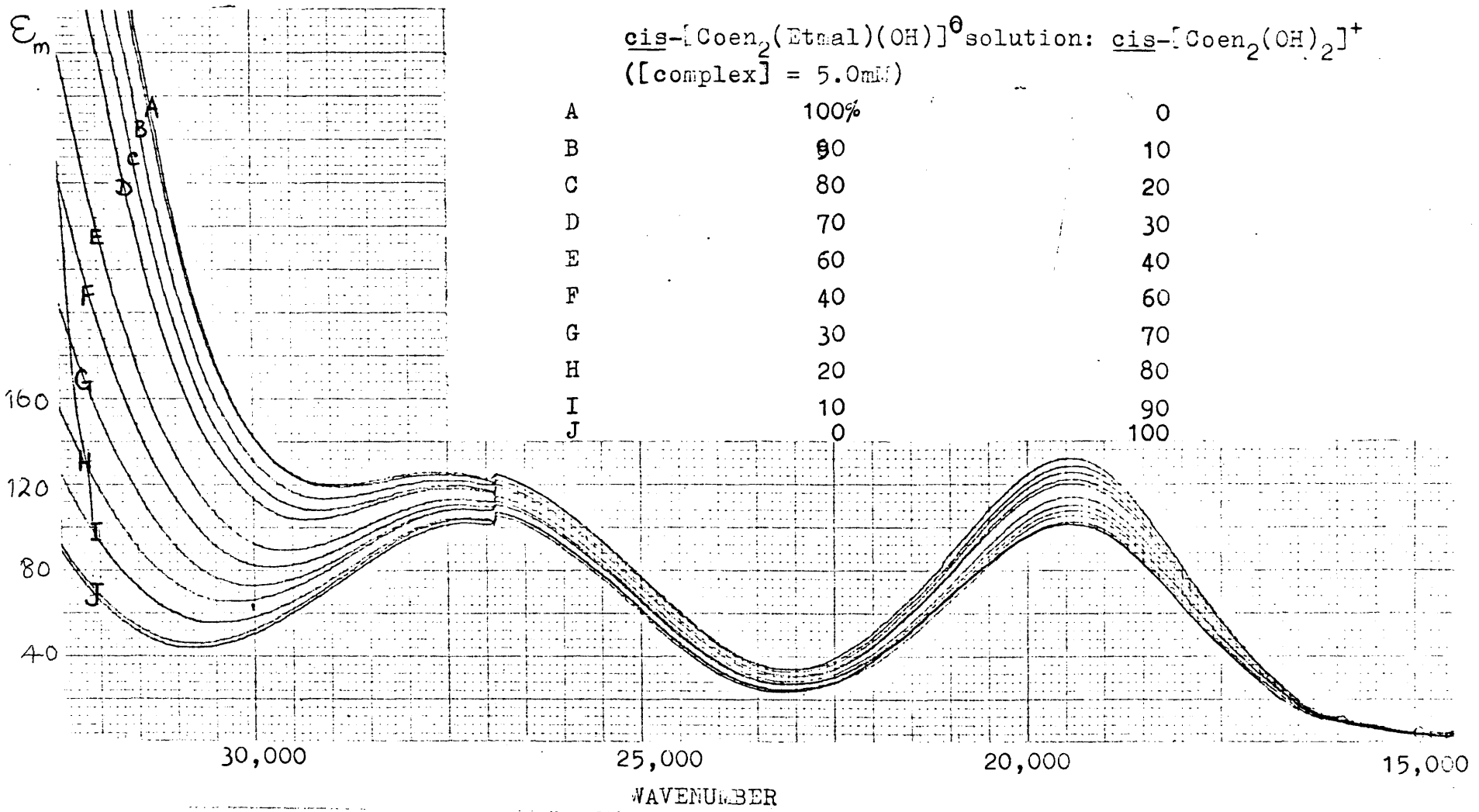

Figure 25. Synthetic equilibrium mixture spectra. Cis-[Coen$_2$(Etmal)(OH)]^0 + cis-[Coen$_2$(OH)$_2$]$^+$. Cis-[Coen$_2$(Etmal)(OH)]^0 generated at [OH$^-$] = 0.50M, T = 28.0°C.

Table 20. Summary of synthetic and observed equilibrium mixtures under varying conditions.
Note: mix = 1:9, cis-$[Coen_2(Rmal)(OH)]^0$ solution: cis-$[Coen_2(OH)_2]^+$
hyd.eq.= the observed equilibrium mixture.

Complex	T°C	$[OH^-]$	19,300cm^{-1}		23,000cm^{-1}		27,200cm^{-1}		30,000cm^{-1}	
			mix.	hyd.eq.	mix.	hyd.eq.	mix.	hyd.eq.	mix.	hyd.eq.
$Coen_2Etmal^+$	28.0	0.50	99	94	21	21	106	110	69	68
$Coen_2Etmal^+$	25.2	2.00	100	103	22	22	104	111	54	55.1
$Coen_2Bzylmal^+$	27.0	0.50	112	110	22	22	116	122	72	72
$Coen_2Bzylmal^+$	25.2	1.50	118	126	21	22	126	136	60	62.7

Conditions were also adjusted so that the isomerisation of cis-$[Coen_2(OH)_2]^+$ was much faster than the hydrolysis. Under these conditions the 1:1 cis/trans mixture, together with $[Coen_2(Rmal)(OH)]^o$ should be observed as the final products. This is only partly true. Spectra recorded after ten half lives, ($10t_{\frac{1}{2}}$), showed ε_m values in the low wavelength part of the spectrum lower than the literature(15) values of cis-$[Coen_2(OH)_2]^+$. (Values of ε_m ca.30,000cm^{-1} are always high, as this region is most sensitive to the intermediate $[Coen_2(Rmal)(OH)]^o$). However, substantial reaction always occurred after $10t_{\frac{1}{2}}$, by which time the cis/trans mixture was expected.

In other words, the cis isomer is always the product of the reaction regardless of conditions. Isomerisation rates found after ten half lives of the hydrolysis reaction agree moderately well with literature values(38,15). Reaction is observed to cease after a period corresponding to $10(t_{\frac{1}{2}}^{hyd.} + t_{\frac{1}{2}}^{isom.})$. Thus, the final amounts of cis-$[Coen_2(Rmal)(OH)]^o$ react to give cis-$[Coen_2(OH)_2]^+$, which only then can isomerise to the trans form.

Conditions employed had a maximum value of $t_{\frac{1}{2}}^{hyd.}/t_{\frac{1}{2}}^{isom.} \sim 4$. Larger values may give the cis/trans mixture as the effective product.

As a result of these observations the stoichiometric and isomeric course of the reaction may be represented as:

$$\text{cis-}[Coen_2Rmal]^+ + OH^- \rightleftharpoons \text{cis-}[Coen_2(Rmal)(OH)]^o \qquad (B')$$

$$\text{cis-}[Coen_2(Rmal)(OH)]^o + OH^- \rightleftharpoons \text{cis-}[Coen_2(OH)_2]^+ + Rmal^{2-} \qquad (C')$$

$$\text{cis-}[Coen_2(OH)_2]^+ \rightleftharpoons \text{trans-}[Coen_2(OH)_2]^+ \qquad (D')$$

If the equilibrium constant for (B') is large, it may be considered as unidirectional and taken as a separate reaction. Isomerisation of cis-$[Coen_2(C_2O_4)(OH)]^o$ has been shown to be very slow, ($t_{\frac{1}{2}} \sim 9$ days)(86). By analogy, the substituted malonato-hydroxo species are also deemed isomerisation-inert. That the reaction (B') proceeds with retention of configuration will be discussed later.

Because an equilibrium mixture is observed as the product of the reaction, the feasibility of the back reaction of (C') was investigated semi-quantitatively.

Cis-$[Coen_2(OH)_2]^+$, generated 'in situ' as previously described (p.115), was allowed to stand at room temperature in solutions, μ = 1.00,1.00M in disodium ethyl- and benzyl-malonate, i.e. in 'first order excess' quantities. The temperature was taken no higher than 21°C because of the isomerisation of cis-$[Coen_2(OH)_2]^+$.

After two weeks under these conditions, the back reaction was well characterised. A distinct rise in absorbance occurred ca.30,000cm^{-1} and the $^1A_{1g} \longrightarrow {}^1T_{2g}$ maximum shifted to 27,500cm^{-1}, (as in Figures 23 and 24). However, since isomerisation of the dihydroxo species occurred unavoidably over this period of time, quantitative assessment was not possible because of the complexity of the processes occurring. i.e:

$$\begin{array}{ccc} \text{cis-}[Coen_2(OH)_2]^+ & \overset{Rmal^{2-}}{\rightleftharpoons} & \text{cis-}[Coen_2(Rmal)(OH)]^0 + OH^- \\ \uparrow\downarrow & & \\ \text{trans-}[Coen_2(OH)_2]^+ & \overset{Rmal^{2-}}{\rightleftharpoons} & \text{trans-}[Coen_2(Rmal)(OH)]^0 + OH^- \end{array}$$

(ii) Equilibrium Constants.

In order to make an accurate assessment of equilibrium constant values, the intermediate$[Coen_2(Rmal)(OH)]^0$ is required. Unfortunately it could not be isolated in the case of either complex. Extraction of the basic solution containing the maximum quantity of the intermediate by such solvents as methylethyl ketone, dioxan and carbon tetrachloride proved unsuccessful; as did attempts at fractional precipitation using dioxan or tetrahydrofuran.

However, the ε_m value of the intermediate may be established as a result of the temperature and hydroxide concentration dependency of equilibrium (B'), at the most sensitive wavelength i.e. 30,000cm^{-1}.

Generally, temperature is proportional to the amount of the intermediate formed. Base concentration is more complicated in its effect.

At any temperature there is an optimum $[OH^-]$ to give an absorbance maximum at 30,000cm^{-1}. Primarily the effect of increasing $[OH^-]$ may be to push equilibrium (B') to the right.

After the optimum value of $[OH^-]$ ($\sim$ 0.75M) the effect is a result of a choice of mechanistic pathways. This became obvious as a result of the kinetics in concentrated base, and will be referred to in greater detail later. Because of this duality of mechanistic pathways and inevitable degrees of consecutiveness of the first and second stages, equilibrium constants for the first stage were not calculated.
The effect of varying conditions on the two stages of the reaction, followed at 30,000cm^{-1}, are demonstrated in Figure 26.
The ε_m values at 30,000cm^{-1}, for the intermediates $[Coen_2(Etmal)(OH)]^o$ and $[Coen_2(Bzylmal)(OH)]^o$ were calculated as follows.
Knowing the velocity of the second stage, the % reaction of the latter during the total observed course of the dechelation stage can be found. When this % is added to the observed maximum ε_m value, that of the intermediate should result. A vital assumption is that the equilibrium constant for equilibrium (B') is high under the conditions chosen. Whether or not it is high <u>enough</u> is impossible to say. However, even if the K values obtained are not absolute, their relative values are of interest.

Conditions chosen were those under which maximum absorbance was observed at 30,000cm^{-1}. That is $[OH^-]$ = 0.75M, T = 58.0°C for the benzylmalonato complex and $[OH^-]$ = 0.75M, T = 55.0°C for the ethylmalonato complex.

$$\varepsilon_{Coen_2(Etmal)(OH)^o} = 164 + (3.5 \pm 0.5\%) = 170 \pm 1$$

$$\varepsilon_{Coen_2(Bzylmal)(OH)^o} = 246 + (3.5 \pm 0.5\%) = 254 \pm 1$$

$$\varepsilon_{Coen_2(OH)_2^+} \quad (30kK) = 41(Ref.15)$$

The % <u>cis</u>-$[Coen_2(Rmal)(OH)]^o$ and <u>cis</u>-$[Coen_2(OH)_2]^+$ in the appropriate equilibrium (C') may then be calculated from:

$$\%\underline{cis}[Coen_2(OH)_2]^+ = \frac{\varepsilon_{Coen_2RmalOH^o} - \varepsilon_{equil.}}{\varepsilon_{Coen_2RmalOH^o} - \varepsilon_{Coen_2(OH)_2^+}} \qquad (46)$$

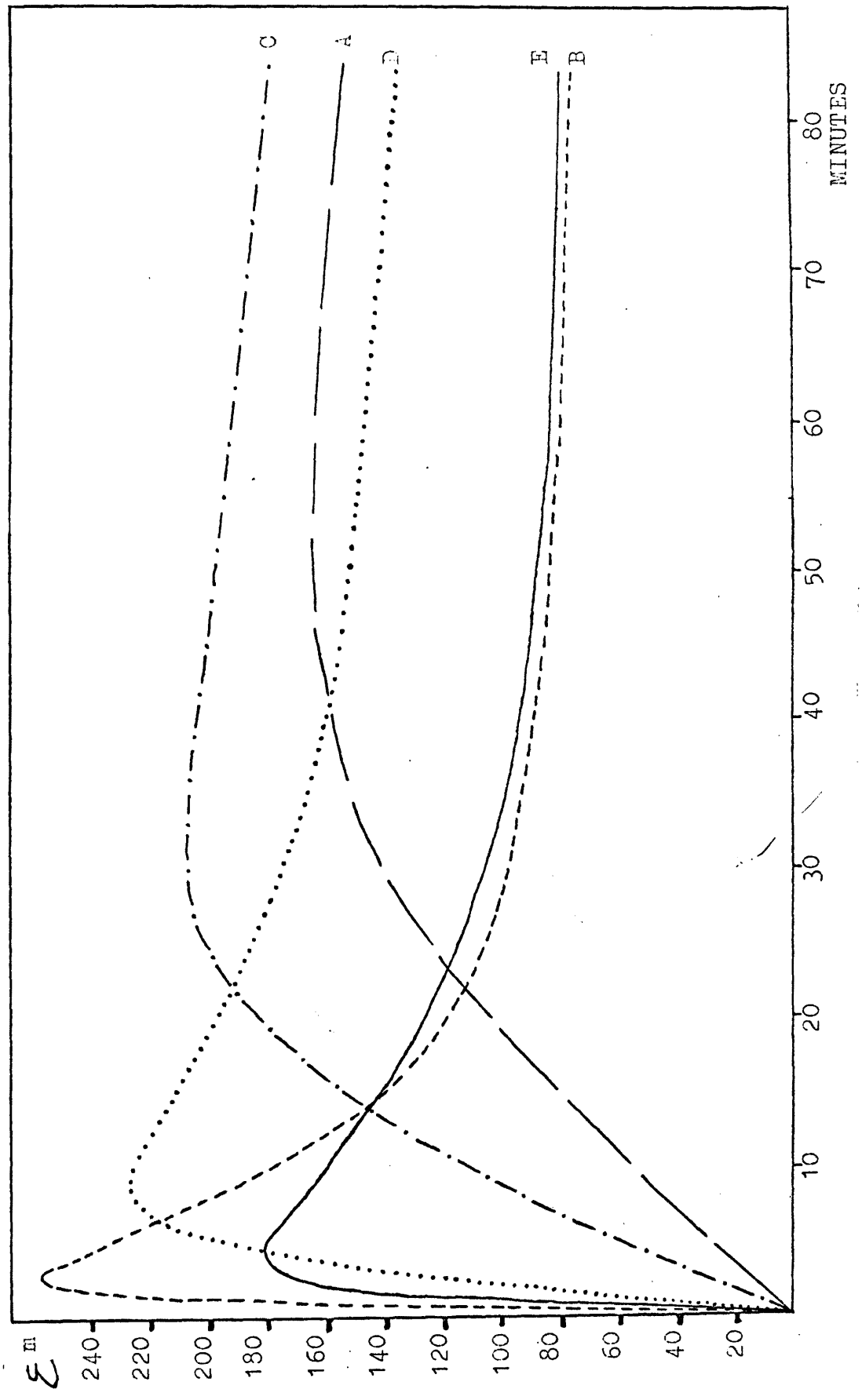

Figure 26. Spectral changes at 30,000cm^{-1} during the base hydrolysis of the $[Coen_2Bzylmal]^+$ ion: A,19.2°, $[OH^-]$=0.75M; B,58.0°, $[OH^-]$=0.50M; C,35.0°, $[OH^-]$=0.125M; D,35.0°, $[OH^-]$=0.75M; E,35.0°, $[OH^-]$=2.50M.

$$\%\underline{\text{cis}}[Coen_2(Rmal)(OH)]^o = \frac{\varepsilon_{equil.} - \varepsilon_{Coen_2(OH)_2^+}}{\varepsilon_{Coen_2RmalOH^o} - \varepsilon_{Coen_2(OH)_2^+}} \qquad (47)$$

where $\varepsilon_{equil.}$ is measured at 30,000cm^{-1}.
Under conditions of large excess of OH^- the equilibrium constant $K_{C'}$ for equilibrium (C') is given by:

$$K_{C'} = \frac{[Coen_2(OH)_2^+][Rmal^{2-}]}{[Coen_2(Rmal)(OH)^o]} \qquad (48)$$

and since $[Coen_2(OH)_2^+] = [Rmal^{2-}]$ at equilibrium (or at any time providing reaction (C') is under way):

$$K_{C'} = \frac{[\underline{\text{cis}}\ Coen_2(OH)_2^+]^2}{[\underline{\text{cis}}\ Coen_2(Rmal)(OH)^o]} \qquad (49)$$

Note.(i) $K_{C'}$ values are only calculated under those conditions where the isomerisation (D') is negligible.i.e. when an ∞ value fitting the observed pseudo first order rate constants is found after the appropriate time ($10t_{\frac{1}{2}}$). Final values obtained when $t_{\frac{1}{2}}^{isom.}/t_{\frac{1}{2}}^{hyd.} < 3$ do not correspond to $\varepsilon_{equil.}$ in equations (46) and (47). Furthermore equilibrium constant calculations involving ε_m values for the 1:1 cis/trans $[Coen_2(OH)_2]^+$ mixture from(15) are invalid, since the isomerisation has been shown to be a non-integral part of the hydrolysis reaction sequence.

(ii) A value of $t_{\frac{1}{2}}^{isom.}/t_{\frac{1}{2}}^{hyd.} = 3$, ($[OH^-] = 0.375M$, $T = 27.0^oC$) results in cis-$[Coen_2(OH)_2]^+$ as the observed product of the reaction after at least ten half lives. However, even a value of $t_{\frac{1}{2}}^{hyd.}/t_{\frac{1}{2}}^{isom.} = 4$,($[OH^-] = 0.125M$, $T = 58.0^oC$) did not result in cis/trans $[Coen_2(OH)_2]^+$ as the effective product.

$K_{C'}$ values, under suitable, unambiguous conditions are summarised in Table 21. They were checked at 19,200cm^{-1}. Error was estimated by the method of mean deviation since several runs contributed to each of the $\varepsilon_{equil.}$ values quoted.

Table 21. Equilibrium constants for the second stage of the base hydrolysis of $[Coen_2Etmal]^+$ and $[Coen_2Bzylmal]^+$.

Complex	T°C	$[OH^-]$M	$\varepsilon^m_{equil.}$(30kK)	%$[Coen_2(Rmal)(OH)]^0$	%$[Coen_2(OH)_2]^+$	$10^{-2}K_c$, M.L.$^{-1}$
$[Coen_2Etmal]^+$	35.0	1.50-3.00	59 ± 2	14 ± 1.5	86 ± 3	5.3 ± 1
		4.00	60 ± 2	15 ± 1.5	85 ± 3	4.8 ± 1
	25.2	1.50	56 ± 2	11.5 ± 1.5	88.5 ± 3	6.8 ± 1.5
		2.50	54 ± 2	10 ± 1	90 ± 3	8.4 ± 1.5
		3.75	56 ± 2	11.5 ± 1.5	88.5 ± 3	6.8 ± 1.5
	28.0	0.65	76 ± 3	27 ± 2	73 ± 3	2.0 ± 0.3
		0.45	76 ± 3	27 ± 2	73 ± 3	2.0 ± 0.3
$[Coen_2Bzylmal]^+$	35.0	1.50	70 ± 2	13.5 ± 1.5	86.5 ± 3	5.6 ± 1
		2.00	68 ± 1	12.5 ± 1	87.5 ± 2	6.1 ± 1
		2.50	67 ± 1	12 ± 1	88 ± 2	6.4 ± 1
		3.00	69 ± 2	13 ± 1	87 ± 3	5.8 ± 1.5
	25.2	1.50-3.75	65 ± 2	11 ± 1	89 ± 3	7.2 ± 1.5
	27.0	0.375	76 ± 1	16.5 ± 1	83.5 ± 2	4.2 ± 0.5
		0.45-0.75	75 ± 1	16 ± 1	84 ± 2	4.4 ± 0.5
	18.0	1.00	60 ± 1	9 ± 0.5	91 ± 2	9.2 ± 2
		0.50	57 ± 1	7.5 ± 0.5	92.5 ± 2	11.5 ± 2
		0.75	57 ± 1	7.5 ± 0.5	92.5 ± 2	11.5 ± 2

(iii) The Kinetic Course of the Reaction.

The kinetic study of the base hydrolysis was divided into two parts according to the two ionic strengths studied. Both parts were conveniently examined by the 'Isolation Method', (p.8). Base concentration was always maintained in large excess and pseudo first order rate constants were derived from the spectrophotometric data according to the standard integrated form of the rate law:

$$\text{Rate} = k_2 [\text{complex}][OH^-] \qquad (50)$$

when $[OH^-] \gg [\text{complex}]$, (p.9). Such pseudo first order rate constants demonstrated that the reaction is first order in complex.

Pseudo first order rate constants for the ring opening stage were derived from Guggenheim's method(41a), since no ∞ values for the reaction are obtainable.

Guggenheim's method applies only to first or pseudo first order reactions. The standard integrated form of a first order rate expression can be expressed as:

$$A_0 - A = A_0 e^{-kt} \qquad (51)$$

where A_0 is the initial absorbance, which is proportional to the initial concentration of the reactant under consideration, and $(A_0 - A)$ is the residual absorbance after time t. If a series of readings A' are taken at <u>exactly</u> regular intervals $(t + t')$ after A, then:

$$A_0 - A' = A_0 e^{-k(t + t')} \qquad (52)$$

Subtracting (52) from (51):

$$A' - A = A_0 e^{-kt}(1 - e^{-kt'}) \qquad (53)$$

i.e. $$kt + \ln(A' - A) = \ln A_0(1 - e^{-kt'}) \qquad (54)$$

The RHS is a constant term since t' was chosen as a constant time interval.

Therefore, $kt + \ln(A' - A) = C$ (55)

and plots of $\ln(A' - A)$ versus t are linear and of slope -k.

In practise, values of A' are chosen at least $1\frac{1}{2}$-2 half lives beyond A. The disadvantage of the method is that since some values of A are used twice, as A and as A', any error in these points is also incurred twice, even if its partner in the term (A' - A) is errorless. In practise, reasonable straight lines are rarely obtained beyond 4 half lives. A specimen Guggenheim plot for the ring opening stage of the base hydrolysis of $[Coen_2Bzylmal]^+$ is shown in Figure 27.

When $t_{\frac{1}{2}}^{isom.}/t_{\frac{1}{2}}^{hyd.} < 3$ and no ∞ value was observed for the second stage, pseudo first order rate constants were again derived from Guggenheim's method. When $t_{\frac{1}{2}}^{isom.}/t_{\frac{1}{2}}^{hyd.} > 3, \infty$ values were observed after 10 $t_{\frac{1}{2}}^{hyd.}$, which, when used in semi-log plots gave excellent straight lines over at least 5 half lives. Semi-log plots for evaluation of second stage data were always employed when $[OH^-] > 1M$, μ = 4.00, but Guggenheim's method was necessary when $[OH^-] < 1M$, μ = 1.00 at T = 35°C, 45°C and 55°C.

In solutions μ = 1.00 and $[OH^-] < 1M$, plots of pseudo first order rate constants versus $[OH^-]$ were found to be linear and passed through the origin: thereby demonstrating that the reaction is first order in $[OH^-]$ and that no neutral, uncatalysed rate exists. These observations apply, within the limits of experimental error, to both ring opening and to malonate-abstraction stages for both complexes.

Kinetic data in μ = 1.00 solutions, having $[OH^-] < 1M$ are summarised in Tables 22(a) and (b), and 23(a) and (b). Overall second order rate constants were derived by dividing pseudo first order rate constants by $[OH^-]$ according to equation(5) (p.9).

Pseudo first and hence second order rate constants for the ring opening stage are denoted; $k_1^{'E}$ and $k_1^{'B}$, and $k_2^{'E}$ and $k_2^{'B}$, where E referes to ethyl and B to benzyl. Net forward reaction pseudo first order and hence second order rate constants for the second stage are; $(k_1^{"E} + k_{-1}^{"E})$ and $(k_1^{"B} + k_{-1}^{"B})$, and $k_2^{"E}$ and $k_2^{"B}$ respectively. Values of $k_1^{"}$ and $k_{-1}^{"}$ were derived between the expressions:

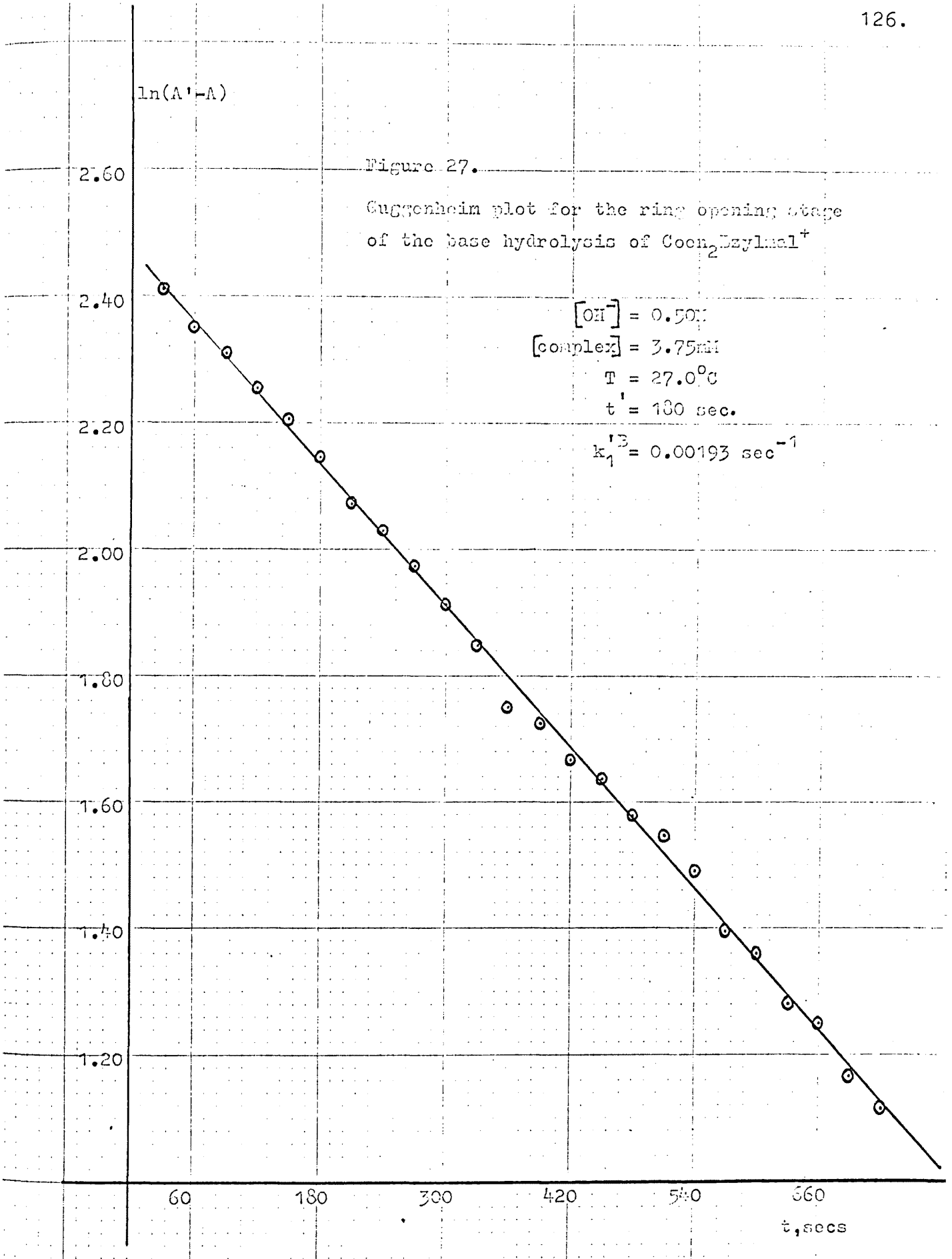

Figure 27.

Guggenheim plot for the ring opening stage of the base hydrolysis of $Coen_2Dzylmal^+$

$[OH^-]$ = 0.50M

[complex] = 3.75mM

T = 27.0°C

t' = 180 sec.

$k_1'^B$ = 0.00193 sec^{-1}

Table 22(a). Observed, pseudo first order and derived, second order rate constants for the ring opening stage of the base hydrolysis of $[Coen_2Etmal]^+$.

[complex] = 5.0mM *[complex] = 3.33mM

T°C	$[OH^-]$M	$10^2 k_1'^E sec^{-1}$	$10^2 k_2'^E$ L.M^{-1}sec^{-1}
18.0 ± 0.1	0.65	0.129 ± 0.005	0.198 ± 0.007
	0.75	0.159 ± 0.005	0.212 ± 0.007
	0.833*	0.181 ± 0.002	0.217 ± 0.003
28.0 ± 0.1	0.45	0.225 ± 0.003	0.500 ± 0.007
	0.50	0.244 ± 0.005	0.488 ± 0.010
	0.65	0.313 ± 0.007	0.482 ± 0.011
	0.75	0.379 ± 0.016	0.505 ± 0.021
35.0 ± 1	0.45	0.380 ± 0.017	0.845 ± 0.038
	0.50	0.445 ± 0.017	0.890 ± 0.034
	0.65	0.550 ± 0.012	0.846 ± 0.018
	0.75	0.632 ± 0.020	0.843 ± 0.027
45.0 ± 0.1	0.45	0.962 ± 0.040	2.14 ± 0.09
	0.50	1.07 ± 0.02	2.14 ± 0.045
	0.65	1.36 ± 0.035	2.10 ± 0.05
	0.75	1.64 ± 0.06	2.16 ± 0.08

Table 22(b). Observed, pseudo first order and derived second order rate constants for the second stage of the base hydrolysis of $[Coen_2Etmal]^+$.

[complex] = 5.0mM; $K_{C'}$ = 2.0 ± 0.3 x 10^2(28°C)$M.L^{-1}$

T°C	$[OH^-]_M$	$10^3(k_1''^E + k_{-1}''^E)$ sec^{-1}	$10^3k_1''^E$ $sec.^{-1}$	$10^6k_{-1}''^E$ $sec.^{-1}$	$10^3k_2''^E$ $M.L^{-1}sec^{-1}$
28.0 ± 0.1	0.45	0.0365 ± 0.0005	0.0363	0.182	0.0811 ± 0.0011
	0.50	0.0400 ± 0.0006	0.0398	0.198	0.0800 ± 0.0012
	0.65	0.0564 ± 0.0015	0.0561	0.267	0.0868 ± 0.0023
	0.75	0.0642 ± 0.0050	0.0639	0.320	0.0855 ± 0.0067
35.0 ± 0.1	0.45	0.105 ± 0.005			0.234 ± 0.011
	0.50	0.118 ± 0.003			0.234 ± 0.008
	0.65	0.150 ± 0.002			0.231 ± 0.003
	0.75	0.177 ± 0.003			0.236 ± 0.004
45.0 ± 0.1	0.45	0.410 ± 0.008			0.911 ± 0.018
	0.50	0.451 ± 0.010			0.903 ± 0.020
	0.65	0.620 ± 0.005			0.954 ± 0.008
	0.75	0.712 ± 0.008			0.949 ± 0.011
55.0 ± 0.1	0.50	1.465 ± 0.025			2.93 ± 0.05
	0.75	1.915 ± 0.010			2.56 ± 0.02

Table 23(a). Observed, pseudo first order and derived second order rate constants for the ring opening stage of the base hydrolysis of $[Coen_2Bzylmal]^+$.

[complex] = 3.75mM *[complex] = 2.81mM

T°C	$[OH^-]$M	$10^2 k_1'^B sec^{-1}$	$10^2 k_2'^B$ L.M^{-1}sec^{-1}
19.2 ± 0.1	0.375	0.0578 ± 0.0016	0.154 ± 0.004
	0.50	0.0689 ± 0.0011	0.139 ± 0.002
	0.75	0.112 ± 0.002	0.149 ± 0.003
27.0 ± 0.1	0.375	0.139 ± 0.002	0.371 ± 0.006
	0.50	0.205 ± 0.022	0.410 ± 0.044
	0.75	0.297 ± 0.015	0.396 ± 0.020
	0.813*	0.322 ± 0.017	0.396 ± 0.021
35.0 ± 0.1	0.125	0.138 ± 0.002	1.10 ± 0.02
	0.375	0.374 ± 0.011	1.00 ± 0.03
	0.50	0.485 ± 0.010	0.970 ± 0.020
	0.75	0.702 ± 0.017	0.940 ± 0.020
48.0 ± 0.1	0.125	0.315 ± 0.020	2.52 ± 0.16
	0.20	0.495 ± 0.020	2.48 ± 0.10
	0.50	1.22 ± 0.09	2.44 ± 0.18
	0.75	1.55 ± 0.04	2.16 ± 0.05

Table 23(b). Observed, pseudo first order and derived second order rate constants for the second stage of the base hydrolysis of $[Coen_2Bzylmal]^+$.

T°C	[complex]	$[OH^-]$M	$10^3(k_1^{"B} + k_{-1}^{"B})sec^{-1}$	$10^3k_1^{"B}sec^{-1}$	$10^7k_{-1}^{"B}$ sec^{-1}	$10^3k_2^{"B}$ $M.L^{-1}sec^{-1}$
18.0	10.7	0.50	0.00795 ± 0.00050	0.00794	0.0690	0.0160 ± 0.0010
	10.1	0.75	0.0129 ± 0.0007	0.0128	0.112	0.0172 ± 0.0009
	11.6	1.00	0.0177 ± 0.0010	0.01755	0.154	0.0177 ± 0.0010
27.0	3.75	0.375	0.0263 ± 0.0013	0.0262	0.610	0.0702 ± 0.0035
	3.75	0.50	0.0333 ± 0.0015	0.0332	0.772	0.0667 ± 0.0010
	3.75	0.75	0.0528 ± 0.0015	0.0527	1.23	0.0705 ± 0.0020
	2.81	0.313	0.0613 ± 0.0027	0.06105	1.42	0.0740 ± 0.0033
35.0	3.75	0.125	0.0308 ± 0.0006			0.246 ± 0.005
	3.75	0.375	0.102 ± 0.002			0.272 ± 0.005
	3.75	0.50	0.134 ± 0.006			0.268 ± 0.012
	3.75	0.75	0.193 ± 0.010			0.257 ± 0.013
48.0	3.75	0.125	0.192 ± 0.002			1.53 ± 0.02
	3.75	0.20	0.307 ± 0.002			1.53 ± 0.02
	3.75	0.50	0.732 ± 0.017			1.47 ± 0.03
	3.75	0.75	1.05 ± 0.03			1.41 ± 0.04
58.0	3.75	0.125	0.576 ± 0.007			4.61 ± 0.06
	3.75	0.50	2.05 ± 0.02			4.10 ± 0.04
	3.75	0.75	2.94 ± 0.03			3.92 ± 0.04

$$k''/k''_{-1} = K_{C'} \quad (56)$$

and

$$(k''_1 + k''_{-1}) = k_{obs} \quad (57)$$

under conditions where $K_{C'}$ was derived unambiguously.

Pseudo first order rate constants, for any given set of conditions, derived from Guggenheim's method were reproducible to within 10%, whilst those from semi-log plots were reproducible to within 7%. At least four runs were measured under any set of conditions and error was estimated from the mean deviation.

Specimen pseudo first order rate constant versus $[OH^-]$ plots are shown in Figure 28. Such plots were found in all cases to be linear, and hence the rate laws governing both stages of the reaction are:

$$\text{Rate} = k'_2[Coen_2Rmal^+][OH^-] \quad (58)$$

$$\text{Rate} = k''_2[Coen_2Rmal.OH^o][OH^-] \quad (59)$$

Arrhenius plots were constructed for both stages of the reaction for both complexes from the mean second order rate constants,(Figures 29 and 30). The Arrhenius relationship was found to be obeyed over the temperature range studied, and the following equations were set up:

$$k'^E_2 = 3.1 \times 10^8 \, e^{-15,000/RT} \quad (60)$$

$$k''^E_2 = 4.8 \times 10^{14} e^{-26,000/RT} \quad (61)$$

$$k'^B_2 = 4.1 \times 10^{10} e^{-18,000/RT} \quad (62)$$

$$k''^B_2 = 1.3 \times 10^{16} e^{-28,000/RT} \quad (63)$$

Summarised activation parameters are listed in Table 24.

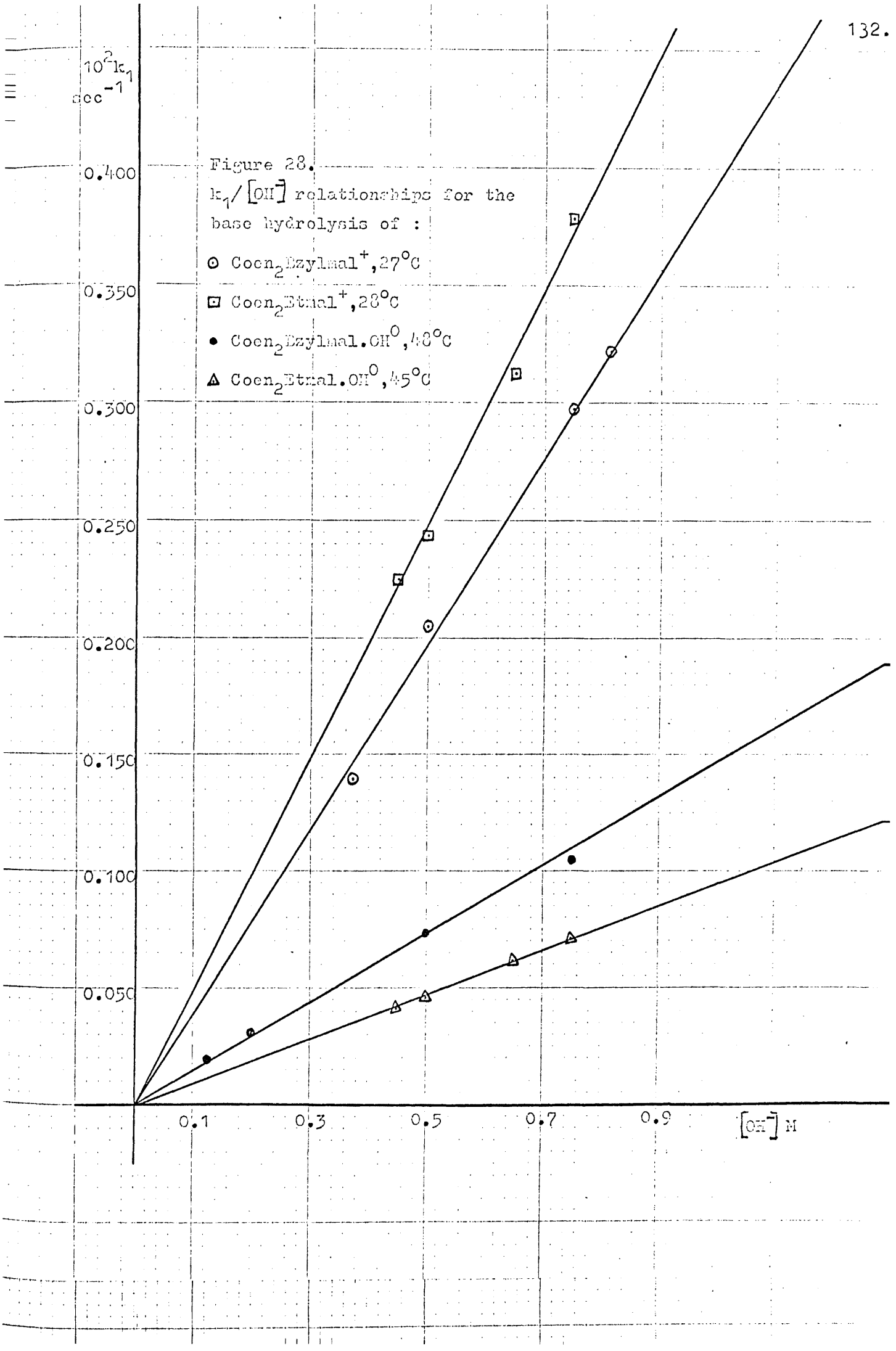

Figure 28.
$k_1/[OH^-]$ relationships for the base hydrolysis of :

⊙ $Coen_2Bzylmal^+$, 27°C

⊡ $Coen_2Etmal^+$, 28°C

• $Coen_2Bzylmal.OH^0$, 48°C

▲ $Coen_2Etmal.OH^0$, 45°C

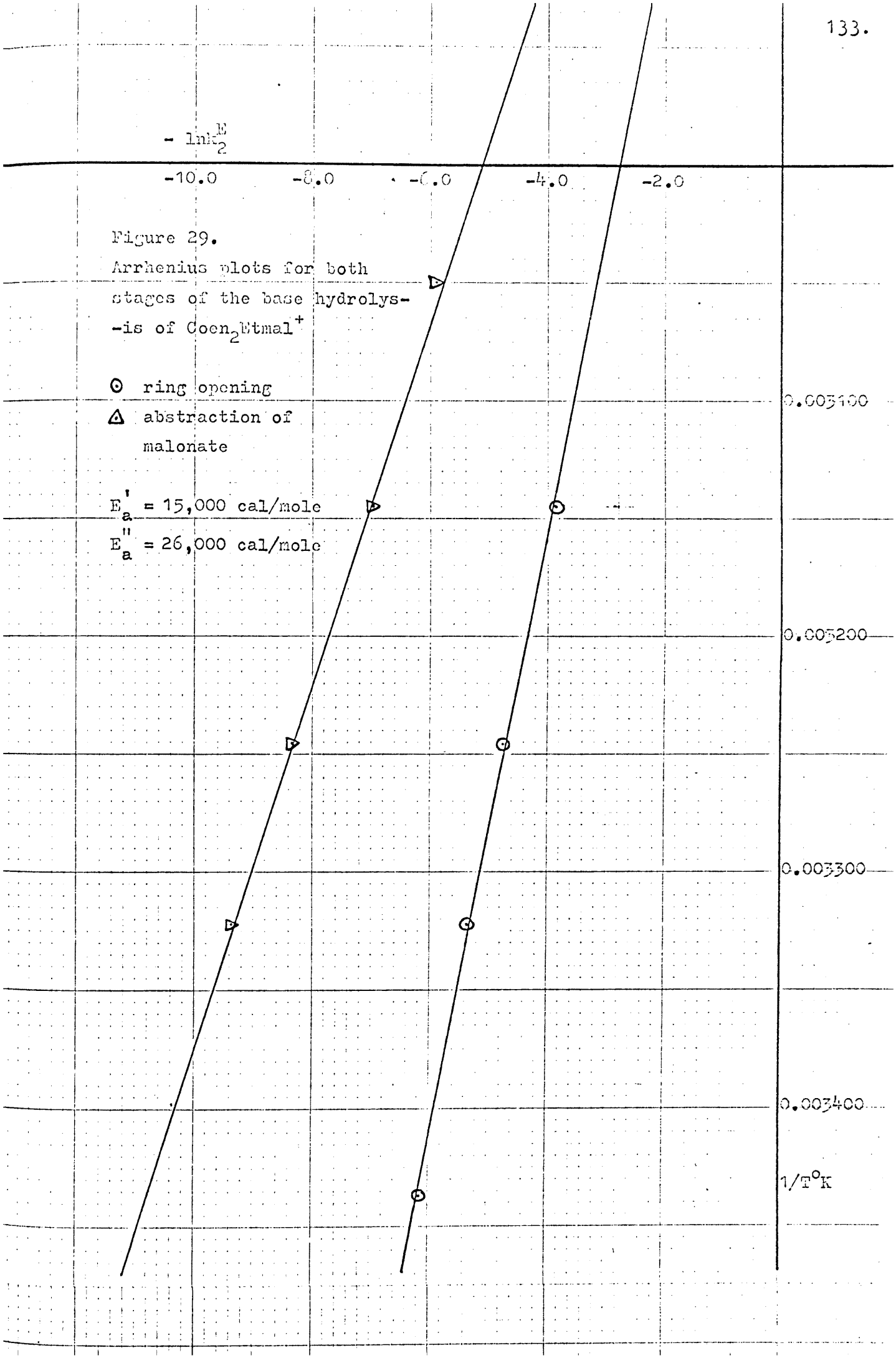

Figure 29.
Arrhenius plots for both stages of the base hydrolysis of $Coen_2Etmal^+$

⊙ ring opening
△ abstraction of malonate

$E_a' = 15,000$ cal/mole
$E_a'' = 26,000$ cal/mole

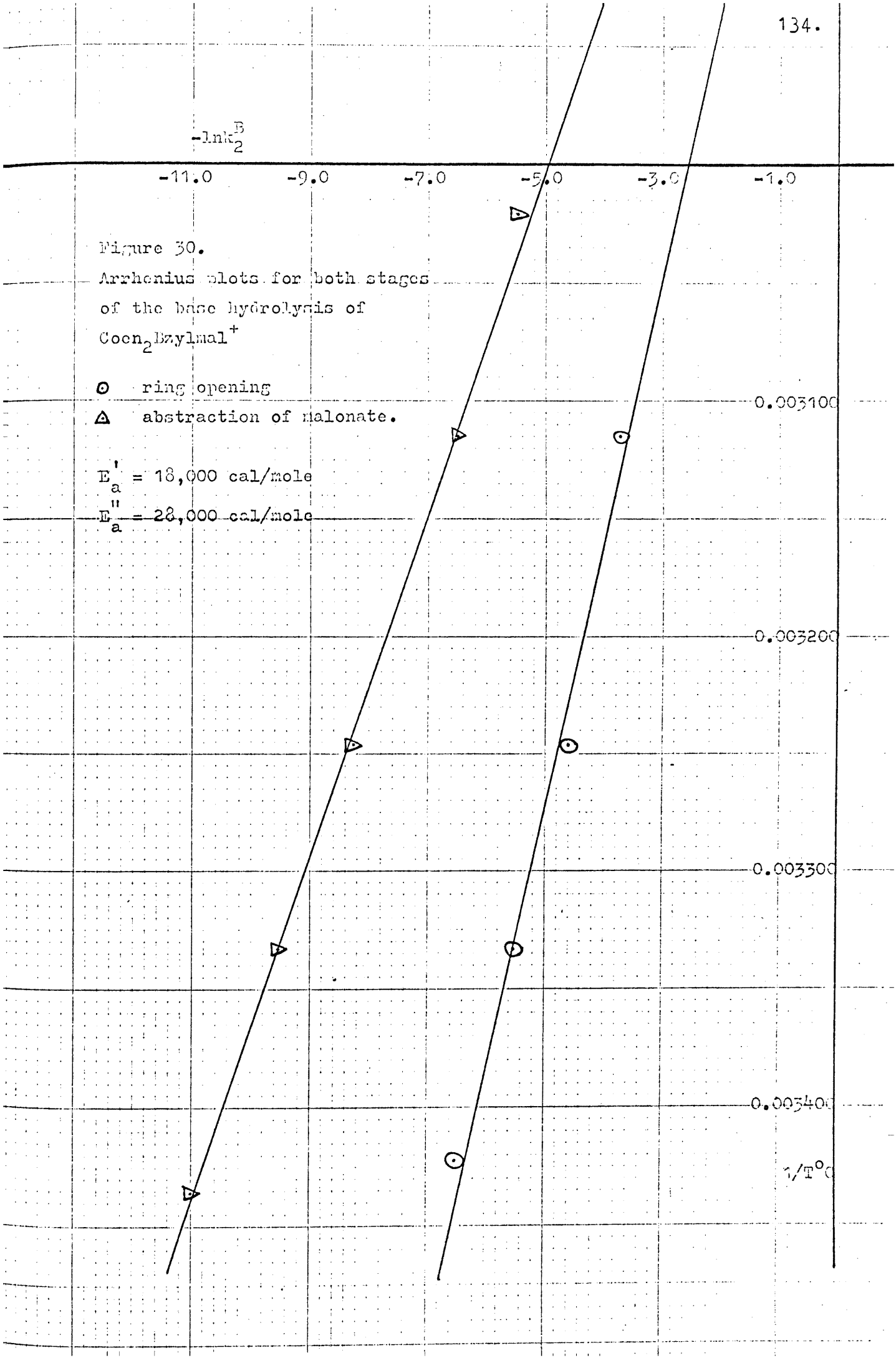

Figure 30.
Arrhenius plots for both stages of the base hydrolysis of $Coen_2Bzylmal^+$

⊙ ring opening
△ abstraction of malonate.

$E_a' = 18{,}000$ cal/mole
$E_a'' = 28{,}000$ cal/mole

Table 24. Activation parameters for the base hydrolysis of $[Coen_2Etmal]^+$ and $[Coen_2Bzylmal]^+$.

Reacting Complex	E_a kcal/ mole.	$\triangle H^{\ddagger}(25^oC)$ kcal/ mole.	$\triangle G^{\ddagger}(25^oC)$ kcal/ mole	$\triangle S^{\ddagger}$ cal/deg/ mole.
$[Coen_2Etmal]^+$	15 ± 1	14.4 ± 1	21 ± 4.5	-22 ± 3
$[Coen_2Etmal.OH]^o$	26 ± 1	25.4 ± 1	23.3 ± 2	+7 ± 3
$[Coen_2Bzylmal]^+$	18 ± 1	17.4 ± 1	21 ± 2	-12 ± 3
$[Coen_2Bzylmal.OH]^o$	28 ± 1	27.4 ± 1	23.5 ± 2	+13 ± 3

In solutions μ = 4.00, $[OH^-] > 1.00M$ a change of kinetics takes place.

Two temperatures were examined, 25.2°C and 35.0°C, to see if the isomeric course of the reaction in concentrated base varies at low temperature, as in the case of $[Coen_2(C_2O_4)]^+$(37).

As in solutions $[OH^-] < 1M$, cis-$[Coen_2(OH)_2]^+$ is always the product of the reaction, in equilibrium with $[Coen_2(Rmal)(OH)]^{\oplus}$. Equilibrium constants were generally greater than those in dilute base (Table 21) but by amounts dependent on the reduced amounts of the intermediates formed compared with the amounts formed in dilute base (Figure 26). A_{Max} at 30,000cm^{-1} is generally 25±5% lower in concentrated than in dilute base. A corresponding increase was observed in K_C, values at the comparable temperature. Synthetic equilibrium mixtures (p.115) demonstrate that cis-$[Coen_2(OH)_2]^+$ is still the product. Therefore, an additional or different mechanistic pathway must come into play in concentrated base that allows production of cis-$[Coen_2(OH)_2]^+$ whilst ring opening is in progress. Subsequent to this extreneous effect the equilibrium for the second stage is not much disturbed by the change in medium.

Pseudo first order rate constants were again found for both ring opening (from Guggenheim's method) and malonate-abstraction (from semi-log plots). Up to $[OH^-] \sim 1.50M$, a linear relationship was found between observed first order rate constants and $[OH^-]$, again passing through the origin. Beyond $[OH^-] = 1.50M$, a considerable deviation from simple second order kinetics was observed, (Figures 31,(a) and (b)) in all cases except ring opening of $[Coen_2Etmal]^+$ at 35°C. The lack of substantial effect here is ascribed to experimental error more than anything else.

When [complex] is kept constant and $[OH^-]$ varied, Initial Rates (p.8) give an order of reaction wrt $[OH^-]$ of 1.85 ± 0.2 (Table 25). In addition, it may be noticed that the values of n, the mean reaction order wrt $[OH^-]$, are higher at 25°C than at 35°C. This is probably indicative of lower temperature favouring the reaction path second order in hydroxide concentration.

Plots of $\ln k_{obs}$ versus $\ln[OH^-]$ show slopes of 1.9 ± 0.1. Such evidence points to the operation of a rate law having one term in $[OH^-]$, second order in $[OH^-]$. Nevertheless the rate law:

$$k_{obs} = k_2[OH^-] + k_3[OH^-]^2 \qquad (64)$$

under high $[OH^-]$ conditions, was tested by $k_{obs}/[OH^-]$ versus $[OH^-]$ plots as well as:

$$k_{obs} = k_3[OH^-]^2 \qquad (65)$$

by k_{obs} versus $[OH^-]^2$ plots. Excellent linearity was found only in the case of (65), except that an intercept was found in all cases, on the k_{obs} axis, (Figures 32(a) and (b)). The rate law:

$$k_{obs} = k_1 + k_3[OH^-]^2 \qquad (66)$$

is therefore postulated as operative above $1.50M[OH^-]$. The rate law (66) operates for <u>both</u> stages for <u>both</u> complexes at the two temperatures studied. k_{obs} values at 1.50M were

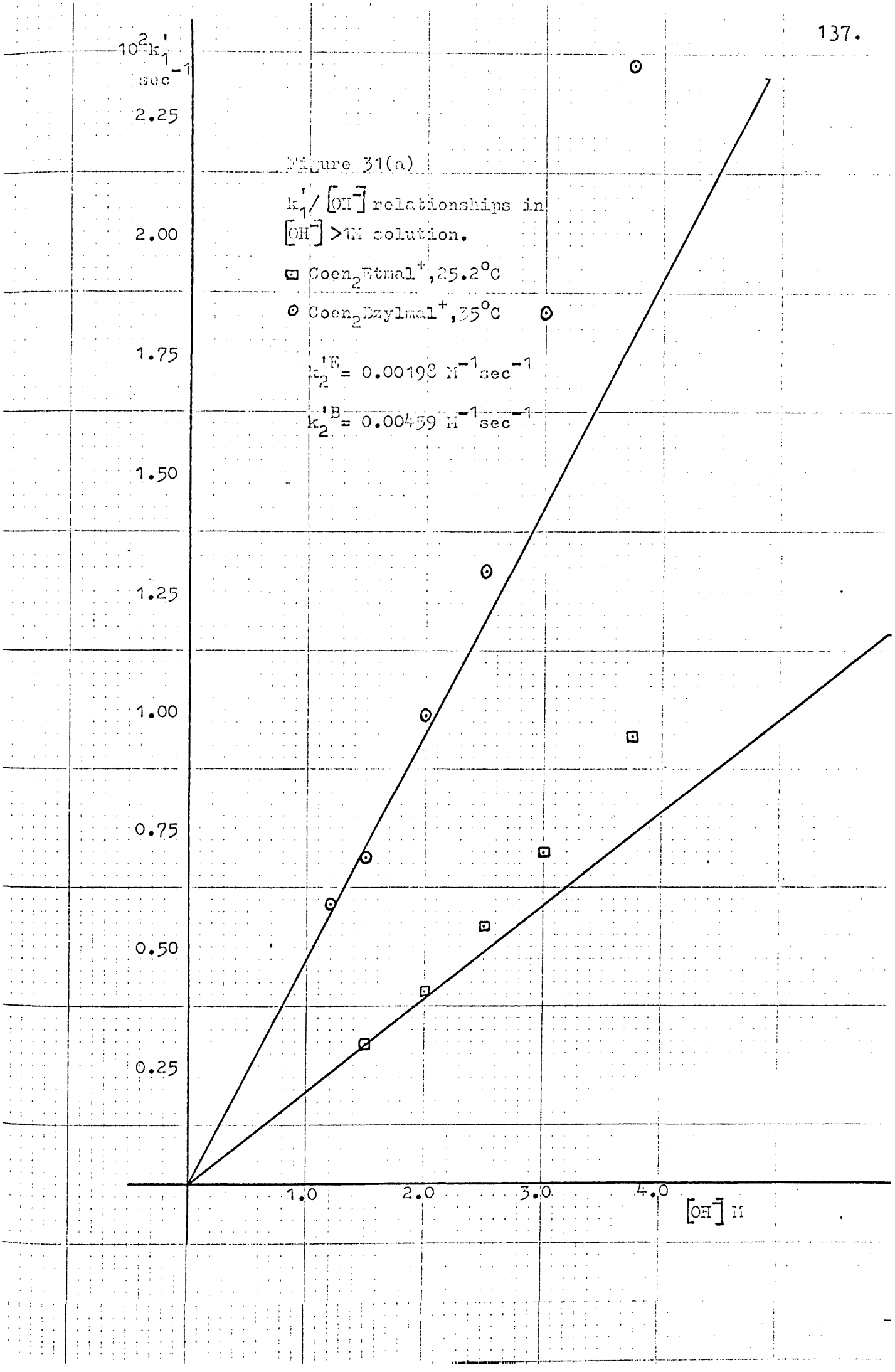

Figure 31(a)

k_1' / $[OH^-]$ relationships in $[OH^-]$ >1M solution.

⊡ $Coen_2$Etmal$^+$, 25.2°C

⊙ $Coen_2$Xylmal$^+$, 35°C

$k_2'^E$ = 0.00198 $M^{-1} sec^{-1}$

$k_2'^B$ = 0.00459 $M^{-1} sec^{-1}$

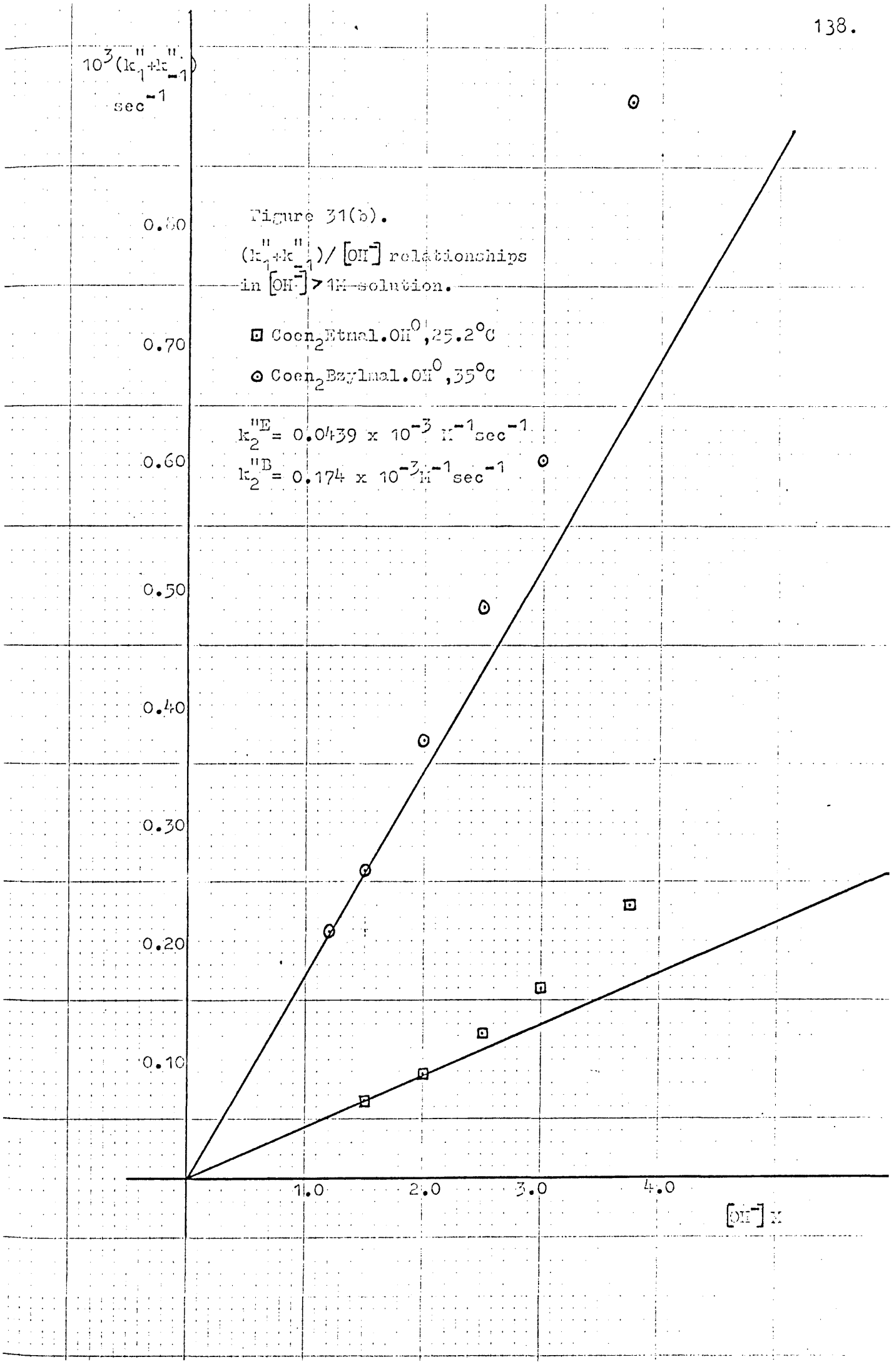

Figure 31(b).

$(k_1''+k_{-1}'')/[OH^-]$ relationships in $[OH^-] > 1M$-solution.

⊡ $Coen_2Etmal.OH^0$, 25.2°C

⊙ $Coen_2Bzylmal.OH^0$, 35°C

$k_2''^E = 0.0439 \times 10^{-3}\ M^{-1}sec^{-1}$

$k_2''^B = 0.174 \times 10^{-3}\ M^{-1}sec^{-1}$

Table 25. Initial Rates[a], μ = 4.00, $[OH^-]$>1.50M.

10^4 Initial Rate $M.L^{-1}sec^{-1}$	$[OH^-]$M	T°C	Reacting Complex	[b]Mean n
1.78	2.70	35.0	$[Coen_2Etmal.OH]^o$	
1.89	3.00			1.8 ± 0.1
2.84	3.75			
0.320	2.50	25.2		
0.460	3.00			2.1 ± 0.1
0.740	3.75			
1.77	2.50	35.0	$[Coen_2Bzylmal.OH]^o$	
2.37	3.00			1.65 ± 0.05
3.40	3.75			
0.400	2.50	25.2		
0.553	3.00			1.9 ± 0.1
0.852	3.75			

[a] Initial rates for ring opening stages were not obtained because of the velocity of the reaction under these conditions. Nevertheless ring opening does demonstrate the same kinetic behaviour as does the second stage.

[b] Mean n, the reaction order wrt $[OH^-]$, is derived between pairs of $[OH^-]$/In.Rate data at each temperature.

included in the k_{obs} versus $[OH^-]^2$ plots, since these constitute borderline cases between the second and third order (wrt$[OH^-]$) rate laws.
Observed pseudo first order rate constants are summarised in Table 26.

Table 26(a). Observed, pseudo first order rate constants for the base hydrolysis of $[Coen_2Etmal]^+$. μ = 4.00.

T°C	$[OH^-]$M	$10^2 k_1'^E$ sec^{-1}	$10^3(k_1''^E + k_{-1}''^E)sec^{-1}$
25.2	1.50	0.298 ± 0.005	0.0664 ± 0.0010
	2.00	0.406 ± 0.003	0.0884 ± 0.0010
	2.50	0.543 ± 0.014	0.121 ± 0.010
	3.00	0.700 ± 0.010	0.160 ± 0.004
	3.75	0.940 ± 0.020	0.230 ± 0.010
35.0	1.20	0.604 ± 0.017	0.220 ± 0.010
	1:50	0.784 ± 0.020	0.254 ± 0.010
	2.00	1.06 ± 0.03	0.390 ± 0.012
	2.30	1.17 ± 0.03	0.422 ± 0.013
	2.70	1.59 ± 0.04	0.553 ± 0.013
	3.00	1.68 ± 0.08	0.590 ± 0.009
	3.25	1.70 ± 0.08	0.702 ± 0.020
	3.75	2.34 ± 0.10	0.898 ± 0.025
	4.00		0.986 ± 0.030

[complex] = 5.0mM

Table 26 (b). Observed, pseudo first order rate constants for the base hydrolysis of $[Coen_2Bzylmal]^+$, μ = 4.00.

T°C	$[OH^-]$M	$10^2 k_1'^B$ sec^{-1}	$10^3(k_1''^B + k_{-1}''^B)sec^{-1}$
25.2	1.50	0.279 ± 0.010	0.0695 ± 0.0025
	2.00	0.392 ± 0.010	0.101 ± 0.005
	2.50	0.576 ± 0.030	0.130 ± 0.002
	3.00	0.708 ± 0.040	0.175 ± 0.002
	3.75	1.10 ± 0.05	0.234 ± 0.005
35.0	1.20	0.586 ± 0.010	0.209 ± 0.010
	1.50	0.686 ± 0.015	0.260 ± 0.013
	2.00	0.988 ± 0.010	0.370 ± 0.013
	2.50	1.29 ± 0.01	0.482 ± 0.020
	3.00	1.83 ± 0.02	0.604 ± 0.030
	3.75	2.35 ± 0.10	0.904 ± 0.020

[complex] = 3.75mM.

First and third order rate constants were calculated from the intercepts and slopes of $k_{obs}/[OH^-]^2$ plots (Figure 32). These are listed in Table 27. Second order rate constants in μ = 4.00 solution calculated from the data when $[OH^-] < 1.50M$, when second order kinetics are still operative, (Figure 31), are included in Table 27.

General rate laws are of the form:

$$k_1' = k_1^{\curvearrowright} + k_2'[OH^-] + k_3'[OH^-]^2 \quad (67)$$

and

$$(k_1'' + k_{-1}'') = k_1^{\curvearrowright\curvearrowright} + k_2''[OH^-] + k_3''[OH^-]^2 \quad (68)$$

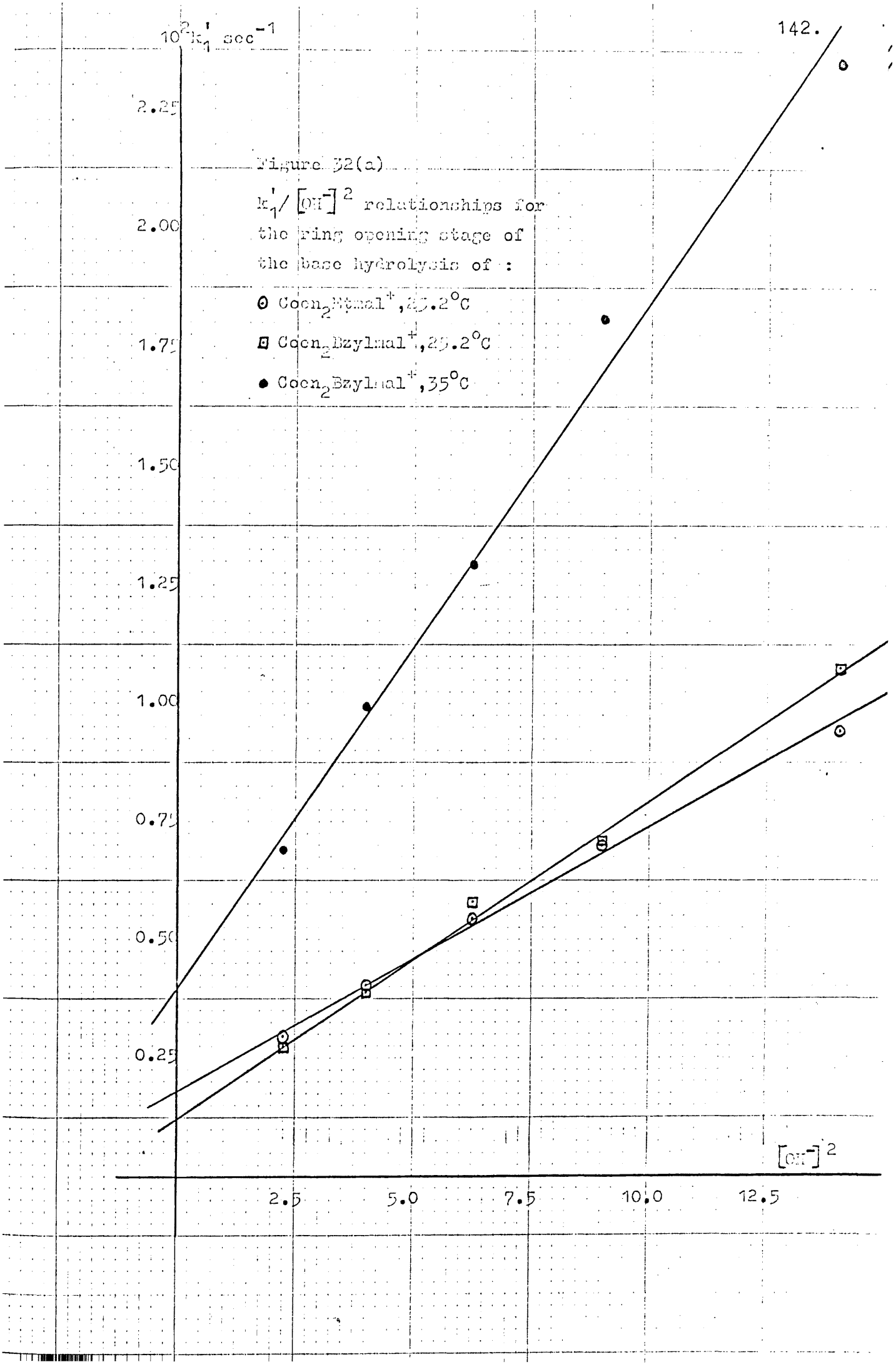

Figure 32(a)

$k_1' / [OH^-]^2$ relationships for the ring opening stage of the base hydrolysis of :

⊙ $Coen_2NHmal^+$, 25.2°C

⊡ $Coen_2Bzylmal^+$, 25.2°C

● $Coen_2Bzylmal^+$, 35°C

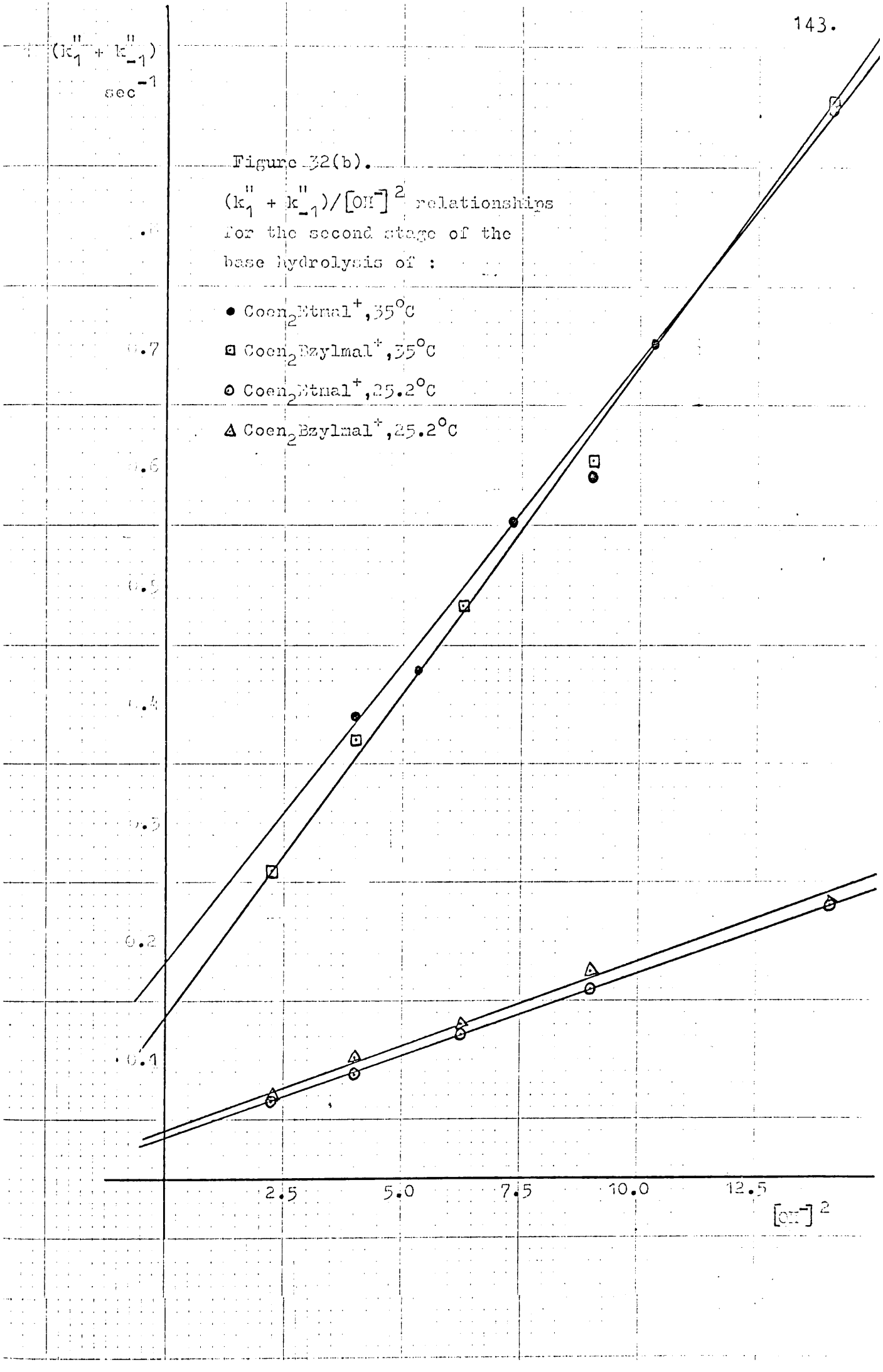

Figure 32(b).

$(k_1'' + k_{-1}'')/[OH^-]^2$ relationships for the second stage of the base hydrolysis of :

- ● $Coen_2$Etmal$^+$, 35°C
- ⊡ $Coen_2$Bzylmal$^+$, 35°C
- ⊙ $Coen_2$Etmal$^+$, 25.2°C
- △ $Coen_2$Bzylmal$^+$, 25.2°C

Table 27 (a). Derived first and third order rate constants for the base hydrolysis of $[Coen_2Etmal]^+$ and $[Coen_2Bzylmal]^+$ in solutions $[OH^-] > 1.50M$, $\mu = 4.00$.

Complex	T°C	$10^2k_1'$ sec^{-1}	$10^3k_3'$ $L^2M^{-2}sec^{-1}$	$10^3k_1''$ sec^{-1}	$10^4k_3''$ $L^2M^{-2}sec^{-1}$
$[Coen_2Etmal]^+$	25.2	0.185	0.562	0.0350	0.139
	35.0	-	-	0.185	0.500
$[Coen_2Bzylmal]^+$	25.2	0.112	0.700	0.0405	0.139
	35.0	0.359	1.48	0.135	0.549

Table 27 (b). Derived second order rate constants for the base hydrolysis of $[Coen_2Etmal]^+$ and $[Coen_2Bzylmal]^+$ in solutions $[OH^-] = 1.00$-$1.50M$, $\mu = 4.00$.

Complex	T°C	$10^2k_2'$ $L.M^{-1}sec^{-1}$	$10^3k_2''$ $L.M^{-1}sec^{-1}$
$[Coen_2Etmal]^+$	35.0	0.525	0.198
	25.2	0.198	0.0449
$[Coen_2Bzylmal]^+$	35.0	0.459	0.173
	25.2	0.183	0.0452

under conditions when $[OH^-] \gg [complex]$. Under normal conditions of $[complex] \approx [OH^-]$ the general rate law:

$$\text{Rate} = k_1[complex] + k_2[complex][OH^-] + k_3[complex][OH^-]^2 \quad (69)$$

operates for both stages of the base hydrolysis of both complexes.

It is observed that the reactions deviate from simple second order kinetics ca.$[OH^-]$ = 1.50M. It is argued, therefore, that the general rate laws (67) and (68) (being specialised cases of (69)), should operate in this region and this region only, provided the seperately operating laws (66) and (50) are correct.
Equations (67) and (68) are quadratics, supposing $[OH^-]$ is the unknown. A small computer programme was therefore devised to solve quadratics for the values of $[OH^-]$ corresponding to values of k_1, k_2 and k_3 derived from the graphical method of analysis, under given temperature conditions. Values of k_{obs} were selected first for 0.1M increments of $[OH^-]$, and having narrowed the range of solutions in this way, for 0.01M increments, where necessary. The narrow range solutions for $[OH^-]$ are given in Table 28.

The solutions of the quadratic rate laws for $[OH^-]$ all lie within less than 0.1M$[OH^-]$ of the points where kinetics are observed to diverge from simple second order (Figure 31). Evidently then, the two rate laws (66) and (50) are correct.

Although the precise solutions of the quadratics are governed by error in the values of k_1, k_2 and k_3, it may be appreciated that the changeover of kinetics is abrupt, since only one solution, within a range of 0.01M$[OH^-]$ is valid.

The brief duration of the quadratic rate laws demonstrated by the computer analysis is good evidence for their validity.

The University of London CDC6600 was used for the analysis. The programme 'GWENO' used, is given in Appendix II.

Table 28. Solutions of the quadratic rate law: $k_{obs} = k_1 + k_2[OH^-] + k_3[OH^-]^2$. Note B and C are k_2 and k_3. The time units of each rate constant are minutes.

A,(-KOBS+K1) NARROW RANGE

HYDROLISIS ETMALOH 35DEG

[OH]	SOLN1	SOLN2	A	B	C
1.70	-.217	1.554	-.00890	.01190	.003000
1.69	-.217	1.573	-.00878	.01190	.003000
1.68	-.218	1.592	-.00866	.01190	.003000
1.67	-.218	1.611	-.00854	.01190	.003000
1.66	-.218	1.632	-.00842	.01190	.003000
1.65	-.219	1.652	-.00830	.01190	.003000
1.64	-.219	1.674	-.00818	.01190	.003000
1.63	-.219	1.696	-.00806	.01190	.003000
1.62	-.220	1.719	-.00794	.01190	.003000
1.61	-.220	1.742	-.00782	.01190	.003000
1.60	-.221	1.766	-.00770	.01190	.003000

HYDROLISIS ETMAL 25DEG

[OH]	SOLN1	SOLN2	A	B	C
1.70	-.239	1.518	-.09300	.11900	.033700
1.69	-.239	1.535	-.09180	.11900	.033700
1.68	-.240	1.553	-.09060	.11900	.033700
1.67	-.240	1.571	-.08940	.11900	.033700
1.66	-.240	1.590	-.08820	.11900	.033700
1.65	-.241	1.609	-.08700	.11900	.033700
1.64	-.241	1.628	-.08580	.11900	.033700
1.63	-.242	1.648	-.08460	.11900	.033700
1.62	-.242	1.669	-.08340	.11900	.033700
1.61	-.243	1.690	-.08220	.11900	.033700
1.60	-.243	1.712	-.08100	.11900	.033700

Table 28 (cont'd).

HYDROLISIS ETMALOH 25DEG

[OH]	SOLN1	SOLN2	A	B	C
1.60	-.263	1.552	-.00204	.00263	.000832
1.59	-.263	1.569	-.00201	.00263	.000832
1.58	-.264	1.587	-.00199	.00263	.000832
1.57	-.264	1.605	-.00196	.00263	.000832
1.56	-.265	1.623	-.00194	.00263	.000832
1.55	-.265	1.642	-.00191	.00263	.000832
1.54	-.266	1.662	-.00188	.00263	.000832
1.53	-.266	1.682	-.00186	.00263	.000832
1.52	-.267	1.702	-.00183	.00263	.000832
1.51	-.267	1.724	-.00181	.00263	.000832
1.50	-.268	1.745	-.00178	.00263	.000832

HYDROLISIS BZYLMAL 35DEG

[OH]	SOLN1	SOLN2	A	B	C
1.60	-.266	1.488	-.22500	.27500	.089000
1.59	-.266	1.504	-.22220	.27500	.089000
1.58	-.267	1.520	-.21940	.27500	.089000
1.57	-.267	1.536	-.21680	.27500	.089000
1.56	-.268	1.553	-.21400	.27500	.089000
1.55	-.268	1.570	-.21120	.27500	.089000
1.54	-.269	1.582	-.20940	.27500	.089000
1.53	-.269	1.599	-.20680	.27500	.089000
1.53	-.269	1.599	-.20680	.27500	.089000
1.52	-.270	1.618	-.20400	.27500	.089000
1.51	-.270	1.638	-.20110	.27500	.089000
1.50	-.271	1.667	-.19700	.27500	.089000

Table 28 (cont'd).

HYDROLISIS BZLMALOH 35DEG

[OH]	SOLN1	SOLN2	A	B	C
1.60	-.260	1.455	-.00870	.01040	.003290
1.59	-.260	1.473	-.00858	.01040	.003290
1.58	-.261	1.490	-.00846	.01040	.003290
1.57	-.262	1.509	-.00834	.01040	.003290
1.56	-.262	1.527	-.00822	.01040	.003290
1.55	-.263	1.547	-.00810	.01040	.003290
1.54	-.263	1.566	-.00798	.01040	.003290
1.53	-.264	1.587	-.00786	.01040	.003290
1.52	-.264	1.608	-.00774	.01040	.003290
1.51	-.265	1.630	-.00762	.01040	.003290
1.50	-.266	1.652	-.00750	.01040	.003290

HYDROLISIS BZYLMAL 25DEG

[OH]	SOLN1	SOLN2	A	B	C
1.50	-.300	1.400	-.10000	.11000	.042000
1.49	-.301	1.414	-.09880	.11000	.042000
1.48	-.301	1.428	-.09760	.11000	.042000
1.47	-.302	1.443	-.09640	.11000	.042000
1.46	-.303	1.458	-.09520	.11000	.042000
1.45	-.303	1.473	-.09400	.11000	.042000
1.44	-.304	1.489	-.09280	.11000	.042000
1.43	-.305	1.505	-.09160	.11000	.042000
1.42	-.305	1.522	-.09040	.11000	.042000
1.41	-.306	1.539	-.08920	.11000	.042000
1.40	-.307	1.557	-.08800	.11000	.042000

HYDROLISIS BZYLMALOH 25DEG

1.60	-.253	1.597	-.00206	.00277	.000832

2. THE ACID CATALYSED HYDROLYSIS.

Unlike $[Coen_2mal]^+$ (p.61) and $[Coen_2(C_2O_4)]^+$(87) which are quite stable for long periods in acid solution , at elevated temperatures, both $[Coen_2Etmal]^+$ and $[Coen_2Bzylmal]^+$ are observed to react readily and in two separate stages.

The first stage is characterised by isobestic points at $21,600cm^{-1}$ and $23,800cm^{-1}$, a general loss of intensity and a shift of the $^1A_{1g} \longrightarrow {}^1T_{1g}$ transition from $19,600cm^{-1}$ to $20,000cm^{-1}$.

This stage was characterised as being due to dechelation of malonate by acidifying an alkaline solution in which the dechelated species had been generated under known conditions in the maximum amount. Whereupon, the spectrum at the end of the first stage in acidic solution was obtained (Figure 33).

The second stage is characterised by a general further loss in intensity, by isobestic points at $18,200cm^{-1}$, $26,900cm^{-1}$ and $28,450cm^{-1}$ and by a marked increase in intensity ca. $30,000cm^{-1}$. The effect is, in fact, very similar to ring opening in alkaline solution. The spectrum could arise from a mixture of cis and trans-$[Coen_2(OH_2)_2]^{3+}$. The spectra of these ions from(15) together with that at the end of the second stage in acid solution is shown in Figure 34. Addition of alkali to pH~12, where hydroxo species are quite stable, produced the spectrum shown in Figure 35. The spectrum may be compared with those of cis and trans-$[Coen_2(OH)_2]^+$(15). Maxima and minima are in the correct positions and the product of the acid hydrolysis appears to have been almost entirely cis-$[Coen_2(OH_2)_2]^{3+}$, subsequently deprotonated to cis-$[Coen_2(OH)_2]^+$. Such a reaction has been shown(31) to occur with full retention of configuration.

The product of the second stage could be cis-$[Coen_2(OH)(H_2O]^{2+}$ as was postulated in the case of the carbonato analogue(52,58). Since this ion isomerises very rapidly(45) a ready path to a cis/trans isomeric mixture of $[Coen_2(OH_2)_2]^{3+}$ is available on protonation of the hydroxyaquo ion. Cis or cis/trans-$[Coen_2(OH_2)_2]^{3+}$ is always the observed product of the acid hydrolysis of $[Coen_2CO_3]^+$(101) in the pH range 2-3. Protonation of product hydroxyaquo ions is therefore an integral part of the mechanism.

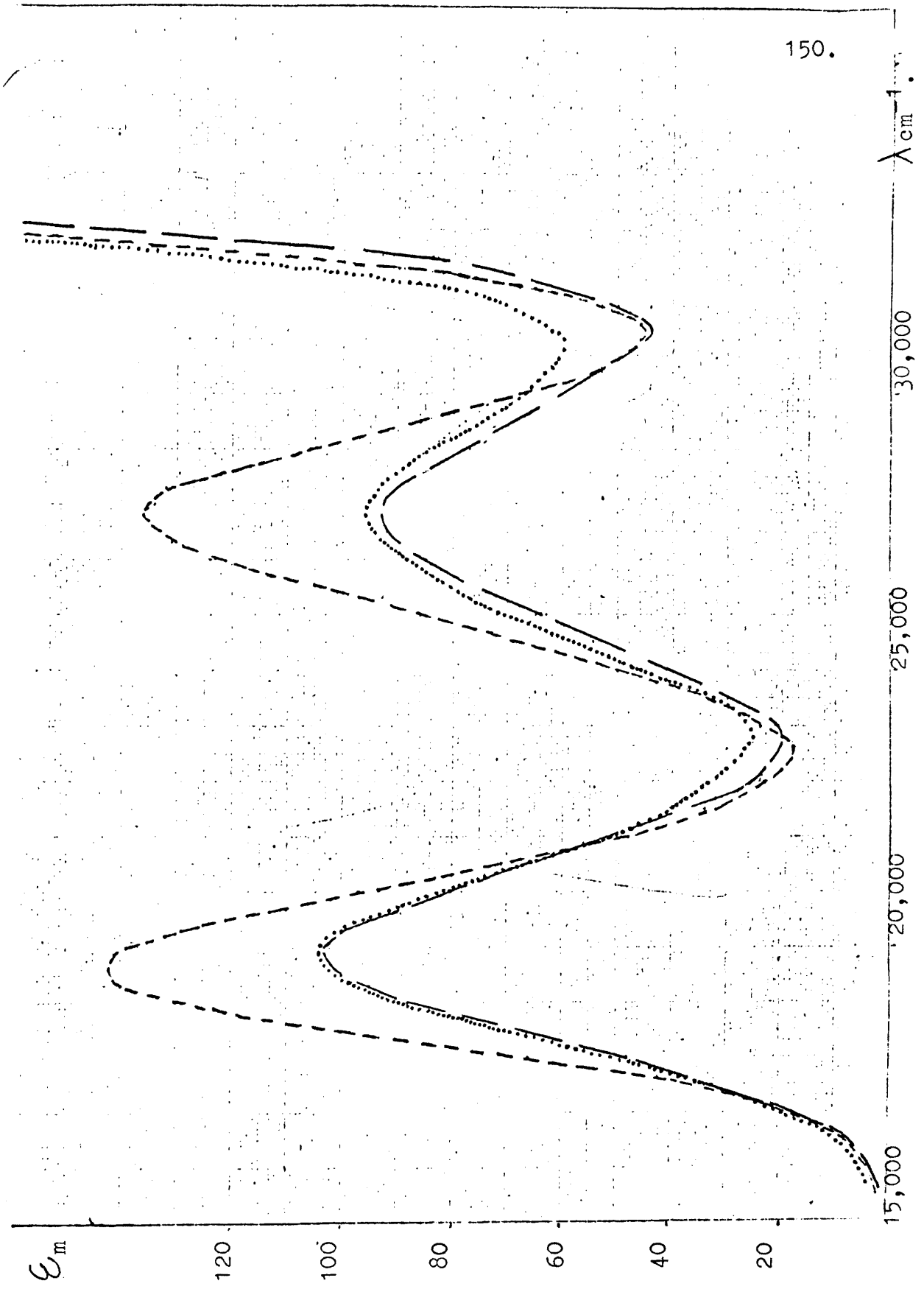

Figure 33. Characterisation of the first stage of the acid hydrolysis of $[Coen_2Etmal]^+$

------ $[Coen_2Etmal]^+$

—— —— After first stage in acid, pH~3

..... Ring opening in alkali + HCl ⟶ pH~3.

Figure 34. uv-visible spectra of :

—— —— cis $[Coen_2(OH_2)_2]^{3+}$

---------- trans $[Coen_2(OH_2)_2]^{3+}$

..... final spectrum after acid hydrolysis of $[Coen_2Etmal]^+$ at pH 3.38

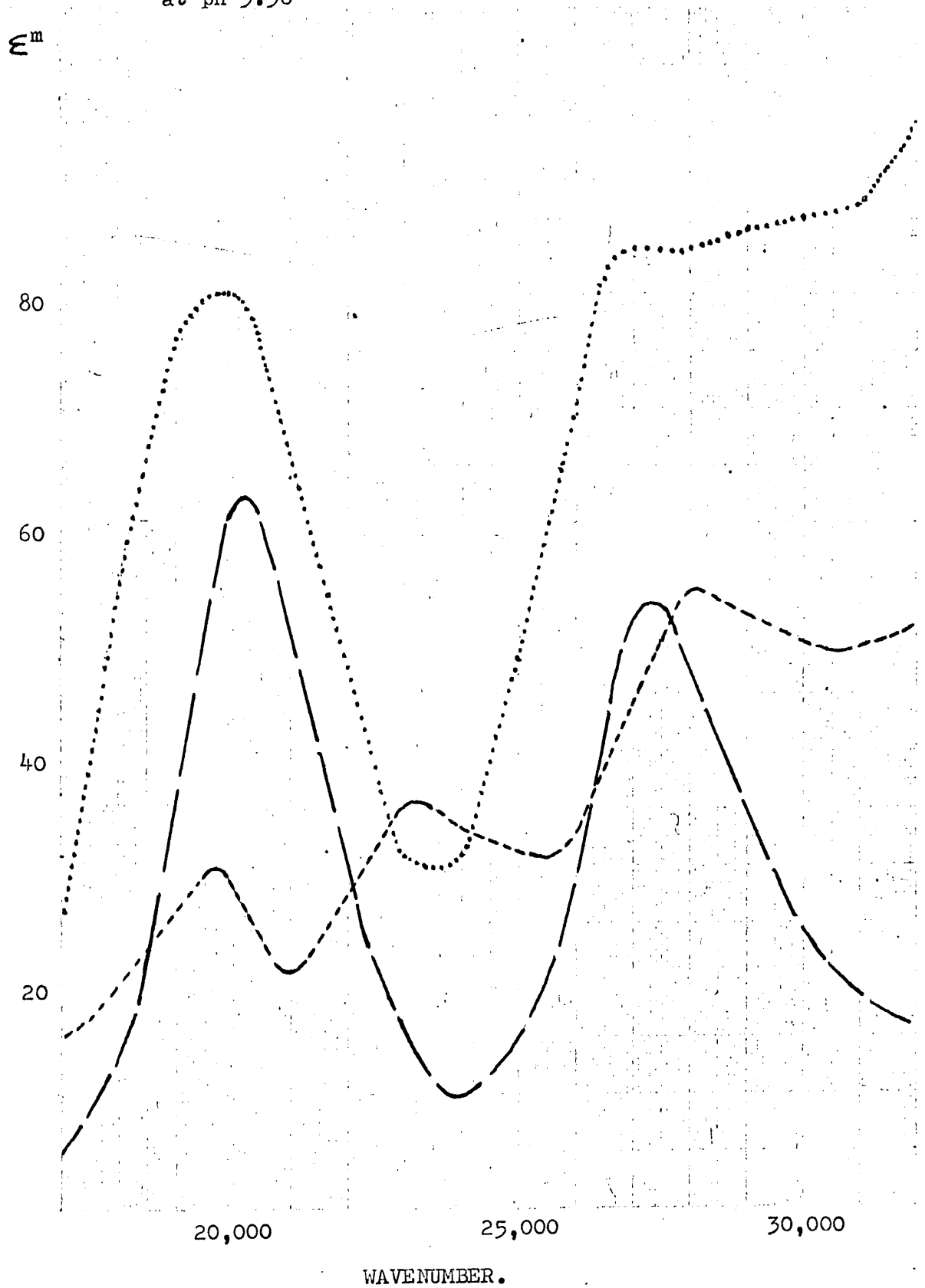

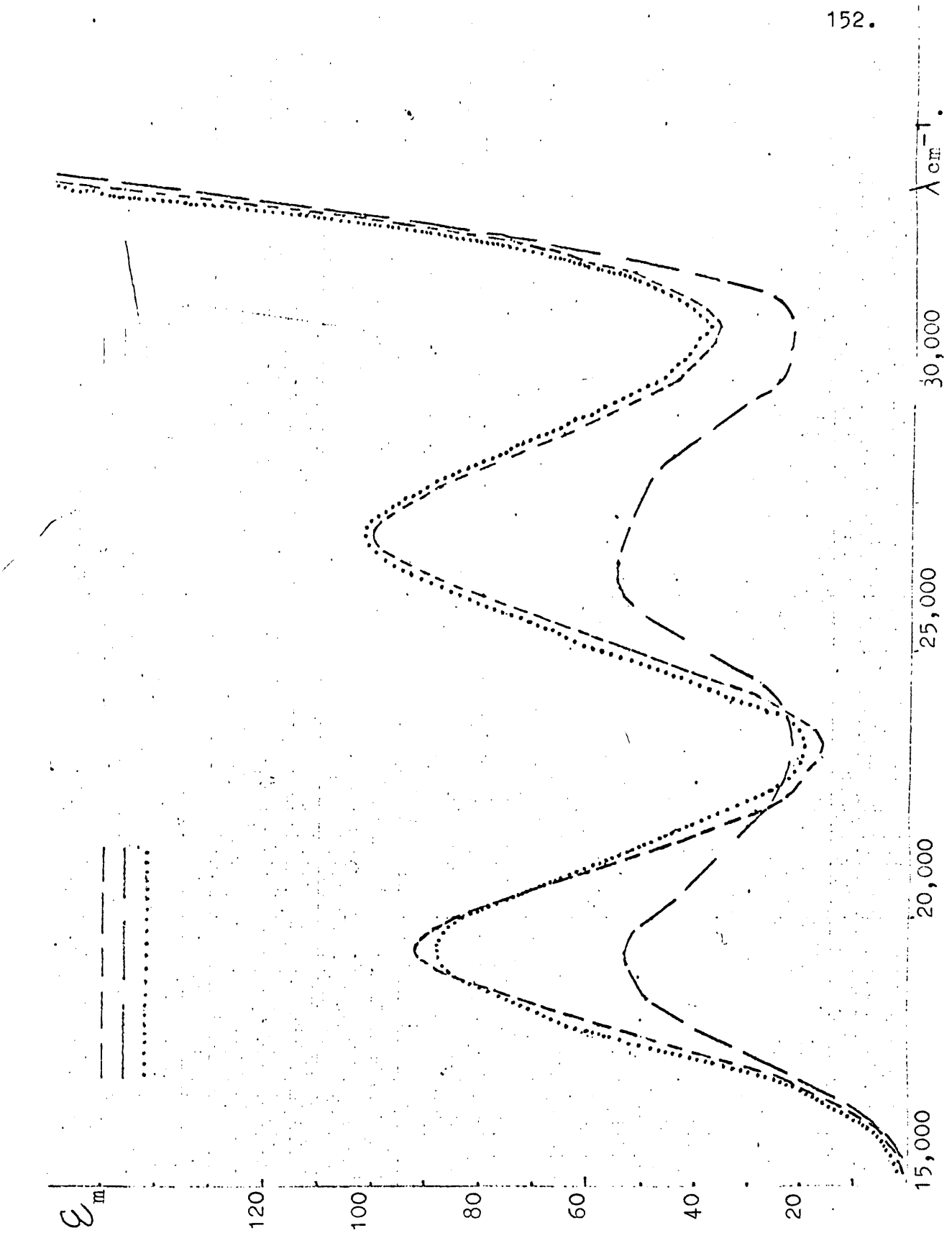

Figure 35. Characterisation of the second stage of the acid hydrolysis of $[Coen_2Bzylmal]^+$.

----- <u>cis</u>-$[Coen_2(OH)_2]^+$

— — <u>trans</u>-$[Coen_2(OH)_2]^+$

..... complete reaction in acid + NaOH ⟶ pH ~12.

The kinetic dependence on $[H_3O^+]$ was studied in the hope of further elucidation.

Observations were made in a similar manner to the base hydrolysis. Ionic strength was maintained at 0.35 by the use of NaCl. 'First order' excess of acid was maintained by the use of sodium acetate/HCl buffer solutions and both stages of the reaction were conveniently studied at 41.4°C. At this temperature and in the acid concentration range studied, the first stage is complete in about 20 minutes,and the second in about four hours.

The first stage was conveniently studied at 28,450cm^{-1},the isobestic of the second, thereby providing an ∞ value and removing all co-incidence with the second stage regardless of the complexity or otherwise of the second stage products.

The second stage was followed at the region of maximum change (31,000cm^{-1}) and the ∞ taken as the final absorbance at that wavelength.

Good pseudo first order rate constants over four half lives, were obtained in this way for both stages for both complexes.

The first stage shows half order dependence on $[H_3O^+]$ whilst the second appears independent of acid, although at the lowest pH studied (1.66) [acid] appeared to inhibit the reaction.

Pseudo first order,k'_{obs},and derived one and a half order rate constants for the first stage and pseudo first order rate constants, k''_{obs}, for the second, are summarised in Table 29.

3. THE EFFECT OF IONIC STRENGTH.

The effect in basic solution is most conveniently assessed by the magnitude of the second order rate constants for the reaction at 25°C. k_2 values at this temperature, μ = 1.00, were obtained from the Arrhenius plots (Figures 29 amd 30) whilst those at μ = 4.00 were obtained directly.

Bronstead's(17) formulation for the effect of ionic strength, equation (10)(p.11) cannot be expected to hold here, since at the concentrations used Debye-Hückel theory is invalid.

Ideally, plotting $\log_{10}k_2$ versus $\sqrt{\mu}$, we would expect a slope of -1.02 at 25°C for the ring opening reactions, and would

Table 29. Observed and derived rate constants for both stages of the acid catalysed hydrolysis of the $[Coen_2Etmal]^+$ and $[Coen_2Bzylmal]^+$ ions, at 41.4 ± 0.1°C.

$[Coen_2Etmal^+]$ = 5.0mM. $[Coen_2Bzylmal^+]$ = 3.75mM.

pH	$[H_3O^+]$ M.L^{-1}	$[H_3O^+]^{\frac{1}{2}}M^{\frac{1}{2}}L^{-\frac{1}{2}}$	Complex	$10^2 k'_{Obs}$ sec^{-1}	$k'_{1\frac{1}{2}}$ $L^{\frac{1}{2}}M^{-\frac{1}{2}}$sec^{-1}	$10^3 k''_{Obs}$
1.66	0.0218	0.148	$Coen_2Etmal^+$	1.46 ± 0.12	9.85 ± 0.80	0.0667 ± 0.0030
			$Coen_2Bzylmal^+$	0.889 ± 0.050	6.00 ± 0.35	0.0840 ± 0.0050
2.66	0.00218	0.0468	$Coen_2Etmal^+$	0.310 ± 0.020	6.62 ± 0.40	0.173 ± 0.008
			$Coen_2Bzylmal^+$	0.280 ± 0.018	5.98 ± 0.38	0.170 ± 0.008
3.38	0.000417	0.0204	$Coen_2Etmal^+$	0.144 ± 0.010	6.95 ± 0.50	0.163 ± 0.007
			$Coen_2Bzylmal^+$	0.131 ± 0.009	6.42 ± 0.45	0.182 ± 0.007
3.78	0.000166	0.0129	$Coen_2Etmal^+$	0.0831 ± 0.005	6.44 ± 0.30	0.333 ± 0.015
			$Coen_2Bzylmal^+$	0.110 ± 0.006	8.53 ± 0.36	0.198 ± 0.008

expect the second stage to be independent of ionic strength, since it involves a species of ionic charge zero. Such a plot would be of little value since only two ionic strength values were studied. However, $\log_{10}k_2/\mu^{\frac{1}{2}}$ values are summarised in Table 30.

Table 30. Ionic strength dependence at 25°C.

$\mu^{\frac{1}{2}}$	$\log_{10}k_2'$	$\log_{10}k_2''$	Complex.
1.00	-2.41	-4.24	$[Coen_2Etmal]^+$
	-2.49	-4.28	$[Coen_2Bzylmal]^+$
2.00	-2.70	-4.38	$[Coen_2Etmal]^+$
	-2.75	-4.34	$[Coen_2Bzylmal]^+$

As expected, ring opening does not obey Bronstead's equation. However, $\log_{10}k_2'$ does show negative dependency on $\mu^{\frac{1}{2}}$ which is expected for a reaction involving one negatively charged and one positively charged ion.
Within experimental error, the second stage of the reaction is independent of ionic strength. This is excellent corroborative evidence for the zero charged intermediate $[Coen_2(Rmal)(OH)]^o$.

Reactions carried out in the presence of Ba^{2+} and K^+ ions showed no change in observed rates. We may, therefore, safely assume that neither ring opening, nor abstraction of malonate is subject to cation catalysis (either specific or general).

DISCUSSION.

It is apparent that the introduction of a large steric factor has raised the energy barrier to the activated complex so as to render the ring opening reaction in basic solution observable.

The unsubstituted complex $[Coen_2mal]^+$ reacts(35) in one observable stage. However, the values of E_a, (15 kcal/mole for $[Coen_2Etmal]^+$ and 18 kcal/mole for $[Coen_2Bzylmal]^+$), are low enough to make the ring opening reaction very fast in comparison to the second stage.

We may deduce that, since ring opening becomes observable as a result of introducing a large steric factor on the α-position, it takes place by carbon-oxygen fission, since the steric factor will have a much more substantial effect in this region than in the region of the cobalt-oxygen co-ordinate bond. Such a conclusion is supported by the lack of steric change during the course of the reaction and also by analogy with $[Coen_2(C_2O_4)]^+$, where carbon-oxygen fission was demonstrated by O^{18} exchange(3).

It is apparent, also, that the effect of the α-substituents is not solely steric. Both ethyl and benzyl are expected to exert an inductive effect on their neighbouring atoms. If carbon-oxygen fission is operative as the dechelation mechanism, the α-substituents would be expected to facilitate the reaction compared to $[Coen_2mal]^+$, by activating the carbonyl carbon with respect to an incoming nucleophile. However, since the net activation energy is increased compared to $[Coen_2mal]^+$, the steric effect of the α-substituents contributes much more to the total than does the electronic effect.

It is interesting to note that the activation energy for the ring opening reaction for the benzyl substituted complex is greater than that for the ethyl substituted complex, whilst the values for the second stage are comparable. The higher value for ring opening is reconcilable with the increased steric barrier to attack on the carbonyl carbon, (outweighing the inevitable increased inductive effect). The fact that E_a for the second stage appears largely independent of the substituent may well be indicative of cobalt-oxygen fission

in this stage, since this is expected to be less sensitive to the α-substituent, both sterically and electronically.

If the carbonyl carbon atoms are activated in the manner described, a different dechelation mechanism is expected for $[Coen_2Etmal]^+$ and $[Coen_2Bzylmal]^+$ than for $[Coen_2mal]^+$. There is no reason why ring opening should not occur in an identical manner in all three complexes in dilute base, but in concentrated base, the combined effects of the medium and of the α-substituents may lead to a continued preference for hydroxide attack on the carbonyl carbon, and its consequences, rather than deprotonation to form the stable conjugate base postulated by Farago(35).

As observed, in concentrated base, ($>1.50M$), a deviation from simple second order kinetics occurs for both stages of the reaction. This involves a term second order in hydroxide concentration and an extra term, first order in complex concentration and zero order in $[OH^-]$. Since a limiting rate is observed at high $[OH^-]$ in the case of $[Coen_2mal]^+$, the base hydrolysis of the substituted malonato complexes goes, in concentrated base at least, by a different mechanism.

In dilute base, it is postulated that ring opening occurs by S_N2 attack on the carbonyl carbon by OH^-, and that this leads to C-O fission.

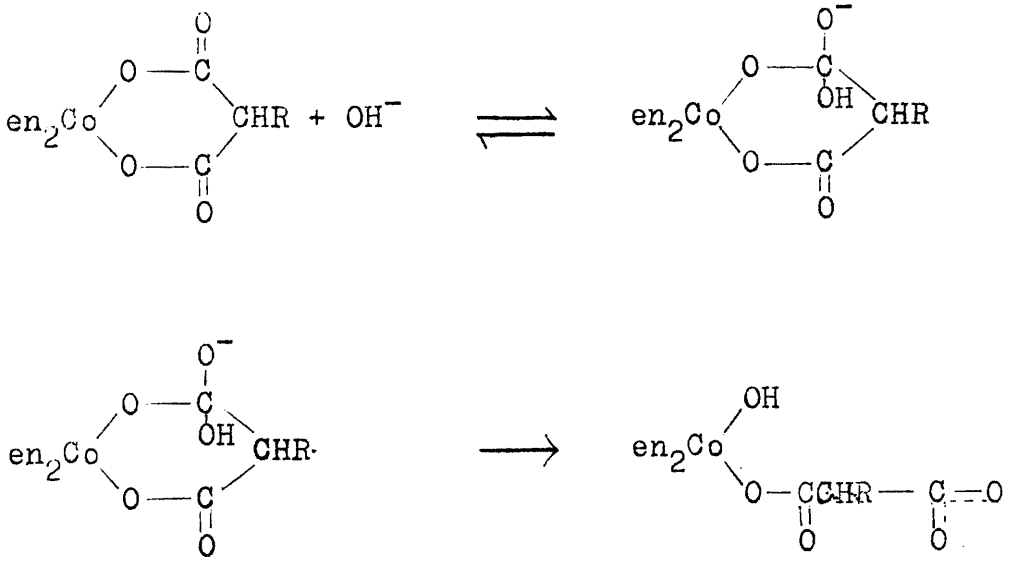

The reaction necessarily proceeds with retention of configuration. The conclusion that C-O fission operates is also supported by the activation entropy values obtained. $\triangle S^{\dagger}$ =-22eu and -12eu, for $[Coen_2Etmal]^+$ and $[Coen_2Bzylmal]^+$ respectively. Such values are typical of reactions involving substantial lack of disordering factors. However, Tobe's correlation(99) (p.27) of activation entropies and steric change does not necessarily apply here, since the metal-chelate bond is not broken.

The mechanism operates up until $\sim$1.50M[OH^-]. The k_2' values found at μ = 1.00 and μ = 4.00 are necessarily different. However, rough E_a values calculated from the data at 25.2°C and 35°C when μ = 4.00 ($\sim$16kcal/mole and $\sim$17.5kcal/mole, for $[Coen_2Etmal]^+$ and $[Coen_2Bzylmal]^+$ respectively), confirm that the same mechanism operates. Such a conclusion also applies to the k_2'' values in μ = 4.00 solution. ($E_a \sim$27kcal/mole for both complexes).

Since the loss of optical activity accompanying base hydrolysis was not followed it is not possible to state exactly by what mechanism the second stage proceeds when the latter shows simple second order kinetics. Co-O bond fission is infered by analogy with the other dicarboxylate complexes that have been studied(3,37) and by consideration of the activation energy's relative insensitivity to the α-substituent. $\triangle S^{\dagger}$ values are sufficiently low(99) for both complexes to conclude that if the mechanism is dissociative, then the intermediate is a tetragonal pyramid. Such a conclusion is supported by the lack of steric change during the second stage. However, both activation entropy and lack of steric change could be reconciled with an associative mechanism. Tobe(99) has further pointed out that even if a mechanism is not truely dissociative but is solvent assisted, the critical stretching of the leaving group-cobalt bond may be accompanied by general rearrangement toward five co-ordinate symmetry, i.e. trigonal bipyramidal to give steric change, and tetragonal pyramidal to preclude it. Such a description, which seems analogous to the I_a(p.19) process, may well pertain here.

The leaving group, either $Etmal^{2-}$ or $Benzylmal^{2-}$ may be seen from the results to have differing effects upon the rate of

reaction. This is again symptomatic of an associative process. In the case of $[Coen_2(C_2O_4)]^+$,(p.101) an S_N1CB mechanism was postulated and accounted well for the observed results. i.e. substantial steric change; racemisation and the production of the trans dihydroxo ion directly from the hydroxyoxalato intermediate. The lack of steric change observed in the case of the α-substituted malonato complexes, irrespective of conditions, makes such a mechanism unlikely. However, it is more likely than a pure S_N1 mechanism, since in this case there is no π donor in the trigonal plane able to stabilise the intermediate by p_x-$d_{x^2-y^2}$ overlap,(p.23). Those intermediates having OH, (the only other π donor present), in the trigonal plane are forbidden if the retentive or inverted cis isomer only is to be the product, (see pp.23 and 26).

Without polarimetric measurements a final conclusion is impossible, but it is felt that since the product of the reaction is always cis$[Coen_2(OH)_2]^+$ and in view of the effect of the leaving groups upon the rate, an associative mechanism is most probable. However, all possible intermediates are outlined in Scheme 3. An amido conjugate base mechanism is not included. This is irrelevant in the absence of polarimetric results, anyway, since it provides only for net inversion, (over the S_N1 mechanism), and this was not studied here. i.e. type B intermediates (p.26) only are envisaged.

see Scheme 3.

Only those intermediates giving retentive or inverted cis product are included. In the associative mechanism these may come about by cis or trans attack. Cis attack seems unlikely on account of the bulky nature of the ethyl- and benzyl-malonato ligands. However, it is difficult to imagine why trans $\angle$ 4,5 attack to give trans dihydroxo product does not occur while the equally likely trans attack at $\angle$ 1,4 and $\angle$ 3,5 does. Cis attack is favoured for this reason.

The product of the base hydrolysis of $[Coen_2mal]^+$ is racemic cis-$[Coen_2(OH)_2]^+$ and racemisation is found to proceed at a rate equal to that of hydrolysis under given conditions. It is likely that in dilute base identical stereochemical

Scheme 3.

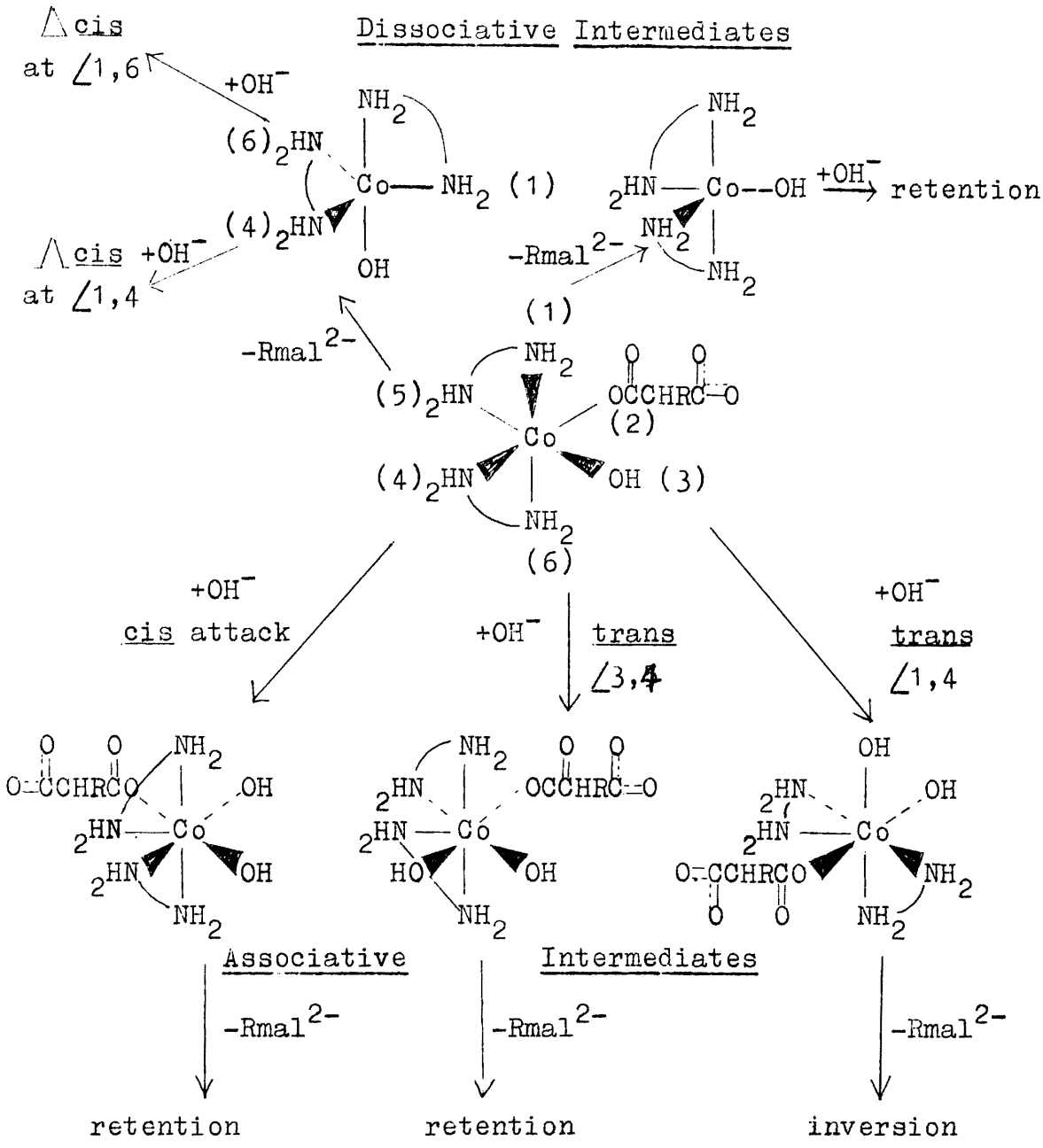

---

mechanisms operate for the substituted and unsubstituted complexes but with the modifications to the kinetic parameters introduced by ethyl and benzyl, as described. Only in the more concentrated medium does the α-substituent alter the mechanistic course of the reaction as observed from the kinetics.

It was postulated(37) that in the case of $[Coen_2(C_2O_4)]^+$ a species of the kind:

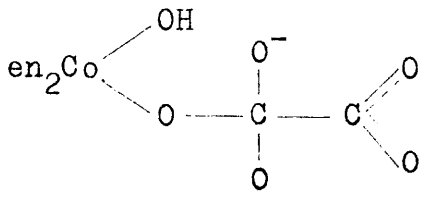

was formed in concentrated base. This would be expected to decrease the acidity of the amine protons and promote a change from a dissociative to an associative mechanism. In view of the activating effect of the ∝-substituents on the carbonyl carbon, such a species is postulated here, during the course of <u>both</u> stages of the reaction.

In the case of ring opening, this is the normal reaction. However, it is postulated that a further molecule of hydroxide attacks the metal directly and syncronously. This may occur by <u>cis</u> or <u>trans</u> attack as outlined already (p.160). The effect probably comes about in the concentrated medium by an effect peculiar to that phase, such as ion pairing, placing the hydroxide in a favourable attacking position.

In addition, it is postulated that since the carbonyl carbon atoms are so activated in the ∝-substituted complexes, a molecule of complex may abstract a molecule of hydroxide in a rate determining step from a neighbouring molecule that is undergoing hydrolysis. It is indeterminate as to whether the ring opened form comes about by carbon-oxygen or by metal-oxygen fission, since both are now possible. What is certain is that the reaction does go without isomerisation.

Having abstracted the molecule of hydroxide that does not actually engage in hydrolysis in its first site, the further molecule of complex then reacts itself in a like manner. The process is a type of chain reaction.

Such a situation is substantially supported by the kinetics. With regard to the second stage of the reaction, where identical kinetics are observed, a similar scheme is envisaged.

Hydroxide attack on the carboxyl group is unlikely in view of the cancelling effect of the delocalised negative charge. Attack is therefore postulated on the remaining carbonyl

carbon in an identical manner to the first stage. Hydrolysis may occur by metal-oxygen or by carbon-oxygen fission so as to always give cis product.

Activation energies were not determined, but it is likely that ring opening has the lower value, since it has two attackable carbonyl carbons, and hence may go effectively to completion before the second stage sets in.

The mechanism is outlined in Schemes 4 and 5.

Scheme 4.

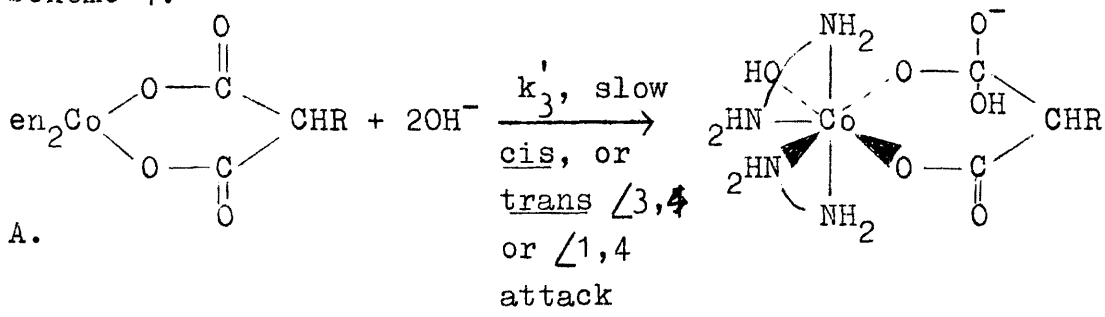

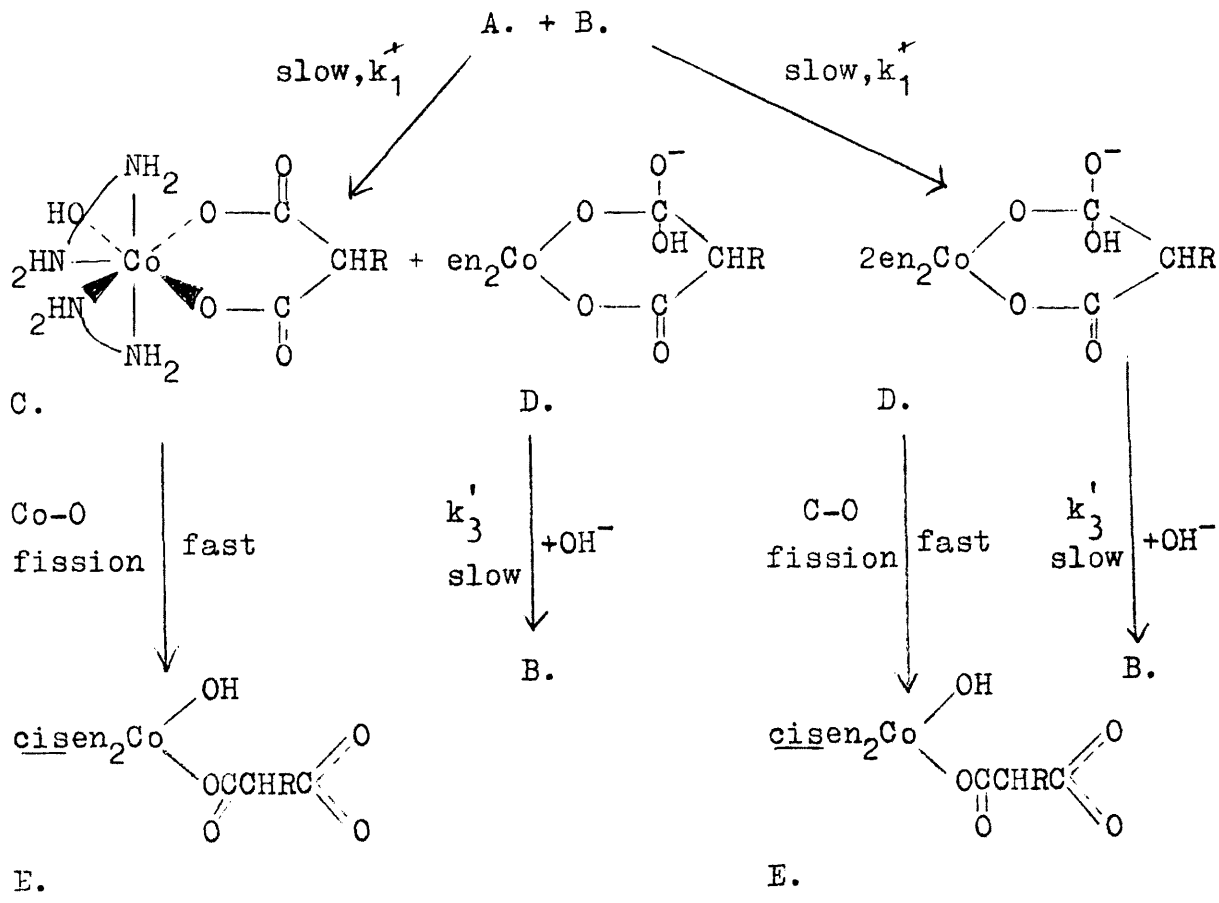

Note that the mechanism involves identical intermediates, D. Since the k_2' path has been shown to be negligable at $[OH^-]$ 1.50M (since the solutions of the quadratic rate laws are invalid beyond this point), these intermediates must engage in the k_3' path in order to achieve the open ring form. For the D intermediate produced by abstraction of the hydroxide bound to the metal in B this would appear to constitute a closed loop process. However, it is proposed that (a) the D intermediate produced in such a manner has become activated (D*) by more molecular collisions than D, and is able to react with C-O fission directly - but in a fast step and in a manner independent of the k_2' path; or (b) that intermediate C is prefered. (b) is deemed more likely
If (b) is the case, O^{18} exchange experiments would elucidate the mechanism more fully.

Scheme 5. The mechanism of the second stage of the base hydrolysis of $[Coen_2Rmal]^+$, $[OH^-] > 1.50M$.

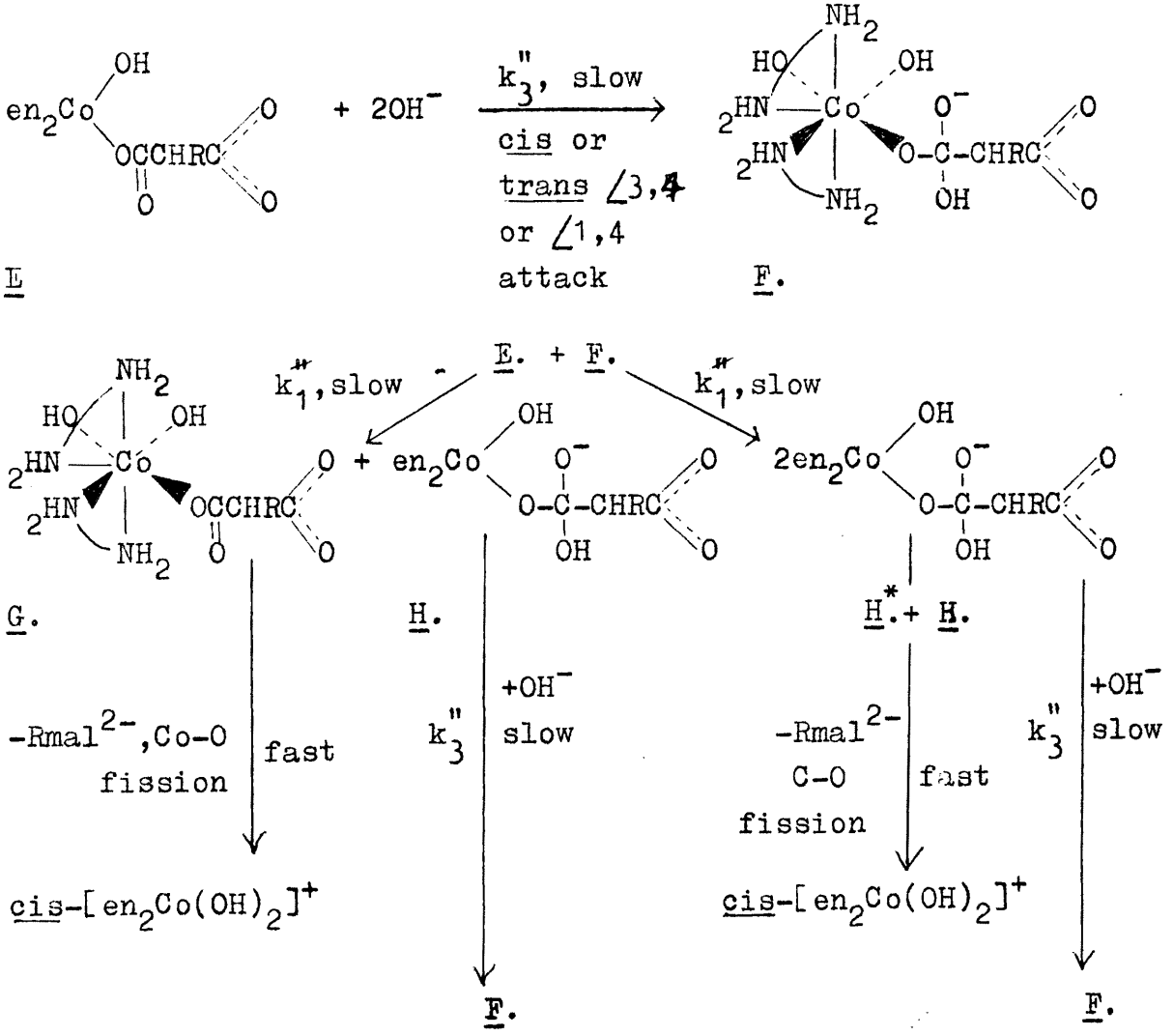

Similar arguments apply to the reaction of either H or H^* in the k_3'' path or in a fast step to give dihydroxo product.

It is worth noting that at 25°C the k_1 and k_3 paths generally dominate earlier than at 35°C. This is deduced from the solutions of the general quadratic rate law (Table 28) and from the order of reaction wrt $[OH^-]$ deduced from the initial rates. In this respect the mechanism is similar to that in $[Coen_2(C_2O_4)]^+$(37) where, if an associative mechanism does operate, it is favoured at lower temperature.

The mechanisms outlined come about as a result of the effect of the medium and of the ∝-substituent (in activating the carbonyl carbon).
The latter effect can also be reconciled with the reversibility of the second stage.

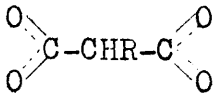
, displaced in the second stage, unlike either

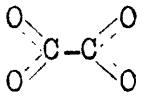
or
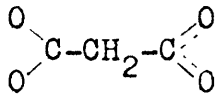
, may retain some polar character of the carboxyl group, i.e. $\overset{\partial+}{C}=\overset{\partial-}{O}$. It is therefore possible that this may displace a molecule of OH^- from cis-$[Coen_2(OH)_2]^+$. Since the product of the base hydrolysis of $[Coen_2(C_2O_4)]^+$ and $[Coen_2mal]^+$ is irreversibly dihydroxo ion, mal^{2-} and $(C_2O_4)^{2-}$ are certainly incapable of this. The result in this case is that an equilibrium is finally established containing some of the hydroxymalonato intermediate.
Equilibrium constants(Table 21) are large as one would expect. Generally, they are larger for the benzylmalonato complex. This is unexpected, since the greater inductive power of the benzyl group might be expected to polarise the $\diagdown C=O$ bonds more and thereby push equilibrium (C') to the left. However, since a large experimental error was incurred, the relative values of K_C, may not be as they appear. Furthermore, 10Dq values (p.110) are less for $Etmal^{2-}$ and $Bzylmal^{2-}$ than for mal^{2-}. This is again contrary to the argument above, since in the light of the ligand field parameters, mal^{2-} appears to be more capable than either $Etmal^{2-}$ or $Benzylmal^{2-}$ of donating an electron pair to the

metal's d orbitals.

Further evidence for the operation of the mechanism described above is also apparent from the amounts of $[Coen_2(Rmal)(OH)]^o$ formed in equilibrium (B')(p.118). As stated (p.135) $K_{C'}$ values in concentrated base are roughly the same amount greater than those in dilute base, than the amount of intermediate formed in concentrated base is less than the optimum quantity (Figure 26) formed in dilute base. This phenomenon was attributed to the production of cis-$[Coen_2(OH)_2]^+$ whilst ring opening was in progress. The mechanism described above allows for this.

Once a molecule of complex has undergone ring opening to give E, by the $k_1^{\leftarrow}$ and k_3' paths there is no reason to suppose why a ring opened molecule should not engage in the $k_1^{\leftarrow}$ path with one having just undergone association in the A + B, k_3' path. Such an interaction is not included in the k_2' path in dilute base. (Although it may occur but be negligable in quantity). Interaction of this nature is not as likely as the A + B, $k_1^{\leftarrow}$ type, since only one carbonyl carbon is relatively activated. However, if it does occur, which seems most likely, reaction along the k_3'' path is then inevitable and cis dihydroxo product results. The $k_1^{\leftarrow}$, k_3', $k_1^{\leftarrow\leftarrow}$ and k_3'' paths are, in fact, intimately interlinked.

At lower temperatures (25.2°C)(in concentrated base), $K_{C'}$ values are higher than at 35°C. This is consistent with the earlier suggestion that the $(k_1 + k_3)$ paths are favoured by lower temperature, thereby allowing more cis-$[Coen_2(OH)_2]^+$ to form during the ring opening stage and increase the value of $K_{C'}$.

Once all the complex is in the ring opened form, this is the only species able to react in the $k_1^{(")}$ path and only cis dihydroxo product can result. As observed, the equilibrium for the second stage is only affected during the course of ring opening.

In comparison to the results for the base catalysed hydrolysis, those for the acid catalysed reaction do not permit as full a description of the operative mechanism. Several facts, are however, apparent.

Since $[Coen_2mal]^+$ and $[Coen_2(C_2O_4)]^+$ are not subject to acid catalysed hydrolysis, once again the α-substituent is responsible for the extreneous effect. It is proposed that the inductive effect of the group makes protonation of the carbonyl oxygens feasible, thereby leading to dechelation and the production of intermediates.

This is inferred from the dependence of the observed pseudo first order rate constants on acid concentration. In addition since that dependence is half-order, the protonating moiety must be associated with two molecules of complex. This is consistent with the generation of bimalonatoaquo and malonatoaquo intermediates.

Since acid hydrolysis is observed only in the case of the α-substituted complexes, the molecule of acid must be associated with a group easily influenced by the substituent. This is one of the carbonyl oxygens. If such a protonation does occur, the observed dechelation must come about by cobalt-oxygen fission, to generate the two intermediate types. i.e.

$$2[Coen_2Rmal]^+ + H_3O^+ + H_2O \longrightarrow [Coen_2(H_2O)(RmalH)]^{2+} + [Coen_2(H_2O)(Rmal)]^+ \qquad (E')$$

This is fully consistent with the suggestions of Harris(52) (p.106) for $[Coen_2CO_3]^+$, where the two forms analogous to those in (E') were proposed (equilibria (T) and (U)), even though the reaction was observed to proceed in one stage.

A comparison to the zero order dependence of the second stage is not found in either the mechanism of Harris(52) or Jordan(58)(p.107) for the acid hydrolysis of $[Coen_2CO_3]^+$, both of which include one acid-catalysed term in the removal of carbonate.

The products of the reaction appear to be both cis and trans -$[Coen_2(H_2O)_2]^{3+}$. Such a result could come about as a consequence of a dissociative mechanism in which H_3O^+ is involved in the fast step or as a result of production of aquohydroxo ion, which has been shown(45) to isomerise extremely rapidly. By analogy with the carbonate complex(34) dechelation probably goes with retention of configuration

even if Co-O fission occurs. Production of the aquohydroxo intermediate in a neutral step from the intermediate followed by rapid isomerisation, would be consistent with the results observed here, and with the analogous step (V) proposed by Harris.

$$\underline{cis}\text{-}[Coen_2(H_2O)(Rmal)]^+ + H_2O \longrightarrow \underline{cis}\text{-}[Coen_2(OH)(H_2O)]^{2+} + RmalH^- . \qquad (F')$$

$$\underline{cis}\text{-}[Coen_2(OH)(H_2O)]^+ \underset{\longleftarrow}{\overset{fast}{\longrightarrow}} \underline{trans}\text{-}[Coen_2(OH)(H_2O)]^{2+} \qquad (G')$$

Reaction of the bimalonatoaquo intermediate in neutral and acid catalysed steps analogous to (W) and (X) of Harris and of Jordon is indeterminate here. If the acid catalysed step does occur as well as the inevitable step:

$$\underline{cis} \text{ and } \underline{trans}\text{-}[Coen_2(OH)(H_2O)]^{2+} + H_3O^+ \longrightarrow \underline{cis} \text{ and } \underline{trans}\ [Coen_2(H_2O)_2]^{3+} + H_2O \qquad (H')$$

then neither figures in the observed kinetics.

Since no neutral rate was observed, even on heating to 95°C, dechelation appears to be rate controlling. This does not necessarily imply that the rate of dechelation controls the rate of subsequent steps, but since the second stage is independent of $[H_3O^+]$ it can only occur in acid solution <u>after</u> acid catalysed dechelation of substituted malonate.

In addition, it is also apparent that the dechelated intermediates, whatever their nature, do not contribute to the final products. This is quite certain in view of the resulting spectrum on adding alkali to the acid solution of products.

GENERAL CONCLUSION.

The pmr studies have demonstrated the stereospecificity of the acid catalysed deuteration of the active methylene group in $[Comal_2en]^-$. Absolute assignment of the inequivalent protons: H_A and H_B was a result of the observation of 'trans-space' coupling in $[CoEtmal_2en]^-$. This is the first report of this phenomenon in the field of transition metal chemistry.
The base catalysed deuteration proceeded at a rate too fast to measure. However, this, as well as the acid catalysed rates confirmed that the lability of the α-protons is sufficient to complement the conjugate base proposed by Farago(34,35).
The results should prove useful in the synthesis of α-mono -substituted (especially deuterium substituted) malonic acid and malonate esters.

The introduction of the α-substituents; ethyl and benzyl, rendered the ring opening stage of the acid and of the base catalysed hydrolysis observable. This stage is <u>not</u> observed in the base hydrolysis of $[Coen_2mal]^+$(34,35) or the acid catalysed hydrolysis of $[Coen_2CO_3]^+$(52,58,101).
In fact, the substituents are responsible for the fact that acid hydrolysis is observed at all.
The hydrolysis of the complex cations $[Coen_2Etmal]^+$ and $[Coen_2Bzylmal]^+$ is therefore subject to specific acid-base catalysis.
In dilute base, the kinetics of hydrolysis are as observed for the $[Coen_2(C_2O_4)]^+$(87) and $[Coen_2mal]^+$(34,35) ions, i.e. simple second order. In concentrated base the kinetic rate law consists of two terms; one second order in $[OH^-]$, (as postulated by Taube(3) and confirmed by Farago(37) for $[Coen_2(C_2O_4)]^+$), and one zero order in $[OH^-]$.
The kinetics were reconciled with the mechanisms proposed on pp.162-3. The mechanisms allow for the formation of dihydroxo product whilst the ring opening stage is still in progress. This accounts for the existence of an optimum value of $[OH^-]$ to give a maximum amount of the intermediate $[Coen_2(Rmal)(OH)]^o$, at a given temperature.

This observation was also made in the case of $[Coen_2(C_2O_4)]^+$(69) but cannot be accounted for by either simple second order kinetics, or kinetics second order in $[OH^-]$ without the zero order term. Further examination of the kinetics of the base hydrolysis of this complex is therefore advocated.
Since the change of kinetics in concentrated base produces the possibility of different bond fission to that in dilute base, O^{18} exchange experiments would be a most useful next step in this research.
Such conclusions as are forthcoming from the acid catalysed hydrolysis, support the conclusions made in the case of $[Coen_2CO_3]^+$(52,58).

One may speculate as to how far the existence of acid catalysed hydrolysis invalidates the pmr spectral assignments made in the case of $[CoEtmal_2en]^-$ and $[Coen_2Etmal]^+$. No chemical shift changes or effects on the line shapes were observed - although spectra were recorded quickly in most cases.
In addition, the definite existence of two geometrical isomers of $[CoEtmal_2en]^-$ precludes a dechelation equilibrium, or pre-equilibrium in anything but very small proportions, as was proposed for $[Comal_2en]^-$.
On this evidence, the spectral assignments may stand, although further work is needed in this respect.

APPENDIX I

The uv-visible spectra of $K_3[Comal_3]3H_2O$ and $K[Comal_2en]H_2O$ were recorded in a range of sodium acetate/HCl buffers (pH 1-4).

(i) $K_3[Comal_3]3H_2O$. Initial spectra were all identical. Therefore, the self-buffering effect of the complex cannot be due to the pre-equilibrium (H)(p. 61) already postulated, since this would be expected to be pH dependent and hence show significant spectral differences in a range of buffers.

However, spectra recorded 10-15 minutes after dissolution (Figure A1) revealed the possibility of acid hydrolysis. The spectra shown are virtually stationary and therefore an acid hydrolysis equilibrium which is pH dependent is postulated.

The spectra are consistent with the formation of aquo complexes, since the ε_m values are low. However, there is no radical change in band positions. Dechelated malonate is therefore a possibility. The buffering effect of the complex could therefore come about by the action of the dechelated malonate rather than by the action previously postulated (p.61)

Further investigation of this system is needed.

(ii) $K[Comal_2en]H_2O$. The complex is quite stable for long periods in all the buffer solutions. Spectra are identical within the limits of weighing error.(Figure A2).
It has been noticed already (p. 54) that the self buffering effect of this complex is considerably less marked than that of $K_3[Comal_3]3H_2O$. There is no evidence as to whether its effect is due to the pre-equilibrium (H)(p. 61) or to small amounts of the hydrolysed form postulated above for the trismalonato-complex. Scheme 2 (p.96) is therefore allowed to stand, with the reservation that the first pre-equilibrium postulated <u>may</u> be invalid. Nevertheless a nonstereospecific pathway is essential in the light of the evidence already presented. If the pre-equilibrium is invalid, then the nonstereospecific pathway probably arises from the protonated complex. This is allowed for in Scheme 2.

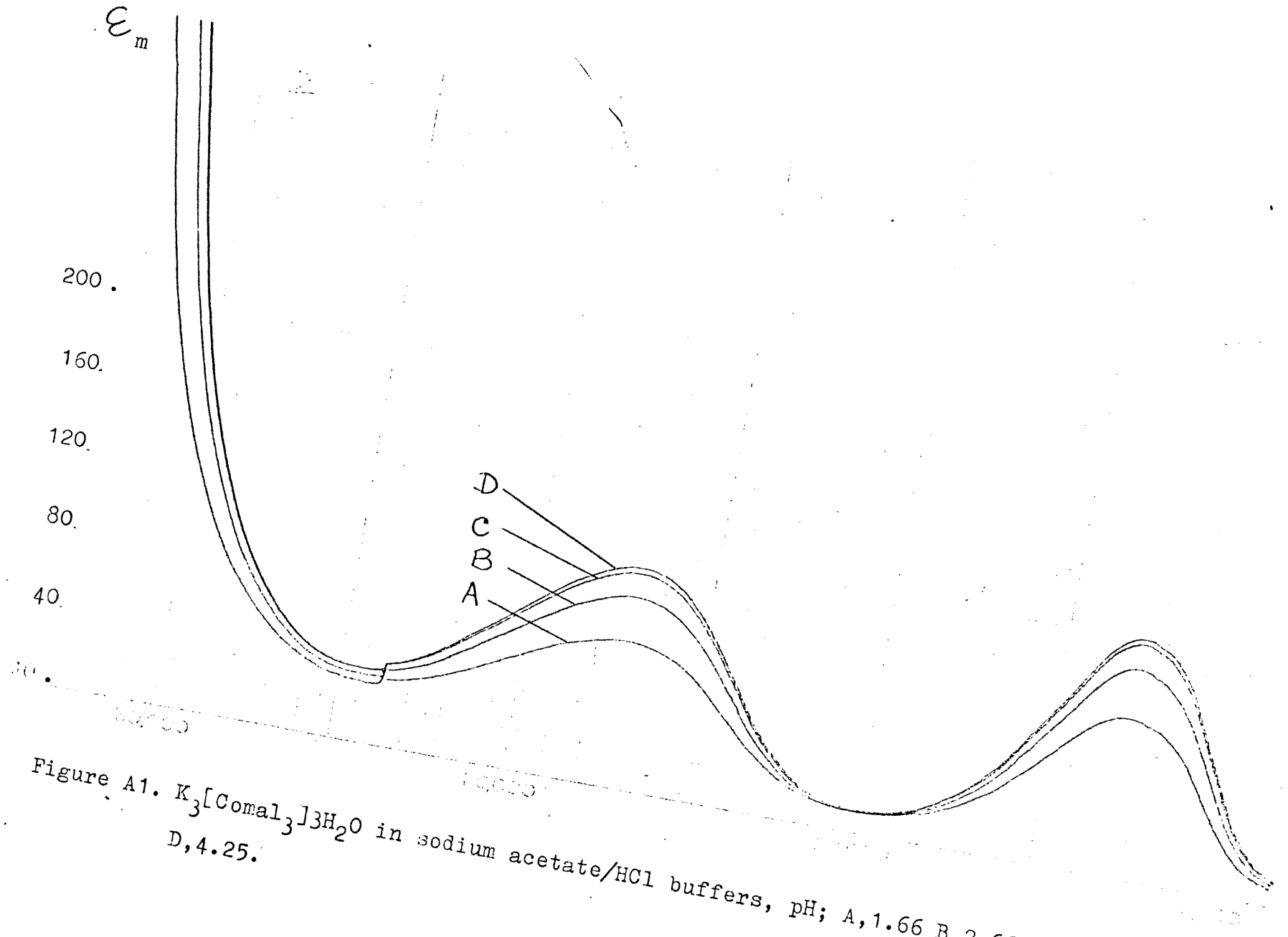

Figure A1. $K_3[Comal_3]3H_2O$ in sodium acetate/HCl buffers, pH; A,1.66 B,2.66 C,3.38 and D,4.25.

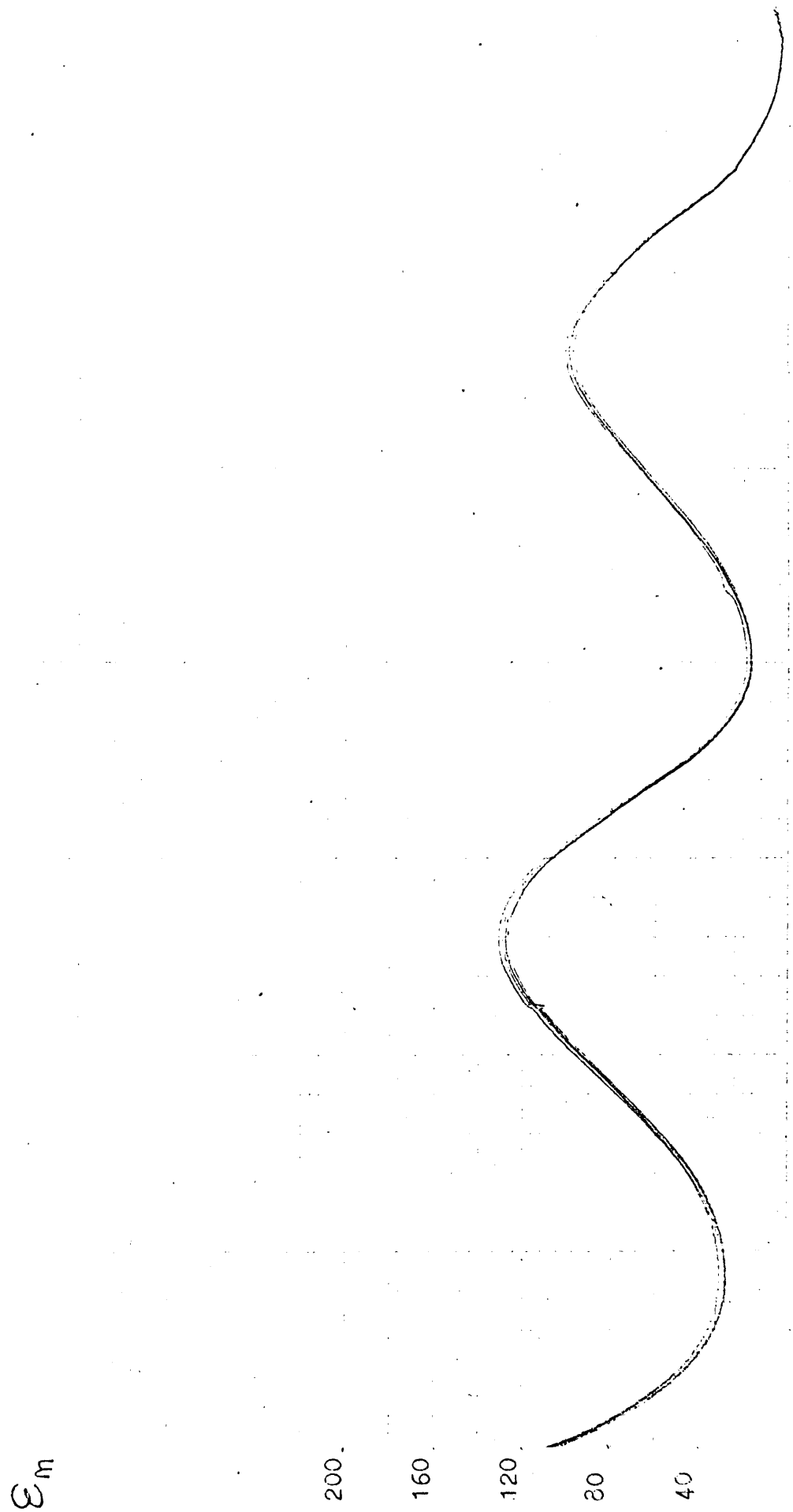

Figure A2. K[Co(ox)$_2$en].$2H_2O$ in a range of sodium acetate/HCl buffer solutions, pH 1.6-4.2

APPENDIX II.

Computer programme for the solution of the quadratic rate laws.

The programme is in Fortran IV.

```
      PROGRAM GWENO(INPUT,OUTPUT)
      REAL OH
      INTEGER HEAD(80)
000003 13    READ 18,(HEAD(I),I=1,80)
000003 18    FORMAT(80A1)
000015       PRINT 17,(HEAD(I),I=1,80)
000015 17    FORMAT(1H1,80A1)
000027 12    READ 10,(HEAD(I),I=1,80)
000027 10    FORMAT(80A1)
000041       PRINT 11,(HEAD(I),I=1,80)
000041 11    FORMAT(1H0,80A1)
000053 4     FORMAT(1H0* [OH]*,12X,*SOLN1*,10X,*SOLN2*,15X,*A*,17X,*B*,
     1 17X,*C*,//)
000053       PRINT4
000057 15    READ 1,OH,A,B,C
000073       IF(OH.EQ.0.0.AND.A.EQ.0.0)GOTO 20
000101       IF(OH.EQ.0.0)GOTO 12
000101 1     FORMAT(F4.2,2F7.5,F8.6)
000101       SOLN1=(-B+SQRT(B*B-4*A*C))/(2*A)
000113       SOLN2=(-B-SQRT(B*B-4*A*C))/(2*A)
000127 2     FORMAT(F6.2,2(10X,F6.3),2(10X,F8.5),10X,F9.6)
000127       PRINT 2,OH,SOLN1,SOLN2,A,B,C
000147       GOTO 15
000150 20    STOP
000152       END

UNUSED COMPILER SPACE
011100
```

APPENDIX III

Survey of uv-visible spectra of cobalt(III) complexes containing co-ordinated malonate.

The preparations of the new malonato complexes are described earlier in this thesis (pp.54-60 and p.108). For the sake of completeness a survey of the complex's uv-visible spectra, compared to previously reported complexes, is given here.

Complex	Transition $^1A_{1g} \longrightarrow {}^1T_{1g}$	ε_m	Transition $^1A_{1g} \longrightarrow {}^1T_{2g}$	ε_m
$[Coen_2mal]^+$	20,100	115	28,000	104
$[Coen_2Etmal]^+$	19,600	144	27,800	133
$[Coen_2Bzylmal]^+$	19,650	202	27,800	181.3
$[Comal_2en]^-$	18,600	90.4	26,050	113.8
$[CoEtmal_2en]^-$	18,300	101	25,800	117.5
$[CoBipy_2mal]^+$	20,100	81.4		
$[CoBipy_2mal][Comal_2Bipy]$	19,100	152		
$[Cophen_2mal]^+$ (2)	19,800	89.8		
$[Cophen_2mal][Comal_2phen]$	19,000	165		

N.B. the $^1A_{1g} \longrightarrow {}^1T_{2g}$ transitions of the complexes containing heterocyclic ligands are hidden by the uv-active chromophores of the latter.

BIBLIOGRAPHY.

1. ABLOV,A.V.,Russ.J.Inorg.Chem.,1961,6, 157.

2. ABLOV,A.V. and PALADE,D.M.,ibid.,1962,7, 1304.

3. ANDRADE,C.A. and TAUBE,H.,J.Amer.Chem.Soc.,1964,86, 1328.

4. ANET,F.A.L.,ibid.,1962,84, 1053.

5. ANET,F.A.L. and BOURN,A.J.R.,ibid.,1967,89, 760

6. ANET,F.A.L.,BOURN,A.J.R.,CARTER,P. and WINSTEIN,S.,ibid., 1965,87, 5249.

7. BALLHAUSEN,C.J.,"Introduction to Ligand Field Theory", McGraw-Hill Book Co.Ltd.,1962,p.107.

8. BASOLO,F.,BALLHAUSEN,C.J. and BJERRUM,N.,Acta Chem.Scand., 1955,9, 810.

9. BASOLO,F.,PALMER,J.W. and PEARSON,R.G.,J.Amer.Chem.Soc., 1960,82, 1073.

10a. BASOLO,F. and PEARSON,R.G.,"Mechanisms of Inorganic Reactions",John Wiley,1967,2nd Edition., Chapter 3.

10b. BASOLO,F. and PEARSON,R.G.,ibid., Chapter 4.

11. BETHE,H.,Ann.Physik.,1924,5, 133.

12. BHACCA,N.S.,JOHNSON,L.F. and SHOOLERY,J.N.,"NMR Spectra Catalog",Vols. 1 and 2,Varian Associates,Palo Alto, California, 1963.

13. BIBLE,R.H.,"Interpretation of NMR Spectra, An Empirical Approach",Plenum Press, New York,1965,p.83.

14. BJERRUM,N.,Z.Physik.Chem.,1924,108, 82.

15. BJERRUM,N. and RASMUSSEN,S.E.,Acta Chem.Scand.,1952,6, 1265.

16. BONTHER-BY,A.A.,Advan.Magn.Resonance,1965,1, 195.

17. BRONSTEAD,J.N.,Z.Physik Chem.,1922,102, 169.

18. BROOMHEAD,J.A.,DWYER,F.P. and KANE-MAGUIRE,L.A.P.,Inorg. Chem.,1968,7, 1388.

19.BUCKINGHAM,D.A.,DURHAM,L. and SARGESON,A.M.,Aust.J.Chem., 1967,20, 268.

20.BUCKINGHAM,D.A.,MARZILLI,L.G. and SARGESON,A.M.,J.Amer. Chem.Soc.,1967,89, 825.

21.BUCKINGHAM,D.A.,MARZILLI,L.G. and SARGESON,A.M.,ibid,91, 5227.

22.BUCKINGHAM,D.A.,OLSEN,I.I. and SARGESON,A.M.,ibid.,1966, 88, 5443.

23.BUCKINGHAM,D.A.,OLSEN,I.I. and SARGESON,A.M.,Inorg.Chem., 1967,6, 1807.

24.CALDIN,E.F.,"Fast Reactions in Solution",Blackwell Scientific Publications,Oxford,1964.

25.CARLIN,R.(Ed.),"Transition Metal Chemistry",Vol.3, Edward Arnold Ltd.,London,1966,p.325.

26.CHAN,S.C.,J.Chem.Soc.,A,1966, 1124.

27.CHRISTIANSEN,J.A.,Z.Physik Chem.,1924,113, 35.

28.COREY,E.J. and BAILAR,J.C.Jnr.,J.Amer.Chem.Soc.,1959,81, 2620.

29.COTTON,F.A. and WILKINSON,G.,"Advanced Inorganic Chemistry", John Wiley and Sons Ltd.,1967,p.856.

30.DWYER,F.P.,REID,I.K. and GARVAN,F.L.,J.Amer.Chem.Soc., 1961,83, 1285.

31.DWYER,F.P.,SARGESON,A.M. and REID,I.K.,ibid,1963,85.

32.EMSLEY,J.W.,FEENEY,J. and SUTCLIFFE,L.H.,"High Resolution NMR Spectroscopy",Vol.1,Chapter 8,pp.280-480,and Appendix I,pp.661-663,Pergamon,London, 1965.

33.ERICKSON,L.E.,YOUNG,D.C.,HO,F.F-L.,WATKINS,S.R.,TERRILL,J.B., and REILLY,C.N.,Inorg.Chem.,1971,10, 441.

34.FARAGO,M.E.,Co-ord.Chem.Revs.,1966,1, 66.

35.FARAGO,M.E. and KEEFE,I.M.,unpublished results.

36.FARAGO,M.E.,KEEFE,I.M. and MASON,C.F.V.,J.Chem.Soc.,A,1970, 3194.

37.FARAGO,M.E. and MASON,C.F.V.,J.Chem.Soc.,A,1970, 3100.

38.FARAGO,M.E.,MASON,C.F.V. and PAGE,B.A.,Inorg.Chem.,1969,8, 2270.

39.FARAGO,M.E. and SMITH,M.A.R.,submitted to Inorg.Chem.

40.FRIESS,S.L. and WEISSENBERGER,A.(Eds.),"Investigations of Rates and Mechanisms",(Vol.3 of "Technique of Organic Chemistry"),Interscience Publishers,London,1953,2nd Edition, 1963,p.180.

41.FROST,A.A. and PEARSON,R.G.,"Kinetics and Mechanism",John Wiley,N.York,1961,(a)p.49,(b)p.132.

42.GARRICK,F.J.,Nature,1937,139, 507.

43.GEISSMAN,T.A.,"Principals of Organic Chemistry", W.H.Freeman and Co.,San Francisco and London,2nd Edition,1962,p.324.

44.GILLARD,R.D.,J.Chem.Soc.,A,1967, 917.

45.GILLARD,R.D.,ibid,1968, 1945.

46.GILLESPIE,R.J. and NYHOLM,R.S.,Quart.Revs.,1957,11, 339.

47.GLASCOE,P.K. and LONG,F.A.,J.Phys.Chem.,1960,64, 188.

48.GODDARD,J.B. and BASOLO,F.,Inorg.Chem.,1969,8, 2223.

49.GREEN,M. and TAUBE,H.,ibid.,1963,2, 948.

50.HAIGH,C.W.,private communication to E.O.Bishop in (73).

51.HALPERN,B.,SARGESON,A.M. and TURNBULL,K.R.,J.Amer.Chem.Soc., 1966,88, 4630.

52.HARRIS,G.M. and SASTRI,V.S.,Inorg.Chem.,1965,4, 263.

53.HOLDEN,J.S. and HARRIS,G.M.,J.Amer.Chem.Soc.,1955,77, 1934.

54.INGOLD,C.K.,"Structure and Mechanism in Organic Chemistry", Cornell University Press,Ithaca,1953.

55.INGOLD,C.K., Weissman Memorial Lecture, 1958.

56.INGOLD,C.K.,NYHOLM,R.S. and TOBE,M.L.,Nature,1962,194, 344.

57.IUPAC COMMISSION, Inorg.Chem.,1970,9, 2.

58.JORDON,R.B. and FRANCIS,D.J., ibid.,1967,6, 1605.

59.KARPLUS,M.,J.Chem.Phys.,1959,30, 11.

60.KARPLUS,M.,J.Amer.Chem.Soc.,1963,85, 2870.

61.LAIDLER,K.J.,"Chemical Kinetics",McGraw-Hill,London,1965, 2nd Edition,pp.205-230.

62.LAPIDUS,G. and HARRIS,G.M.,J.Amer.Chem.Soc.,1963,85, 1223.

63.LEGG,J.I.,COLEMAN,P.F. and STEELE, J.Inorg.Chem.,1970,9, 937.

64.LEGG,J.I. and COOKE,D.W.,ibid.,1965,4, 1576.

65.LEGG,J.I. and COOKE,D.W.,ibid.,1966,5, 594.

66.LIEHR,A.D.,J.Chem.Phys.,1964,68, 3629.

67.LONGFORD,C.H. and GRAY,H.B.,"Ligand Substitution Processes", W.A.Benjamin Inc.,1965,Chapter 3.

68.LUMRY,R.,SMITH,E.L. and GLANZ,R.R.,J.Amer.Chem.Soc.,1951, 73, 4330.

69.MASON,C.F.V.(née Pearce),PhD.Thesis submitted to the University of London,1967,p.148.

70.McCAFFERTY,A.J. and MASON,S.F.,Proc.Chem.Soc.,1962,338

71.MILLAR,J.D. and PRINCE,R.D.,J.Chem.Soc.,A,1969, 519.

72.MOELWYN-HUGHES,E.A.,Proc.Roy.Soc.,(London),1936,A155, 308.

73.MOONEY,E.F.(Ed.),"Annual Review of NMR Spectroscopy", Academic Press,London and New York,1968,Volume 1,Table 1.

74.MYHRE,P.C.,EDMONDS,J.W. and KRUGER,J.P.,J.Amer.Chem.Soc., 1966,88, 2459.

75.NORDMEYER,F.R.,Inorg.Chem.,1969,8, 2780.

76.AL-OBADIE,M.S. and SHARPE,A.G.,J.Inorg.Nucl.Chem.,1969, 31, 2963.

77.ORGEL,L.E.,J.Chem.Phys.,1955,23, 1819.

78.PAULING,L.,"Nature of the Chemical Bond",Oxford University Press,London,3rd Edition,pp.331-339

79.PEARSON,R.G. and BASOLO,F.,J.Amer.Chem.Soc.,1956,78, 4878.

80.PEARSON,R.G. and BASOLO,F.,Inorg.Chem.,1965,4, 150.

81.PEARSON,R.G.,MUNSON,R.A. and BASOLO,F.,J.Amer.Chem.Soc., 1958,80, 504.

82.PIPER,T.S.,J.Amer.Chem.Soc.,1961,83, 3908.

83.POON,C.K. and TOBE,M.L.,Chem.Comm.,1968, 156.

84.RAMEY,K.C. and BREY,W.S.,J.Chem.Phys.,1964,40, 2349.

85.SCATCHARD,G.,Chem.Rev.,1932, 10, 229.

86.SCHEIDEGGER,H. and SCHWARZENBACH,G.,Chimia,1965,19, 169.

87.SHEEL,S.,MELOON,D.T. and HARRIS,G.M.,Inorg.Chem.,1962,1, 170.

88.SHRINER,R.L.,ADAMS,R. and MARVEL,C.S.,"Organic Chemistry,An Advanced Treatise",2nd Edition,H.Gilman(Ed.),John Wiley, New York,1943,pp.402-413.

89.SMITH,B.B. and SAWYER,D.T., Inorg.Chem.,1968,7, 922.

90.SMITH,B.B. and SAWYER,D.T.,ibid,1968,7, 2020.

91.SMITH,B.B. and SAWYER,D.T.,ibid,1969,8, 379.

92.SMITH,B.B. and SAWYER,D.T.,ibid.,1969,8, 1154.

93.SUDMEIER,J.L. and OCCUPATI,G.,ibid.,1968,7, 2524.

94.SUDMEIER,J.L.,SCHWARTZ, and SENZEL,A.J.,ibid.,1969,8, 2815.

95.SUDMEIER,J.L. and SENZEL,A.J.,Chem.Comm.,1968, 1646.

96.SUDMEIER,J.L.,SENZEL,A.J. and BLACKMER,G.L.,Inorg.Chem., 1971,10, 90.

97.TERRILL,J.B. and REILLEY,C.N.,ibid.,1966,5,1988.

98.TOBE,M.L.,Sci.Progress,1960,48, 483.

99.TOBE,M.L.,Inorg.Chem.,1968,7, 1260.

100.TOBE,M.L.,"Studies on Chemical Structure and Reactivity", J.H.Ridd (Ed.),Methuen and Co. Ltd.,London,1966,p.215.

101.TONG,J.Y.,KEEN,E.S.A., and HALL,B.B.,Inorg.Chem.,1964,3, 1103—

102.WEAKLIEM,H.A. and HOARD,J.L.,J.Amer.Chem.Soc.,1959,81, 549.

103.WIENER,A.,Leib.Annalen,1912,80, 386.

104.WILLIAMS,D.H. and BUSCH,D.H.,J.Amer.Chem.Soc.,1965,87, 4644.

105.WOLDBYE,F.,personal communication to A.M.Sargeson in (19).

106.YONEDA,H. and MORIMOTO,Y.,Inorg.Chim.Acta,1967,1, 413.

107.JONAS,J.,ALLERHARD,A., and GUTOWSKY, H.S.,J.Chem.Phys., 1965,42, 3396.

108.POPLE,J.A. and BONTHER-BY,A.A.,J.Chem.Phys.,1964,42, 1339.